IEEE

WORKSHOP ON

WIRELESS LOCAL AREA NETWORKS

at

WORCESTER POLYTECHNIC INSTITUTE

MAY 9–10, 1991

May 9

Tutorial on Wireless
Indoor Communications

May 10

Invited Lectures by Leading
Researchers and Industrialists

Sponsored by

Wireless Information Network Group at WPI
IEEE Communication Society
WINDATA Inc., Northboro, MA

PREFACE

In 1979, Gfeller and Bapst published a paper in the IEEE Proceedings reporting an experimental wireless local area network using diffused infrared communications. Shortly thereafter, in 1980, Ferrert reported on an experimental application of a single code spread spectrum radio for wireless terminal communications in the IEEE National Telecommunications Conference. In 1984, a comparison between Infrared and CDMA spread spectrum communications for wireless office information networks was published by the author in IEEE Computer Networking Symposium which appeared later in the IEEE Communication Society Magazine. In May 1985, the efforts of M. Marcus led the FCC to announce experimental ISM bands for commercial application of spread spectrum technology. Later on, M. Kavehrad reported on an experimental wireless PBX system using code division multiple access. These efforts prompted significant industrial activities in the development of a new generation of wireless local area networks and it updated several old discussion in the portable and mobile radio industry.

The first generation of wireless data modems was developed in the early 1980's by amature communication groups. They added a voice band data communication modem, with data rates below 9600 bps, to an existing short distance radio system such as a walkie talkie. The second generation of wireless modems was developed immediately after the FCC announcement in the experimental bands for non-military use of the spread spectrum technology. These modems provided data rates on the order of hundreds of Kbps. The third generation of wireless modem now aims at compatibility with the existing LANs with data rates on the order of Mbps. Currently, several companies are developing the third generation products with data rates above 1 Mbps and a couple of products have already been announced.

This workshop addresses issues associated with wireless local area networks. Its aim is to increase the participants' awareness of the current and future direction in the area and to create an interaction between researchers, leading industry developers and end users. The workshop begins with tutorials on the first day and continues on the second day with invited lectures by leading researchers in academia and industry.

The workshop is scheduled to follow the meeting of the IEEE 802.11 Wireless Access Methods and Physical Layer Standardization Committee for wireless local area networks, held from May 6 to May 9 at Worcester, Mass.

The tutorial is designed for researchers, design engineers, computer scientists, students, and users who are interested in getting a general overview of technical aspects of wireless indoor radio networks. It will prepare the general audience for the lectures and discussions on the second day. The main lecture in the tutorial will cover principles of wireless indoor communications. This will be followed by three short tutorials on implementation issues. At the end of this day, a group of network managers will hold a panel discussion on the applications and issues regarding wireless LANs in an end user environment.

The invited lectures will start with an overview of wireless local networks and the existing regulations and standards. The following sessions concern measurement and modeling of the indoor radio and optical propagations, spread spectrum application, and other emerging technologies. At the end of the second day, the workshop features a panel discussion on the future direction of wireless technology.

Prof. Kaveh Pahlavan
Department of Electrical Engineering
Worcester Polytechnic Institute

May 10: Invited Lectures

PROGRAM

May 9: Tutorial: Wireless Indoor Communications

9:00–2:30 p.m. MAIN TUTORIAL (K. Pahlavan)

- Motivations and Examples
- Digital Communicatitions Over Indoor Radio Channel
- Basic Principles of Spread Spectrum
- Infrared Communications

2:30–4:00 p.m. SHORT TUTORIALS

4:30–5:30 p.m. USERS PANEL

Discussion among a group of invited network managers from various end user companies on the application of wireless LANs.

SPEAKERS

Dr. H. Arnold
Bell Communicaton Research, Red Bank N.J.

Dr. C. Bass
Bass Assoc., Palo Alto California

Mr. J. Cheah
Hughes Network Systems, California

Dr. D. Devasirvatham
Bell Communication Research, Red Bank, N.J.

Prof. D. Falconer
Carlton University, Ottawa, Canada

Mr. T. Freeburg
Motorola Inc., Arlington Heights, IL

Mr. V. Hayes
NCR Systems Engineering, B.V. Nieuwegein, The Netherlands

Dr. P. Hortensius
IBM, Westchester County, N.Y.

Dr. J. Kahn
University of California, Berkeley

Prof. M. Kavehrad
University of Ottawa, Canada

Mr. S. Lipoff
Arthur D. Little Co., Cambridge, Mass

Dr. M. Marcus
FCC, Washington, D.C.

Prof. D. Schilling
City College, N.Y.

Mr. B. Tuch
NCR, Systems Engineering, B.V. Nieuwegein, The Netherlands

Mr. S. Wilkus
AT&T Bell Labs, N. Andover, Mass.

SHORT TUTORIALS

Implementation Issues for Wireless Spread Spectrum Data Communications Links for use in License Free Applications

Stuart J. Lipoff
Electronic Systems Laboratory
Arthur D Little
Cambridge, Mass 02140 USA

IEEE Workshop
on
Wireless Local Area Networks
Worcester Polytechnic Institute
May 9-10, 1991

OUTLINE

- Introduction
- Review FCC rules
- Electromagnetic environments
- Review available systems
- Generic system architectures
- Conclusions

INTRODUCTION
PRESENTATION OBJECTIVES

- Objectives

To explore practical and cost effective hardware realizations of short range, license free spread spectrum data communications systems in consideration of:

  - Electromagnetic interference environment
  - Constraints of FCC rules
  - Alternative system architectures
  - Minimum acceptable performance requirements

- Scope

  - USA regulatory environments
  - FCC Part 15.247 rules in 902-928 MHz band
  - Indoor, general office environment
  - Exploring existing hardware as examples of alternative implementations

INTRODUCTION
BACKGROUND

- Despite slow start since 1985 FCC rule action a wide variety of short distance, unlicensed, spread spectrum devices have been introduced for or are in development for such applications as:
  - Wireless LANs
  - Source data collection
  - Point of sale devices
  - Transportation ID systems
  - Highway toll systems
  - Portable computers
  - Security systems
  - Access control media
  - Automatic ID tags
  - Environmental control
  - Utility remote meter reading
  - Stock exchange trader's terminals
  - Process control systems
  - Home bus communications
  - Personal communications networks
- Presently 11 manufacturers have received FCC approval for one or more of the product categories above in the 902-926MHz band
- Product development now underway in the higher frequency bands (see below)
- The appeal of reliable unlicensed communications is so great we expect the list of applications and manufacturers to grow rapidly

REVIEW FCC RULES

- FCC rule reference 47CFR15.247
  - 1st published 6/85
  - Modified 7/90
- Frequency bands

Within ISM bands and shared with other <u>licensed</u> and <u>unlicensed government</u> and <u>non-government</u> radio allocations

--902 to 928 MHz --2400 to 2483.5 MHz --5725 to 5877 MHz

- Power output of up to 1 watt and maximum 6dB gain antenna (or equivalent)
- Three modes of operation defined
  - Direct sequence
  - Frequency hop
  - Pulsed FM

REVIEW FCC RULES
FREQUENCY HOP

- Minimum number of discrete channels
  - >=50 in 902-928MHz band
  - >=75 in 2400-2483.5 and 5725-5850MHz bands
- Maximum dwell time/channel
  - <=0.4S (20S window) in 902-928MHz band
  - <=0.4S (30S window) in 2400-2483.5 and 5725-5850MHz bands
- Minimum channel spacing the larger of
  - >=25KHz or
  - The 20dB occupied bandwidth of the modulated channel
- Maximum occupied bandwidth/channel
  - <=500KHz in 902-928MHz band
  - <=1MHz in 2400-2483.5 and 5725-5850MHz bands
- Must use each channel equally on average

REVIEW FCC RULES
DIRECT SEQUENCE

- 6dB bandwidth >=500KHz
- Maximum power density limit of 8dBm/3KHz in 1 second window
- Minimum processing gain of 10dB

ELECTROMAGNETIC ENVIRONMENT
902-928MHZ BAND

- The potential sources of interference are mainly narrow band and include:
  - Licensed non-government systems
    - Part 97 Amateur radio
    - Part 90 AVM
  - Licensed government systems
    - Airborne radiolocation systems
  - Part 15 Subpart C narrowband unlicensed systems
    - Part 15.231 periodic operation (garage doors)
    - Part 15.243 material measurement systems
    - Part 15.245 field disturbance sensors (excluding intrusion)
    - Part 15.247 spread spectrum
    - Part 15.249 general use
  - Part 18.301 ISM systems, e.g:
    - Industrial heating
    - Medical diathermy
    - Industrial microwave ovens

ELECTROMAGNETIC ENVIRONMENT
PROTECTION REQUIRED

Interference Source	Equivalent Xmit Power (dBW)	Required Separation in Miles (Square Law)	Required Separation in Miles (Plane Earth)
Part 90 AVM	+30	0.5 to 13 miles	0.1 to 0.5 miles
Part 97 Amateur	+32	0.7 to 17 miles	0.1 to 0.6 miles
Government Radiolocation	?	?	?
Part 15 Periodic Operations	-43	16 feet	39 feet
Part 15 Material Measurement	+9	246' to 1.2 miles	158' to 0.1 miles
Part 15 Field Disturbance	-11	26' to 0.1 miles	49 to 246 feet
Part 15 General Use	-31	3 to 62 feet	16 to 79 feet
Part 15 Co Spread Spectrum	+/-0	89' to 0.4 miles	92' to 0.1 miles
Part 18 ISM	-68		3 to 10 feet

NOTES

1) Assumes operation of desired signal transmitter at 30 meters distance from receiver terminal

2) When range is shown above, best case assumes building penetration loss of 28dB from those signals likely to originate from outside the building (i.e: Part 90 and 97)

3) Assumes 10dB protection required between desired and interfering signal (without consideration of processing gain)

4) Assumes 17dB location variability factor to account for differential fading

ELECTROMAGNETIC ENVIRONMENT SUPPORTING CALCULATIONS

			<---Equiv---->		<---------no bldg loss--------------			
Case	Field Strength (uV/M)	FCC Meas Distance (Meters)	Power Watts	Power dBW	Square Law (Meters)	Plane Earth (Meters)	Square Law (Miles)	Plane Earth (Miles)
P90 AVM			1000	30	21238	798	13.2	.5
P97 Ham			1500	32	26738	896	16.6	.6
P15 Per	12500	3	4.687e-5	-43	5	12	0	0
P15 Mat	500000	30	7.5	9	1893	238	1.2	.1
P15 FD	500000	3	.075	-11	189	75	.1	0
P15 Gen	50000	3	.00075	-31	19	24	0	0
P15 SS			1	0	672	142	.4	.1
P18 ISM	70	30	1.47e-7	-68	0	3	0	0

AVAILABLE SYSTEMS APPLICATIONS

COMPANY	APPLICATION
Agilis	Wireless LAN
California Microwave	Wireless LAN
Gambatte	Wireless MIDI (musical instrument) Bus
Life Point Systems	Wireless Smoke Detector Bus
Metricom	Remote Utility Meter Reading
NCR	Wireless LAN
Nynex	Wireless LAN
O'Neill Communications	Wireless LAN
Proxim	Wireless LAN
Telesystems SLW	Wireless LAN

AVAILABLE SYSTEMS
REALIZATION

SYSTEM	MODULATION	DEMODULATION
A)	Direct Sequence	Homodyne
B)	Direct Sequence	Nonlinear demodulator post correlator
C)	Direct sequence	?
D)	Frequency Hop	Synchronous channel following
E)	Direct sequence	Nonlinear demodulator post correlator
F)	Direct Sequence	Nonlinear demodulator post correlator
G)	Direct Sequence	Predemodulator I.F. de-spreading using delay lock loop tracking and scan acquisition

AVAILABLE SYSTEMS
TYPICAL BLOCK DIAGRAMS
DIRECT SEQUENCE NONLINEAR

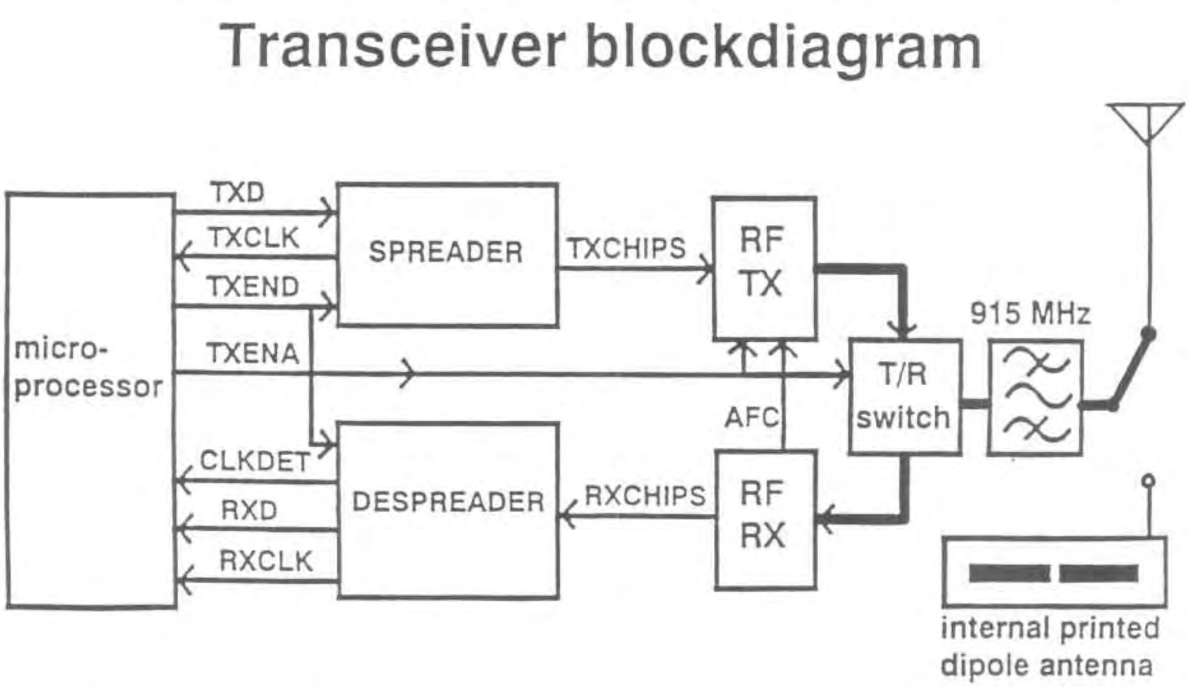

Source: FCC part 15 application system E)

AVAILABLE SYSTEMS
TYPICAL BLOCK DIAGRAMS
DIRECT SEQUENCE NONLINEAR (CONTINUED)

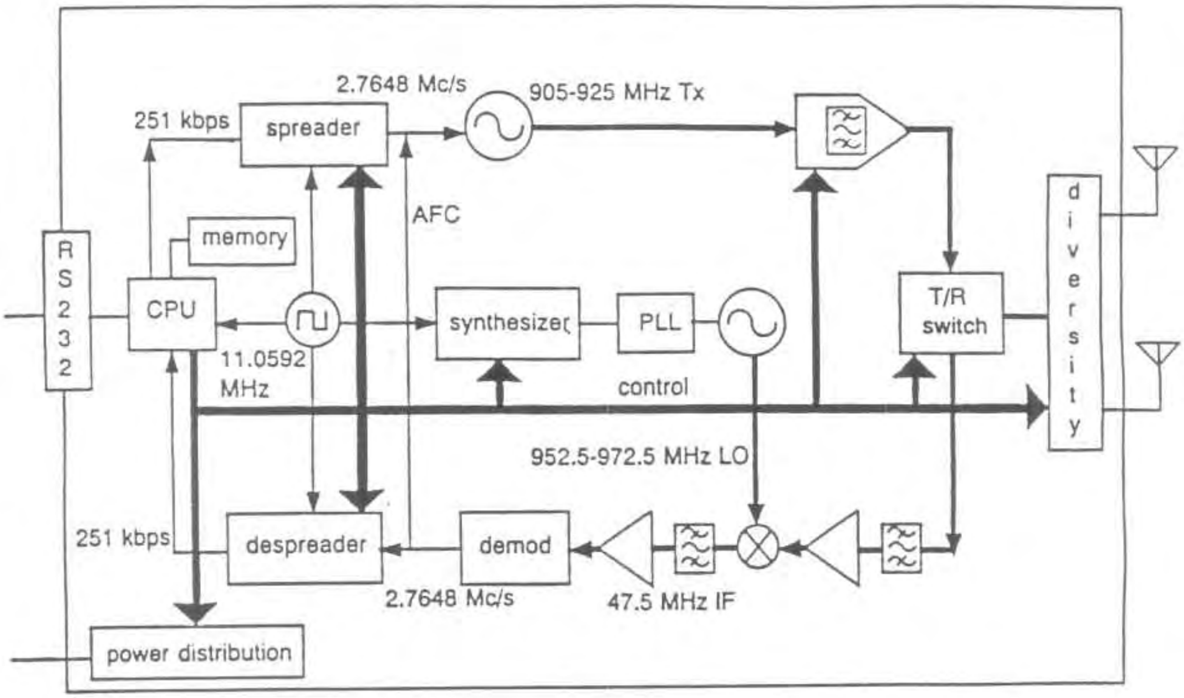

Source: FCC part 15 application system E)

AVAILABLE SYSTEMS
TYPICAL BLOCK DIAGRAMS
DIRECT SEQUENCE NONLINEAR (CONTINUED)

Direct Sequence Spread Spectrum (DSSS)

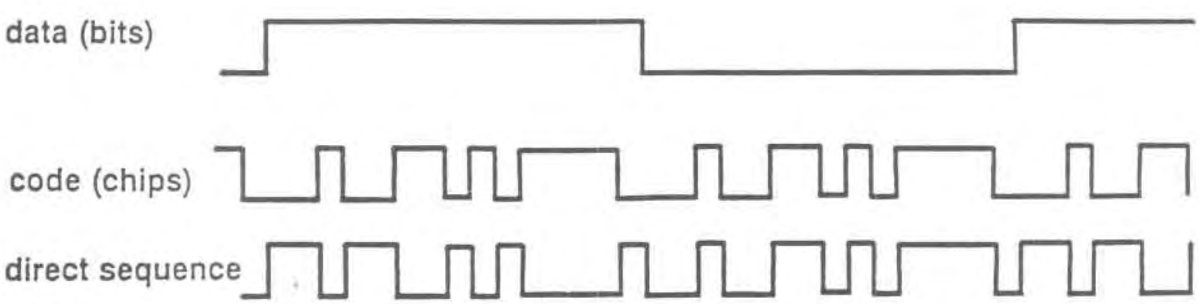

direct sequence = databits ⊕ spreading sequence

15 chips/bit = 11.8 dB spreading gain

Source: FCC part 15 application system E)

AVAILABLE SYSTEMS
TYPICAL BLOCK DIAGRAMS
DIRECT SEQUENCE NONLINEAR (CONTINUED)

Spreader blockdiagram

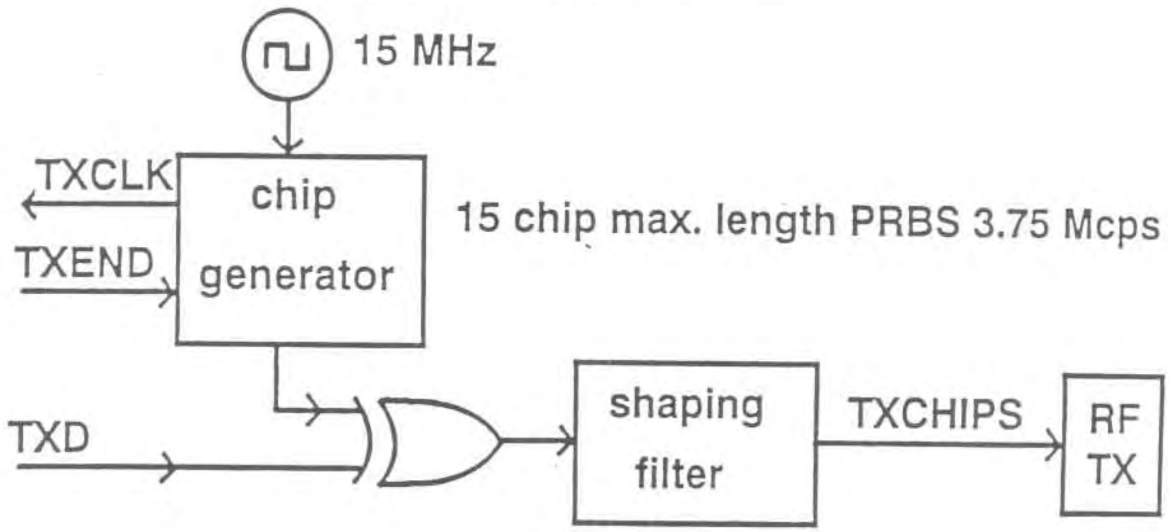

Source: FCC part 15 application system E)

AVAILABLE SYSTEMS
TYPICAL BLOCK DIAGRAMS
DIRECT SEQUENCE NONLINEAR (CONTINUED)

RF Transmitter blockdiagram

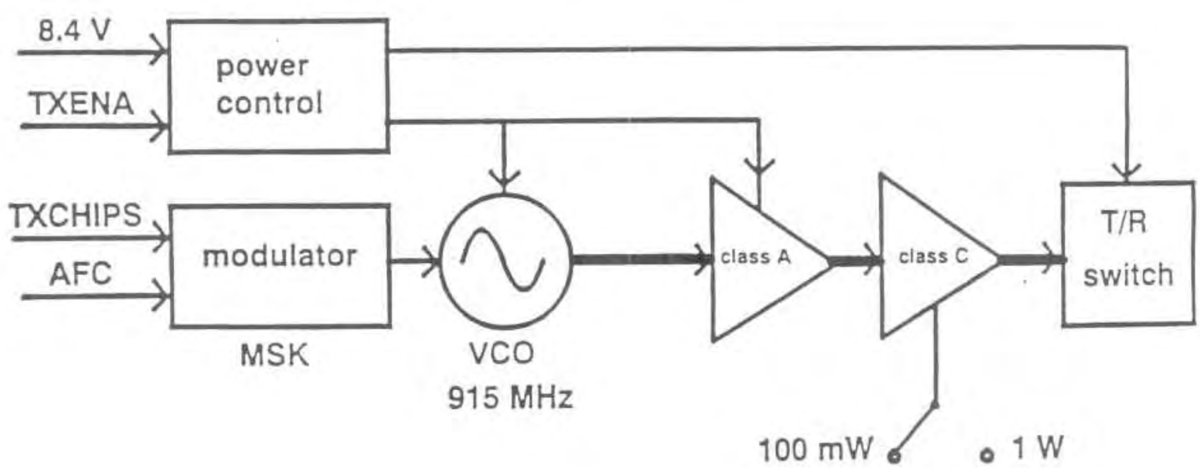

Source: FCC part 15 application system E)

AVAILABLE SYSTEMS
TYPICAL BLOCK DIAGRAMS
DIRECT SEQUENCE HOMODYNE

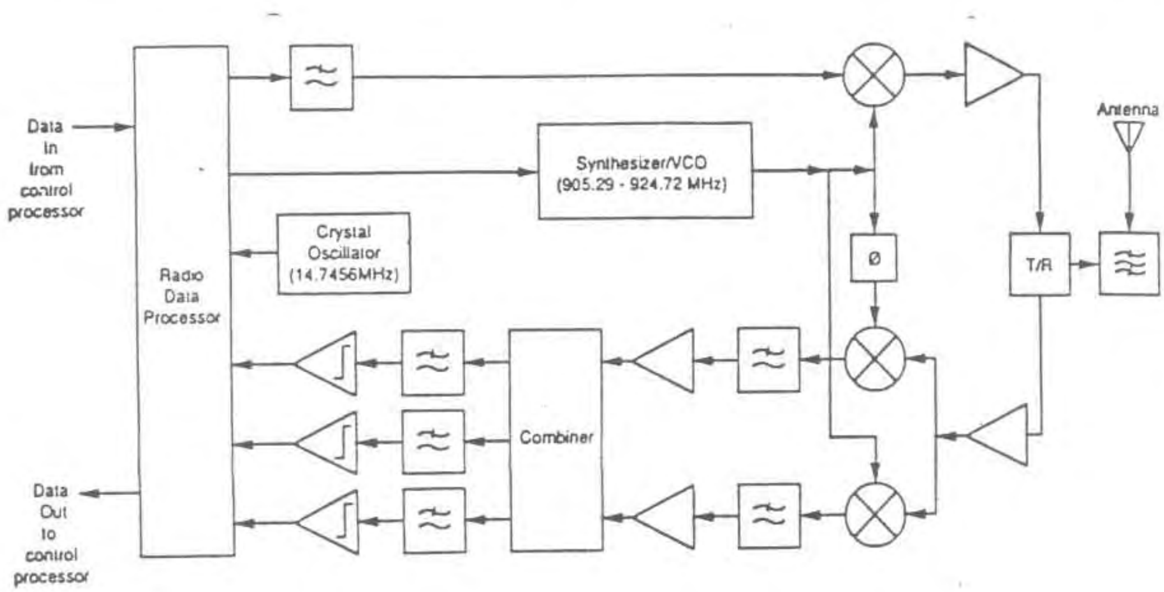

Source: FCC part 15 application system A)

AVAILABLE SYSTEMS
REVIEW

- Most products are direct sequence based transceivers for local area networks, typical operation
  - — 19.2 to 230.4 KBPS data rates
  - — PSK/MSK modulation
  - — 16 chips/bit
  - — 614.4 KChips/sec to 3.68 MChips/sec
- Most common form of direct sequence demodulation is nonlinear demodulator post correlator, other include:
  - — Homodyne linear processing
  - — Code tracking IF despread

GENERIC SYSTEM ARCHITECTURES
FREQUENCY HOP

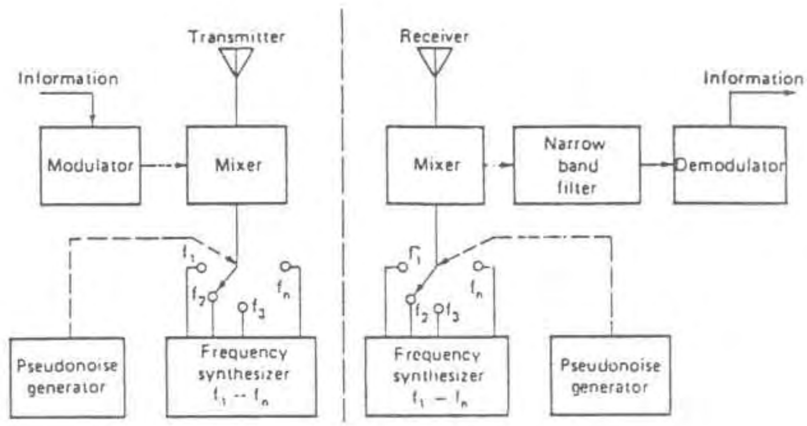

Source: Communications Receivers by Rohde and Bucher

GENERIC SYSTEM ARCHITECTURES
D.S. SYNCHRONIZATION

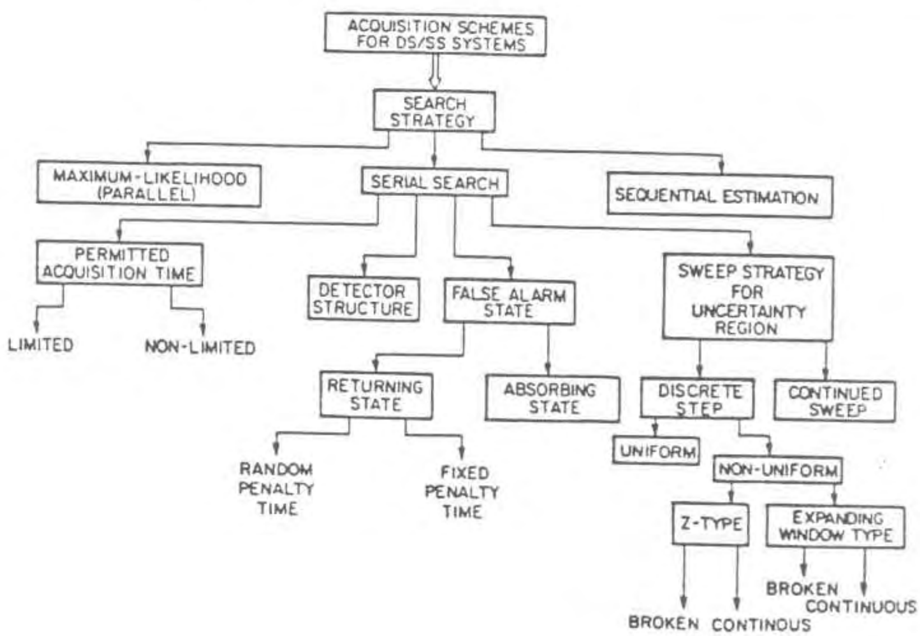

Source: Spread Spectrum Communications by M. Simon et al

GENERIC SYSTEM ARCHITECTURES NONLINEAR POST DEMOD CORRELATOR

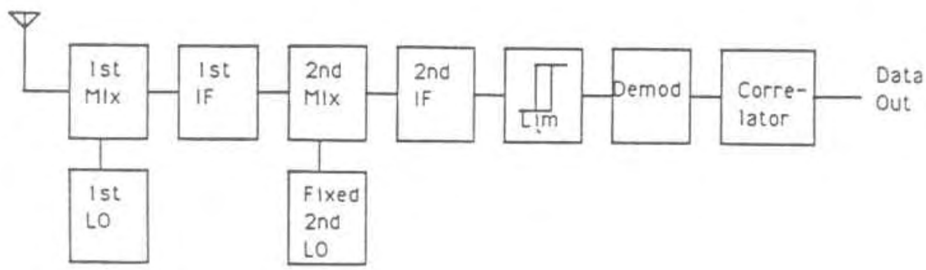

GENERIC SYSTEM ARCHITECTURES PREDEMOD IF DESPREADING

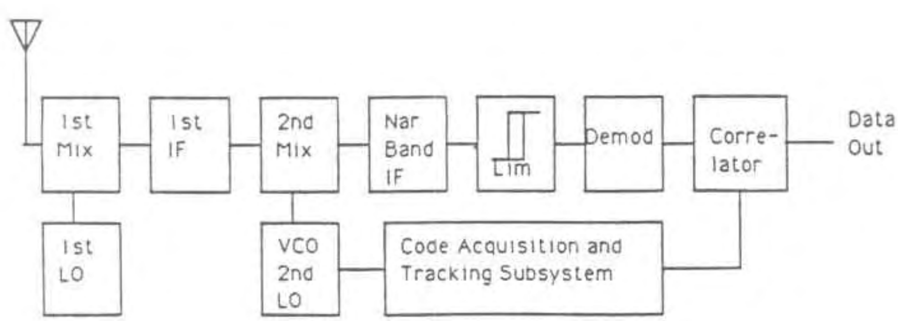

GENERIC SYSTEM ARCHITECTURES
HOMODYNE

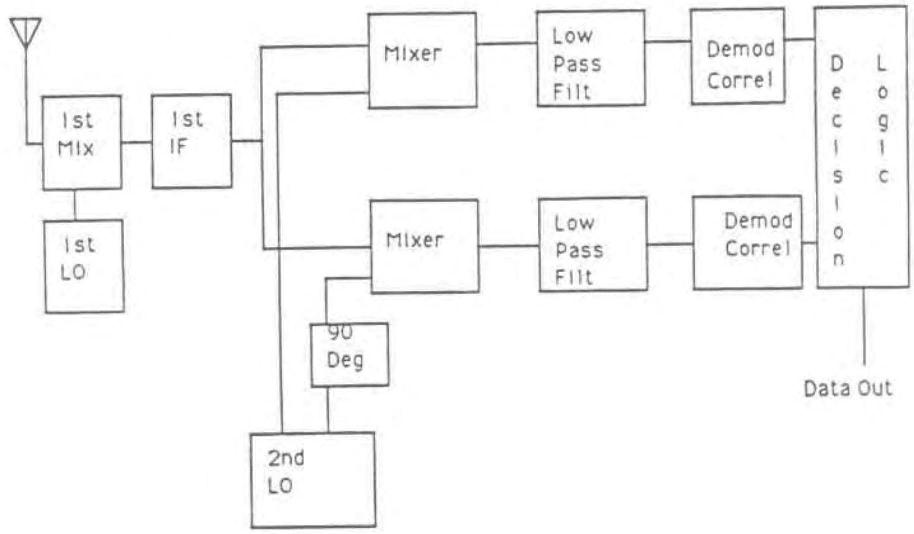

GENERIC SYSTEM ARCHITECTURES
TYPICAL DIRECT SEQUENCE RECEIVER

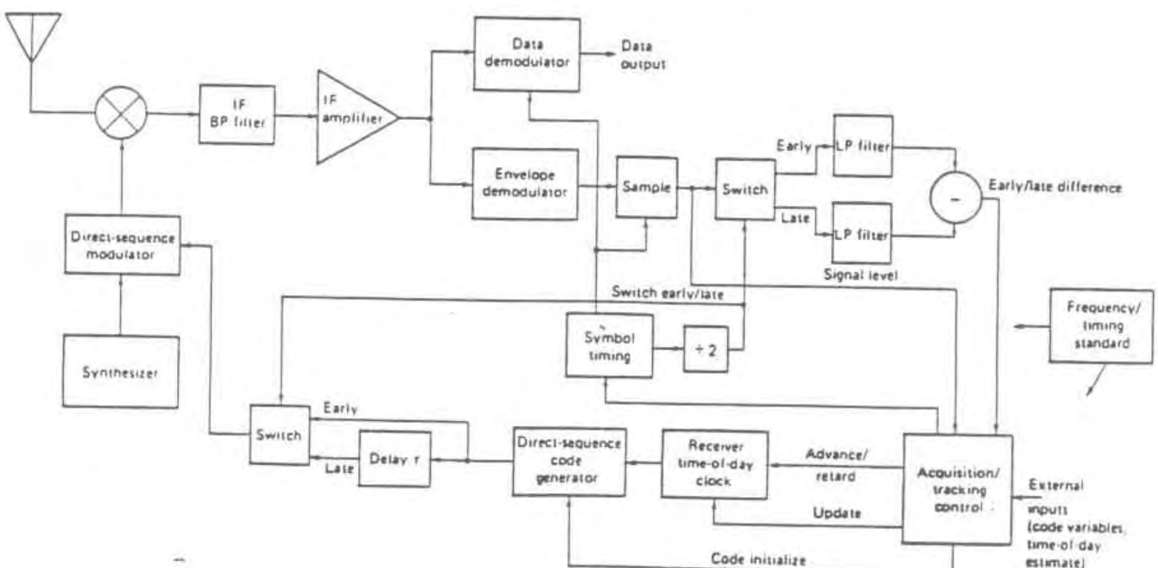

Correlation receiver with dither tracking channel for direct sequence.

Source: Communications Receivers by Rohde and Bucher

GENERIC SYSTEM ARCHITECTURES
TYPICAL FREQUENCY HOP RECEIVER

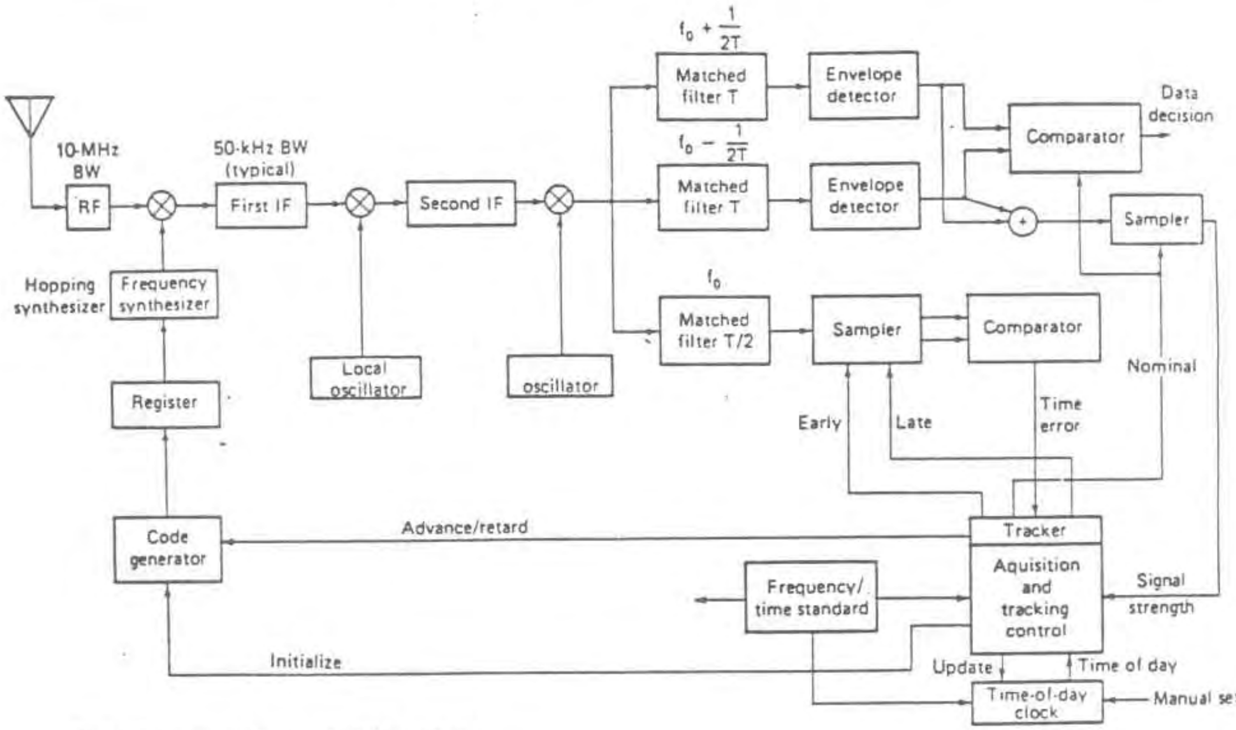

Source: Communications Receivers by Rohde and Bucher

CONCLUSIONS

- The most common system hardware realization is
  - — Direct sequence
  - — Broadband IF
  - — Nonlinear post demodulation correlation
- Such a system offers some benefits
  - – Meets FCC rules
  - – Low cost
  - – Simple, compact realization

However, the tradeoffs relative to performance in an interference environment are likely to result in marginal performance

- – External high power, narrow band licensed operations can disable communications from up to 17 miles away
- – Co-Channel and co-located (or nearby) internal spread spectrum systems can disable communications with up to 0.4 mile separation even when codes are near orthogonal

CONCLUSIONS (CONTINUED)

- Two commercially available systems employ linear processing followed by narrow band filters at the expense of hardware complexity

  – Code tracking and acquisition hardware for despreading solution
  – Multiple mixers and high stability oscillators for homodyne solution

However

  – Even in the best case, the direct sequence approach requires a broadband IF on the order of 10X a comparable frequency hop solution

- On first analysis, the direct sequence approach appears to offer many benefits but simple solutions may be unreliable

- Several approaches, including moving to higher frequencies, are available to improve direct sequence receivers to employ processing gain for added interference rejection however

  – These approaches add complexity, power drain, and physical size
  – The direct sequence receiver front end is broadband and still subject to dynamic range overload

- While the frequency hop solution is employed by only two manufacturers due to its' apparent complexity, when the burdens of designing a reliable direct sequence system are considered the frequency hop approach may offer higher performance at a comparable cost and complexity

Interference Characteristics of Microwave Ovens in Indoor Radio Communications

J. Y. C. Cheah

Hughes Network Systems
San Diego

Abstract

The scarcity of suitable radio spectrum for indoor radio communications under the regulatory constraints has prompted endeavors to investigate means of utilizing the valuable channel bandwidths available within these constraints. The interference potential of the microwave oven is characterized in an attempt to render the ISM band it occupied useful for indoor radio communications. The characterization process included an in-depth power spectral measurement of the radiation. A theoretical model of the radiation characteristics is then proposed. The interference characterization results point to a possible valuable frequency bandwidth that may be available for high speed indoor communications usage in the "low cost" consumer product arena.

1 Introduction

The advent of the regulatory rulings regarding the much relaxed power emission levels and bandwidth occupancy requirements of the 2.4 Ghz ISM band using spread spectrum technique, has spurred interest in its exploitation for indoor communications. 2.4 Ghz is also well within the implementation realm of the low-cost, high-frequency silicon technology.

The ISM band of 2400-2483.5 Mhz is designated by FCC Part 15 Subpart C, 15.247 for spread spectrum usage. The similar lower band of 902-928 Mhz is extremely congested, and narrow for regular LAN operations. The higher band of 5725-5850 Mhz is currently limited by the cost of technology for consumer products. Unfortunately, the 2.4 Ghz band supports the wide spread use of microwave ovens. As a result of the omnipotence interference potential of microwave oven spurious radiations, as well as the ubiquity of its use that coincides with the indoor communications operation domains, utilization of this band for communications and other ISM purposes has been largely ignored. Moreover, the hardware cost to operate at this frequency band was perceived as beyond what a "low cost" market place can bear only a few years ago.

It is therefore appropriate to investigate the characteristics of microwave oven radiation so that this valuable ISM band can be reclaimed for suitable communications usage.

An interference power spectrum measurement effort was expended[1] in characterizing the radiation characteristics. The measurement was conducted with various resolution bandwidths equally distributed across the interference spectrum. The measurement results present a compact interference behaviour that can be readily identified. A theoretical model was formulated to describe the observed spectral phenomenon so as to facilitate designs to accommodate this interference source in the communications channel.

2 Measurement Setup

The measurement was conducted using a Hp 8566 spectrum analyser calibrated using its internal automatic calibration procedure. A test antenna was designed to provide an overall return loss performance of better than 10 dB over the measurement frequency range. The performance of the test antenna was calibrated by a HP 8753 network analyser coupled with a Hp 85046A S parameter test set. The intent was to prevent the test antenna in exerting a significant frequency response of its own onto the test results.

Figure 1 shows the calibration results of the test antenna used.

The measurement was conducted within the near field region at the bore-sight of the oven door. The following near field assumptions were made[2]:-

- The radiation near field region of the radiation is determined by the smallest dimension D of the oven using the following relationship.

$$d \leq \frac{2D^2}{\lambda} \qquad (1)$$

$$\text{where} \begin{cases} d \text{ is the distance from the oven door.} \\ \lambda \text{ is the wavelength.} \end{cases}$$

- D represents the effective radiation antenna dimension of the oven.

- The effective radiation propagation is directed from the oven door.

The reason for conducting the measurements within the near field of the oven under test was to eliminate any possible radiation antenna effect that may be present from the oven. Precaution was also taken to select a constant load for the oven. It was determined arbitrarily that a 12 oz water load at an initial temperature of about 25 degree C was to be used. For "Max-hold" spectrum measurements, a fixed 10 second cooking time is used. The measurement time for "Zero frequency span" time domain measurement is one single sweep. The same test conditions were used to ensure the uniformity of the test environment. Several makes of ovens were tested using the measurement regime shown in Figure 2. This represents over 30 measurements per oven.

3 Measurement Results

Spectrum measurements with various resolution bandwidths and sweep times are necessary to determine the complicated interference characteristics as observed. Representative plots are shown in Figures 3a, 3b, 3c, 3d.

The following general observations were made:-

- The interference radiation emission is synchronous to the 60 Hz mains frequency and the interference energy exists only for half of the period.

- The interference power measured was approximately proportional to the measurement resolution bandwidth. This relationship held true from 30 Hz to 3 Mhz bandwidth.

- There were very rapid amplitude bursting characteristics which might have a rise time much shorter than 300 nsecs.

- There was no evidence of a detectable single frequency spectrum line during the measurement. The rapid and abrupt amplitude variation behaviour precluded this possibility.

- In the wide frequency span measurement, it could be seen that the detected signal levels in the measurement results were not exactly reduced by the same amount of the resolution bandwidth reduction. This phenomenon implied that the spectra measured was not really white. The small amount of error indicated the impulsive nature of the signal where the effective impulsive resolution bandwidth is related to the amplitude response $V(t)$ of the impulse [3]:-

$$BW_{impulse} = \frac{V_{pk}}{\int_{-\infty}^{\infty} V(t)dt} \qquad (2)$$

Figure 3a shows a representative plot of this measurement.

- A typical plot for the narrow frequency span measurement is shown in Figure 3b. The need to limit the resolution bandwidth to 1 Khz in this case is governed by the resolution bandwidth filter shape factor K and frequency span F_{span} where[4],

$$T_{sweep-time} \geq \frac{KF_{span}}{BW^2_{res}} \qquad (3)$$

- Figure 3c shows the fine grain structure of the impulse characteristics in a wide resolution bandwidth time domain measurement. An observation can be made that the interference can in fact exist for up to 8 milliseconds at any given frequency within the frequency range. The fine oscillatory power variations are most likely caused by an impulse that approaches a Delta function with respect to the filter bandwidth at 3 Mhz. The measured $|S(t)|^2$ was a result of an impulse such that,

$$S(t) = \frac{2A}{\pi(t-t_0)} \sin(\pi(f_2 - f_1)(t-t_0)) \cdot \cos(\pi(f_2+f_1)(t-t_0)) \quad (4)$$

where f_1 and f_2 are the lower and the upper frequencies of the resolution filter.

- Narrow resolution bandwidth time domain measurement shows a near perfect impulse response of the 10 Hz resolution bandwidth as shown in Figure 3d.

4 An Interference Model

From the measurement effort described above, a theoretical model of the interference signal structure is proposed as shown in Figure 4a. Since the 60 Hz component is clear, it is only of interest to investigate the time window when the interference exists. A time series for this general basic structure can be written as,

$$S(t) = \sum_{k=-(m-1)}^{m-1} \delta(t - k\Delta t) + \sum_{k=m}^{m+n-1} \left(1 - \frac{k-m+1}{n+1}\right) \cdot [\delta(t+k\Delta t) + \delta(t - k\Delta t)] \quad (5)$$

The corresponding Fourier Transform is,

$$\mathbf{S}(\omega) = \frac{\sin[(\frac{2m-1}{2})\omega\Delta t]}{\sin[\frac{\omega\Delta t}{2}]} + \sum_{k=0}^{n-1} \left(1 - \frac{k+1}{n+1}\right) \cdot [2\cos[(k+m)\omega\Delta t] \quad (6)$$

A more compact equation can be derived from Equation (6) without significantly affecting the accuracy from that of the proposed model. It can be obtained by making $n = 1$. Then, the Fourier Transform is simplified to,

$$\mathbf{S}(\omega) = \cot[\frac{\omega\Delta t}{2}] \sin[m\omega\Delta t] \quad (7)$$

There are two derivatives of this general basic model. If one takes Δt =0 at some interval between $-m$ and m, the resultant wave shape will represent most of the interference structures observed, as depicted in Figure 4b. One can also expect a break in the impulse train for a few multiple of Δts. This is shown in Figure 4c. The value of Δt was determined to be approximately 3 μsecs, and n is between 1 to 10. There is also a low frequency amplitude envelope function which is omitted. This interference structure has a carrier frequency of 2.45 Ghz.

The study of this interference model will hopefully point to a number of solutions that can result in efficient use of this band.

5 Conclusion

A detailed study of the interference characteristics of microwave ovens is presented. A theoretical representation of the interference structure is also proposed. The aim is to stimulate efforts in reclaiming this valuable spectrum resource for indoor communications use.

References

[1] J. Y. C. Cheah, "IEEE 802.4L submission on microwave oven interference measurement", *IEEE p802.4L/90-08a.*, Feb. 1990.

[2] J. Appel-Hansen, "Seminar on Electromagnetic antenna and scattering measurements", Part I, *CSIRO Division of Applied Physics, National Measurement Laboratory, Australia*, Nov., 1982.

[3] F. Ball, "Measure the real impulse bandwidth", *Microwaves & RF*, Jan. 1987, pp.93-96.

[4] New England Microwave Corp, "Power spectral analysed in PIN-diode switching transients", Application Note, *MSN*, Dec. 1986, pp. 101-105.

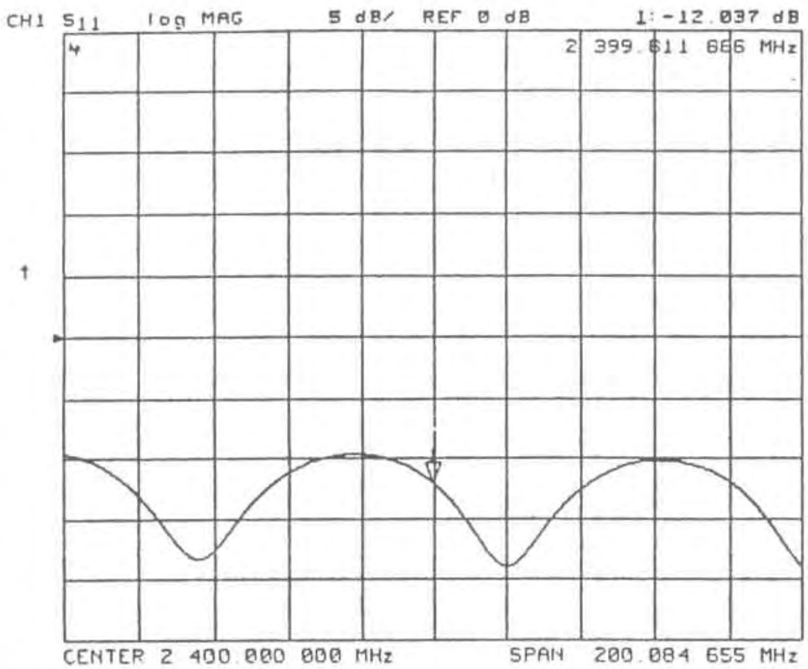

Figure 1: The frequency response of the specially designed antenna in terms of return loss.

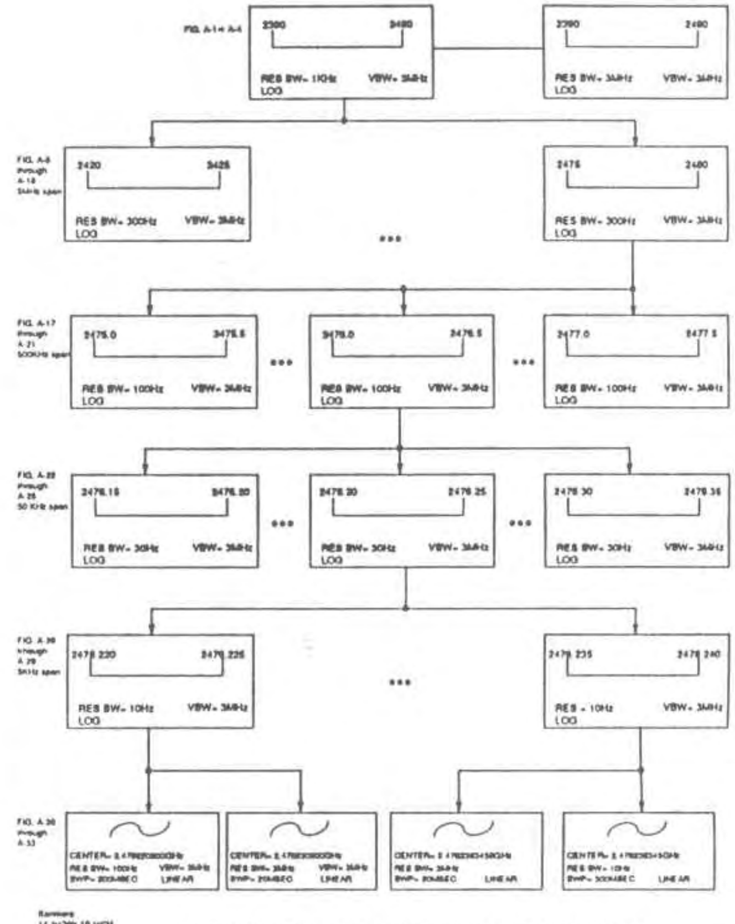

Figure 2: The spectrum measurement regime over the measurement frequency range.

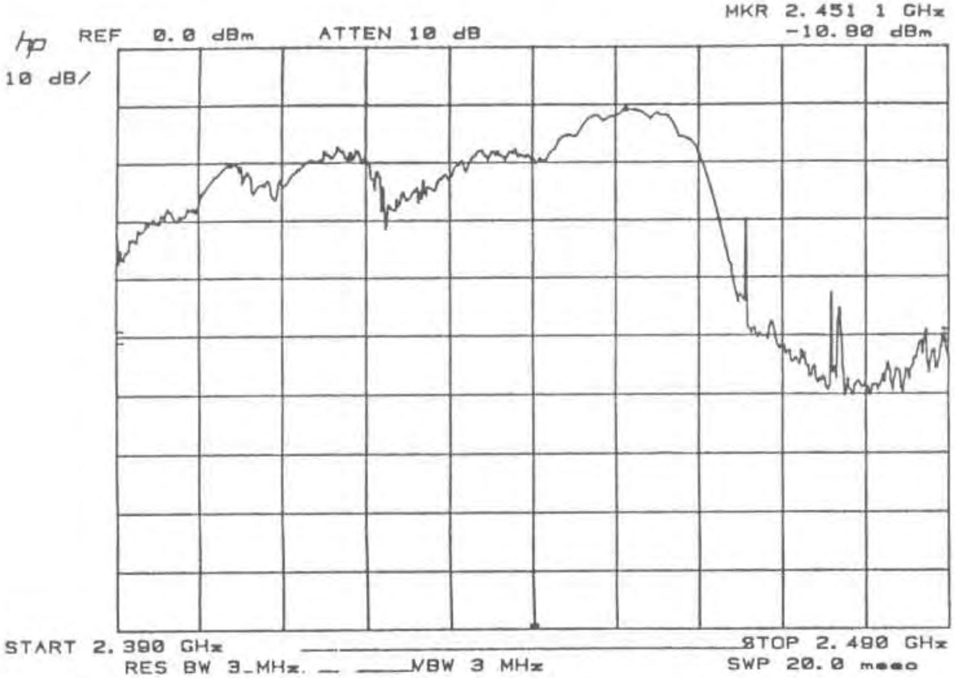

Figure 3a: A representative plot for the wide frequency span measurement.

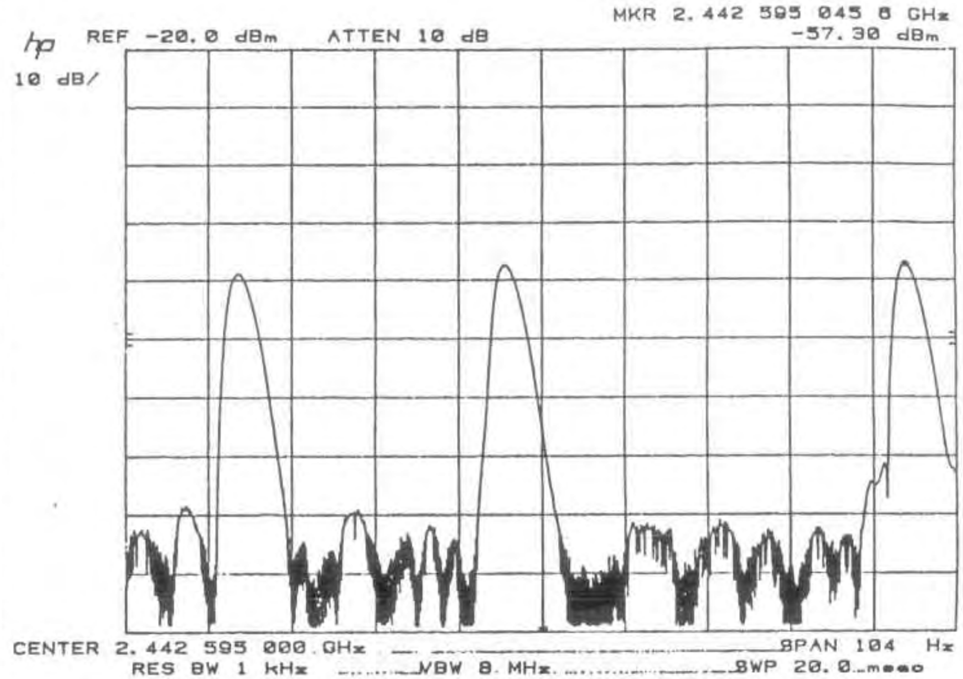

Figure 3b: A representative plot for the narrow frequency span measurement.

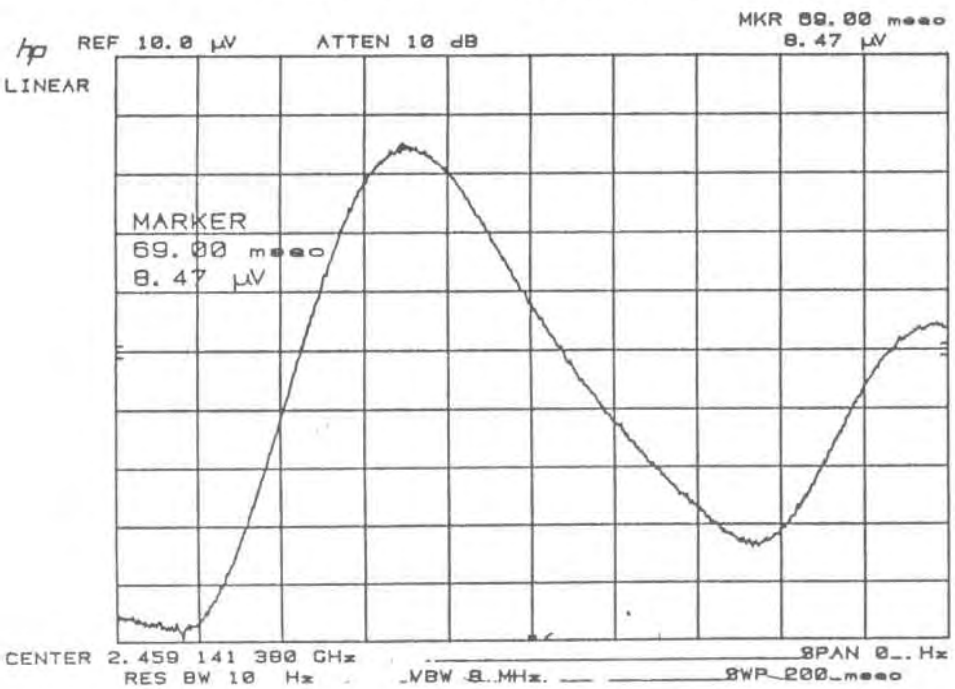

Figure 3d: A representative plot for the narrow resolution bandwidth time domain measurement.

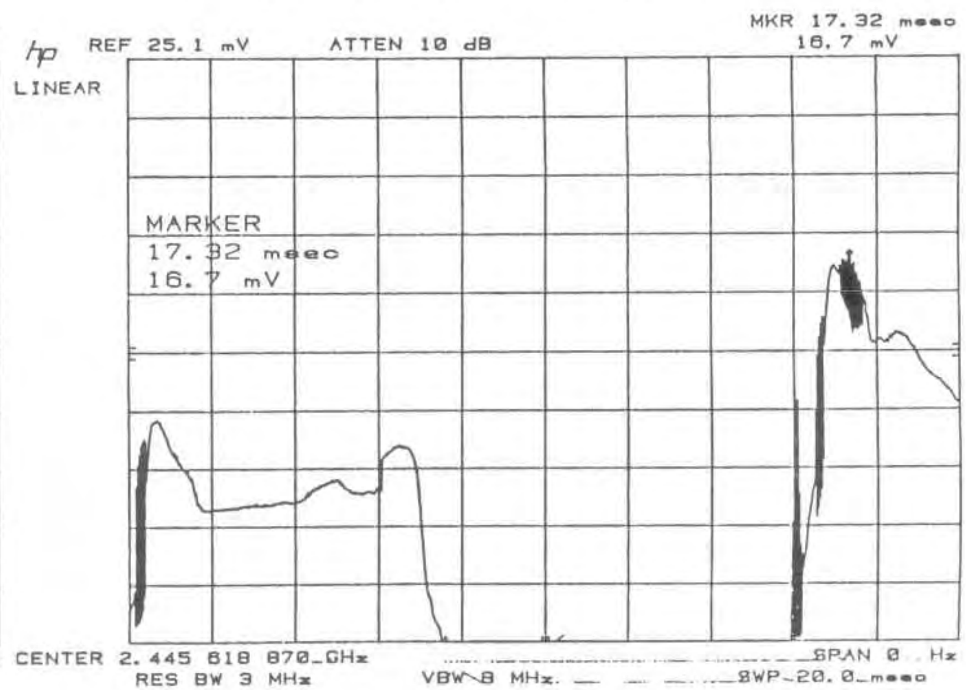

Figure 3c: A representative plot for the wide resolution bandwidth time domain measurement.

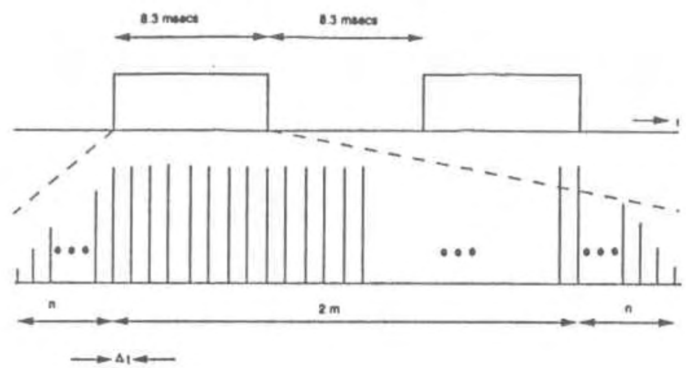

Figure 4a : The general microwave oven interference model.

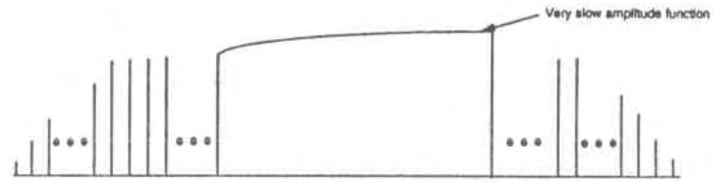

Figure 4b: The pulse interval collapses to form a contiguous radiation pattern.

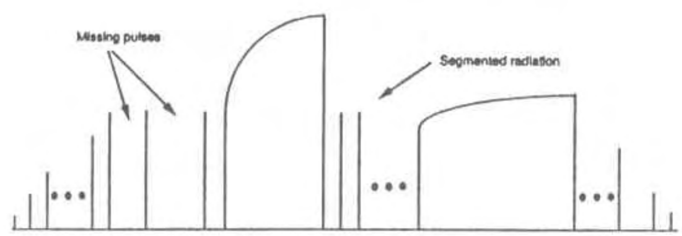

Figure 4c: The pulse train may have missing pulses, and the contiguous radiation patterns may also be segmented.

Standards and Regulatory Aspects of Wireless Local Communications

Stephen A. Wilkus
AT&T Bell Laboratories
N. Andover, Ma.

Abstract: Over 7 different international standards bodies are developing various wireless standards. Hearings and rulemaking proceedings are taking place in the regulatory agencies in many of the industrialized nations. This paper presents an overview of the wireless standards and regulatory arenas, and attempts to clarify some of the distinctions among the emerging standards.

The international, European, and U.S. standards and regulatory organizations will be reviewed with an emphasis on how wireless LAN standards will evolve. Additionally, particular details of the Digital European Cordless Telecommunications (DECT) system, CT2, CT2+, and the emerging work of Bellcore (Universal Digital Portable Communications System) will be compared and contrasted.

1. Introduction

In the past two years the Federal Communications Commission (FCC) has received over 50 applications for experimental licenses for Personal Communication Service (PCS) trials, as well as related petitions for rulemaking (Table 1). The Canadian Department of Communications has authorized 11 similar trials. The European Commission (EC) and the UK have gone further and allocated frequencies on a primary basis to specific wireless systems. The European Council of Ministers and other European nations have signed a memorandum of understanding setting aside the band 1880 to 1900 MHz on a primary basis for DECT[1], 864-868 MHz for CT2, and 890-915 MHz and 935-960 MHz for GSM (1800-1860 for the UK's implementation of GSM).

Standards, as well as regulatory groups, are actively involved in shaping the emerging wireless systems. The international CCIR, the American ANSI, TIA, T1, Europe's ETSI, and the IEEE all have significant efforts underway to set various wireless standards.

Needless to say, there is a comparably diverse array of organizations that are intending to provide some order to the chaotic wireless efforts. Principle among these, is the international CCIR (Comité Consultatif International des Radiocommunications) and the ITU (International Telecommunication Union) to which it reports. Figure 1 highlights the relevant standards and rulemaking bodies involved in wireless issues. Section 2 of this paper describes these standards bodies, their interrelationships, and their wireless efforts. Section 3 discusses the regulatory organizations and their activities. Section 4 explains the nature of some of the principle emerging standards, particularly CT2, DECT, and Bellcore's UDPCS.

2. Standards Organizations

There have been many sobering stories of well engineered products produced at good prices with willing customers that have failed because of the lack of a standard. Anyone with a Beta videotape recorder can appreciate the importance of standards. These standards efforts provide vendors with larger, less fragmented markets, the service providers with more common equipment, and the end-users benefit from a competitive marketplace. One price we pay for standards, it seems, is to be inundated with acronyms.

In some technical efforts, regulatory bodies also determine the standards to be used, particularly for the broadcast standards. For example, the U.S. HDTV standard is to be chosen by the FCC. However, the current trend in the U.S. appears to be for the regulatory bodies, and the FCC in particular, to allocate frequencies and to set interference controls but to leave the specific standards up to industry forums. For example, the FCC has allowed the cellular operators to provide service without using the analog AMPS standard.[2] Consequently, it is reasonable to consider the regulatory and standards bodies separately. This section presents an overview of the standards organizations that are active in developing wireless standards at the international level as well as in Europe and United States.

Figure 1 - Wireless Standards and Regulatory Bodies

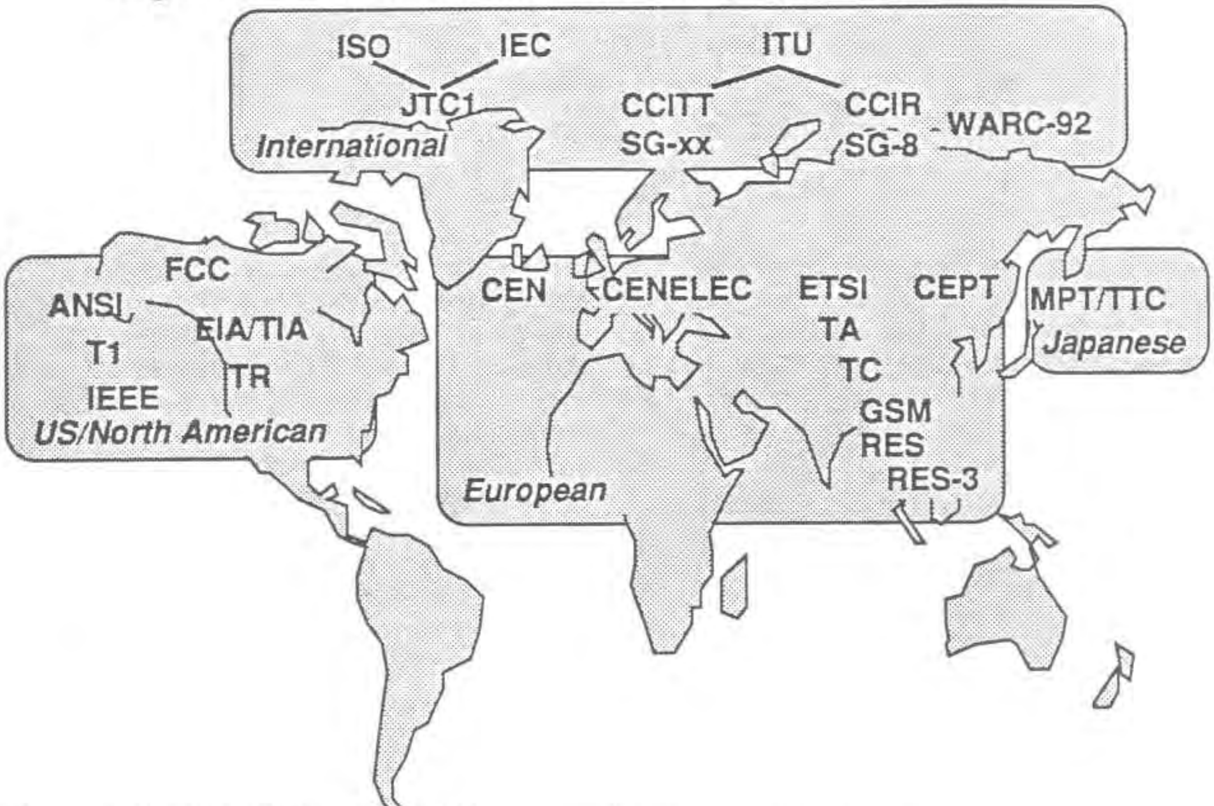

ANSI	American National Standards Institute
CCIR	Comité Consultatif International des Radiocommunications
CCITT	Comité Consultatif International Télégraphique et Téléphonique
CEN	Comité Européen de Normalisatoin
CENELEC	Comité Européen de Normalisation Electrotechnique
DECT	Digital European Cordless Telecommunications
EIA	Electronics Industry Association
ETSI	European Telecommunications Standards Institute
GSM	Global System Mobile (Groupe Spécial Mobile)
IEC	International Electrotechnical Commission
IEEE	Institute of Electrical and Electronic Engineers
ISO	International Organization for Standardization
ITU	International Telecommunication Union
JSA	Japanese Standards Association
JTC1	Joint Technical Committee
NTIA	National Telecommunications & Information Adm.
RES3	Radio Equipment and Systems, sub-group 3
T1	Standards Committee T1 – Telecommunications
TA/TC	Technical Assembly/ Technical Committee
UDPCS	Universal Digital Portable Communications System
WARC	World Administrative Radio Conference

2.1. International

ISO / IEC

The International Organization for Standardization (ISO), founded in 1946, and the International Electrotechnical Commission (IEC) have had an important role in adopting several of the IEEE 802 standards on an international basis. The IEEE 802.2, .3, and .4 standards have been adopted as ISO/IEC 8802.2, .3, and .4 international standards. An IEEE 802.11 wireless LAN standard is also likely to come before ISO/IEC for adoption. Typically, ISO has been active in computer and information technology standards but has not been active in radio issues. It remains to be seen how a Wireless LAN standard will be treated by ISO.

The scope of the IEC is the development of international standards for electrotechnology while the ISO's includes everything *not* covered by the IEC. In recognition of the technical overlap that takes place in the Information Technology field, these two organizations formed a Joint Technical Committee, JTC1. Interestingly, the American ANSI is the world secretariat for JTC1, but the administrative work for the technical advisory groups within each member nation is spread throughout several organizations, including the IEEE. Consequently, the development of an IEEE 802.11 Wireless LAN standard will ultimately pass through the TJC1 approval process.[3]

2.2. United States Standards Bodies

In the United States, the American National Standards Institute (ANSI) serves to coordinate and accredit many of the U.S. standards organizations. It does not write standards but reviews the procedures by which accredited committees produce standards, and represents these standards development organizations in the international bodies such as ISO. It gets most of its funding from private companies and member standards bodies. The relevant standards bodies working on wireless under the ANSI umbrella are the IEEE, EIA, and the Standards Committee T1. "T1" is composed predominantly of Common Carriers and Local Exchange Carriers and is sponsored by the Exchange Carriers Standards Association. However, T1 is an open forum with organizational membership. The Committee T1 consists of technical subcommittees T1E1 concerned with Network interfaces; T1M1 Maintenance; T1Q1 Performance; T1S1 Services Architecture, Signalling, ISDN Access, and SS7; T1Y1 Speech Coding, and T1X1 for network to network interfaces. Several of these subcommittees have an interest in wireless access.

In mid 1990 COMSAT proposed to T1E1 the creation of a new project concerning mobile to PSTN interfaces. The T1 Administrative Group, recognizing the complexity and scope of the project formed T1P1 to coordinate and oversee the standardization of Universal Personal Communications (UPT) and wireless access in particular. It met for the first time in December 1990 and has just recently established its own structure *vis*.:

- T1P1.1 program management and standards planning
- T1P1.2 system engineering for wireless access and terminal mobility
- T1P1.3 systems engineering for Personal Communications Service (PCS) and network aspects

In addition to coordinating the standardization process, the mission and scope of T1P1 includes defining the interface specifications for wireless access to the public telephone and data networks, including the PSTN and ISDN. Currently, T1P1 has established liaisons with CCIR US Task Group 8/1, TIA, and IEEE 802.11.

IEEE

Although strictly international in membership, the IEEE standards activities have been predominantly driven by and viewed as a U.S. organization, hence it is accredited by ANSI. In the case of the IEEE 802.11 wireless LAN working group, the chair and a substantial part of the membership are from outside the US but it has only filed comments with the US FCC and no other nation's regulators. It has a liaison with T1P1, and with ETSI/RES-3.

This group has set for itself the task of defining a common air interface for wireless LANs operating in the 1 to 50 Mbit/s range with the possibility of several distinct physical layer definitions running at different data rates. A major decision for this group is the question of voice/data versus data-only support, following the 802.9 standards work on a voice/data LAN. Data-only supporters are concerned that the standard not be overburdened with voice capabilities, while others see a need for voice-like isochronous data for control automation applications, as well as interactive voice applications.

EIA/TIA

The Electronic Industries Association (EIA) working together with the Telecommunications Industry Association (TIA) has been the principle organization responsible for American cellular telephone standards. This has included the AMPS (IS-3) standard as well as the new Dual-Mode (IS-54) digital system. Active groups within EIA/TIA working on Technical Requirements (TRs) include: TR-8 for Land Mobile Service, TR-45.1 continuing work on Analog Terminal Interface Standards (AMPS), TR 45.2 Inter-system standards (Mobile Application Part, MAP), and TR 45.3 Subcommittee on Digital Cellular Systems.

In 1987 the Electronics Industries Association (EIA) filed a petition for rule making seeking a permanent allocation for cordless telephones in the 800/900 MHz band. Finding that an allocation in that portion of the spectrum for cordless telephones was not justified, the Commission denied EIA's proposal on November 19, 1989[4], and made the 46/49 MHz allocation permanent.

2.3. Europe

CEN / Cenelec

About 20 years ago, while "Europe-92" was a wistful dream, separate European national standards organizations recognized the need for a European standards body to parallel the international standards bodies. The European Committee for Standardization (CEN) was formed for non-electrical products and parallels the ISO, while the

European Committee for Electrotechnical Standardization (Cenelec) complements the IEC. The national standards bodies that comprise CEN and Cenelec - from the 12 European Commission (EC) countries as well as six European Free Trade Association (EFTA) countries - are obligated to adopt the CEN/Cenelec standards. CEN and Cenelec like CEPT, the Conference of European Posts and Telecommunications Administrations, have apparently not been an efficient body for responding to the rapid changes in telecommunications. The European Commission has taken a firmer role in creating a stronger set of European standards bodies such as ETSI.

ETSI

Because of difficulties with network operators, Cenelec had been unable to make much headway in the area of telecommunications standards, which the twelve member nations recognized would be crucial to the success of a single market. Consequently, the EC established the European Telecommunications Standards Institute (ETSI) in 1988 to complement the CCITT, the international group that develops telecommunications standards.

ETSI is comprised of organizational members (as opposed to individual membership as in IEEE) with a significant membership fee required. Its membership is limited to European based organizations and European operations of multinational corporations. It currently consists of approximately 94 manufacturers, 43 administrations, 18 user organizations, 2 private service operators, and 3 research bodies from the 12 EC countries, the six EFTA countries, and Cyprus, Malta, and Turkey.[5] There are also more than 20 officially accredited observers, including the U.S. State Department and the Japanese Trade Association.

Since its formation by the EC in 1988, this organization has been extraordinarily active and has been responsible for adopting the United Kingdom's specification for CT2[6,7], the Global System Mobile (GSM) specifications[8], the Digital European Cordless Telecommunications system (DECT)[9], as well as the European Radio Messaging System (ERMES) for pan-European paging. ETSI is also considering a common dedicated mobile data air interface standard.[10]

The Global System Mobile (GSM), was previously established by the CEPT but moved to ETSI. It is a broadranging pan-European digital cellular system which specifies everything from the handset keyboard interface to the signalling between switching centers. It parallels the TR45 cellular radiotelephone group in TIA.

The RES-3 sub technical committee has recently adopted the CT2 specification[11], and also has responsibility for the DECT standard. This sub technical committee is composed of about 56 participating organizations and is supported by paid staff (PT-10) that has at least 50 staff months allocated in 1991. This effort is expected to yield a 900 page specification for DECT by early 1992.

A new group, NA7, has been formed on Universal Personal Telecommunications (UPT) to lay out a work program in Spring of 1991.

Japan's TTC and JSA

In mid 1989, the Japanese Ministry of Posts and Telecommunications (MPT) completed specification of a digital mobile telephone system and submitted it to the Telecommunication Technology Council (TTC). In order to reduce friction with the U.S., this development included sharing specifications with a U.S. trade delegation. The Radio System Development Center, set up by electronic equipment makers and other, helped develop this system that is designed to work well in outdoor environments. This system is planned for commercial introduction by the spring of 1992.

The Japanese Standards Association (JSA) is also reportedly active in developing and promoting both a Universal Digital Cellular (UDC) system standard and an Advanced Cordless (DECT-like) system.

3. Regulatory Activities

3.1. ITU (International Telecommunication Union)

Dating back to 1865 (as the International Telegraph Union), the ITU is currently an agency of the United Nations. The ITU has divided the world into three geographic regions where localization of the rules apply (Europe in region 1, the U.S. in 2, Asian in 3). The increased mobility of radio units integrated with laptop computers and pocket phones may present new challenges to this regional approach to allocations.

The organization of the ITU includes: (1) the Plenipotentiary Conference, which is the supreme organ of the ITU and meets approximately every five years; (2) two World Administrative Conferences, one for telegraph and telephone and one for radio (WARC) which meets as needed, (3) the Administrative Council, which meets annually and is responsible for executing decisions of the Plenipotentiary Conference; (4) the General Secretariat, responsible for administrative and financial services; (5) the International Frequency Registration Board, concerned with the assignment of radio frequencies; (6) the International Telegraph and Telephone Consultative Committee (CCITT); and (7) the International Radio Consultative Committee (CCIR), which conducts technical studies in the radio field.[12]

A recent ITU Plenipotentiary Conference (Nice, 1989) resolved that a World Administrative Radio Conference (WARC) shall take place in the first quarter of 1992 for dealing with frequency allocations in certain parts of the spectrum, particularly the mobile radio allocations and the Future Public Land Mobile Telecommunications Systems (FPLMTS). This "WARC-92" conference is scheduled for Feb. 3 - March 5, 1992 in Malaga, Spain. Such general WARCs are rare, with the last one held in 1979. So far the FCC has issued three notices of inquiry concerning agenda items for this conference, and the state department has held formal discussions with other national regulators to coordinate WARC contributions.

This conference should produce a draft watershed treaty calling for the allocation of spectrum for FPLMTS as well as other blocks of spectrum for Low Earth Orbit Mobile Satellite Services and high definition TV satellite broadcast. It generally takes several years for the signatory nations to ratify the treaty and to implement the revised Radio Rules through national rulemaking procedures.

CCIR (International Radio Consultative Committee)

CCIR Study Group 8 studies technical and operating aspects relating to all the mobile services, radiolocation, amateur, and their satellite services. In 1985 CCIR Study Group 8 formed a special international group to identify the requirements for FPLMTS. This Interim Working Party IWP8/13 is composed of approximately 40 administrations and international organizations. At the CCIR Plenary in May 1990, CCIR Study Group 8 was reorganized and IWP8/13 was renamed as Task Group TG8/1.[13,14]

This group, in preparing a thorough analysis of FPLMTS, has estimated the total spectral requirements for universal services, both for private intra-premises and public outdoor application, at 230 MHz, with 60 MHz for the exclusive use of low power personal communications services. This estimate was based upon an exclusive allocation with no sharing with alternative service providers. Such sharing would inevitably increase the spectral requirements of such a system. Recently, a new Question (AM/8) was adopted by TG 8/1 to initiate studies concerning radio local area networks.

CCITT (International Telegraph and Telephone Consultative Committee)

CCITT Study Group XVIII has developed a baseline document concerning Universal Personal Telecommunications (UPT). This document recommends that specific Study Groups develop recommendations that will facilitate mobile services. In the past they have been active in such areas as numbering plans, location registration in ISDN networks and system signalling 7 (SS7) protocols, X.400 email, and X.25 type packet-switched network standards that will likely be used for such things as visitor location registrations and authorization.

These Study Groups have the following charters: SG I: Service Definition; SG II: Network Operations; SG III: Charging and Accounting Principles; SG IV: Maintenance; SG VIII: Terminals; SG XI: Signaling architecture, MSAP (Mobility Services Application Part), SS7; SG XV: Transmission; and SG XVIII: ISDN, network architecture.

For privately owned, local area networks, the CCITT will likely not have a significant role in the standardization of the network hardware. Rather the CCITT will address the logical level of the data content, i.e. the X.400 email standards and the packet formatting of X.25, and ISDN.

3.2. U.S. Regulatory Activities

In the United States, the Congress, the FCC and the Department of Commerce's National Telecommunications and Information Administration (NTIA) are actively involved in wireless rulemaking. House Resolution 531 (the so-called "Dingell Bill" from Rep. John Dingell, D-Mich.), and Senate Bill 218, "Emerging Telecommunications Act of 1990" both call for the Department of Commerce and the FCC to reallocated from government use to commercial use a minimum of 200 MHz located below 5 GHz. The bills call for identifying the spectrum within 2 years and making it available for commercial use in two stages, the first within 4 years of the enactment of the bill. The second part of the reallocation is to take not less than 10 years to allocate - as a reserve. In the 1990 congressional session, the bill pass the House but failed in the Senate.

The FCC, too, has been active in issuing Notices of Inquiries (NOIs) concerning PCS and the WARC convention, and dealing with various petitions for specific allocations, as shown in Table 1. The commission received over 100 comments to its PCS NOI, many recommending reallocation of the 1,880 - 1,990 MHz band for PCS. PCN America, Inc. has petitioned the FCC to allocate frequencies in the 1,700-2,300 MHz range. The FCC expressed that, "it is anticipated that the 1992 WARC will consider allocating spectrum in the 1700 MHz to 2300 MHz band for PCNs in Region 1 and possibly will address a similar allocation for the other Regions as well. The 1992 WARC may even consider providing a worldwide allocation for PCSs in this portion of the spectrum."[15] In preparing for WARC-92, the Commission has indicated that it does not feel that a common world-wide allocation is needed but that some compatibility (perhaps by having nearby bands) would be desirable. Industry comments have been mixed on this issue. Apple Computer Inc. has specifically requested an international allocation for "Data-PCS".[16] Currently, the 1880 MHz to 1990 MHz band is licensed to more than 8,100 non-government fixed service users, particularly point-to-point microwave users such as railroads, power, petroleum, and common carriers. Some of these users are converting these facilities over to fiber optic cables — contributing to making this an attractive band to request allocations in.

Of equal interest, Janice Obuchowski, Assistant Secretary for Communications and Information for the Department of Commerce, and Administrator of the National Telecommunications and Information Administration (NTIA), advocates market-based spectrum allocation.[17] This refers to an alternative to lottery and comparative hearings as a way to select licensees, perhaps even as a way to allocate the services associated with a frequency band. Under this scheme, a license would confer some property rights that could be bought and sold. As described, this scheme is not currently provided for in law (currently, radio licenses may not be sold even though a company that holds a license may, subject to FCC authorization.) Even so, the current Federal budget includes a line item for income from the auctioning of spectrum. The original version of the "Emerging Telecommunications Act of 1989" specifically forbade the auctioning of spectrum but the current drafts do not. A recent NTIA report[18] recommends the adoption of these auctions as a way for the federal government to sell spectrum and let the marketplace place a value on the real worth of a band. It could also provide an incentive for various Federal agencies to release spectrum for private use. The NTIA has estimated that the aggregate spectrum value to cellular license holders is between $46B and $80B.[17]

4. Specific Standards

CT2

The U.K. has been most aggressive in introducing new wireless systems – typically without waiting for international standardization. CT2 (cordless telephone–second generation) is one such British initiative, launched commercially in September 1989 – a full year before standardization by ETSI. A conflict arose within ETSI in 1990 over whether CT2 was to be made an interim standard or skipped entirely in lieu of the forthcoming DECT standard. The issue had to be elevated to the ETSI Technical Assembly for a decision where it was decided to make CT2 an interim standard.

This cordless phone standard is the most developed of the emerging digital phone systems. Currently there are several British manufacturers that produce "CT2" phones and full compliance with the Common Air Interface that insures inter-operability is scheduled for later this year.

As indicated in Table 2, the distinctive feature of CT2 is that there is only one voice channel per RF carrier. Time Division Duplexing (TDD) is used to "ping-pong" between transmit and receive so that a base station with antenna diversity can infer the mobile unit's received signal strength over the reciprocal channel. The TDD then helps reduce the cost and complexity of the mobile unit. However, by allocating a single voice server to the radio channel (no TDMA) there is no provision for bandwidth on demand or variable data rate applications. Also, as improvements are made to voice coders this CT2 system will have difficulty taking advantage of them. No more or less than 32 kbits/s are supported. Moderate-speed voiceband modems can work over CT2's ADPCM codec but a 32 kbits/s pure digital channel could be supported if the A/D D/A converters and codec are bypassed

CT2+

In recent comments to the FCC[19], Northern Telecom Inc. proposed a Personal Communications Interface (PCI), commonly known as CT2+, that enhances the CT2 system. The enhancements to CT2 include additional frequency channels in the 930-931 and 902-928 MHz (ISM band) ranges, as well as the 900-959.95 MHz band where sharing agreements with fixed services permit. The enhancements also include a more efficient control channel scheme that is more appropriate given the increase in the number of channels, support for handoffs, and registration for two way calling in a visited location.

With these enhancements, CT2+ becomes a impressive wireless system that has the virtues of simplicity and availability while still providing many of the same functions of the more advanced TDMA systems. It is doubtful that ETSI will reconsider CT2 specifications but the T1P1 organization may consider aspects of CT2+ for application in the U.S.

It is worth noting that the proposal allows for frequency sharing with fixed microwave services — if there are no fixed service license holders nearby to interfere with, then a CT2+ base station could be configured to use that additional spectrum in that particular territory. This should be attractive to the FCC given their interest in reuse of spectrum.

DECT

The Digital European Cordless Telecommunications (DECT) standard is nearing completion by ETSI's RES-3 Technical Committee with full approval expected late this year. This highly advanced system was initiated by Ericsson as a basis for wireless PBX, with the support and sponsorship of governments of Scandinavia (not members of the EC but members of ETSI). The EC has consistently supported the notion that Universal Personal Communication be realized through the harmonious interworking of DECT, GSM, and ERMES.

Technically, DECT is an aggressive system that multiplexes 12 voice channels (32 kbits/s, ADPCM) onto 11 frequency carriers thus providing 132 possible servers, enough for a dense office environment. In order to simplify the handset, TDD is used with the consequence that the radio channel raw data rate is an uncomfortably high 1152 kbits/s. Given multipath delay spreads in an outdoor or spacious indoor environment, this high data rate may require equalization to work well. Alternatively, antenna diversity, frequency diversity, and port diversity may compensate for the multipath fading concerns. Only field experience will tell. DECT uses dynamic channel allocation so that base stations determine what frequencies to operate on dynamically as load and adjacent base stations permit.

In order to gain field experience, Ericsson has developed a "pre-DECT" product, DCT-900, with 8 time slots operating in the 860-870 and 940-944 MHz bands. Unlike the CT2 system, DECT supports variable data rates for wireless LAN applications including BRI ISDN as well as 32 kbits/s through 736 kbits/s (23 of the 24 time slots can be assigned in one direction). (Current specifications call for a software imposed limit of 30% of the system capacity to be tied up with data transmission but it is not clear how it knows what is data versus what is voice.) It is important to remember that this data service can be provided off of a privately owned PBX or LAN server, there need be no airtime charges or end-user licensing hurdles to using this system. Both public and private base stations are envisioned. This appears to be the way moderate-speed wireless LANs are to operate in Europe.

UDPCS

After the breakup of the Bell System on January 1, 1984, part of AT&T Bell Laboratories was "spun off" to form Bell Communications Research, or Bellcore. Bellcore serves the research needs of the regulated side of the seven regional holding companies. In this capacity, Bellcore has had a longstanding research program to explore wireless loop access. This has resulted in two issuances of a framework advisory for a standard Universal Digital Portable Communication System (UDPCS).[20] These documents propose a UDPCS system and solicit industry comments. The key aspects of the currently proposed specification for UDPCS are given in Table 2. Unlike the DECT system that was developed first for indoor wireless PBX applications, the UDPCS system is optimized for operation in outdoor environments were large delay spreads are expected. In order to combat these large delay spreads, the symbol rate was reduced by using Frequency Division Duplexing (FDD instead of TDD) and 4 level modulation (QPSK). Consequently its 250 kbaud channel rate is less than 1/4 of DECT, yet it serves nearly as many lines as DECT (10 instead of 12). As with DECT, data rates from 32 kbits/s to 320 kbits/s are supported by allocating one or more time slots to a data terminal.

With many Frequency Division Duplexing systems, an expensive duplexing filter is required to filter the strong transmit signal from the weak received signal. However, the proposed UDPCS system staggers the transmit and receive timeslots so that the terminal does not need a duplexer.

Bellcore typically facilitates the development of standards by first issuing Framework Advisories such as this, then transferring the work to a standards organization such as T1 that defines the *interface* specifications. Bellcore then writes equipment requirements that include those interface specifications but also include power, size, cooling, etc.,. specifications.[21]

Bellcore can unilaterally specify the technical requirements of equipment, but typically committee T1 is used to agree upon a specification in a multilateral way. T1P1 may be that forum for making UDPCS a standard, in fact Bellcore has been an active contributor to T1P1.

As a rule, Bellcore specifies only telephone network equipment, not the privately owned equipment such as a PBX or a LAN. However, a standard evolving out of T1P1 may be general enough to include such applications. One difficulty, however, will be the aversion to offer a tariffed service over spectrum that is shared with private systems. This will likely require that separate frequency allocations be made for public and private wireless networks, while sharing a common air interface.

Other Notable Systems

CDMA

Qualcomm Inc., together with NYNEX, Ameritech, PacTel, and AT&T have announced an alternative digital cellular system that uses spread spectrum Code Division Multiple Access (CDMA) for multiplexing different channels over a common frequency band. A trial of this system is scheduled for late this year or early 1992 in New York City. This is a proprietary system that uses the standard cellular frequency band under the provisions of FCC Report and Order, Gen. Docket No. 87-390, 65 RR 2d. 983 (1988), which allows a cellular operator to provide services that do not use current cellular standards, provided that out-of-band emissions limits are not exceeded. This system will provide standard cellular mobile phone type services but with a digital air interface that could support some low data rate metropolitan area networking applications.

WIN (Wireless Indoor Network)

Motorola Inc. has pioneered the use of the 18 GHz Digital Termination Service (DTS) bands to provide an indoor wireless LAN that operates at 15 Mbit/s and connects up to 32 Ethernet nodes via radio. This product was made possible by recent changes to the DTS rules in the FCC Report and Order, PR Docket No. 88-191, adopted Feb. 8, 1990, specifically ¶94.88. Currently another proprietary interface, this system suffers from the high propagation losses of 18 GHz. Consequently, coverage is limited to about 500 feet of the base(s). These also require licensing with the FCC, but the vendor (Motorola) can coordinate that for the customer, provided that the network is not moved out of the confines of the building.

5. Summary

The development of a Personal Communications System, for voice, data, or both, is a worldwide effort requiring coordination and cooperation among many hundreds of companies and organizations. Current FCC rules have some allowances for the emerging new products, cordless phones and wireless LANs have been available on the market now for several years. But in order to introduce a product that can truly interwork with and not against a variety of other products of different manufacturers, the standards and regulatory process must be followed. It is not a gantlet, but a process that brings together many others that can add to the value and intellectual basis of a product. Standards do not reduce competitive forces but provides a context for competition. There does not appear to be a single wireless standard emerging but rather a variety of standards from which the marketplace may choose.

There have been substantial, perhaps revolutionary, changes in the technology of wireless devices, with advanced microprocessor control and frequency agile synthesizers being cost competitive with previously less advanced systems. There have also been substantial changes in the thinking and scope of the standards and regulatory bodies. The internationalization of standards, particularly in the European arena, as well as the prospect of auctioned spectrum, are both nearly revolutionary in character and may have as profound an effect as the technological advances.

It is risky to make any predictions about the what the various bodies will do, but it is doubtful that the FCC would allocate any frequencies to a Personal Communication Service that might be superseded by potential WARC-92 allocations. Consequently, it is doubtful that any permanent frequency allocation for PCS or "Data-PCS" will be made by the FCC prior to the WARC-92 deliberations. In addition, given the support that the 12 European Commission (EC) countries as well as six European Free Trade Association countries have given to PCS it can be expected that a significant allocation to PCS will come out of the WARC-92 conference, at least for Region 1. The FCC is also supportive of innovation and is anxious to insure that the U.S. does not fall behind in this area. The FCC has been encouraging experiments and products that use novel techniques such as spread spectrum to share spectrum - easing the conflicts between current license holders and new applicants. While these experimental results are not yet conclusive, the FCC and the NTIA are also exploring other, market based, approaches to contend with these conflicts through auctions and legalized license sales.

Acknowledgements

The author would like to express gratitude for the patient discussions and help provided by Gary Fishman, Ernest Gleit, Dale Wisler, and Gene Rappoport during the preparation of this paper.

References

[1] Minutes of the Eleventh Meeting of Sub-Technical Committee RES-3 held in Munich, December 10-14, 1990. RES-3 (90)126.

[2] FCC Report and Order, Gen. Docket No. 87-390, 65 RR 2d. 983 (1988)

[3] IEEE Relationships and Interfaces to international Standards Organizations, Prepared by the IEEE Standards Board, February 1991.

[4] FCC Report and Order, RM-4780, 2 FCC Rcd 7278 (1987).

[5] "Global Standards," Karen Fitzgerald, IEEE Spectrum, June 1990, pages 44-46.

[6] MPT 1375, "Common Air Interface Specification," Department of Trade & Industry, Radiocommunications Division, London SE1 8UA.

[7] European Telecommunications Standards Institute BP 152 F-06561, September 10-14, 1990

[8] European Telecommunications Standards Institute, Interim European Telecommunication Standard, European digital cellular telecommunications system (phase 1); Draft prl-ETS-xxx.

[9] European Telecommunications Standards Institute, ETSI Secretariat: B.P.152.F-06561 Valbonne Cedex, France, RES-3N Chapters 1-6.

[10] "Europe's Wireless Revolution," Arthur H. Hill, ©1991 Telephony (a Div. of Intertec Publishing Corp) Chicago Il. page 10.

[11] European Telecommunications Standards Institute I-ETS:1990 Version 1.0.0 Approved in Paris by ETSI TC/RES September 10-14, 1990.

[12] Encyclopædia Britannica, Volume V, page 395, ©1983, Fifteenth edition.

[13] Michael H. Callendar, Chairman, CCIR Task Group 8/1 (Formerly IWP 8/13). Minutes of CCIR meeting 12/90.

[14] CCIR IWP 8/13 Report M/8 on "Future Public Land Mobile Telecommunication System".

[15] Federal Communications Commission Docket No. 90-314, June 14, 1990, ¶ 5.

[16] Federal Communications Commission Supplementary Notice of Inquiry Relating to WARC-92 Preparations, SNOI 91-73.

[17] "Wireless Communications and Spectrum Conservation: Sending a Signal to Conserve," IEEE Communications Magazine, February 1991, pg. 26-29.

[18] "U.S. Spectrum Management Policy: An Agenda for the Future," NTIA Special Publication 91-23, February 1991.

[19] Northern Telecom, Response to Notice of Inquiry Relating to Establishment of New Personal Communications Services," Federal Communications Commission Docket No. 90-314, October 1, 1990.

[20] Bellcore FA-NWT-001013 "Generic Framework Criteria for Universal Digital Personal Communications Systems", issue 2, December 1990.

[21] Conversation with Gerald R. Boyer, Bellcore District Manager, Advanced Access Requirements and Systems Engineering, May 8, 1991.

Table 1 – Petitions Before the FCC Concerning PCS and Related Issues

Report and Order on GEN. Docket 89-354	June 14, 1990	Amending Parts 2 and 15 of the rules with regard to the operation of spread spectrum systems. particularly ¶15.247, to require 10dB of processing gain for DSSS operation, 17dB for FHSS.	902-928 MHz 2400-2483.5 MHz 5725-5850 MHz
Cellular 21, Inc.	Sept. 21, 1989	Allocation for CT2 Service	941-944 MHz
PCN America, Inc. (Millicom)	RM-7175 Nov. 7, 1989	Allocation for PCN based upon CDMA and microcell technologies	1700-2300 MHz
McCaw Cellular Communications	Jan. 16, 1990	Establishment of a Cellular Digital Data Network (CDDNS) to link mobile computers.	901-902 MHz 940-941 MHz
American SMR Network Association	March 9, 1990	Allocation for Private Land Mobile Radio Services (PLMRS)	901-902 MHz 940-941 MHz
Land Mobile Communications Council	April 13, 1990	Allocation for PLMRS	901-902 MHz 940-941 MHz
Pioneer Preference Proposal	April 27, 1990 Gen Docket 90-217	NPRM to adopt rule that would provide preferential treatment in its licensing process associated with the development of new communication services.	all (This proposal applies accross the board to all radio licenses — not just PCS.)
Telecommunications Industry Association (TIA)	April 30, 1990	Allocation of 25 duplex channel pairs to cordless telephone service (up from 10)	46.61- 46.97 MHz (from Base) 49.62-49.98 MHz (from handset) 15 kHz spacing
FCC Report and Order	January 8, 1991	To Permit Cordless Telephone Operation on Offset Frequencies (Ordered)	46.61- 46.97 MHz (from Base) 49.67-49.97 MHz (from handset) from -45 to 175 kHz spacing
Apple Computer Company	RM-7618 Jan. 28, 1991	Initiate a Rulemaking to allocate 40 MHz for "Data PCS"	40 MHz in the 1850 - 1990 MHz band
Motorola	Report and Order, PR Docket No. 88-191, adopted Feb. 8, 1990, specifically ¶94.88.	Allows for low power indoor use of the 18 GHz band for Aries type Wireless LANs.	18.820-18.870 and 19.160-19.210 GHz

Table 2

Comparison of Various Wireless Systems

	CT2	CT2+	DECT	GSM	PCN	IS-54	AMPs (EIA-IS3)	UDPCS
Band (MHz)	864-868	930-931	1880-1900	890-915	1710-1785	824-849	824-849	.4 – 4 GHz ?
		940-941 +		935-960	1805-1880	869-894	869-894	
Bandwidth (MHz)	4 MHz	2 MHz +	20 MHz	50 MHz	150 MHz	50 MHz	50 MHz	60 MHz
Channelization	FDMA	FDMA	TDMA/FDMA	TDMA/FDMA	TDMA/FDMA	TDMA/FDMA	FDMA	TDMA/FDMA
Channel Spacing (kHz)	100 kHz	100 kHz	1.728 MHz	200 kHz	200 kHz	30 kHz	30 kHz	300-400 kHz
# of Freq. Channels	40	20 +	11	125	375	832	832	~170
Voice Ch/Freq Ch	1	1	12	8	16	3 (or 6)	1	10
Total Duplex Channels	40	20 +	132	1000	6000	2496	832	1700
Duplex Method	TDD	TDD	TDD	FDD	FDD	FDD	FDD	FDD
Equiv. BW / Duplex Chan.	100 kHz	100 kHz	144 kHz	50 kHz	25 kHz	20 kHz	60 kHz	80 kHz
Channel bit rate	72 kBPS	72 kBPS	1152 kBPS	270 kBPS	270 kBPS	97.2kbps?	NA	450 kbps raw
Data Service	32 kbps	32 kbps	32-736 kbps	16 kbit/s	8 kbit/s	8 kbit/s	Voiceband only	32 to 320 kbps
Speech coder	ADPCM	ADPCM	ADPCM	RPE-LTP	RPE-LTP	VSELP	NA	ADPCM
Bit rate	32 kBPS	32 kBPS	32 kBPS	13 kbps	6.7 kbps	8 kbps	NA	32 kbps
Frame Time (mSec)	2 mSec	2 mSec	10 mSec	4.6 mSec	4.6 mSec	40 mSec	NA	2 mSec
Modulation	GMSK	GMSK	GMSK	GMSK	GMSK	π/4 DQPSK	Analog FM	DQPSK
Voice & Data	~no	~some	yes	yes	yes	yes?	~no	yes
Ave xmit power (Watts)	5 mW	5 mW	10 mW	2, 5 MS	2, 5 MS	0.6, 1.2, 3.0	0.6, 1.2, 3.0	400-800mW down
Peak Transmit Power (W)	10 mW	10 mW	250 mW	8, 20 MOB	8, 20 MOB	0.6, 1.2, 3.0	0.6, 1.2, 3.0	100-200 mW uplink
Handoff ?	no	yes	yes	yes	yes	yes	yes	
Cell Radius	41-140 m	40-140 m	40 - 140 m	1 - 5 miles	0.4 - 5 miles	30 miles ?	30 miles ?	2000 feet
Availability	1989	1991	1992	1991?	1993	Late 1991	1983	1994?

CT2 from MPT 1375 "Common Air Interface Specification" 1990.
DECT (Digital European Cordless Telecommunications System from ETSI Draft prl-ETS-xxx.
IS-54: Newly adopted "dual mode" Cellular System providing new digital services with backward compatibility with AMPS.
AMPS: Advanced Mobile Phone Service. The current analog FM cellular standard (vs. the European TACS, NMT NET, and RTMS systems)
Bellcore: from FA-TSY-001013 Issue 2, Dec 1990. A wide area loop access approach for data and voice, proposed for comments.

SAW 4/1/91

SESSION I

OVERVIEW OF WIRELESS LANs

BASS ASSOCIATES

TRENDS IN NETWORKING

Charlie Bass

Bass Associates

BASS ASSOCIATES

TRENDS IN NETWORKING

Political

Economic

Technology

Application

BASS ASSOCIATES

POLITICAL TRENDS IN NETWORKING

Deregulation
- U.S.
- U.K.
- JAPAN

International Standards
- CCITT
- ISO
- IEEE

Private vs. Shared Facilities

ECONOMIC TRENDS IN NETWORKING

Competition

Voice Message Units
Time x Distance

Data Message Units
Data Rate x Time x Distance

Private vs. Switched

BASS ASSOCIATES

TECHNOLOGY TRENDS IN NETWORKING

End to End Digitzation

Fast Circuit vs Fast Packet Switching

ISO Reference Model

Standards in Hard and Soft Silicon

More Speed - More Compression

Copper to Fiber to Air

STANDARDS

Ethernet

Token Ring

TCP/IP

OSI

X.400, X.500, X.Y ^{n}

V.32

ISDN

Group IV Fax

Px64

SMDS

Sonet

ATM

FDDI

DVI, JPEG, MPEG

DECT

BASS ASSOCIATES

APPLICATION TRENDS IN NETWORKING

Virtual Private and Hybrid Networks

Data Overtaking Voice

Group to Premises to Enterprise to Industry to Universal

Personal Connectivity

Network Computing

Multimedia

Regulatory Policy Considerations for Radio Local Area Networks

Michael J. Marcus
Assistant Chief for Technology
Field Operations Bureau
Federal Communications Commission
Washington, DC 20554

Abstract

A variety of technical approaches are available to to implement radio LANs. Since the radio technology area is highly regulated in all countries these must be considered in the context of regulatory policy. Several technical options and their present and proposed regulatory status in the U. S. envvironment are reviewed. It appears that such systems could have a major economic impact if a successful combination of technical and regulatory approaches is found.

Introduction

In recent years there has been an ever increasing interest in local area networks (LANs) as an important adjunct to office automation. Most work on this area has been based on transmission media based on wire, coaxial cable, and optical fibers. While these media can sustain wide bandwidths and multiple access, they also require often costly installations which restrict terminals to specific locations and need modification in case routine office reassignments, remodeling, or relocation. Motorola has estimated that the annual cost for moving LAN terminals for a major corporation with sales of $4 billion and a terminal population of 40,000 could reach $10 million/year with present costs of $1000/terminal relocation. They also estimated that the total cost to U.S. industry of relocating LAN terminals could reach $5.6 billion by 1990 [1].

This type of economic projection has spurred interest in LAN technologies that do not depend on dedicated cabling. Three approaches to this are radio-based systems, carrier current systems using normal power distribution wiring, and optical systems. In considering these alternatives one must consider both the nature of the propagation medium and the regulatory environment - concerns which are not usually considered for cable-based LANs. Optical systems are not subject to government regulation (except with respect to safety concerns) but have practical limitations due to the line of sight nature of the propagation media and therefore have limited applications. Both radio and carrier current approaches involve unusual propagation factors and subject the technology to government regulation--not a direct factor for other cable-based systems. In this paper we review both the technical and regulatory issues involved with the two approaches. The regulatory discussion will focus on the U. S. environment although the same basic issues will apply to other countries.

The basic propagation media issues which must be considered for these alternatives are similar to those for other communications media. These are channel bandwidth, multipath spectrum (resulting from reflections of signals), and backround noise characteristics. The problem facing the system designer is to come up with a modulation and channel access mechanism combination that can achieve the desired throughput goals at a reasonable cost.

Regulatory Background

In the U. S. all radio transmitters used by private users and local governments must be licensed by the Federal Communications Commission (FCC)[2] and comply with FCC rules. (Systems operated by federal agencies are covered by similar provisions administered by the National Telecommunications and Information Administration under delegated authority from the President[3]). Systems that are not explicitly designed as transmitters but are capable of causing interference are also subject to FCC regulation[4]--a provision that encompasses power line carrier systems. At present the FCC Rules contain no explicit provisions for radio LANs but several provisions of the FCC Rules are broad enough to permit radio LANS.

Spread Spectrum

Spread spectrum radio technology was originally developed for military applications where resistance to jamming and/or covertness were of major concern. In a spread spectrum system, an information-bearing signal is combined with a wideband noise-like signal of a much larger bandwidth using a balanced modulator or equivalent approach to yield a signal that has appears to be a wideband noisy signal. At the receiver the noise-like signal is replicated and used to demodulate the transmission and derive an estimate of the origonal information.

Spread spectrum has two characteristics that make it of particular interest for LAN use. These are resistance to multipath interference and the ability to use code division multiple access (CDMA). In buildings with metallic objects such as furniture or structures, multipath propagation can limit the achievable data rate and coverage area of radio systems by causing intersymbol interference and fading nulls. While impact of fading nulls can be controlled with the use of diversity antennas, the intersymbol interference problem may require the time resolution of spread spectrum for control.

CDMA is a method of sharing a communications medium by the use of orthogonal noise-like modulating signals or spreading sequences. The spreading sequences are normally derived from the ouput of linear-feedback shift registers. Other methods of channel sharing, such as time division multiple access (TDMA) or frequency division multiple access (FDMA) require explicit cooperation between those sharing the channel. In CDMA, no cooperation is needed once the shift register designs are selected separately for each user. (Indeed, since there are a large number of shift registers and which which can be used there may not even be a need for explicit cooperation in selecting the design.)

The Hewlett-Packard Company (H-P) has reported two experimental spread spectrum radio LANs. The first H-P system transmitted 5 mw of power at a center frequency of 1.5 GHz and was capable of delivering 100 kb/s with a range of 300 m[(5)]. A 25.5 MHz chip rate was used which which resulted in a processing gain of 24 dB. This system used a surface acoustic wave receiver that could acquire new signals in 1 ms and was used in a polling arrangement.

The second H-P system explored the feasibility of sharing spectrum with the Instructional Television Fixed Service (ITFS) in the 2500-2650 MHz band[(6)]. ITFS is intended for the distribution of educational video programming by educational institutions and is technically similar to the Multipoint Distribution Service (MDS) which uses an adjacent band for similar commercial activities. Both ITFS and MDS receivers usually use highly directional antennas - a factor which simplifies the feasibility of spectrum sharing. The technical parameters of the second H-P system were similar to the first except for the frequency. The significance of the test was its demonstration of non-interfering coexistence with the ITFS system which was being operationally used at the H-P facility to receive programming from Stanford University.

A theoretical thesis on the use of spread spectrum for radio LANs explored many of the system engineering aspects of a CDMA system. Small systems, say less then 50 terminals, may be possible with CCD receivers that do not require synchronization. However, larger systems require greater processing gains to be used in a pure CDMA mode. Such gain requires an active correlator in the receiver and either overall system synchronization or a long preamble which will reduce throughput.[7]

In 1981 the FCC originally began exploring the feasibility of civil uses of spread spectrum technology[8]. While the formal responses to the original FCC Notice of Inquiry were generally negative, emphasizing the point of view of users seeking to defend present allocations, the Commission nevertheless formulated specific proposals which it issued in 1984 [9]. In May 1985 the Commission adopted a subset of its proposals[10].

The rule change which is most relevant to the radio LAN application is contained in Section 15.247 of the FCC Rules[11]. This allows unlicensed transmitters of an approved design to transmit up to 1 w of spread spectrum emissions in any of the following bands: 902-928 MHz, 2400-2483.5 MHz, and 5725-5850 MHz. The minimum spreading permitted is specified in the rules for both direct sequence and frequency hopping systems. These systems can be used for any application such as radio LANs and cordless microphones but are secondary (must not cause interference to other users and can not complain about interference received) to other uses of these frequencies such as microwave ovens in the case of the 2400 MHz segment, radar systems, and amateur radio in the case of the 900 MHz segment.

Several commercial spread spectrum radio LANs have been developed and marketed although the commercial success has been limited to date. An interesting application of this technology and policy provision has been a MIDI (musical instrument digital interface) unit to carry digital information from digital musical instuments to synthesizers. The system is used in concerts by several.prominent rock musicians Amateur radio use of the 900 MHz band is rare at present and in any case will usually be limited to residential areas[11a]. Although industrial radio frequency heating equipment is permitted in all three bands, such equipment is rare in most areas with the exception of the ubiquitous consumer microwave oven. Fortunately, safety regulations severely limits the external emissions from such consumer equipment.

Motorola Radio LAN Petition

In June 1985 Motorola, Inc. filed a petition before the FCC requesting a frequency allocation for radio LAN use in the 1700-1710 MHz band and appropriate technical and licensing rules [12]. The petition proposed a maximum 100 mw effective radiated power and a maximum bandwidth of 10 MHz and no other technical design restrictions such as modulation type or channel access mechanism. After reviewing comment that were received on the petition, the FCC issued a Notice of Proposed Rulemaking (NPRM) in May 1986[13].

The NPRM modified the Motorola concept slightly to provide for 2 MHz channels in the 10 MHz wide proposed allocation and allowing a user to use one or more contiguous channels. It retained the original concept of no detailed technical specification in the rules, proposing to leave such choices to individual manufacturers. Thus some designers could use spread spectrum while others used more traditional modulation. The NPRM also raised the question of how to handle multiple users in close proximity with the possibility of either giving them licenses in nonoverlapping frquency segments or giving them overlapping licenses with the understanding that they would developing a sharing technique (such as FDMA or TDMA) among themselves.

The basic controversy in this proceeding was not with the technical details of the proposed rules or even the need for a radio LAN service, but rather with the fact that the proposed frequencies are allocated on a primary basis to the Meteorological Satellite Service and that any LAN use must be secondary to this service. Motorola's petition assumed that these frequencies were only used for satellite downlinks at 10 locations in the United States, however, the comments in this proceeding indicated NOAA's plans to encourage much more widespread reception of this weather information which might make sharing with LANs impractical. As a result, the FCC turned down Motorola's petition in July 1988 but indicated that it would "welcome .. any further proposals that might prove more promising for a RLAN service"[13a]

LANs as a Fixed Service under Section 90.257 of FCC Rules

At least one firm, Electronic System Technology, Kennewick, WA, has marketed a radio LAN system that can be licensed under Section 90.257 of the FCC Rules[14] in the band 72-76 MHz. This system transmits up to 9600 b/s with a power of 1 w. Ranges of up to 50 km are claimed, depending on the antenna used and the propagation environment. Such systems operate on a secondary basis between television channels 4 and 5 and attention is needed to avoid interference to this primary service. The licensing provisions of Section 90.257 seek to avoid such interference and may limit the applicability of such a system.

RLANs Under the 18 GHz Operational Fixed Microwave Service

Apparently reponding to the FCC's invitation in Docket 86-174, Motorola filed comments in Docket 88-191, which was initiated as a general examination of rules for point-to-multipoint operations in the Private Operational Microwave Service, proposing that multiple low power (100 mw) systems be permitted in the 18 GHz band. (This band had been allocated for the Digital Termination Service, which in turn is the generalization of a late 1970's proposal from Xerox for a system originally called XTEN.) In March 1990 the FCC approved Motorola's request under a regulatory regime that simplified licensing and technical standards[14a]. In February 1991 Motorola introduced a TDMA radio LAN product called ALTAIR™.

Millimeter Wave Systems

Work at British Telecom Research Laboratories has explored the feasibility of radio LANs in the millimeter wave part of the spectrum[15]. Even though the wave propagation in this region is ray-like, many types of building materials reflect such energy and have the net effect of providing reasonable coverage within an enclosed area. It was found that this multipath effect would allow transmissions speed up to 2 Mb/s using straightforward equipment. Atmospheric absorbtion of 16 dB/km at 60 GHz was found to have little impact on such a system at the short ranges involved in LAN communications. Indeed such absorbtion might be beneficial in limiting intersystem interference and opportunities for unwelcome interception of signals.

At resent there are no regulatory provision in the U.S. for radio LANs in the millimeter wave region. However, due to the large amount of spectrum available and the present uncrowded nature of the region it may be rather simple to obtain a LAN allocation and other necessary rule changes in this region if technical feasibility is established and a specific proposal is made.

Carrier Current Systems

One can construct useful communications systems that use the power mains as a transmission medium. This can be appealing for LAN use since most equipment receives external power in any case. Carrier current systems have been used by the power utility industry for a long time and have been recently introduced into consumer products for remote control of light and appliances in the home. Such systems generally use signalling carriers of 3-500 kHz and have data rates of less that 100 b/s[16,17]. The limiting factors in such systems are background noise, both harmonics of the line frequency and white noise, and intersymbol interference that results from multiple impedance mismatches in the power mains at the signalling frequency. The power mains with typical buildings provide reasonable path loss for frequencies up to 20 Mhz[18]. The impedance of transformer windings effectively limits the propagation of signals above 1 MHz and this effect can be used to control intersystem interference.

Spread spectrum may be used to control the impact of the multipath propagation in power mains as in radio systems. H-P has demonstrated a system which used the band 3-10 MHz and achieved a 30 m range with a power density of 1μW/kHz and 100 m range with a power density of 10 μW/kHz. The experiments showed that the incidental free space radiation from the power mains was too low to cause radio interference.[19]

Other work with spread spectrum carrier current technology [0] has demonstrated a point-to-point system with a capacity of 6 kb/s and an error rate of 10^{-4}. While the work to date is promising, more research is necessary to develop the appropriate modulation techniques for this complicated communications medium.

The Further Notice in Docket 81-413 raised the question of possible authorization by the FCC of spread spectrum carrier current systems. Only H-P commented on this matter and the Commission decided to defer the issue without prejudice and left the rulemaking open for further comment. Thus, regulatory action in this area might be relatively easy if a specific proposal was received.

Other Options

The author has frequently heard casual remarks suggesting that "idle" UHF television channels could expeditiously used for radio LANs. From the technical and regulatory viewpoint, such an approach is fraught with difficulties. First, high quality video reception requires a signal to noise ratio at the receiver input of 40-60 dB. Random noise is tolerated better subjectively than interfering signals that result in beats with components of the video signal. Consumer-grade television receivers also have limited adjacent channel and IF image rejection capability. Secondly, the use of UHF television allocations by other services has been very contentious for over twenty years in this country. While the American Stock Exchange did receive a waiver from the Commission for a 1 mw voice system in the UHF television band within its building such waivers are reviewed on a case-by-case (location-by-location) basis and can expect strong opposition from a variety of parties. Thus it is unrealistic to expect the sale of commerical systems in the foreseeable future that share these frequencies for LAN use.

Infrared communications are another option and have the advantage, especially compare to the previous paragraph, of requiring no regulatory approval. Pahlavan has recently reviewed this technology(14). The main limitation of this technology is the line-of-sight nature of propagation in the transmission path which limits its applicability.

Channel Access Issues

Radio LANs like most other communications systems have the issue of how to share a communications channel among many users at separate locations. The classic approaches of FDMA, TDMA, CDMA, ALOHA, and hybrids and variants of these techniques are available in the system engineers toolbox. Relatively little has been done in the radio LAN area dealing with the channel access problem because of the need to address the basic communications channel design problem first. In the case of spread spectrum systems CDMA appears to be a preferred approach but it remains to be seen whether is is really practical to budget some of the processing gain for interunit interference or use it in total to reject multipath signals and other sources of interference.

Privacy Issues

The widespread use of radio LAN systems by business raises a new type of privacy concern. Such systems are vulnerable to interception by unauthorized parties at a relatively low cost and risk. The digital information on such systems is also much easier to sort and analyze than voice telephone conversations. While in most cases the interception of such information is illegal in the U. S., such laws may be difficult to enforce.

In the U.S. the issue of communications security for private entities has been left to marketplace forces. Encryption equipment is available and its use in the private sector has been encouraged by the federal government. The cost of having information intercepted may not be apparent to the system owner. In the case of interception by foreign entities there may be economic externalities which do not affect the owner at all but do affect the national economic welfare (as in the case of large scale industrial espionage in high technology areas). There may be a need for increased review of privacy issues as radio LANs are developed. Developers should also consider integrating encryption into system design at an early stage to minimize the cost of security and broaden the market for radio LANs.

Conclusions

A variety of technical options are available for implementing radio LANs and the closely related carrier current LANs. The regulatory status of these concepts are in different stages but are all making progress through the regulatory mechanisms in the U. S. or have been already authorized. A disappointment to the author has been the very limited involvement of the technical community to date in the development of public policy in this area. It is hoped that this articles and others like it will improve the quality of the policy discussions in this area.

The views expressed in this paper are those of the author and not necessarily those of the Federal Communications Commission.

References

(1) Motorola, Inc., Petition for Rulemaking , RM-5072, June 14, 1985

(2) 47 USC 301

(3) 47 USC 305

(4) 47 USC 302

(5) Payne Freret, Ralph Eschenbach, Dick Crawford, and Paul Braisted,"Applications of Spread-Spectrum Radio to Wireless Terminal Communication", Proc. Nat. Telecomm. Conf. 1980, p. 69.7.1-69.7.4

(6) Brian Elliott, "Hewlett-Packard's Experience with Wireless Data Terminals", Attachment to Reply Comments of Hewlett-Packard Company, General Docket No. 81-413, Filed Oct. 24, 1984

(7) James Elder,"Spread Spectrum for Indoor Wireless Data Communications", S.M. Thesis, Department of Electrical Engineering and Computer Science, Massachusetts Institute of Technology, Feb. 1987

(8) Notice of Inquiry, Docket 81-413, 87 FCC 2d 876

(9) Further Notice of Inquiry and Notice of Proposed Rulemaking, Docket 81-413, 49 Fed. Reg. 21951

(10) First Report and Order, Docket 81-413

(11) 47 CFR 15.247 (Formerly 47 CFR 15.126)

(11a) The ARRL Spread Spectrum Sourcebook, American Radio Relay League, 1991

(12) Motorola, Inc., op. cit.

(13) Notice of Proposed Rulemaking, Docket 86-174, May 1, 1986

(13a) Report and Order, Docket 86-174, 4 FCC Rcd 7654

(14) M. David Stone, "Modems Take to the Airwaves", PC Mag., January 14, 1986, p. 184-193

(14a) Report and Order, Docket 88-191, 5 FCC Rcd 1220

(15) S. E. Alexander and G. Pugliese, "Cordless Communications Within Buildings: Results of Measurements at 900 MHz and 60 GHz", Br. Telecom Technol. J., Vol. 1, No. 1, p. 99-105 (July 1983)

(16) J. B. O'Neal, Jr., "Overview of Power Distribution Line Carrier Communications Systems", Proc. Nat. Telecomm. Conf. 1980, p. 14.1.1-14.1.4

(17) Power System Communications Committee, "Summary of an IEEE Guide for Power-Line Carrier Applications", IEEE Trans., Vol. PAS-99, No. 6, p. 2334-2337 (Nov./Dec. 1980)

(18) Comments of Hewlett-Packard Company, Docket 81-413, Sept. 1984

(19) IBID

(20) Peter van der Gracht and Robert Donaldson, "Communications Using Pseudonoise Modulation on Electric Power Distribution Circuits", IEEE Trans., Vol. COM-33, No. 9, p. 964-974 (September 1985)

(21) Kaveh Pahlavan, "Wireless Communications for Office Information Networks", IEEE Comm. Mag., Vol. 23, No. 6, (June 1985), p. 19-26

Wireless LANs — a Portable Communications View

H. W. Arnold
S. Ariyavisitakul
D. M. Devasirvatham

Bell Communications Research
Red Bank, NJ
(908) 758-2982

Bellcore
Bell Communications Research

Current Tetherless Communications

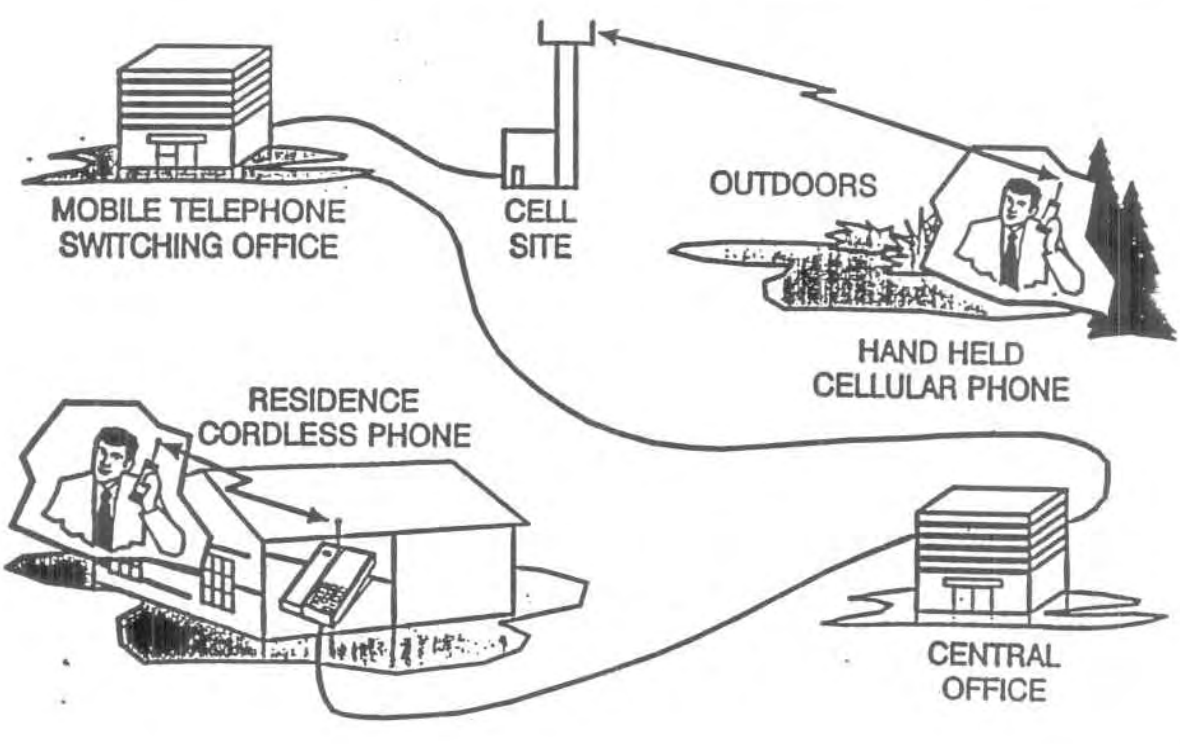

Data On Radio

- Voiceband data modems for cellular mobile
- Wide area radio data systems
  - Motorola KDT technology with IBM (ARDIS)
  - Ericsson Mobitex technology (RAM mobile data)
- Radio Local Area Networks (RLANS)
  - Several vendors

Converging Technology Trends

- Evolution to digital transmission technology
- Advances in CMOS Very Large Scale Integrated Circuits (VLSI)
- Advances in Microwave Integrated Circuits
- Increasing intelligence in networks
  - High speed digital processors
  - Access to large data bases
  - High speed Common Channel Signaling (CCS7)

Objectives For Universal Portable Communications

- Quality and reliability equivalent to wireline
- Ubiquitous integrated services for all portable sets
- Small easy-to-use portable sets
- Maximum time-of-use between rechargings
- Low power for portable sets
- Privacy and security equivalent to wireline
- Economical service comparable to wireline
- Compatibility with the environment
- Efficient use of radio spectrum

PY87 2TS87ADC.006

Digital Portable Communications

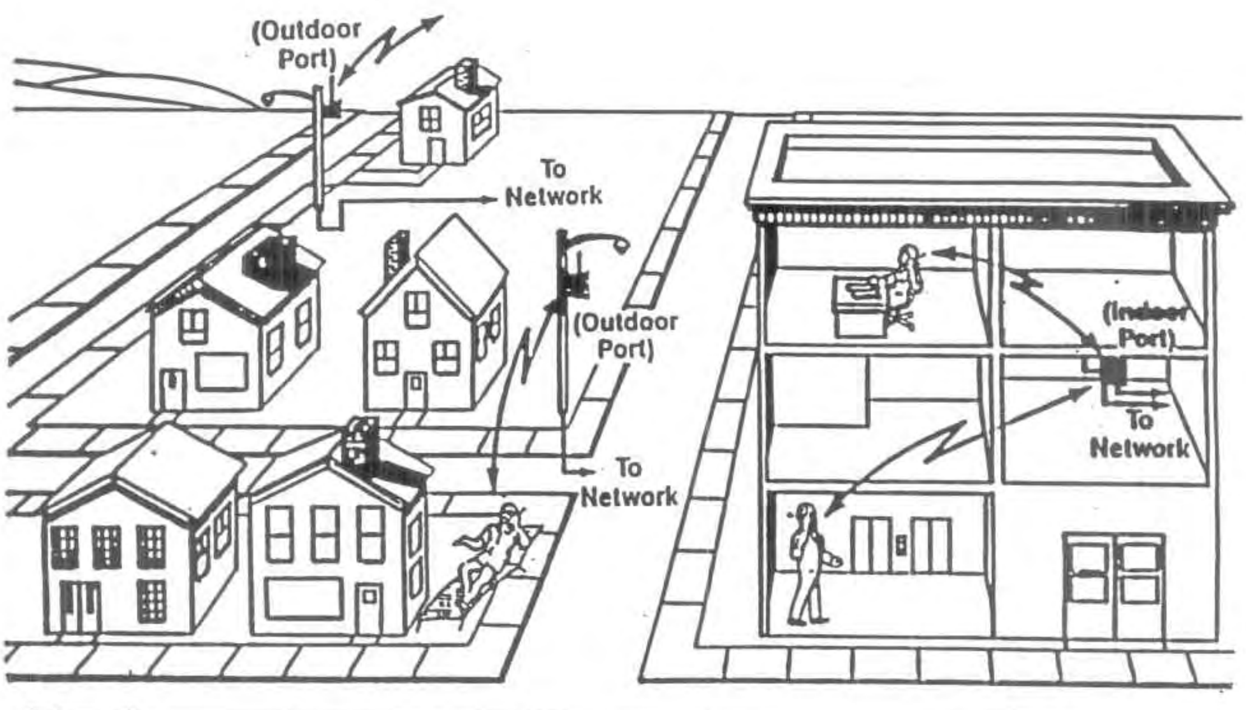

Low-Power Exchange Access Digital Radio Integrated With Network And Intelligence

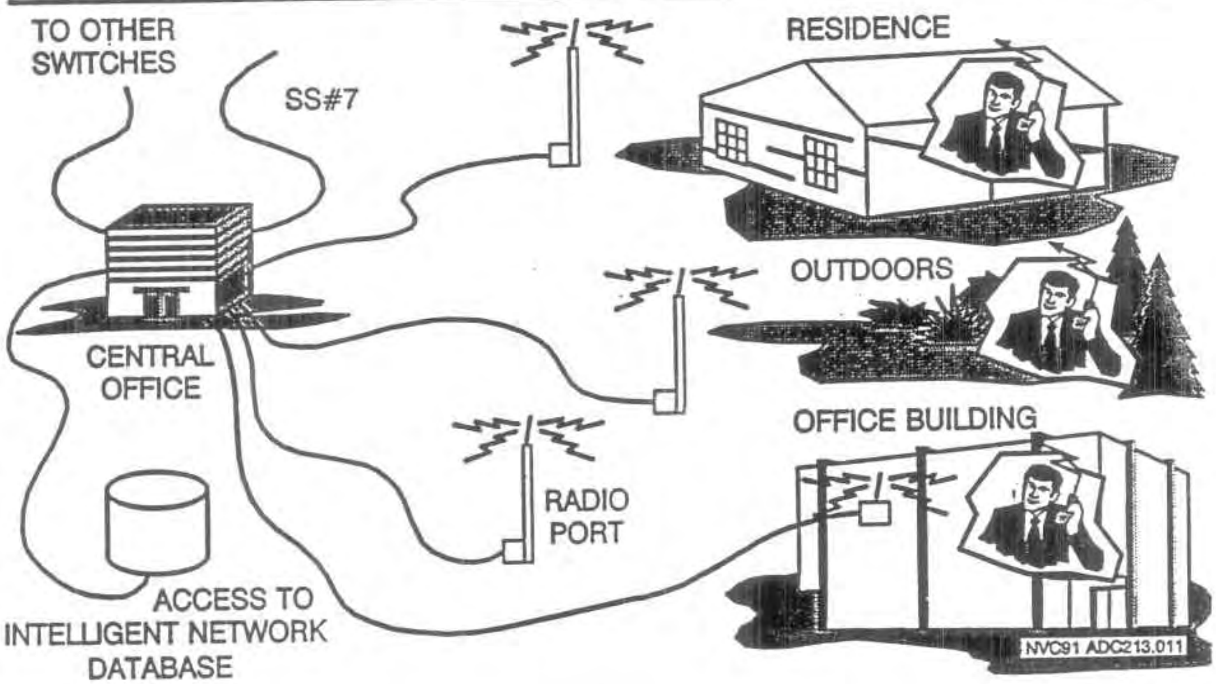

Frequency Assignment And Access

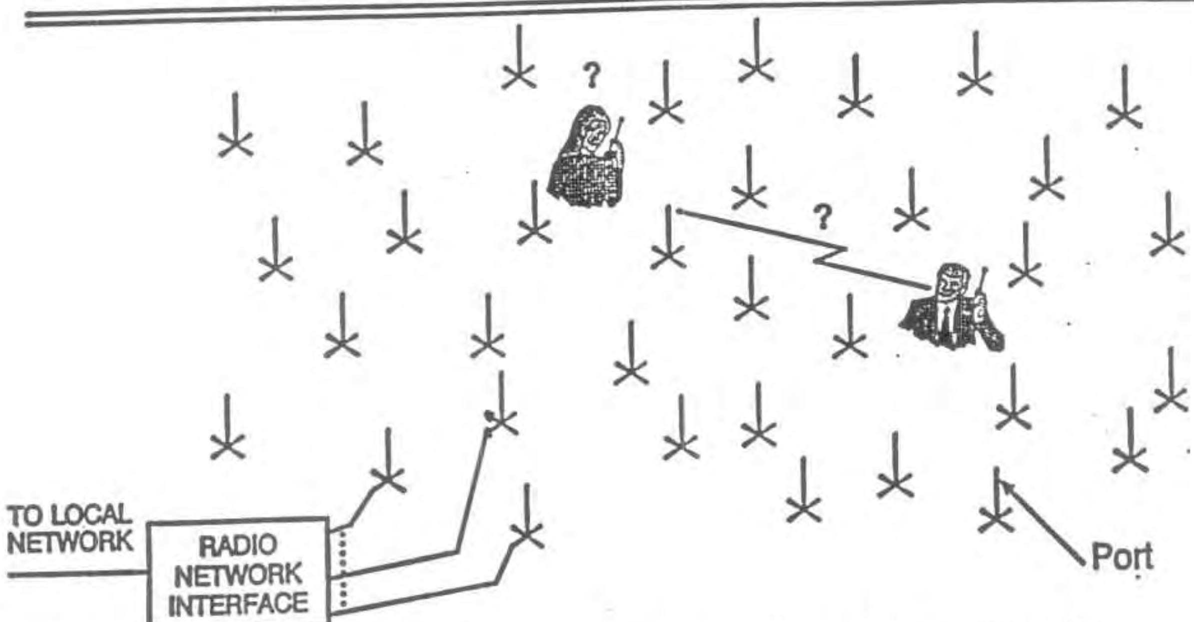

(1) What frequency pair should be assigned to a Port?

(2) What Port should be accessed by a portable user? NVC90 BJC21

Example

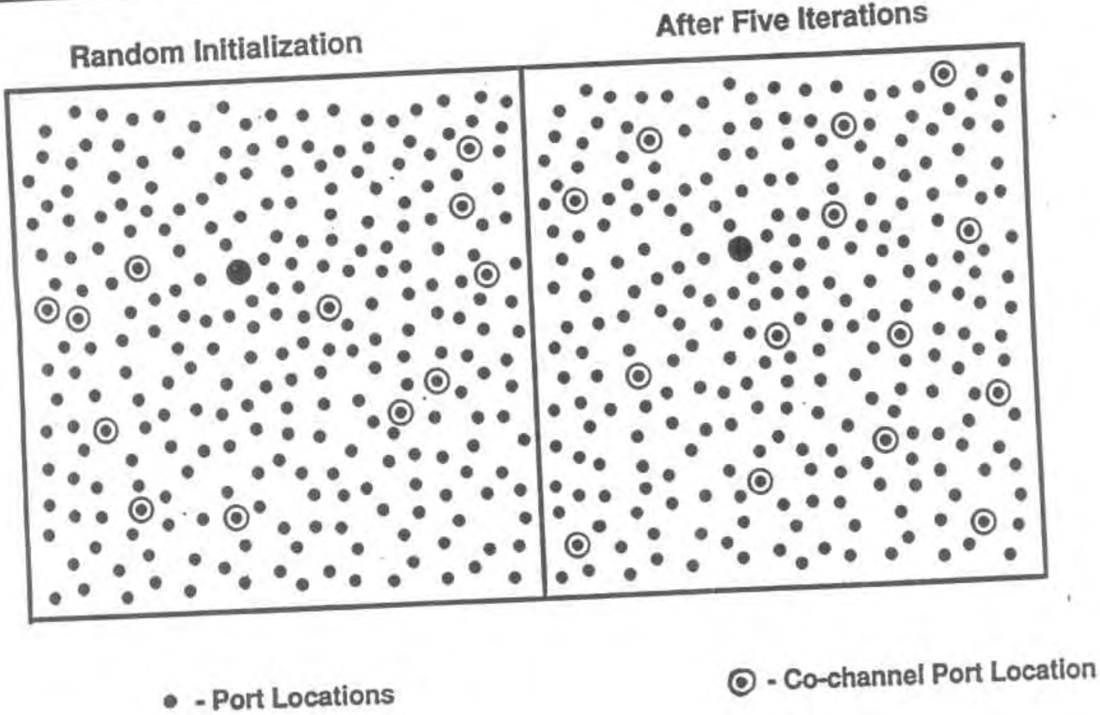

Demand Assigned Digital Radio Link

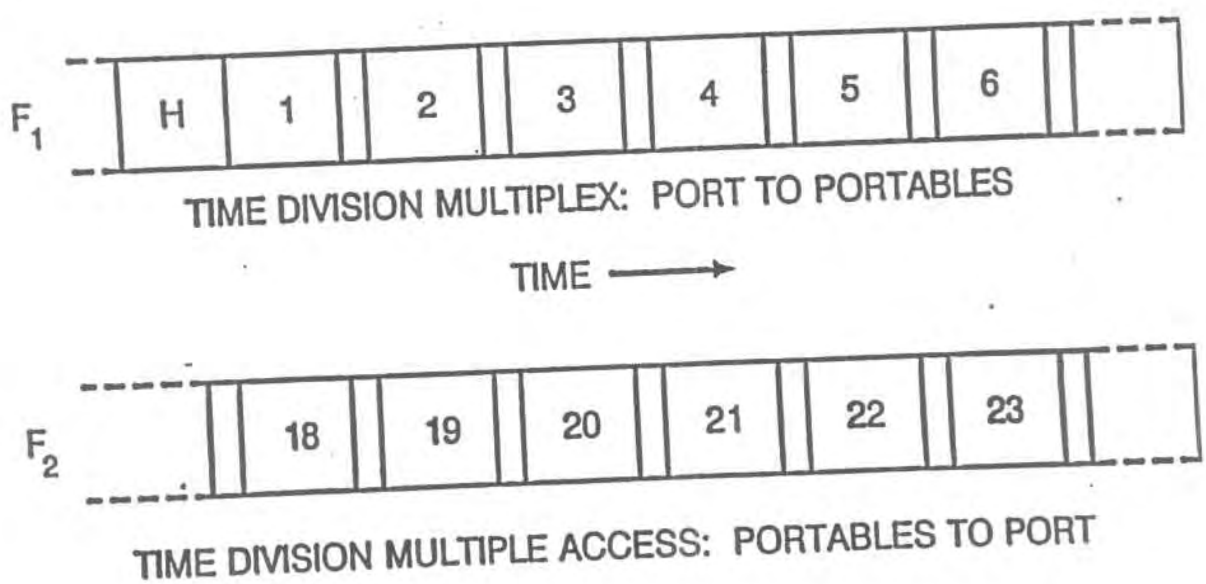

Innovative Techniques for Minimizing TDMA Overhead

- Block symbol timing and carrier recovery
  - Data driven - NO overhead for training sequences
  - Quality measure available without added complexity
  - Modest hardware complexity
- Combined error detection and burst synchronization
  - Only 3 - bit overhead for synchronization
  - Reuses error detection hardware for synchronization

Symbol Timing/Quality Measure

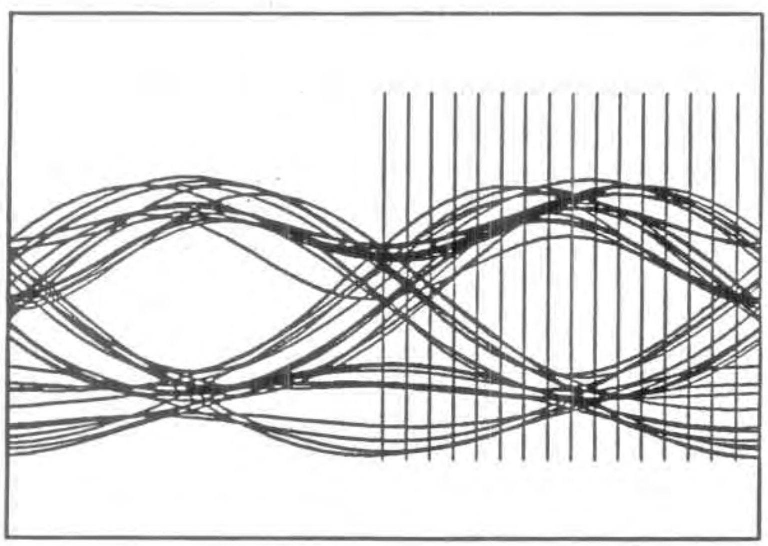

- **Symbol timing: "widest" eye opening**
- **Quality measure: noisiness at symbol timing point**

Typical System Parameters

- 5 mW portable transmitter average power
- 16-32 kbps speech coding
- 500 kbps 4-level digital modulation
- Frequency reuse, autonomous assignment
- 99+ % coverage within service area

Residential areas
- Port separation ~ 2000 ft
- Port antenna height ~ 30 ft

In large buildings
- Port separation ~ 200 ft

Time-Reversal Reception

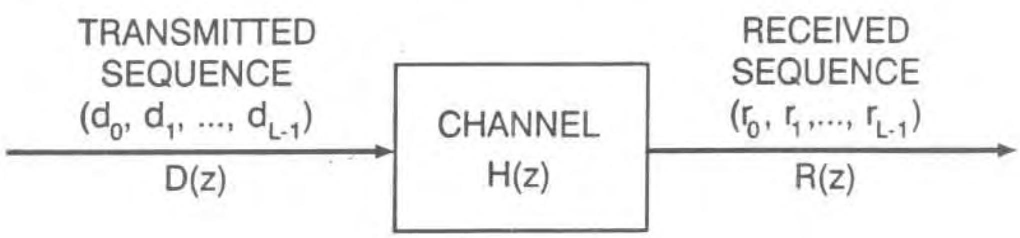

Channel filtering: $R(z) = D(z)H(z)$

Time reversal: $R(z^{-1}) = D(z^{-1})H(z^{-1})$

NVC90 4IEEALA.009

Why Time Reversal Useful

A DFE with time reversal

- Performs equally well in minimum-phase and maximum-phase channels
- Converges fast with LMS adaptation

In fading

- Performs as well or better than using 2x forward filter taps without time reversal

NVC90 4GLBALA.003

Single-Forward-Tap DFE

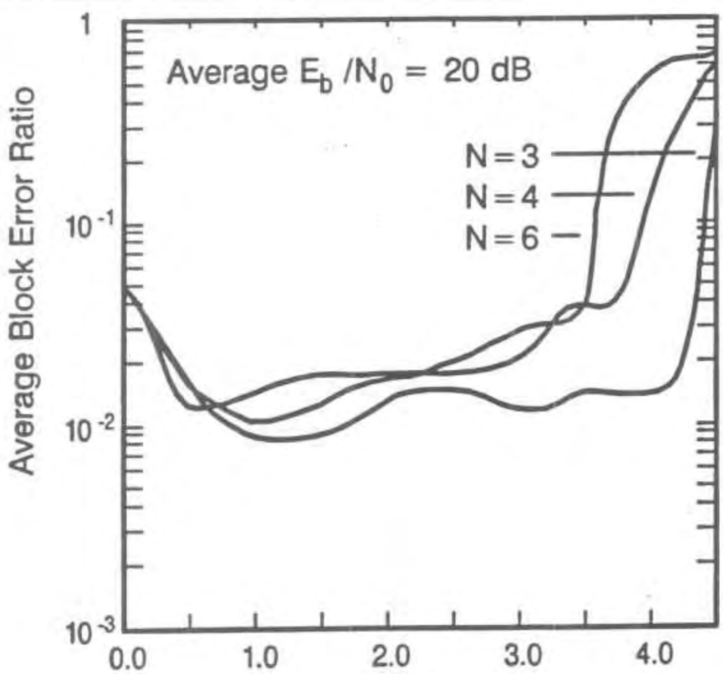

- 5 feedback taps with time reversal
- N equal-strength Rayleigh paths
- Optimum timing

NVC90 4GLBALA.005

Wireless LANs
Standard activity in IEEE

25 March, 1991

Outline

IEEE Profile

IEEE Project 802 profile

IEEE Project 802.11 profile

IEEE Project 802.11 Objectives (Chairman's view)

Conclusion IEEE work

Wireless LANs
Standard activity in IEEE

IEEE Profile

Founded in 1884

Over 320 000 members

In more than 130 countries

Activities: Professional, Educational, Publications, Regional, Technical and Standards

Over 600 standards published, 60 new or revised per year

Computer Society largest of 36 societies (90 000 members)

Wireless LANs
Standard activity in IEEE

25 March, 1991

IEEE Project 802 Profile

Established in 1980

9 Working Groups (1 accomplished task)

2 Technical Advisory groups (1 accomplished task)

3 plenary meeting per year (350-400 participants)

Over 450 voters

Over 600 observers

Recognized as the Experts in Information Technology

Published as ANSI/IEEE Standards:

802.2:1985	Logical Link Control (superseded)
802.3:1985	Carrier Sense Multiple Access with Collision Detection (CSMA/CD) Access Method and Physical Layer Specifications (superseded)
802.4:1985	Token-Passing Bus Access Method and Physical Layer Specifications (superseded)
802.5:1985	Token-Passing Ring Access Method and Physical Layer Specifications
802.7:1989	IEEE Recommended Practice for Broadband Local Area Networks,

Just Published IEEE standards

- 802.1 -1990	Overview and Architecture
- 802.1e-1990	System Load Protocol
- 802.1d-1990	Media Access Control (MAC) Bridges.
- 802.3i-1990	- System considerations for multisegment 10 Mbit/s Baseband Networks - Twisted Pair Medium Attachment Unit (MAU) and Baseband Medium, type 10BASE-T
- 802.3h-1990	Layer Management

Wireless LANs

Standard activity in IEEE

25 March, 1991

IEEE Project 802 Profile

Expected soon:

- 802.1b	LAN/MAN Management
- 802.1f	Recommended practices for the development of layer management standards
- 802.1i	FDDI Supplement
- 802.3	CSMA/CD AUI Abstract Test Suite
- 802.4k	Redundant media
- 802.5b	Voice grade media station attachment for Token-passing ring
- 802.5c	Reconfigurration for a dual ring stations for Token-passing ring
- 802.6	Distributed queue dual bus subnetwork for Metropolitan Area Networks (MAN)
- 802.10b	Standard for interoperable Local Area Network (LAN) Security (SILS), Secure Data Exchange

Standards adopted by ISO

ISO/IEC 8802-2:1989	Information processing systems - Local Area Networks - Logical Link Control Standard
ISO/IEC 8802-3:1989	Information processing systems - Local Area Networks - Carrier sense multiple access with collision detection (CSMA/CD) access method and physical layer specifications
ISO/IEC 8802-4:1990	Information processing systems - Local Area Networks - Token-passing bus access method and physical layer specifications

Wireless LANs
Standard activity in IEEE

25 March, 1991

Profile of IEEE 802.11

- Established in July 1990
- Five meetings held to date
- Officers:

* Chair	Vic Hayes	NCR Corporation
* Vice-Chair	Jim Neeley	IBM Corporation
* Secretary	Michael Masleid	Inland Steel Corporation

- 59 Voting members a.o.

  Apple, Fairchild Data, IBM, ICL, NCR, OKI, Sharp, Sun, Toshiba
  Hughes Network Systems, Motorola, O'Neil, Symbionics, Telemark,
  Telesystems, Symbionics, Symbol Technologies, Norand, OPTA, WIN Data
  NYNEX, General Motors, Honeywell, Inland Steel, AT&T, Symbionics
  Norand, Sonneville Associates, Teledyne

- 77 Observers (Aspirant members) a.o.

  Compaq, Hewlett-Packard, Hitachi
  AT&T, Racal, Retix, Bicc Networks, British Telecom, TI

- 98 On mailing list

Wireless LANs
Standard activity in IEEE

25 March, 1991

IEEE Project 802.11 Objectives (Chairman's View)

- establish IEEE Standard
- introduce IEEE Standard to ISO for consideration as International Standard
- standard would be used by Government Agencies for regulation of the band
- include work on Conformance Standard
- unlicensed use
    * merely type approval by manufacturer
    * no site license required
    * no fee to "private carrier"
- encourage Government Agencies to allocate bands for Radio LANs
    * initial work for ISM bands
- equal opportunity in the bands with existing services in that band
- include limited voice service in standard
- allow electromagnetic cohabitation in the geographic area
- "Local Area" to refer to property
    * whole building
    * campus
    * outdoor storage area / parking
- independent of device implementation
    * independent of vendor
    * independent of computer type
- set ambitious schedule

NCR

Wireless LANs
Standard activity in IEEE

25 March, 1991

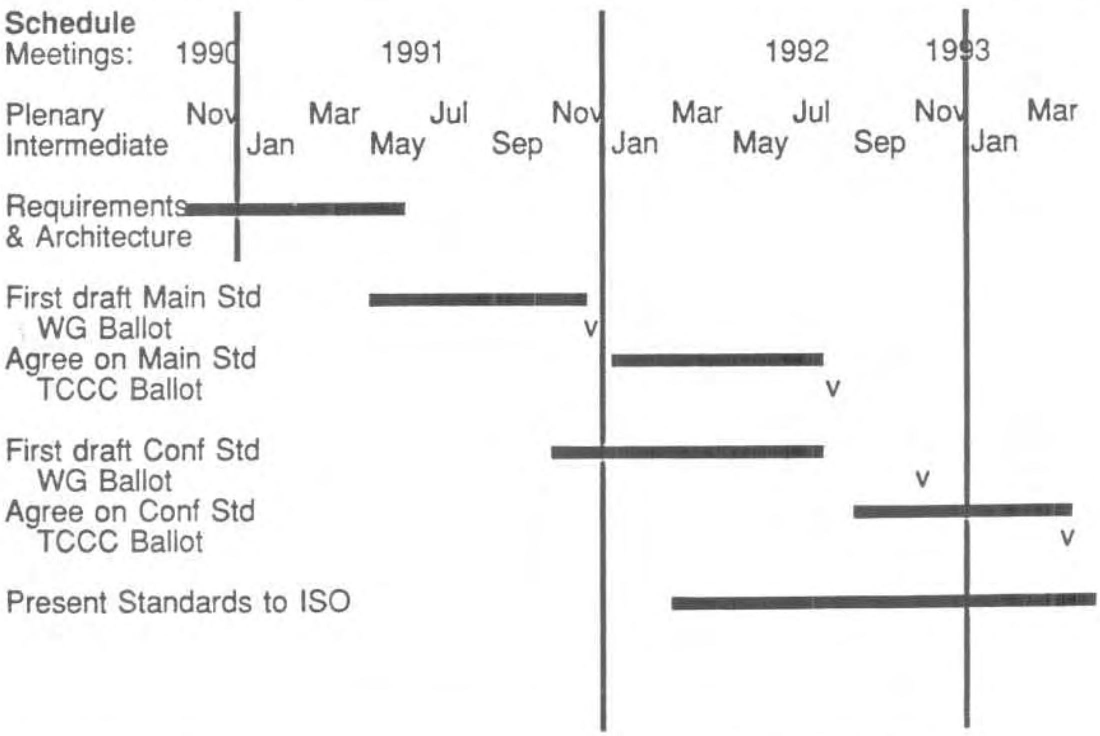

Wireless LANs
Standard activity in IEEE

25 March, 1991

Next Meeting

- July 8-12, 1991
- Hyatt Regency Kauai (HI)

Wireless LANs
Standard activity in IEEE

Conclusion of IEEE presentation

- Ambitious plan set
- Opportunities for allocation of radio spectrum for Information Technology
- Broad interest

SESSION II

CHANNEL CHARACTERIZATION

MULTI-FREQUENCY RADIOWAVE PROPAGATION MEASUREMENTS IN THE PORTABLE RADIO ENVIRONMENT

D. M. J. Devasirvatham, C. Banerjee, M. J. Krain and D. A. Rappaport

Reprinted from IEEE Communications Society
"IEEE International Conference on Communications"
April 16-19, 1990

ICC '90

MULTI-FREQUENCY RADIOWAVE PROPAGATION MEASUREMENTS IN THE PORTABLE RADIO ENVIRONMENT

D. M. J. Devasirvatham, C. Banerjee, M. J. Krain & D. A. Rappaport*

Bellcore
Red Bank, NJ 07701-7040

**NYNEX Science and Technology*
White Plains, NY 10604

ABSTRACT

Time delay spread and signal level measurements were made in two dissimilar office buildings at 850 MHz, 1.7 GHz and 4.0 GHz. No significant statistical difference in time delay spread was found at the three frequencies. The maximum rms time delay spread at the three frequencies did not exceed 270 nanoseconds at the larger building and 100 nanoseconds at the smaller building. Attenuation, while very nearly the same at the three frequencies, decreased slightly with increasing frequency, within the limits of the experiment's accuracy. The variation of the received signal level with distance could be characterized by free space propagation together with attenuation per unit distance. This attenuation coefficient decreased slightly with increasing frequency. The fractional error was found to be a useful measure of the spread of the data.

INTRODUCTION

Universal digital portable communications requires radio equipment which will work reliably within buildings in an environment which has multipath propagation, shadow fading, and moderate motion [1]. The intersymbol interference produced by this radio channel is related to the root mean square (rms) time delay spread of its impulse response [2] [3].

The first measurements of time delay spread at three office buildings and two residences were reported earlier by Devasirvatham [4] [5] [6] [7]. These studies, at 850 MHz, consistently measured root mean square time delay spreads under 100 ns within the buildings when there was a direct path between the transmitter and receiver. In the absence of a direct path, rms delay spreads of as much as 250 ns were seen. Other measurements in offices and factories have also been reported [8] [9].

The first time delay spread measurements at both 850 MHz and 1.7 GHz inside a metropolitan office building were reported by Devasirvatham, Murray and Banerjee [10]. This paper reports the results of the first measurements conducted at 850 MHz, 1.7 GHz and 4.0 GHz, inside two other dissimilar office buildings.

THE EXPERIMENT

Details of the experimental setup to measure the impulse response of the radio propagation channel have been reported earlier [5] [6]. Briefly, an 850 MHz, 1.7 GHz or 4.0 GHz carrier, bi-phase modulated by a 40 Mbit/s pseudonoise code, is broadcast by a transmitter. The signal suffers time-smear in the propagation channel and is then correlated at the receiver with an identical pseudonoise code, running 4 kbit/s slower. As the codes sweep past each other, the receiver traces out the power-delay profile of the channel and its envelope is recorded.

The transmitting and receiving antennas were wideband omni-directional units, at heights of 1.5 m and 2 m, respectively. At every measurement location the receiver antenna was rotated through a horizontal 1.2 m (4 foot) diameter circle. Eight power-delay profiles were obtained at equally spaced positions around the perimeter of this area. For each profile, 2048 points, representing either 2048 or 4096 ns depending on the time scale, were digitized and stored after verifying that there was no signal at greater time delays. The eight individual profiles were then power averaged at each time delay to calculate an averaged power-delay profile. After noise clipping, the area under the curve gives the received power level, while the square root of its second central moment, the rms time delay spread, is the measure of channel dispersion that has the most significant effect on the digital error rate [2] [3].

A total of 50 averaged power-delay profiles were obtained at each frequency in Building OFC/NCO and 28 at Building OFC/NST.

SITE DESCRIPTIONS

The experiment was conducted in one large and one medium sized office building. The larger building, henceforth referred to as OFC/NCO, was the Corporate Headquarters of NYNEX Corporation in White Plains, New York. This large four-floor L-shaped structure measures 121 x 75 m in plan. The building is shadowed to the north by a hill and to the south-east by another large building of the same height. The south and west faces are open. Offices and conference rooms opening off corridors in the longer arm are partitioned using sheet rock walls. The shorter arm is laid out mostly with office cubicles. Usually, line of sight was found only in the aisles and corridors. The floors are constructed using reinforced concrete. The metallized glass outer walls are shaded with venetian blinds. All the measurements were made on the top floor.

The medium sized office building, referred to as OFC/NST, was the NYNEX Science and Technology Center at White Plains, New York. It is a rectangular two-level structure, with a hill to the north. It measures 104 x 47 m in plan. Inside, the two floors have been divided, using rectangular layouts, into aisles, corridors, laboratories and rooms utilizing metallic partitions with a 0.67 m high glass upper portion. Once again, line of sight was only found in the same aisle or corridor. The floor is constructed of concrete and raised false floors are provided throughout the facility. There is a significant amount of laboratory equipment in the rooms. The building's conventional 1950's stone and brick facade has been completely replaced by an aluminum panel system with large metallized glass windows which have metallic venetian blinds. All the measurements were made on the second floor.

In both locations, the receiver was placed, in an aisle or corridor, often at an intersection. The transmitter was moved to locations in aisles, corridors and office rooms. Laboratories were also included in the measurements at OFC/NST.

RESULTS

An averaged power-delay profile at 850 MHz in OFC/NCO is shown as the solid curve in Figure 1. The dotted curve shows the averaged profile at 1.7 GHz and the dashed curve that at 4.0 GHz at the same place, taken immediately afterward. Each curve has been separately normalized to the peak power value of a power-delay profile received at that frequency at a reference distance of 0.3 m in free space. This corrects for frequency dependent system parameters such as transmitted power and antenna gains, and path loss to the reference distance. These three profiles match very closely, indicating that they suffer the same impairments over the multiple echo paths in this location. The higher receiver noise tails at 1.7 GHz and 4.0 GHz are artifacts of the normalization, since the absolute received signal levels were lower at those frequencies and hence closer to the noise floor of the receiver.

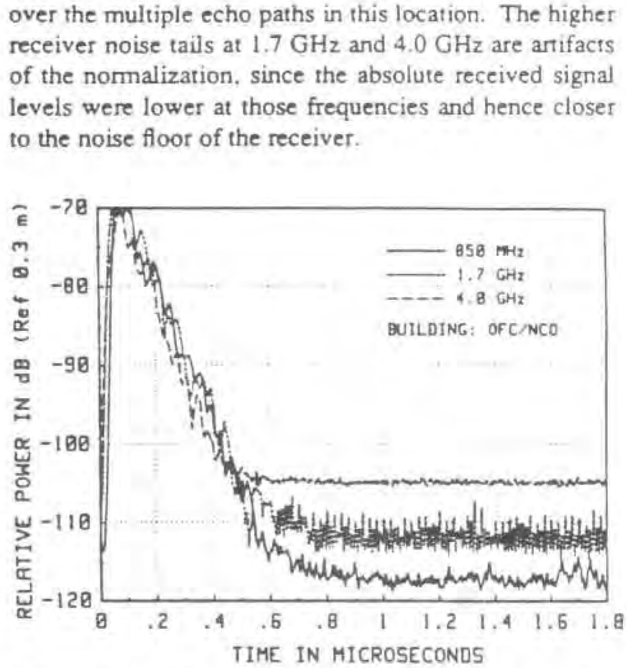

Figure 1. Typical averaged power-delay profiles at 850 MHz (solid curve), 1.7 GHz (dashed curve), and 4.0 GHz (dotted curve) at a location in Building OFC/NCO.

The rms time delay spread measured inside the buildings OFC/NCO and OFC/NST, respectively, was calculated at the three frequencies for all locations measured. The maximum rms delay spread in OFC/NCO at 850 MHz was 270 ns, while it was only 150 ns at 1.7 GHz and 130 ns at 4.0 GHz. This significant anomaly was found at a single location where the 850 MHz profile was much wider than the other two. It appeared that echoes from outside the building were visible at 850 MHz, but not at the other two frequencies. This result is puzzling, but repeatable at that spot.

The rms delay spread did not exceed 100 ns at any frequency at OFC/NST. It was also seen that, excluding the above-mentioned single anomaly at 850 MHz, the three distributions plotted from the data at each site were quite similar. The worst-case value is much less than the worst-case results measured in other larger buildings. Many locations had blocked direct paths, since the transmitter was positioned in conference rooms and in individual suites separated from the main area by walls. The fact that the worst-case results are still not much greater than the direct-path results seems to indicate that the interior walls and partitions are quite transparent at these frequencies.

Figures 2 and 3 show the rms time delay spread at 1.7 GHz and 4.0 GHz, plotted against the rms time delay spread at 850 MHz at the same positions of the transmitter and receiver in the two buildings.

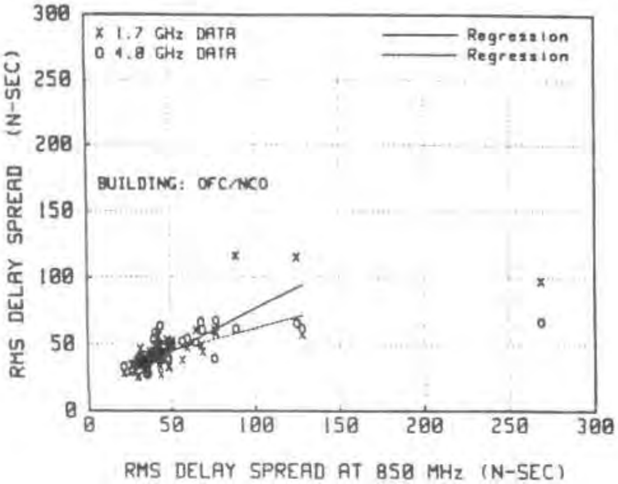

Figure 2. Root mean square time delay spread at 1.7 GHz (X symbols) and 4.0 GHz (O symbols) plotted against the results at the same locations at 850 MHz in OFC/NCO. The regression line for all the data is shown as the central solid curve (1.7 GHz) and dotted curve (4.0 GHz).

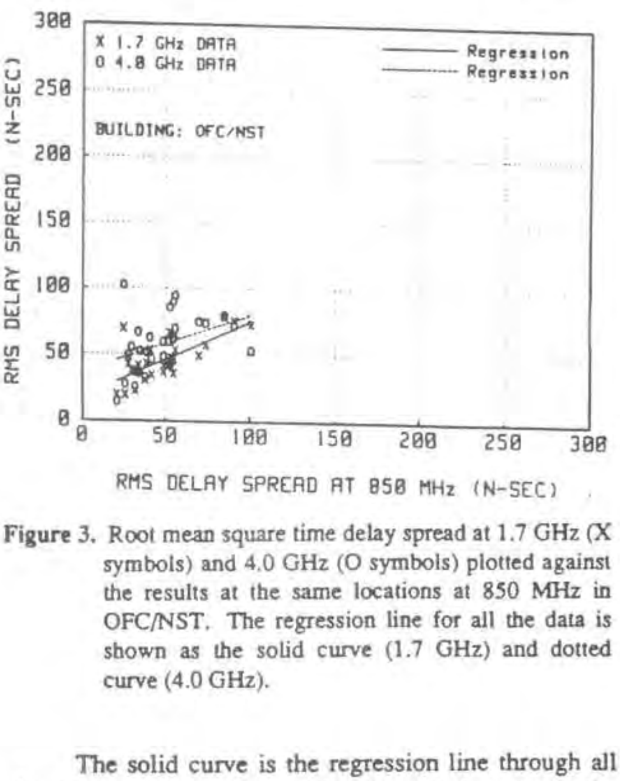

Figure 3. Root mean square time delay spread at 1.7 GHz (X symbols) and 4.0 GHz (O symbols) plotted against the results at the same locations at 850 MHz in OFC/NST. The regression line for all the data is shown as the solid curve (1.7 GHz) and dotted curve (4.0 GHz).

The solid curve is the regression line through all the points at 1.7 GHz, while the dotted curve is the regression line for the 4.0 GHz results. The single outlying point at 850 MHz is excluded from the regression.

These regression results are not very meaningful, quantitatively. This is because the data are clustered about small values of delay spread. The few larger delay spread values exert a disproportionate influence on the regression lines. Nevertheless, it may be said that as the frequency ratio increases, the delay spreads at a particular location tend to be less correlated. Furthermore, the worst-case rms delay spreads at the higher frequencies are not larger, statistically. This also agrees with earlier results at 850 MHz and 1.7 GHz inside a metropolitan office building [10]. This is a very useful result since it suggests that rms delay spread will not, by itself, limit the use of the higher frequencies for a communications system operating within a large building. More data in buildings that produce large delay spreads are needed, however, to confirm this.

Figures 4 and 5 show the received relative power at 1.7 GHz ('X' symbols) and 4.0 GHz ('O' symbols) plotted against the corresponding power at 850 MHz for the same locations of the transmitter and receiver in the two buildings. The power levels are normalized to the power received at each frequency at 0.3 m (1 foot), a convenient distance. This normalization removes system dependent parameters such as transmitted power and antenna gains from the results and gives a measure of the relative path loss at each frequency. The relative power levels range from -35 dB to -95 dB at OFC/NCO and -22 to -85 dB at OFC/NST. The regression lines for all the data at each frequency are shown in the figures as the center line of the set of three lines shown at that frequency. The line above and below it are a set of bounds, which will be discussed below.

It is apparent, when looking at the data, that the spread of the data from the regression line increases as the relative signal level decreases. This behavior is commonly seen in other measurements also [11]. In order to study this behavior, the ratio of the deviation of the data point from the regression, to the regression value, itself, was taken. This was called the "Fractional Deviation" of the data. Therefore, the fractional deviation of the power, $d_f(P_{dB})$, was defined as,

$$d_f(P_{dB}) = \frac{(P_{dB} - P_{dB_{reg}})}{P_{dB_{reg}}} \qquad (1)$$

where P_{dB} is the received power relative to the received power at 0.3 m, in decibels, and $P_{dB_{reg}}$ is the regression value of relative received power in decibels. The rms value of all d_f values will be denoted by σ_4.

We note that the fractional deviation of power is implicitly dependent on the reference power relative to which the denominator is calculated. Intuitively, one may postulate that it should be measured close to the transmitter. In our measurements, this reference was at 0.3 m. Fortuitously, it gave good results. No other justification is given.

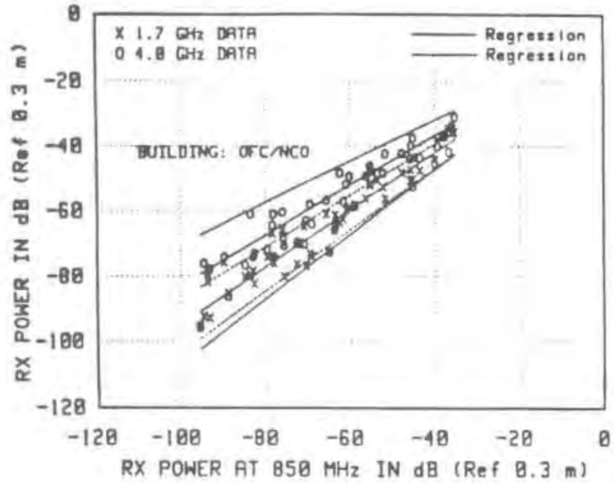

Figure 4. Relative received power normalized to the power at 0.3 m separation at 1.7 GHz (X symbols) and 4.0 GHz (O symbols) plotted against the results at the same locations at 850 MHz in OFC/NCO. The regression line for all the data is shown as the central solid curve (1.7 GHz) and central dotted curve (4.0 GHz). The corresponding lines on either side show ± two fractional deviations.

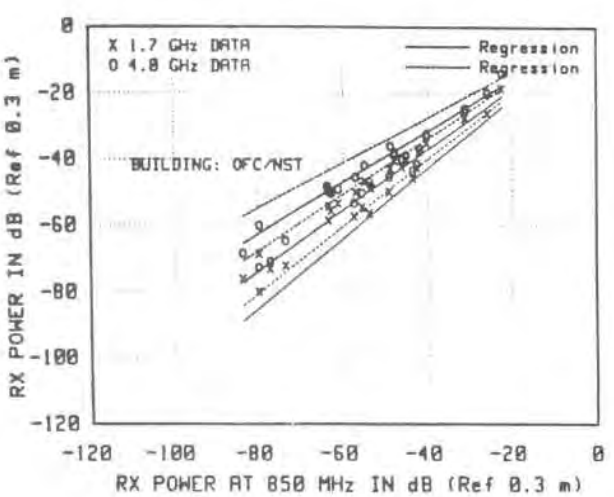

Figure 5. Relative received power normalized to the power at 0.3 m separation at 1.7 GHz (X symbols) and 4.0 GHz (O symbols) plotted against the results at the same locations at 850 MHz in OFC/NST. The regression line for all the data is shown as the central solid curve (1.7 GHz) and central dotted curve (4.0 GHz). The corresponding lines on either side show ± two fractional deviations.

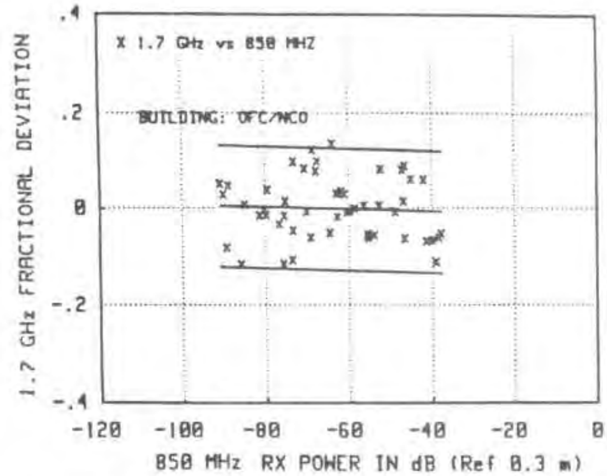

Figure 6. Fractional deviation of power at 1.7 GHz from the regression line, plotted against the power in dB at the same locations at 850 MHz in building OFC/NCO.

Figure 6 shows the fractional deviation of power for the 1.7 GHz - 850 MHz pair of data at the building OFC/NCO, plotted against the power at 850 MHz. It is seen that the spread is now independent of the received relative power. It was found, using statistical analysis, that the spread was not Gaussian, but was better approximated by a uniform distribution. The rms fractional spread, $\sigma_{d(P_m)}$ for this data was 0.064 . It was further found, experimentally, that curves drawn at $\pm 2\sigma_{d(P_m)}$ about the regression curve enclosed virtually all the data points at each frequency at each building. These curves are also drawn in Figures 4 and 5. This is a new and useful result that enables reasonable bounds to be estimated for the propagation data.

The regression results are tabulated in Table 1. They clearly show a small but significant departure from the 45 degree line as the frequency increases. While the lines converge to common values at the higher power levels, i.e., close in, somewhat unexpectedly they deviate so that the relative received power is higher at the higher frequency as the path loss increases.

The 4.0 GHz data lie, in general, at higher relative power values than the 1.7 GHz points or 850 MHz data. The differences in some cases are as much as 15 dB. It is also useful to note that the enhancement of relative level above the 850 MHz data occur where the signals are the weakest (i.e., where the path loss is greatest). Since the frequency-related free space path loss would increase only about 6 or 12 dB at 1.7 or 4.0 GHz, respectively, absolute signal levels could be higher at the higher frequency as well, in this region. This agrees with visual observations at 4.0 GHz on several occasions while making the measurements. The enhancement of the 1700 MHz signal is not as great, and was not obvious during the measurements.

While the intercepts for 1.7 and 4 GHz regression lines are close at each building, the deviation of the intercepts from zero at OFC/NCO is puzzling. There may be some error introduced in extrapolating the data into the close-in region, since this extrapolation must be extended further at OFC/NCO.

Next, the variation of relative received power with distance was studied. Figures 7 and 8 show examples of the relative power, referenced to the power at 0.3 m, at two frequencies in building OFC/NCO. The distance is plotted on a logarithmic scale. As expected, the power falls off with distance. Characterizing this fall-off was somewhat challenging. Piecewise linear approximations, as well as a two-path model together with an attenuation term, were considered. Neither model is intuitively satisfying in this cluttered environment. Hence the approach taken was to apply a simple free space + linear path attenuation model. The signal clearly expands from the transmitting antenna. It passes through walls and other obstructions. As the number of these obstructions increase, their effect may be approximated by some attenuation coefficient in dB/m.

When this model was applied to the data, the results were as good or better than the first two approaches outlined above over the span of the data. Since this model is also closer to the physical reality, it was decided to use it on all the data. However, it must be borne in mind that the model may not apply outside the range of the data, and that it should be used only inside the building.

In figures 7 and 8, the model fit was optimized by varying the attenuation coefficient alone. No offset to the free-space portion of the model was allowed. The model regression lines and suggested upper and lower bound lines, based on twice the rms fractional deviation from the regression for that data, are shown as well. Table 2 shows the regression parameters for the free space + linear path attenuation model, at these locations.

The figures and table 2 show that the model fits the data satisfactorily. The variation of the linear attenuation coefficient with frequency is small, yet consistently decreasing with increasing frequency. Their effect in dB over long distances is sufficient to account for the observed reduction in path attenuation with increase in frequency. Their values at each frequency are also somewhat different for the two buildings. The building OFC/NST, with more metallic walls and partitions, shows smaller attenuation coefficients at corresponding frequencies. This may imply that the propagation in this building is more by reflection than direct transmission through walls.

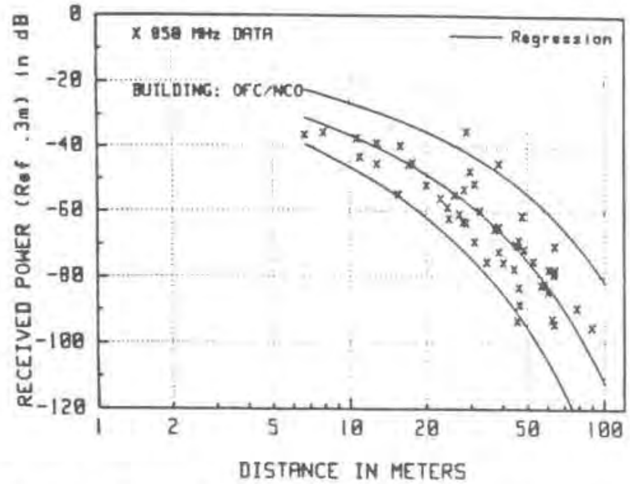

Figure 7. Received power at 850 MHz in OFC/NCO, relative to the power at 0.3 m shown against the distance on a logarithmic scale. The central curve is the model regression line. the side curves are the ± two fractional deviation bounds.

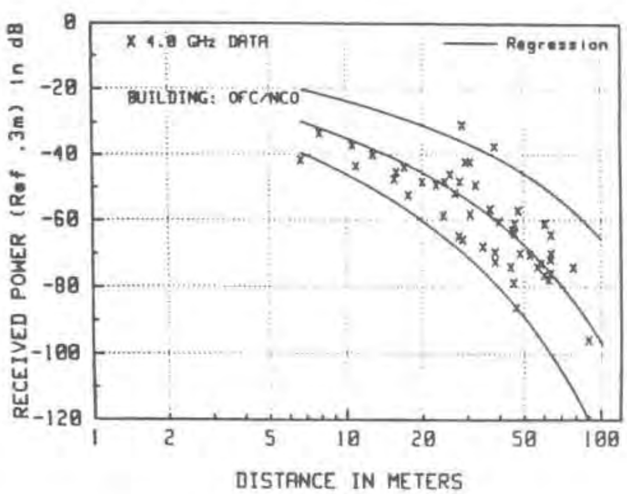

Figure 8. Received power at 4.0 GHz in OFC/NCO, relative to the power at 0.3 m shown against the distance on a logarithmic scale. The central curve is the model regression line. the side curves are the ± two fractional deviation bounds.

The standard deviation of the power data from the regressions are all between 8 and 10 dB. This difference is not significant for practical purposes. Since the data again exhibits increasing spread as the distance between the transmitter and receiver increases, the rms fractional deviation was found to be a more useful parameter in bounding the data. The data bounds drawn in these figures are also at $\pm 2\sigma_d$, chosen conservatively to enclose most of the data points. The few points that lie significantly above the upper bound line were found to be direct line-of-sight data.

The variation in the standard fractional deviation is slightly larger in OFC/NST. This may be due to the smaller data sample in this building.

DISCUSSION

Universal portable communications could be provided with low power transmitters and low antenna heights, using relatively small coverage areas compared to today's mobile radio systems. In such a system, a densely inhabited area such as a multi-story office building would have a large number of small coverage areas located within the building, perhaps a few per floor. Therefore, interference between neighboring buildings or other floors is a significant concern.

The two buildings under study, while different in interior construction, were covered with metal or metallized glass skins. This may explain the relative similarities in the delay spread results. Observation of the delay-spread profiles indicated that the signals appeared to be mostly confined inside the buildings, especially at the higher frequencies. At 850 MHz, some small returns at larger distances were occasionally visible. Thus the delay spread profiles would essentially measure the size of the buildings. In the absence of interior "cavity-like" effects, the delay spread numbers would also be bounded. This may explain why the rms delay spread results are quite low for these two buildings. This would also indicate that interference between adjacent buildings may not be great. Furthermore, the interference may be reduced by operating at the higher frequencies.

The linear path attenuation also appeared to decrease as the frequency increased. As indicated earlier, even the absolute 4.0 GHz signal level was, on occasion, stronger than the other two frequencies. There may also be "waveguide" effects, especially in OFC/NST which had more metal partitions and walls.

If the primary propagation impairment is absorption as the radio waves travel through the interior walls, any difference in absorption at the two frequencies would show up as a deviation of the slope of the power vs. power regression line from unity. If, on the other hand, the primary mechanism in the propagation channel is reflection from the walls and structures, any differences at the two frequencies would be seen as an offset of the intercept from the origin.

Table 2 seems to indicate that the metallic partitions and walls in OFC/NST reflected all frequencies equally well. OFC/NCO, with its greater use of non-metallic structures, seems to show differences in both the transmitted and reflected components as the frequency increases. However, it must be emphasized that these comments are tentative, and based on relatively small samples. Furthermore these comments are based on extrapolation to short distances where there were no data points.

The behavior of relative path loss with distance was also studied. The present results could be reasonably fitted to a free-space + linear path attenuation model. This approach is intuitively satisfying and does not result in unexplainable distance exponents. Clearly, caution must be exercised if the model is used outside the present range of measurements. It, most certainly, should not be extended to locations outside a building.

It is worthwhile re-iterating that these results are relative to the power received at 0.3 m. The absolute power levels at that reference distance would, of-course, depend on the frequency, transmitter power, and the antennas, and could be easily calculated using Friis' transmission formula.

SUMMARY

Time delay spread and signal level measurements were made at 850 MHz, 1.7 GHz and 4.0 GHz inside two dissimilar office buildings. These are the first reported comparative three-frequency measurements.

The relatively open construction and low absorption of the interior walls, coupled with the strongly attenuating exterior walls, kept the rms time delay spread mostly under 100 ns in OFC/NCO. In OFC/NST, the metallic baffle-like interior construction produced the same result. Rms time delay spreads measured at the three frequencies appear to be statistically equal to a first order, within the observed range of values.

Received power levels, relative to the power at 0.3 m separation, were statistically nearly equal at the three frequencies to a first order. The 4.0 GHz relative signal, however, was often stronger in the more metallic building, OFC/NST.

The power-distance relationship could be represented by a free-space + linear path attenuation model. The fitted model curves showed a smaller linear path attenuation coefficient as the frequency increased. The differences in the attenuation coefficients may reflect the dissimilarities in the buildings.

The rms value of fractional deviation of power from the regression line was a good measure of the spread of the data in all cases, when the power was calculated relative to the received power at 0.3 m.

Overall, it was concluded that radiowave propagation was the same over the range of frequencies studied within these buildings. More measurements are needed to draw generalized conclusions.

ACKNOWLEDGEMENTS

We thank H. W. Arnold and D. C. Cox at Bellcore for their support, guidance, commentary and suggestions. We also thank T. Walzman, J. Waldhuter, and W. Beaver of the NYNEX Science and Technology Center.

REFERENCES

1. Cox, D. C.: "Universal Digital Portable Radio Communications", Proc. IEEE, Vol. 75, No. 4, pp 436-477, April 1987.
2. Bello, P. A. and Nelin, B. D.: "The Effect of Frequency Selective Fading on the Binary Error Probabilities of Incoherent and Differentially Coherent Matched Filter Receivers", IEEE Trans. Commun. Syst., Vol. CS-11, pp 170-186, June 1963.
3. Jakes, W. C: editor, "Microwave Mobile Communications", John Wiley and Sons, 1974.
4. Devasirvatham, D. M. J.: "Time Delay Spread Measurements of Wideband Radio Signals Within a Building", Electronics Letters, Vol. 20, No. 23, pp 950-951, 8th November 1984.
5. Devasirvatham, D. M. J.: "Time Delay Spread and Signal Level Measurements of 850 MHz Radio Waves in Building Environments", IEEE Trans. Ant. and Prop., Vol. AP-34, No. 11, pp 1300-1305, November 1986.
6. Devasirvatham, D. M. J.: "A Comparison of Time Delay Spread and Signal Level Measurements Within Two Dissimilar Office Buildings", IEEE Trans. Ant. and Prop., Vol. AP-35, No. 3, pp 319-324, March 1987.
7. Devasirvatham, D. M. J.: "Multipath Time Delay Spread in the Digital Portable Radio Environment", IEEE Communications Magazine, Vol. 25, No. 6, pp 13-21, June 1987.
8. Pahlavan, K., Ganesh, R., and Hotaling, T.: "Multipath propagation measurements on manufacturing floors at 910 MHz.", Electronics Letters, Vol. 25, No. 3, pp 225-227, February 2, 1989.
9. Rappaport, T. S.: "Characterization of UHF Multipath Radio Channels in Factory Buildings.", IEEE Trans. Ant. and Prop., Vol. AP-37, No. 8, pp 1058-1069, August 1989.
10. Devasirvatham, D. M. J., Murray, R. R., and Banerjee, C: "Time Delay Spread Measurements at 850 MHz and 1.7 GHz Inside a Metropolitan Office Building", Electronics Letters, Vol. 25, No. 3, pp 194-196, 2nd February 1989.
11. Murray, R. R., Arnold, H. W., and Cox, D. C.: "815 MHz Radio Attenuation Measured Within A Commercial Building", Proc. IEEE Antennas and Propagation International Symposium, 1986, Vol. 1, pp 209-212, Philadelphia, Pennsylvania, June 8-13, 1986.

Table 1. Power Regression against 850 MHz Relative Power Data

Relative Power Regression						
Location	Freq.	Slope	Intrcpt dB	Corr.	Std. Dev. dB	Std. Fract. Dev
OFC/NCO	1.7 GHz	0.88	-6.6	0.97	4.1	0.064
	4.0 GHz	0.79	-7.6	0.93	5.6	0.096
OFC/NST	1.7 GHz	0.92	-0.5	0.97	3.8	0.076
	4.0 GHz	0.85	+0.6	0.96	3.9	0.094

Table 2. Free Space + Linear Path Attenuation Model Regression

Path attenuation Regression					
Location	Freq.	Atten dB/m	Corr.	Std. Dev. dB	Std. Fract. Dev.
OFC/NCO	850 MHz	0.62	0.87	8.4	0.13
	1.7 GHz	0.57	0.84	8.5	0.13
	4.0 GHz	0.47	0.82	8.6	0.15
OFC/NST	850 MHz	0.48	0.85	8.0	0.14
	1.7 GHz	0.35	0.77	9.5	0.18
	4.0 GHz	0.23	0.77	8.7	0.19

TIME AND FREQUENCY DOMAIN MODELS FOR INDOOR RADIO PROPAGATION

K. Pahlavan and R. Ganesh

Electrical Engineering Department
Worcester Polytechnic Institute
Worcester, MA 01609. USA

S. J. Howard

Raytheon Company
1001 Boston Post Road
Marlboro, MA 01752. USA

Abstract

Time domain and frequency domain statistical models for computer simulation of the fading multipath indoor radio channels are compared. In the time domain model, channel pulse response is formed by addition of several pulses arriving at the receiver from different paths . The statistics of arrival time and strength of paths determined from propagation measurements in [1][12] are used for computer simulation of the channel wideband characteristics. In the frequency domain model, the frequency response of the channel is modeled as an autoregressive (AR) process identified by the location of its poles. The statistics of the location of the poles determined from propagation measurements in [2] are used to regenerate the channel wideband characteristics. The models are then compared in terms of simplicity of the computer simulations and accuracy to represent the vital parameters used in performance prediction of wideband communication systems.

1. Introduction

Analysis of radio propagation in an indoor environment is very complex, because the received signal usually arrives by several paths reflected by walls, ceilings, and other fixed and moving objects around the transmitter and the receiver. The difference in the arrival time of the signal from various paths is proportional to the length of the path traveled, which is affected by the size and architecture of the building and the location of the objects around the transmitter and the receiver. The strength of the signal arriving by such paths depends on the attenuation caused by passage or reflection of the signal from various objects in the area. The deterministic analysis of radio propagation in such an environment is extremely difficult, and one may resort to statistical analysis. A mathematical model is formed for the channel, and the statistics of the model parameters are determined by using the measured channel characteristics for various locations of the transmitter and the receiver in a building.

The first narrowband measurements of radio propagation within buildings was performed by British Telecom [3] and the first multipath spread measurements by Bell Comm. Research [4]. The first statistical model of the channel was introduced by the AT&T Bell Laboratories [5] and further expanded in [1][12]. All these measurements and modeling as well as numerous other works in recent years in this area are concerned with time domain modeling of the channel. More recently, the autoregressive modeling of the indoor radio channel based on frequency domain measurements has been studied [2]. In this paper time domain [1][12] and frequency domain statistical models [2] for the indoor radio channel are examined and compared.

The frequency domain measurement [2] provides coherent measurement of the frequency domain characteristics of the channel from which the time domain response can be determined. Since the time domain measurements [1,3,4,6] are not coherent, the phase associated to each path is not measured and exact calculation of the frequency domain characteristics is not feasible. With the frequency domain autoregressive model, the paths can be classified into clusters easily [2], while it is not that simple to identify the clusters in

This work was supported in part by National Science Foundation under grant NCR-8703435 and a fellowship from the Raytheon Company.

the time domain modeling. With the time domain measurement system, wideband channel impulse response can be measured at twice the rate of variations of the channel when either the transmitter (receiver) is moved or moving objects get close to them [7]. The frequency domain measurement system explained here is not fast enough for these measurements.

Section 2 describes the experimental systems used for the measurements of the channel characteristics in time and frequency domains. Section 3 provides the mathematical model for the time domain characteristics of the channel and gives the statistics of the parameters of the model obtained from the experimental measurements. Section 4 describes the autoregressive model for the frequency domain characteristics of the indoor radio channel. Section 5 provides results and section 6 gives the summary and conclusions.

2. Measurement System

The main component of the frequency domain measurement system is a network analyzer which outputs a swept frequency signal and analyzes the received signal [2]. The signal generated by the network analyzer is used as the input to a $45\ dB$ transmitter RF amplifier. The output of the RF power amplifier is propagated by a dipole antenna. The signal from the receiver dipole antenna is passed through an attenuator and a series of amplifiers with a gain of $60\ dB$. The output of the amplifiers is returned to the network analyzer to determine the frequency response of the channel. The measured data is then read and stored by the PC controller for further analysis. The network analyzer is also equipped with the Fourier transform board which provides the time domain response of the channel.

For the results presented in this paper, the center frequency is $1\ GHz$ and a $200\ MHz$ bandwidth is swept by the network analyzer. The $200\ MHz$ bandwidth in the frequency domain gives an equivalent resolution in the time domain of $5\ ns$, which is what many of the time domain systems are capable of producing. The components used in the construction of the measurement system are rated for linear operation in the $1\ GHz$ range.

Fig. 1 shows a plot of the magnitude and phase of a typical frequency response $H(f, x)$ measured at a location x, and the corresponding magnitude of the time domain response $|h(\tau, x)|$ obtained from the inverse Fourier transform. The magnitude of the frequency response in dB, the phase of the frequency response in degrees, and the magnitude of the time response on a linear scale are shown. The frequency response consists of 801 complex samples at a frequency spacing of $0.25\ MHz$ for a frequency span of $200\ MHz$, which is centered at $1\ GHz$. From this frequency response a time response of $4000\ ns$ duration is derived. The time response is truncated to show only that portion with significant energy. The frequency selective nature of the channel is seen to result in deep nulls at certain frequencies. The phase is linear for most of the frequency band, except for those frequencies at deep nulls where a phase jump is observed. The time domain response illustrates the multipath propagation which causes the frequency selectivity.

Alternatively, the time domain response could be measured directly by modulating narrow pulses [12]. A carrier frequency of around 1 GHz is modulated by a train of narrow pulses providing 5nsec resolution for the received signal. The pulses are repeated every 500 ns. The modulated carrier is input to a $45\ dB$ amplifier and the output is transmitted with a quarter-wave dipole antenna placed about 1.5m above the floor level. The stationary receiver also uses a similar antenna to capture the radio signal. This is followed by a step attenuator and a low-noise high gain ($\simeq 60dB$) amplifier chain. The signal is then demodulated using an envelope detector whose output is displayed on a digital storage oscilloscope coupled to a PC with a GPIB instrument bus. The components used in the measurement set-up have a flat frequency response in the $1GHz$ range.

There are three phenomena affecting the channel characteristics at any location in an indoor channel. The first is the fluctuations in the received power. The second is the effect of multipath caused by fixed objects such as walls or ceiling, and the third is the effect caused by moving humans or objects, close to the transmitter and/or the receiver. All the measurement data used in this work, were collected when there was no traffic near the transmitter and the receiver. The effects of traffic and local antenna movements is reported in [7].

3. Time domain modeling

The mathematical model used for the complex low-pass impulse response of the indoor radio channel was originally suggested by Turin [6] for the mobile radio and is given by,

$$h(\tau, x) = \sum_{k=1}^{L} \beta_k(x)\delta(\tau - \tau_k(x))\ e^{j\theta_k(x)} \tag{1}$$

where $h(\tau, x), \beta_k(x), \tau_k(x), \theta_k(x)$ are the channel impulse response, path amplitude, path delay, and path phase associated with location x of the transmitter and the receiver.

In order to regenerate a set of measured profiles with a computer simulation, several statistics are required. The statistics of the arrival times are needed to identify the existence of a path at a given delay. The fluctuations in the path amplitudes should be fitted to a known probability distribution, identified with a set of parameters (usually mean and standard deviation). The functions relating the mean and standard deviation of this distribution to the path delay should be determined to regenerate the path amplitude accurately. Similar to [5,6] the phases θ_k are assumed *apriori* to be statistically independent uniform random variables over $[0, 2\pi)$.

The rest of this section provides the statistics for the data base described in [12] collected from two subclasses: manufacturing floor areas and college campus areas. Manufacturing floor areas represent large areas occupied by different machinery. The college campus areas represent a floor of a building, consisting of several rooms with different sizes having typical office furniture and various electronic equipment.

A simple statistical model for the arrival of the paths is a Poisson process [5], since the multipath propagation is caused by "objects", located randomly. However, the path arrival distribution governed by a Poisson hypothesis does not show close agreement to the empirical data [12]. This discrepancy reflects a tendency of the paths to arrive in groups, rather than in a random manner. To explain similar discrepancies, a Modified Poisson model was proposed by Suzuki for urban radio channel modeling [10] which was later on adopted for the modeling of indoor radio propagation [1][12].

For the Modified Poisson process, the probability of having a path in bin i is given by λ_i , if there was no path in the $(i-1)$st bin, or by $K_N\ \lambda_i$, if there was a path in the $(i-1)$st bin.

The comparison between the empirical path index distributions and the Modified Poisson distributions shows considerable improvement over those of the Poisson model [12]. This suggests that the paths do not arrive randomly but in groups, and the presence of a path at a given delay is greatly influenced by the presence or absence of a path in the earlier bins. Mathematically speaking, the Modified Poisson model utilizes the empirical probability of occurrence for each bin, while the Poisson model just uses the sum of the probabilities of occurrence for all bins. For the areas considered in this paper, the λ_i and K_i determined from the empirical data are given in [12].

The simple distribution for the statistics of the amplitude of the arriving paths is Rayleigh [5]. However, comparison between the theoretical and empirical data for Rayleigh, Weibull, Nakagami, Suzuki and lognormal distributions for the measurements used in this paper yields the closest fit for the log-normal distribution [12]. Usually, the Rician distribution is not considered for curve fitting, because it's theoretical moments can not be calculated on the dB scale. This results in less accurate curve fits [1,10,11] as compared with the other distributions.

The inhomogeneities of the indoor channel result in variations in the mean and variance of the amplitudes for different delays. To simulate these changing parameters, the distribution for their variations should be known. The scatter plots of mean and standard deviation of the Lognormal distribution versus delays are fitted to decaying exponentials of the form $Ae^{-\frac{\tau}{\Gamma}} + B$ where Γ is the decay rate, τ is the delay and A and B are constants. Fig. 2 shows these fits for the manufacturing areas. Note that the scatter plots give the values of the mean and standard deviation for the path amplitude, given the existence of a path at that delay. The Modified Poisson process decides whether or not, a path exists at a given delay. For the manufacturing floors, the decay rate Γ was 25 ns for the mean and 20 ns for the standard deviation. In these areas most of the received power is concentrated in the initial paths resulting in a faster decay of the received power with delay. On the other hand, the college office areas exhibited a wider spread of power in delay and thus a slower decay for the received power with delay. In the college offices, the decay rate Γ was 177 ns for the mean and 141 ns for the standard deviation.

An important parameter in the time domain channel impulse responses is the RMS delay spread which is given by:

$$\sigma_\tau \equiv (\overline{\tau^2} - (\overline{\tau})^2)^{0.5} \qquad (2.a)$$

where

$$\overline{\tau^n} \equiv \frac{\sum_k \tau^n_k(x)\, \beta^2_k(x)}{\sum_k \beta^2_k(x)}, \qquad n = 1, 2. \qquad (2.b)$$

The RMS delay spread is a measure of the spread of the transmitted signal for the given location of the transmitter and the receiver. For radio communication in the indoor environment, the rms delay spread of the channel gives a measure of performance degradation in the system, caused by intersymbol interference. It is an important parameter for determining data rate limitations of standard and equalized modems [8] and it is also used for performance prediction of spread spectrum modems [9].

4. Autoregressive Modeling in Frequency domain

Fig. 1 shows a sample frequency response of the indoor radio channel measured with a network analyzer. The measurement has been made at a set of evenly spaced frequencies,

$$f_n = f_o + nf_s, \qquad (3)$$

where $f_o = 900MHz$ is the lowest frequency in the band of study and $f_s = 0.25MHz$ is the frequency sample spacing. Assuming an autoregressive model for the measured frequencies we have:

$$H(f_n, x) = \sum_{i=1}^{p} a_i\, H(f_{n-i}, x) + V(f_n). \qquad (4)$$

where $H(f_n, x)$ is the nth sample of the complex frequency domain measurement at location x, p is the order of the model, and $V(f_n)$ is a complex white noise sequence. The parameters of the model are the coefficients of the linear filter, a_i, that predicts the value of $H(f_n, x)$ based on previous values. Autoregressive modeling of the time domain data used for spectral estimation and the techniques for determination of the coefficients of the AR process are well known in the literature [2].

In the AR modeling of the channel it is assumed that the observed samples of the process are the outputs of a linear filter with transfer function

$$G(z) = \frac{1}{1 - \sum_{i=1}^{p} a_i\, z^{-p}} \qquad (5)$$

driven by a white noise signal $V(f_n)$. This filter is also represented by the p poles in the complex z-plane. Having solved for the a_i, one sample of the random process $H(f, x)$ can be generated from (2) using a random sequence $V(f_n)$.

To determine the validity and the order of the model 128 frequency domain measurements taken in two office areas were analyzed. A scattered plot of the poles that resulted from a 5th order process for these measurements is shown in Fig. 3. Similar to the earlier reports, the dominance of the two poles confirms the adequacy of the second order model for all the measurements. Table 1. represents the first and second order statistics of the location of the first and the second pole. Two significant poles can be interpreted as two significant clusters of multipath arrivals [2]. The interpretation of a pole as defining a cluster of paths and the distance from the unit circle as defining the power in the cluster provides a useful physical interpretation for the AR model introduced in this paper.

In the conventional parametric spectral estimation, a pole close to the unit circle represents significant power at the frequency related to the angle of the pole. The frequency is calculated as $f = arg(z_i)/2\pi T_s$, where T_s is the sampling time. In our application, the modeling is in the frequency domain and a pole close to the unit circle represents significant power at the time related to the angle of the pole. The time is calculated as $t = -arg(z_i)/\omega_s$, where $\omega_s = 2\pi f_s$ ($\frac{1}{0.25}\,MHz = 4000\ ns$). The arrival of the significant paths in all measurements are from $150\ ns$ to $550\ ns$, which corresponds to the angular range of $-3\pi/40$ to $-11\pi/40$.

An important function in frequency domain modeling is the complex autocorrelation function of the frequency response defined as:

$$R(k, x) = \frac{1}{N} \sum_{n=1}^{N-k} H(f_n, x) H^*(f_{n-k}, x)\ df, \qquad k => 0. \quad (6)$$

The $3\ dB$ width of $|R(\Delta f, x)|$ is a measure of the similarity or coherence of the channel in the frequency domain, which is inversely proportional to the RMS multipath spread of the channel.

For the time responses derived from frequency domain measurements, the RMS delay spread τ_{rms} is computed by (3). Using the inverse relationship between width in the frequency domain and duration in the time domain, a relationship of the form $B_c = C\tau_{rms}^{-\beta}$ between the $3\ dB$ width (MHz) of the frequency correlation function and the RMS delay spread (ns) of the channel in time domain is determined from a linear regression of the logarithms. Fig. 4 shows the scatter plot of $3\ dB$ width of the frequency correlation function versus the corresponding RMS delay spread of two experiments on a log-log scale and the lines with the MMSE fit to the logarithm of the data. In this plot $C = 80$ and $\tau = .95$.

5. Results of Simulations

This section provides the results of computer simulations for the frequency and time domain modelings of the channel. Results of simulation are compared to those obtained empirically.

The first step in time domain simulation is to generate the path arrival times. The basic model for simulation of the arrival times is the Modified Poisson branching process. The delay axis is divided into bins of length 5 nsecs. The simulation for each profile starts with bin 1. The optimum values of K_i and λ_i, are used to determine the presence or absence of a path in bin i. For the simulation of the Poisson arrivals the average arrival rate is used for all bins and $K_i = 1$.

Next the path amplitudes are generated from the Lognormal distribution for each bin with a path. The means and the standard deviation of the Lognormal distribution are determined from the associated exponential fits. To complete the picture, the phase angles could be chosen from a uniform distribution and added to each path.

To evaluate the performance of this simulation model, the cumulative distribution of rms delay spreads computed from the simulated profiles is compared with that obtained from the measured profiles. Fig. 5 and Fig. 6 show these comparisons for the manufacturing floors and college offices respectively. The dashed lines in these figures are the cumulative distributions of the rms delay spreads computed from simulation. The path amplitudes are simulated based on the exponential fits to the scatter plots of the means and standard deviations. The solid lines in Fig. 5 and Fig. 6 represent the actual cumulative distribution of the rms delay spreads measured from the two areas respectively. The match between the empirical and the simulated distributions can be seen to be very good.

As mentioned in Section 1, the statistical model given in [5] considers Poisson path arrivals and Rayleigh amplitudes. For purposes of comparison, simulation was also carried out for this Poisson/Rayleigh combination. For the Poisson arrivals, the mean path arrival rate was used to determine the presence or absence of a path in any bin. The measured powers in each bin were used to determine the Rayleigh amplitude of an existing path. The rms delay spread was computed for each of these simulated profiles and their distribution function is shown in Fig. 5 and Fig. 6 for the two areas, respectively. The match between the Modified Poisson/Lognormal simulation and the empirical results is significantly better than that provided by the Poisson/Rayleigh simulation. The weakness of the Poisson/Rayleigh simulation is more obvious in the case of manufacturing floors.

For the frequency domain measurements the statistics of the location of the poles are used to identify the poles associated with each location. Then the channel impulse frequency response is generated by driving a filter with the given poles with white noise. The inverse Fourier transform of the process is taken to represent the time domain response of the channel. It is assumed that the variations of the magnitude and the phase of both poles form a Gaussian random variable with the first and second order statistics given in Table 1. t Fig. 7 shows the CDF of the $3\ dB$ width of the frequency correlation function for both the original measurements and the regenerated data from the two pole model. Fig. 8 shows the CDF of the RMS delay spread for both the original measurements and the regenerated measurements. The frequency domain characteristics shows a closer agreement with the original measurements, because the parameters of the model are determined from the second order statistics of the frequency domain autocorrelation function.

6. Summary and Conclusions :

The statistical parameters required for the generation of the channel characteristics in time and frequency domain were given. For the time domain modeling, the Poisson/Rayleigh model and modified Poisson/log-normal model were examined. To simulate the Poisson/Rayleigh model the statistics of the variance of the paths at each bin and the average arrival rate of the paths were needed. For the modified Poisson/log-normal model, the average arrival rate, modified Poisson process coefficient K_i, the mean and the standard deviation of the log-normal distribution for each bin were needed for simulation. It was shown that all these parameters decay exponentially with the arrival time of the paths. The best fit to the CDF of the RMS multipath spread was provided by the Modified Poisson/Lognormal model.

The frequency domain model required generation of location of two poles which needed even less parameters than those of the Poisson/Rayleigh model. Both frequency domain and time domain responses were generated from the two pole autoregressive model of the channel. It was shown that the channel simulation using frequency domain AR model provides very close results with the empirical data related to CDF of the 3-dB width of the frequency correlation function. The CDF of the RMS multipath spread generated from frequency domain channel simulation model showed closer agreement than Poisson/Rayleigh model. However, the modified Poisson/log-normal model shows the closest fit to the empirical CDF's of the RMS delay spread of the channel.

REFERENCES

1. R. Ganesh and K. Pahlavan, "On the Modeling of the Fading Multipath Indoor Radio Channels", IEEE Globecom, Dallas, Texas, Dec. 1989.
2. S.J. Howard and K. Pahlavan," Statistical Autoregressive Models for the Indoor Radio Channel", IEEE Globecom, San Diego, CA, Dec. 1990.
3. S.E Alexander,"Radio Propagation within Buildings at 900MHz", IEE Elect. Lett., pp913-914, Oct. 14, 1982.
4. D.M.J. Devasirvatham, "Time Delay Spread Measurements of Wideband Radio Systems Within a Building", IEE Electronics Letters, pp. 949-950, November 1984.
5. Saleh A A M and Valenzuela R A : 'A Statistical Model for Indoor Multipath Propagation', IEEE-JSAC, vol SAC-5, No. 2, Feb 1987, pp 128-137.
6. Turin G L, Clapp F D, Johnston T L, Fine S B and Lavry D : 'A Statistical model of urban multipath propagation', IEEE Trans.Veh.Technol., Feb 1972, pp 1-9.
7. Ganesh R and Pahlavan K : 'Statistics of Short Time Variations of Indoor Radio Propagation', Proceedings of the IEEE ICC, 1991.
8. Sexton T A and Pahlavan K : 'Channel modeling and Adaptive equalization of Indoor radio communication', IEEE JSAC, Jan 1989.
9. Pahlavan K and Chase M : 'Spread Spectrum Multiple Access performance of orthogonal codes for Indoor Radio Communication', IEEE Trans. on Communication, May 1990.
10. Suzuki H : 'A Statistical Model for Urban Radio Propagation',IEEE Trans. on Comm, Vol COM-25, July 1977, pp 673-680.
11. Lorentz R W : 'Theoretical distribution of multipath fading process in mobile radio and determination of parameters by measurements', Deutsche Bundepost Forschungsinstitut technical report 455 TBr 66, March 1979. (in German)
12. Ganesh R and Pahlavan K : 'Statistical Modeling and Computer Simulation of the Indoor Radio Channel', to be published in IEE Proceedings on Communications, Speech and Vision, England in June/August 1991.

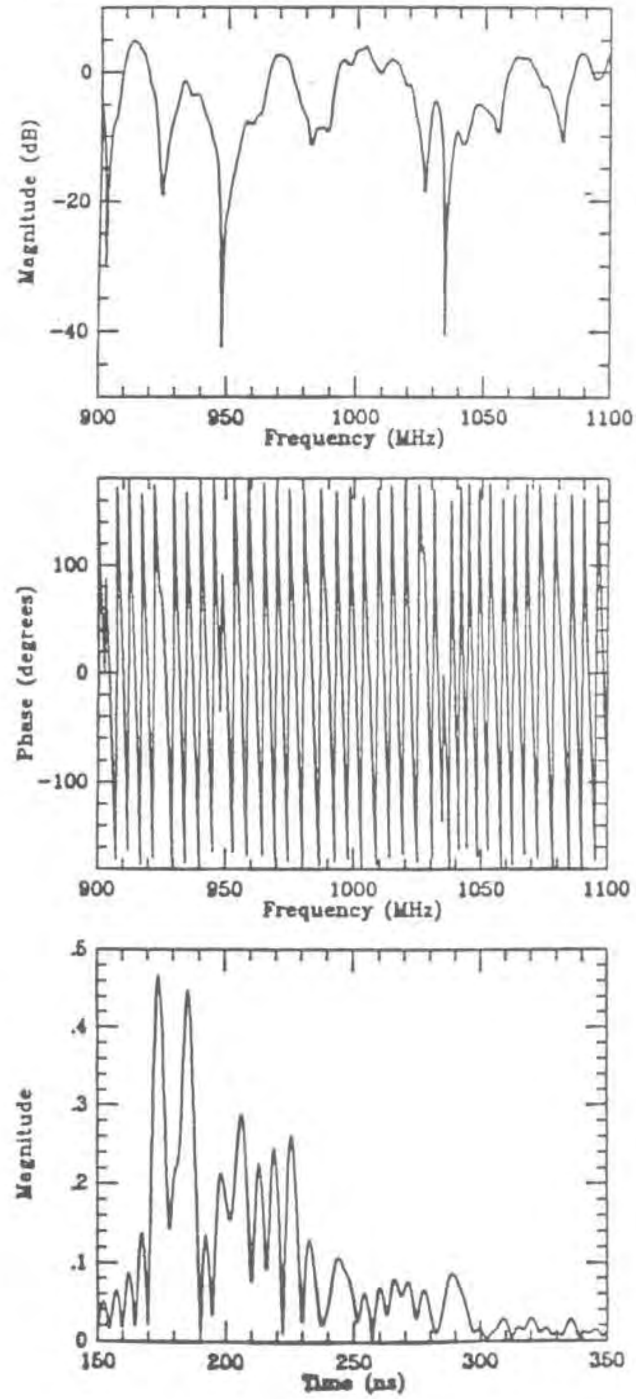

Figure 1. A sample time-frequency response of the indoor radio channel measured with a network analyzer. The top is the magnitude and the middle is the phase of the frequency response; the bottom is the time domain impulse response of the channel.

TABLE 1
Statistics of the location of the first two poles for the office experiment.

EXPERIMENT	parameter	average	stan. dev.	minimum	maximum
office	$\lvert p_1 \rvert$	0.9874	0.006098	0.9648	0.9986
	ANG(p_1)	-18.92	1.919	-22.75	-14.73
	$\lvert p_2 \rvert$	0.849	0.08524	0.5701	0.978
	ANG(p_2)-ANG(p_1)	-7.202	1.691	-10.81	-2.459

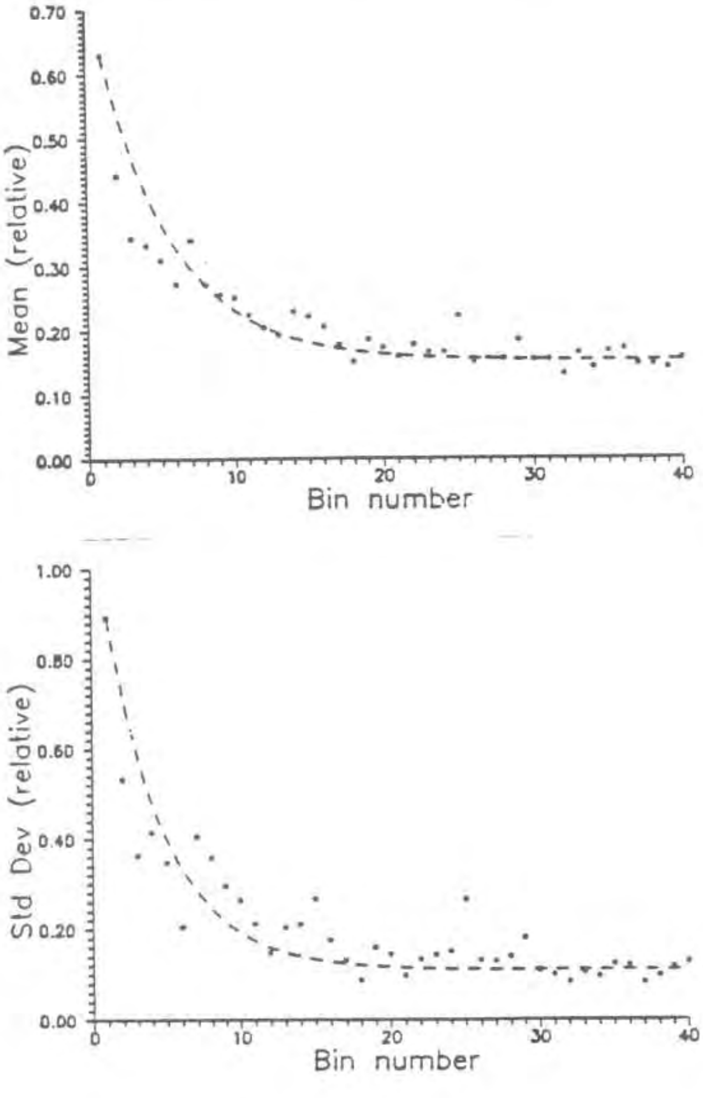

Figure 2. The mean and standard deviation of the lognormal distribution for the path amplitudes, in the manufacturing floor areas. The dashed lines are the exponential fits.

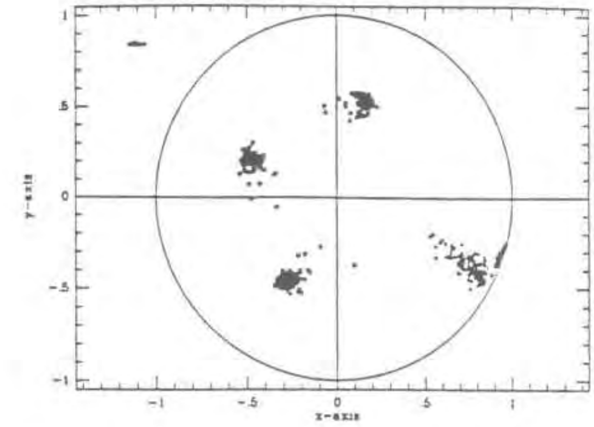

Figure 3. The scattered plot of the poles for the fifth order AR model collected from 128 measurements in the office environment.

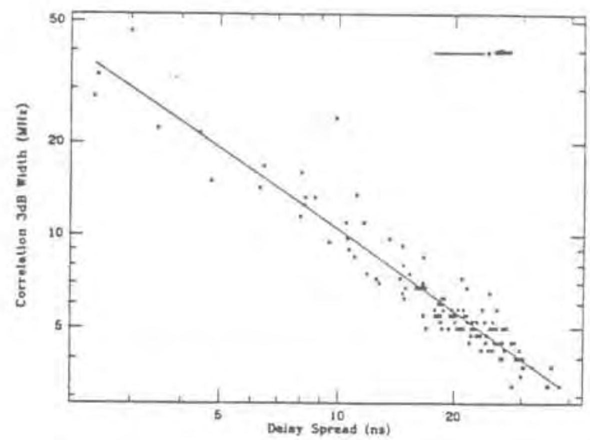

Figure 4. Scattered plot of the 3-dB width of the frequency correlation function versus RMS multipath spread in the log-log scales and the best fit line for two sets of measurements.

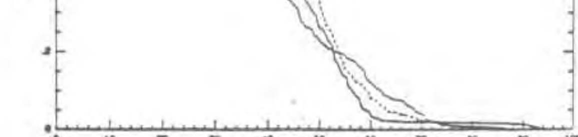

Figure 5. The CDF of the RMS multipath spread from the original measurements and the regenerated profiles from the Poisson/Rayleigh model and modified Poisson/log-normal time domain models in manufacturing floors.

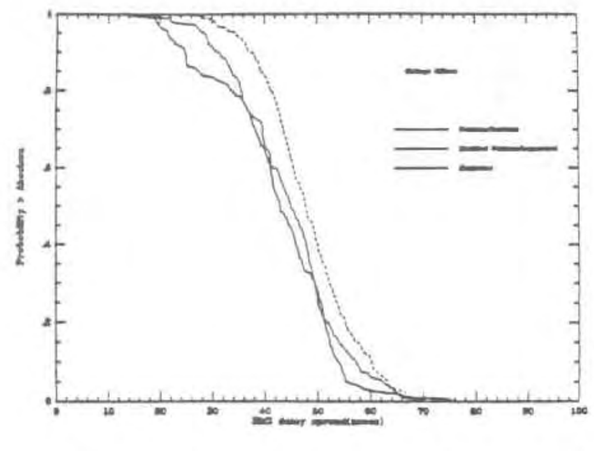

Figure 6. The CDF of the RMS multipath spread from the original measurements and the regenerated profiles from the Poisson/Rayleigh model and modified Poisson/log-normal time domain models in office environments.

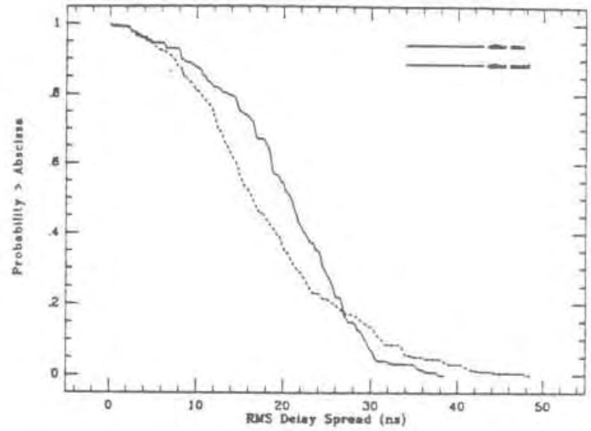

Figure 8. The CDF of the RMS multipath spread from the original measurements and the regenerated profiles from a two pole AR model.

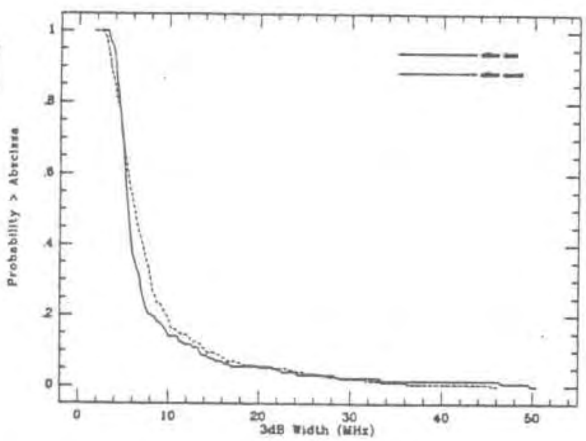

Figure 7. The CDF of the 3-dB width of the correlation function from the original measurements and the regenerated profiles from a two pole AR model.

Simulation of Multipath Impulse Response for Indoor Diffuse Optical Channels

John R. Barry
Joseph M. Kahn
Edward A. Lee
David G. Messerschmitt

Department of Electrical Engineering and Computer Sciences
University of California
Berkeley, CA 94720

ABSTRACT

We present a recursive method for evaluating the impulse response of an indoor free-space optical channel with Lambertian reflectors. The method, which accounts for multiple reflections of any order, enables accurate analysis of the effects of multipath dispersion on high-speed indoor optical communication. We present a simple algorithm for computer implementation of the technique. We also present some computer simulation results, which indicate that reflections of multiple order are the dominant source of intersymbol interference for an indoor optical communication system, and that that reflections of multiple order have a significant effect on the capacity of the indoor optical channel.

1. INTRODUCTION

The desire for inexpensive and high-speed data links in wireless local-area network applications has prompted the recent interest in indoor optical communication [1—11]. In an indoor environment, an optical signal in transit from transmitter to receiver undergoes temporal dispersion due to reflections from walls and other reflectors; this dispersion causes *multipath fading*—a primary impediment to communication at high speeds.

Multipath dispersion is completely characterized by an impulse response $h(t)$, defined such that the intensity of the optical signal detected by the receiver is the convolution of $h(t)$ with the intensity of the transmitted optical signal. In this paper we present a method for numerically calculating the impulse response of a room with an arbitrarily placed transmitter and receiver. Once calculated, the impulse response can be used to analyze or simulate the effects of multipath dispersion on indoor optical communications systems.

Other researchers have modeled indoor reflections of infrared with the purpose of determining the distribution of power throughout a room. Gfeller and Bapst present such an analysis in [1] that accounts for single reflections only; Hash et. al. extended their procedure to include double reflections as well [12]. The simulations in these works were meant for a link budget analysis; thus, only the total power reaching the receiver was estimated. In other words, they were concerned only with the time integral of $h(t)$. Since power budgets typically have built-in safety margins, the accuracy provided by considering only first and second order reflections was sufficient. Hortensius [13] extended the Gfeller and Bapst model to calculate an impulse response, accounting for single reflections only.

In contrast to prior work, the method described here can compute the impulse response accounting for any number of reflections. This allows accurate power distribution analysis, and, more importantly, accurate impulse-response analysis. The latter is necessary because signal power undergoing two or more reflections, although having a reduced amplitude, arrives at the receiver much later than lower-order reflections. This temporal spread is critical in high-speed applications, in which case higher-order reflections cannot be ignored.

In the next section we define the models upon which our procedure is based. In section 3 we describe our recursive algorithm for simulating a room's impulse response. In section 4 we discuss an implementation of this algorithm, and in section 5 we present some simulation results. In section 6 we briefly examine the effects the higher-order reflections have on system design.

2. MODELS

The impulse response of an actual room can be approximated by considering a rectangular cavity with the walls, ceiling, and floor modeled as Lambertian reflectors with different reflectivities. In this section we define the models for the source, reflectors, and receiver.

2.1. Source and Receiver Models

A diffuse optical source can be represented by a position vector $\mathbf{r}_S$, a normalized orientation vector $\hat{\mathbf{n}}_S$, a power P_S, and a radiation intensity pattern $R(\phi,\theta)$, where $R(\phi,\theta)$ is the optical power emitted from the source, per unit solid angle, at position (ϕ,θ) with respect to the source orientation $\hat{\mathbf{n}}_S$. Following Gfeller [1], we will model a source using a generalized Lambertian radiation pattern having uniaxial symmetry (independent of θ):

$$R(\phi) = \frac{n+1}{2\pi} P_S \cos^n(\phi), \qquad \phi \in [-\pi/2, \pi/2]. \quad (1)$$

Here, n is the *mode order* of the radiation lobe, which specifies the directionality of the source. This is illustrated in figure 1, where sources with higher directionality are seen to have larger mode numbers. The coefficient $(n+1)/2\pi$ ensures that integrating $R(\phi)$ over the surface of a hemisphere results in the source power P_S. Note that a Lambertian source has mode order $n = 1$.

To simplify notation, a point source $\mathbf{S}$ that emits a unit impulse at time zero will be denoted by

$$\mathbf{S} = \begin{bmatrix} \mathbf{r}_S \\ \hat{\mathbf{n}}_S \\ n \end{bmatrix} \quad (2)$$

where $\mathbf{r}_S$ is its position, $\hat{\mathbf{n}}_S$ is its orientation, and n is its mode number. Linearity allows us to consider only sources with unity power, since the resulting impulse response can be scaled for other sources.

Similarly, a receiving element $\mathbf{R}$ with position $\mathbf{r}_R$, orientation $\hat{\mathbf{n}}_R$, differential area A_R, and field of view FOV will be denoted by

$$\mathbf{R} = \begin{bmatrix} \mathbf{r}_R \\ \hat{\mathbf{n}}_R \\ A_R \\ FOV \end{bmatrix} \quad (3)$$

A receiver's field of view is represented by an angle FOV; the detector only sees light whose angle of incidence (with respect to the detector normal) is less than FOV. A limited field of view may be an inadvertent effect of detector packaging, or it may be used intentionally to reduce unwanted reflections or noise.

2.2. Reflector Model

In general, a reflection from a surface consists of a specular and a diffusive component [14]. We make the simplifying assumption that all reflectors are purely diffusive, ideal Lambertian [1, 12]. Hence, the radiation intensity pattern $R(\phi)$ emitted by a differential reflecting element is independent of the angle of the incident light. This allows us to decompose a reflection into two sequential steps: to find the reflection from a differential reflecting element with area dA and reflectivity coefficient ρ, first consider the element as a receiver with area dA, and calculate the power it receives dP. Next, model the differential reflector as a source with power $P = \rho dP$ and a Lambertian radiation intensity pattern ($n = 1$):

$$R(\phi) = (1/\pi) P \cos(\phi). \quad (4)$$

2.3. Line-of-Sight Impulse Response

Consider a source $\mathbf{S}$ and receiver $\mathbf{R}$, as specified by (2) and (3), in an environment with no reflectors; see figure 2. Using the models described above, we find the impulse response for this simple system to be a scaled and delayed delta function:

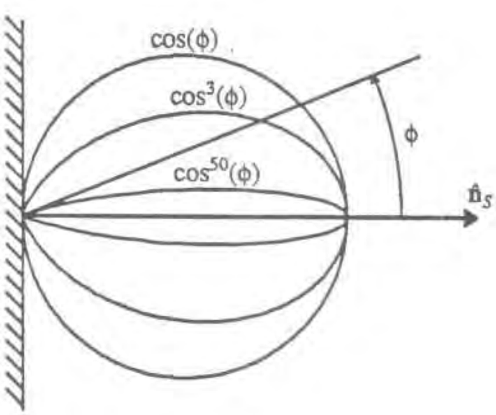

Figure 1. Normalized shape of the generalized Lambertian radiation intensity pattern. Reflectors are modeled with $n = 1$; their radiation pattern is a sphere. Sources with narrower beamwidths are modeled by $n > 1$.

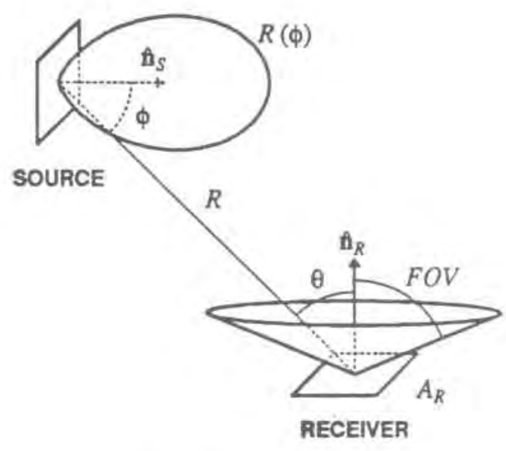

Figure 2. Geometry of source and detector, with no reflectors. The receiver field of view is illustrated by a cone.

$$h^{(0)}(t;\mathbf{S},\mathbf{R}) = \frac{n+1}{2\pi}\cos^n(\phi)\, d\Omega\, \mathrm{rect}(\theta/FOV)\, \delta(t - R/c),$$

where $d\Omega$ is the solid angle subtended by the receiver's differential area (assuming $A_R \ll R^2$):

$$d\Omega = \cos(\theta)\, A_R/R^2, \tag{6}$$

R is the distance between the source and receiver:

$$R = \| \mathbf{r}_S - \mathbf{r}_R \|, \tag{7}$$

θ is the angle between $\hat{\mathbf{n}}_R$ and $(\mathbf{r}_S - \mathbf{r}_R)$:

$$\cos(\theta) = \frac{\hat{\mathbf{n}}_R \cdot (\mathbf{r}_S - \mathbf{r}_R)}{R}, \tag{8}$$

ϕ is the angle between $\hat{\mathbf{n}}_S$ and $(\mathbf{r}_R - \mathbf{r}_S)$:

$$\cos(\phi) = \frac{\hat{\mathbf{n}}_S \cdot (\mathbf{r}_R - \mathbf{r}_S)}{R}, \tag{9}$$

the rectangular function is defined by

$$\mathrm{rect}(x) = \begin{cases} 1 & \text{for } |x| \le 1 \\ 0 & \text{for } |x| > 1 \end{cases}, \tag{10}$$

and c is the speed of light. Identities (8) and (9) rely on the fact that the orientation vectors $\hat{\mathbf{n}}_S$ and $\hat{\mathbf{n}}_R$ are normalized to have unit length.

3. MULTIPLE BOUNCE ALGORITHM

We will now describe our algorithm for calculating an impulse response. Given a particular source $\mathbf{S}$ and receiver $\mathbf{R}$ in a room with reflectors, light from the source can reach the receiver after any number of reflections. Thus, the impulse response can be written as an infinite sum:

$$h(t;\mathbf{S},\mathbf{R}) = \sum_{k=0}^{\infty} h^{(k)}(t;\mathbf{S},\mathbf{R}) \tag{11}$$

where $h^{(k)}$ is the response of the light undergoing exactly k reflections. The line-of-sight response $h^{(0)}$ is given by (5), while higher-order terms ($k > 0$) can be calculated recursively:

$$h^{(k)}(t;\mathbf{S},\mathbf{R}) = \frac{n+1}{2\pi}\int_S h^{(k-1)}\left(t - R/c; \begin{bmatrix} \mathbf{r} \\ \hat{\mathbf{n}} \\ 1 \end{bmatrix}, \mathbf{R}\right) \frac{\rho \cos^n(\phi)\cos(\theta)}{R^2}\, d\mathbf{r}^2 \tag{12}$$

The integration is performed with respect to $\mathbf{r}$ on the surface S of all reflectors. Here, $\hat{\mathbf{n}}$ is the normal to the surface S at position $\mathbf{r}$, ρ is the reflectivity of the reflector at position $\mathbf{r}$, $R = \|\mathbf{r} - \mathbf{r}_S\|$, $\cos(\phi) = \hat{\mathbf{n}}_S \cdot (\mathbf{r} - \mathbf{r}_S)/R$, and $\cos(\theta) = \hat{\mathbf{n}} \cdot (\mathbf{r}_S - \mathbf{r})/R$.

Equation (12) is our main theoretical result. Intuitively, it says that the k-bounce impulse response from a single point-source $\mathbf{S}$ can be found by first finding the distribution and timing of the power from $\mathbf{S}$ onto the reflecting walls; then, using the walls as a distributed light source, computing the $(k-1)$-bounce impulse response.

4. IMPLEMENTATION

The integral in (12) can be calculated numerically by breaking the reflecting surfaces into numerous small reflecting elements, each with area ΔA. Thus, $h^{(k)}(t)$ can be approximated by

$$h^{(k)}(t;\mathbf{S},\mathbf{R}) = \frac{n+1}{2\pi}\sum_{\text{all elements}} h^{(k-1)}\left(t - R/c; \begin{bmatrix} \mathbf{r} \\ \hat{\mathbf{n}} \\ 1 \end{bmatrix}, \mathbf{R}\right) \frac{\rho \cos^n(\phi)\cos(\theta)}{R^2}\Delta A \tag{13}$$

This spatial discretization will cause temporal discretization as well, turning the normally piecewise-continuous function of time $h^{(k)}$ into a finite sum of scaled delta functions; temporal smoothing can be achieved by subdividing time into bins of width Δt and summing the total power received in each bin.[1] The resulting histogram closely approximates the actual $h^{(k)}$, achieving equality as ΔA and Δt approach zero.

Direct implementation of (13) is not efficient for reflection orders k greater than two, because identical computations would then be performed multiple times. To see this, consider a room with walls subdivided into a total of N reflecting elements. Then, in calculating (13), a total of N^k *elementary* computations are performed, where one elementary computation is defined as the calculation of differential power and delay from a point source to a differential receiver, as in (5). Thus, an elementary computation consists of the collection of multiplications and vector dot-products described in (6) through (10). However, there are only $(N+1)^2$ unique elementary computations, corresponding to the line-of-sight impulse response from any element (including source) to any element (including receiver). Therefore, a more efficient approach would be to construct two look-up tables, each consisting of $(N+1)^2$ entries. The first, call it `dP(i,j)`, contains the differential power between element i and element j; the second, call it `tau (i,j)`, contains the delay between element i and element j. With these two tables, a numerical procedure is easily implemented, as illustrated by the following pseudocode:

```
function h(i, j, k)
begin
   if (k=0)
     return dP(i,j) × delta(t-tau(i,j))
   else
     return
       sum from r = 1 to N
          dP(i,r) × delta(t-tau(i,r))*h(r,j,k-1)
end
```

Here, `h(i,j,k)` is a function that returns the k-bounce impulse response $h^{(k)}(t)$ with element i as the source and

[1] Empirical evidence suggests that a good choice for the bin width is $\Delta t = \sqrt{\Delta A}/c$, where c is the speed of light.

element j as the receiver. Delays are obtained by convolving—the symbol $*$ denotes convolution—with a Dirac delta function. The reflectivity ρ_i of the i^{th} reflecting element is absorbed into the `dP(i,j)` table in the following way: first, the table is initialized to so that `dP(i,j)` contains the total line-of-sight power from element i received by element j; then, all entries `dP(i,j)` in which i is a reflector are scaled by ρ_i.

5. SIMULATION RESULTS

A computer program was written that implements the algorithm described in the previous section. The user can specify the various parameters listed in table 1. The elevation angles are defined with respect to the horizontal plane; thus a source that is pointing straight down has an elevation of −90°, and a receiver that is pointing straight up has an elevation of 90°. The final set of parameters in the table control the resolution of the simulation. Here, Δt is the bin width of the power histogram that approximates the impulse response, and *bounces* is the maximum number of reflections that are considered. The spatial resolution of the simulation is specified by the number of partitions per dimension; the total number of differential reflecting elements is then given by

$$N = 2(N_x N_y + N_x N_z + N_y N_z).$$

In figure 3 we show the simulated impulse responses $h^{(k)}$, $k \in \{0, \cdots, 5\}$, for the particular room configuration given in table 1. We were able to use higher spatial resolutions for the lower-order reflections, because their run-times are short; the number of reflectors for each bounce are indicated in table 2. The time origin is defined by the arrival of the line-of-sight impulse. Each of the responses are labeled by the total power they would carry if the source had power 1 Watt. Thus, $h^{(0)}$ is a delta function, scaled by 1.23 μW. The first-order response is seen to have four peaks, corresponding to the four walls of the room; the total power from once-reflected light is 0.505 μW. Total power is seen to decrease for each of the higher-order impulse responses; however, they tend to add to a significant amount, as shown in the sum impulse response at the bottom of the figure. Furthermore, this power arrives much later than that from lower-order reflections.

	parameter	value
room:	length	5 m
	width	5 m
	height	3 m
	ρ_{NORTH}	0.8
	ρ_{SOUTH}	0.8
	ρ_{EAST}	0.8
	ρ_{WEST}	0.8
	$\rho_{CEILING}$	0.8
	ρ_{FLOOR}	0.3
source:	mode	1
	x	2.5 m
	y	2.5 m
	z	3 m
	elevation	−90°
	azimuth	0°
receiver:	area	1 cm^2
	field of view	85°
	x	0.5 m
	y	1.0 m
	z	0 m
	elevation	90°
	azimuth	0°
resolution:	Δt	0.2 ns
	bounces	5
	no. x partitions (N_x)	50
	no. y partitions (N_y)	50
	no. z partitions (N_z)	30

Table 1. Simulation parameters for room, source, receiver, and resolution.

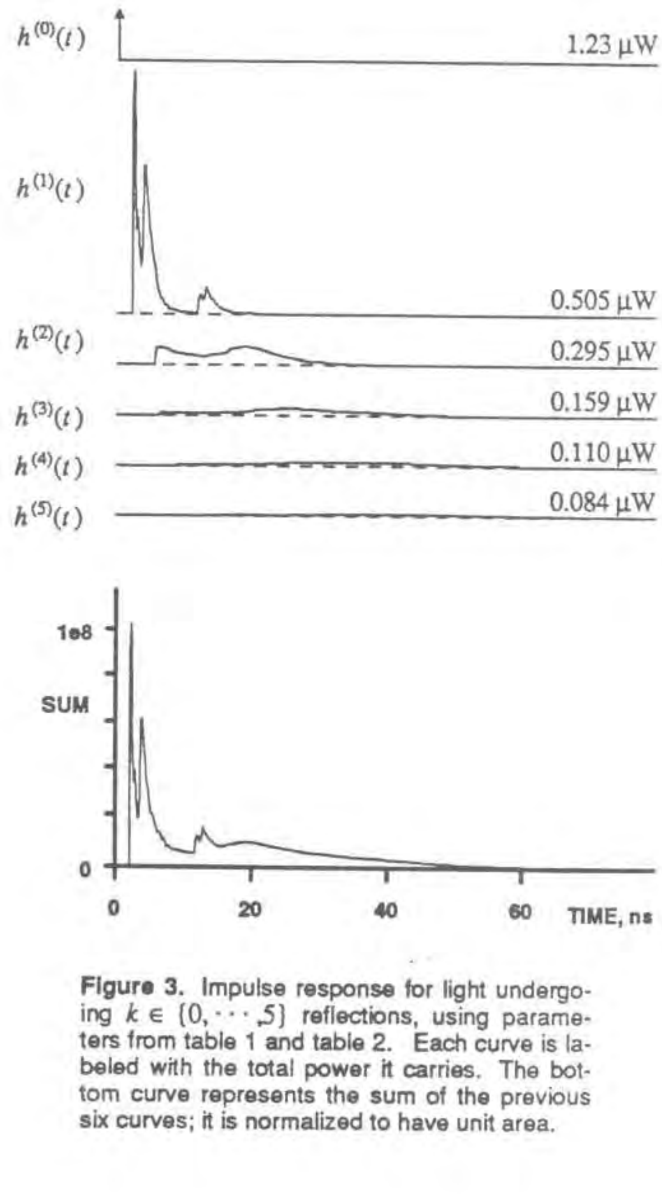

Figure 3. Impulse response for light undergoing $k \in \{0, \cdots, 5\}$ reflections, using parameters from table 1 and table 2. Each curve is labeled with the total power it carries. The bottom curve represents the sum of the previous six curves; it is normalized to have unit area.

k	N_x	N_y	N_z
0	-	-	-
1	50	50	30
2	50	50	30
3	15	15	15
4	7	7	7
5	4	4	4

Table 2. Spatial resolution for simulation shown in figure 3.

The net result is that, contrary to previous beliefs, higher-order reflections are significant. This may be easier to see in the frequency domain. Using the results shown in figure 3, we can estimate the frequency response of the channel:

$$H(\omega) = \int_{-\infty}^{\infty} h(t) e^{-j\omega t}\, dt$$
$$\approx \sum_{n=-\infty}^{\infty} h(n\,\Delta t) e^{-j\omega n \Delta t}\, \Delta t = \Delta t\, H(e^{j\omega\Delta t}), \tag{14}$$

where $H(e^{j\omega\Delta t})$ is the discrete-time fourier transform of the discrete-time signal $h(n\Delta t)$. In figure 4 we plot $|\Delta t H(e^{j\omega\Delta t})|$ for impulse responses accounting for up to one through five reflections. In figure 4(a) and (b), the amplitude responses are normalized to have unity d.c. gain, whereas in (c) the absolute amplitude responses are shown. These figures illustrate the need for considering higher-order reflections. Each additional reflection tends to lengthen the duration of the impulse response, which decreases the bandwidth of the channel. Notice how the -3 dB bandwidth of the channel tends to decrease as the number of reflections increases; the one-bounce impulse response has a bandwidth of 83 MHz, while the five-bounce impulse response has a bandwidth of only 12 MHz.

In figure 5 we show the phase and group-delay response of the channel. The group delay is defined as $-(\partial/\partial\omega)\angle H(\omega)$, so that a linear-phase channel has constant delay. The line-of-sight impulse response, being a delta function, has zero phase and thus zero delay. As the number of reflections increases, the phase response becomes less linear, and the delay response exhibits more variability.

A previously published result states that, without equalization, multipath restricts the symbol rate of an indoor infrared data link to 260 Mbps $\times$ meter/d, where d is the length (and width) of the room (with a 3 meter ceiling) [1]; this was based on single-reflections only. If we equate the -3 dB bandwidth with maximum symbol rate, then our single-reflection impulse response for a $d = 5$ meter room indicates a 83 MHz $\times$ 5 meter or 415 Mbps $\times$ meter/d symbol rate restriction, which is close to the previous restriction. However, the higher-order reflections cause the actual restriction to be more severe; our five-reflection result indicates a 12 MHz $\times$ 5 meter or 60 Mbps $\times$ meter/d symbol rate restriction. Of course, our data is only applicable to the particular room configuration

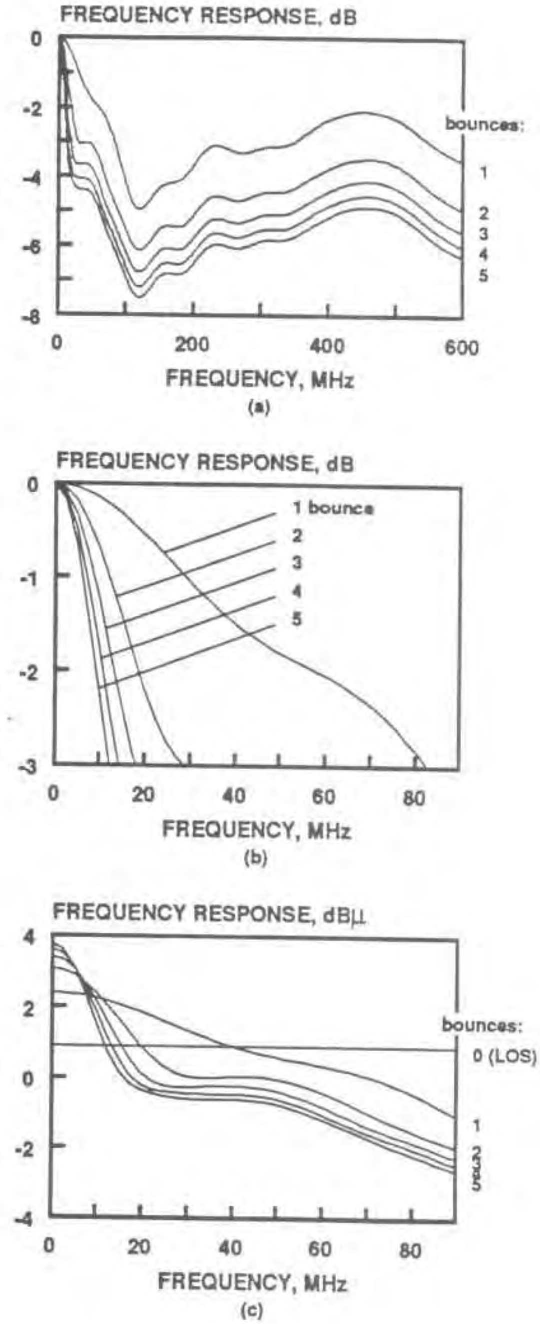

Figure 4. Effects of high-order reflections on amplitude response: (a) range is 600 MHz; (b) range is 90 MHz, to highlight the -3 dB bandwidths. Both (a) and (b) are normalized to have unit d.c. gain, whereas (c) is not. Thus, in (c) we can see the higher d.c. gain provided by the multiple reflections. The curves are labeled by the highest number of considered reflections.

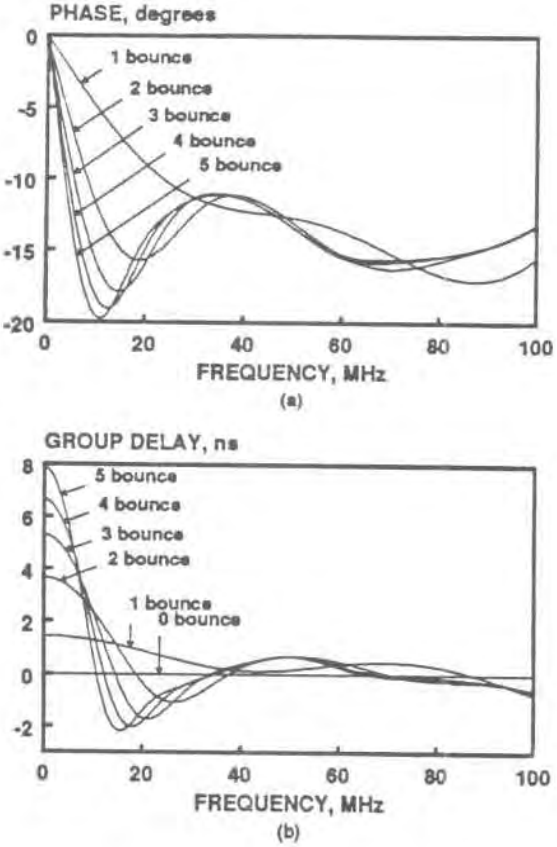

Figure 5. Effects of high-order reflections on (a) phase and (b) group-delay response. The curves are labeled by the highest number of considered reflections.

specified by table 1, so we cannot make a general statement about all room configurations. Nevertheless, to the extent that this particular simulation is indicative of other similar configurations, 60 Mbps × meter/d is a more realistic upper limit.

6. IMPLICATIONS OF HIGH-ORDER REFLECTIONS ON SYSTEM DESIGN

In this section, we examine the implications of the extra multipath dispersion introduced by higher-order reflections. The effect on power penalty is shown in figure 6 [15]. Here, we define power penalty as the extra power required to overcome the intersymbol interference and achieve a bit-error rate of 10^{-9}, measured relative to the power required with a dispersionless channel. We assume a baseband on-off keyed (OOK) system with white zero-mean additive gaussian noise and an integrate-and-dump receiver.

We see that the higher-order reflections have a severe impact on the power penalty. Accounting for only single reflections leads to a power penalty of 1.2 dB at 100 Mb/s, which is misleading; accounting for five reflections yields a more realistic result of 4.9 dB. Reflections of order greater than five will raise the penalty even higher. We thus conclude that, since most of the power penalty is due to reflections of order greater than one, the high-order reflections are the dominant source of intersymbol interference.

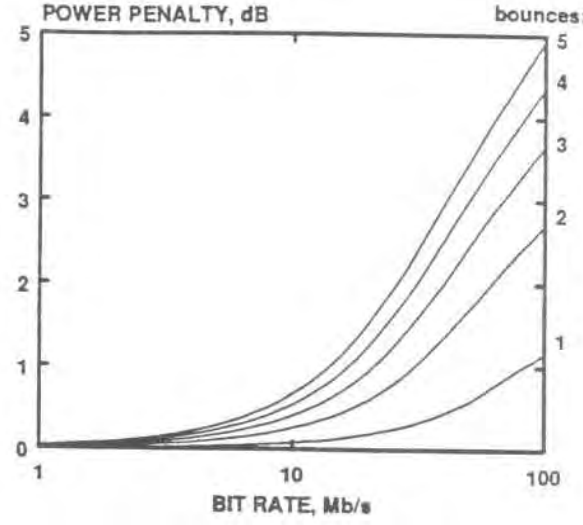

Figure 6. The effect of higher-order reflections on power penalty, plotted versus bit rate for a baseband OOK system.

The effect of higher-order reflections on channel capacity is shown in figure 7. The capacity derivations, which used a numerical water-pouring technique [16], will be omitted here for brevity [17]; we only want to illustrate the effects of higher-order reflections on capacity. Basically, the capacity calculations assume the receiver consists of an array of 16 avalanche photodiodes, each with mean gain of 100, and each with its own transimpedance

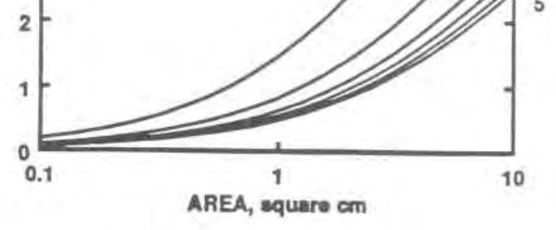

Figure 7. Effect of higher-order reflections on Shannon capacity, plotted versus total detector area.

amplifier and feedback resistance of 1 KΩ. The capacitance per unit area of the photodiodes is 100 pF/cm^2, and the background-light irradiance is 300 μW/cm^2.

The effects of higher-order reflections on channel capacity is also seen to be significant. Specifically, at a total area of 10 cm^2, the capacity for the single-reflection channel is 3.7 Gb/s, while that for the five-reflection channel is only 2.5 Gb/s.

Both figure 6 and figure 7 are based on the specific room configuration in table 1. Although it is difficult to quantify exactly how these results will generalize to other room configurations, we see no reason to think the power-penalty and capacity results of figure 6 and figure 7 will change considerably, and we thus view them as representative of rooms with similar dimensions.

7. SUMMARY

We have presented a method for evaluating the impulse response of an arbitrary room with Lambertian reflectors. This method can account for any number of reflected paths. A simple algorithm suitable for computer implementation has been presented. The results of computer simulations indicate that reflections of multiple order are the dominant source of intersymbol interference for an indoor optical communication system. The reflections of multiple order also have a significant impact on the capacity of the indoor optical channel. The design of a high-speed indoor communication link using infrared will require careful attention to the multipath response described in this paper.

REFERENCES

1. F. R. Gfeller and U. H. Bapst, "Wireless In-House Data Communication via Diffuse Infrared Radiation," *Proceedings of the IEEE* **67**(11) pp. 1474-1486 (November 1979).
2. J. R. Barry, J. M. Kahn, E. A. Lee, and D. G. Messerschmitt, "High-Speed Non-Directed Optical Communication for Wireless Networks," *submitted to IEEE Network Magazine*, (March 13, 1991).
3. T. Minami, K. Yano, and T. Touge, "Optical Wireless Modem for Office Communication," *National Computer Conference*, pp. 721-728 (1983).
4. Y. Nakata, J. Kashio, T. Kojima, and T. Noguchi, "In-House Wireless Communication System Using Infrared Radiation," *Proceedings of the International Conference on Computer Communication*, pp. 333-337 (1984).
5. I. A. Parkin and J. Zic, "An Application of Infra-red Communications," *Journal of Electrical and Electronics Engineering, Australia — IE Aust. & IREE Aust.* **4**(4) pp. 331-336 (December 1984).
6. Osamu Takahashi and Takashi Touge, "Optical Wireless Network for Office Communication," *JARECT (Japan Electron. Rev. Electron. Comput. Telecomm.)* **20** pp. 217-228 (1985/1986).
7. K. Pahlavan, "Wireless Intraoffice Networks," *ACM Transactions on Office Information Systems* **6**(3) pp. 277-302 (July 1988).
8. Chu-Sun Yen and R. D. Crawford, "The Use of Directed Optical Beams in Wireless Computer Communications," *IEEE Globecom '85*, pp. 1181-1184 (December 2-5, 1985).
9. M. D. Kotzin and A. P. van den Heuvel, "A Duplex Infra-Red Systems for In-Building Communications," *IEEE conference proceedings*, pp. 179-185 (1986).
10. Y. Yamauchi, M. Sato, and T. Namekawa, "In-House Wireless Optical Digital SSMA," *Electronics and Communications in Japan, Part 1* **70**(6) pp. 87-101 (1987).
11. T. S. Chu and M. J. Gans, "High Speed Infrared Local Wireless Communication," *IEEE Communications Magazine* **25**(8) pp. 4-10 (August 1987).
12. D. Hash, J. Hillery, and J. White, "IR RoomNet: Model and Measurement," *IBM Communication ITL Conference*, (June 1986).
13. P. Hortensius, "Research and Development Plan of the Infrared Portable Data Link," *IBM T. J. Watson Research Center, Yorktown Heights, New York*, (January 4, 1990). Internal Report.
14. A. S. Glassner, ed., *An Introduction to Ray Tracing*, Academic Press, San Diego (1989).
15. J. R. Barry, "Simulation of Multipath Impulse Response for Indoor Diffuse Optical Channels," *U.C. Berkeley*, (to be published).
16. R. G. Gallager, *Information Theory and Reliable Communication*, John Wiley & Sons, New York (1968).
17. J. R. Barry, "Capacity of a Non-Directive Indoor Optical Channel with Diffusive Reflectors," *U.C. Berkeley*, (to be published).

SESSION III

SPREAD SPECTRUM COMMUNICATIONS

Spread Spectrum PBX System Using CDMA

M. Kavehrad
University of Ottawa
Dept. of Electrical Engineering
Ottawa, Ont., K1N 6N5
Tel.: (613) 564-7079

Abstract- Spread spectrum techniques are universally accepted in hostile communication environments that occur in military applications. In commercial sector, spread spectrum is not yet widely accepted, in spite of recent FCC encouragements and rulings. We present a commercial application of direct sequence, spread spectrum technique. This involves office, factory or laboratory based wireless, small or large PBX applications. Experimental results, as well as a discussion of the advantages of spread spectrum in harsh indoor, multipath environments, are included. Some sample calculations of multipath outage will complete the article.

I. Introduction

There have been analyses published [1,2] in the last decade that show Direct Sequence Spread Spectrum (DSSS) is as efficient as FDMA or TDMA in multiple access communications for channels that do involve signal fading. FCC is actively encouraging spread spectrum development in commercial applications for its frequency reuse capability [3]. Recent rulings have also appeared regarding SS usage [4]. A variety of techniques have been presented for wireless indoor office communications [5], including spread spectrum techniques. This is exactly the case for the situation examined herein. That is, for a wireless PBX for offices, laboratories or factories where the transmission medium involves severe multipath fading. In addition, wireless applications could play a major role in the automated offices and factories of the future [2] through wireless control of robotic devices. Detailed arguments will be supplied for the merits of the case we present for the application of DSSS to Indoor Radio Local Area Networks that use a star architecture: further results can be found in [6-10].

II. Wireless PBX

Our application treats the wireless PBX scenario depicted in Fig. 1. This represents the upstream transmission mode (from user to base station) of an indoor, wireless, local area network with star architecture. Each user has a unique DSSS code and a correlator exists for each user in a channel bank structure at the base station. The output of the bank of correlators is fed to the usual PBX circuitry and call set-up is handled using standard PBX features. Average power control is necessary in such a system to avoid the classical near/far problem. This is easily achieved on the downstream (from base station to user), as considerable computer power is available at the base station. On the upstream, it is a little more difficult since the user terminals are meant to be small and cheap. We will address this important point later.

For a wideband indoor radio we have a severe multipath problem. It is really a classical Rayleigh multipath, fading channel. One must assume or develop a model that has detailed structure for the multipath fading since the received SS signal attributes are to be used for inherent diversity reception. DSSS has been tested for a variety of theoretical models and it was found that performance is about the same in all cases [9] for indoor environments, because the maximum delay spread is so small compared to typical bit time in ISDN applications that delay distribution does not play a significant role. In this sense DSSS is robust. A DSSS system holds some advantages and disadvantages. On the positive side, DS radio links offer:

1) Asynchronous multiple access
2) Inherent diversity in multipath fading channels
3) Frequency reuse by signal overlay
4) Ease of implementation and low cost
5) Robust relative to varying channel conditions
6) Built-in addressing and security

On the negative side, with DS radio links:

1) Power control is needed to combat near/far problem.
2) Minor interference is introduced into existing systems in an overly signaling mode.

The role of asynchronous transmission is clear. A user transmits at random. The signal arrives at the correlator bank and is detected, along with interfering signals. The latter limits the user population and we will say more about this later.

The inherent diversity of SS modulation, an important point, is clear referring to Turin's discrete multipath channel [11]. A correlator, or matched filter, outputs M peaks of resolved signals for a single transmission and thus, (inherent) Mth-order diversity. The idea goes back to the time of the RAKE system [12, p. 471] for HF communications. Using selection diversity [7], it turns out that fairly large orders of diversity are needed in indoor digital radio. Spread spectrum system can offer this with minor complexity. Such is a major advantage in commercial systems, where complexity and cost are directly related.

An operating radio band may not be needed in DSSS over a lightly loaded part of the radio spectrum as we spread the signal so wide that it is undetectable by other than the reference user's correlator in Fig. 1. This concept is borrowed from the Low-Probability-of-Intercept mode of communications in military systems. Peak power is low anyway as the operating radius of the system in Fig. 1 is at most a 100 feet or so. The concept here is the signal overlay mode of operation [3]. For this reason we do not discuss the bandwidth efficiency of DSSS herein. This subject is discussed in reference [7].

The fourth point mentioned in advantages of DSSS is the implementation issue. The main component in the receiver structure in Fig. 1 is the SAW correlator [13]. Low cost, non-programmable, passive correlators, one for each possible system user, exist in the correlator bank in Fig. 1. Such correlators are available from a number of manufacturers. In volume, the cost is low; say, a few dollars per correlator.

Finally, the addressing and security features for DSSS are well known. Call set-up and addressing are easily related to the unique user code [14]. Alternatively, call set-up could use the Aloha-like random access techniques.

A minus for DSSS is the need for average power control. On the average, which includes the fading statistics, all signals should arrive at the receiver with the same average power in order to get a reasonable throughput. It has been shown in [7] that the number of simultaneous users drops in step with a fixed reduction of the reference user's average power. However, in star LANs average power can be controlled [10]. In wider-area fully connected networks, such a control may not be possible.

For the interference radiated into other systems, the main concern regards signals transmitted into other buildings, or into other LANs in the same building. The SAW correlator can be used to advantage here. The SAW correlator we have in mind will be realized at an appropriate IF. Such correlators exhibit a frequency capture phenomenon [10]. If these correlators are detuned by a modest amount, incoming signals are rejected. Thus, LANs in other buildings, or in adjacent cells within buildings, are operated at a frequency offset. This offset is greater than the frequency stability of the RF sources used in any LAN application. Of course, this discussion assumes all LANs are using DSSS with SAW correlators as the basic receiver element.

III. Receiver Structures

A receiver structure that can be analyzed is shown in Fig. 2 where K users and L paths per user are depicted. In buildings where the maximum delay spread is very small compared to typical information bit time, a simple formula [6] for L is:

$$L = \left\lfloor \frac{T_m}{T_c} \right\rfloor + 1$$

where T_m is the multipath delay spread, T_c is a chip time of the DS code and $\lfloor \cdot \rfloor$ is the floor function; that is x is the largest integer less than or equal to x. This formula is based on the time-resolution of DSSS signals, which is T_c seconds, namely one chip period. This point is illustrated in Fig. 3. Thus, the time T_m is divided into segments of T_c time units and L follows accordingly.

Although in our performance analysis we rely on delay spread as the main factor, actual power delay profile of the resolved multipath peaks and its impacts have been addressed in [9] where the performance analysis is based on actual indoor radio channel characteristics measurements as well as an intuitive model.

We note that the simple formula above has been demonstrated experimentally [10]. This is illustrated in Fig. 4 where two resolvable peaks from the SAW correlator output are shown. The IF spectrum is also displayed and a 20*db* fade notch is displayed.

The receiver in Fig. 2 is based on the selection diversity rule. First, the largest spread-spectrum correlation peak envelope is chosen per RF antenna. Finally, the larger signal between the two RF antennas is selected. This peak is then coherently demodulated. A more practical receiver, based on differential phase shift keying (DPSK) and noncoherent integration is illustrated in Fig. 5. In this, all correlation peaks are differentially demodulated and an integrator adds up the results over the delay spread T_m, noncoherently. Remarkably, this receiver can also be analyzed [9]. The simple receiver in Fig. 5 is the one to use in any system implementaion. A more elaborate method is to sample the peaks and find a sum of the weighted samples. This method has also been evaluated in [9]. As is common in fading channels, about 3*db* in SNR or 50 percent of the active user population is lost in using DPSK relative to coherent PSK [9]. However, this loss can be compensated by using error correcting codes. Here we are taking other than the reference users signal as the total system noise.

IV. Performance Analysis

The two basic measures of performance in digital systems are the average bit error rate (BER) and the multipath multipath outage. First the average BER is discussed. For multipath outage, a few calculations are included later in this section.

Average BER

For the average BER analysis, [6] presents the basic model and the nondiversity performance. Turin's [11] structural model was used with parameters set to values appropriate for indoor digital radio. For each user, the impulse response is

$$H_k(\tau) = \sum_{l=1}^{L} \beta_{lk}\delta(\tau - \tau_{lk})e^{j\phi_{lk}}$$

where $\delta(t)$ is the Dirac-delta function, β_{lk} is the path gain, ϕ_{lk} is the path phase and τ_{lk} is the path time delay. The path gain β_{lk} is assumed Rayleigh and independent, with ϕ_{lk} and τ_{lk} being independent and uniformly distributed. In the equation above, L represents the SS diversity available to the receiver while $L(K-1)$, K the number of active users, is the total number of interference terms.

The scenario for analysis used in [6-9] was to analyze selection diversity in a closed form. Then performance for a Gaussian model for the interference was computed and compared with the exact results. Finally, the differentially coherent case with a noncoherent integrator in Fig. 5, as well as its perfectly coherent counterpart, were analyzed using Gaussian assumption.

The bottom line is to estimate the number of active users. Such curves can be found in Figs. 6 and 7. These curves are for a $32\ Kb/s$ packet speech application with 1000 bit packets. Speech interpolation can be used for word error rates 10^{-1} or so, and thus the basic BER of interest is around 10^{-4}. Figures 6 and 7 give estimates for the user population for maximal ratio combining (MRC) (that is, the coherent, weighted integrator version of Fig. 5) and for selection diversity with forward error correction. In the latter case, the environment must give independent symbol errors as it would occur in the system implementations here and in the 30-60 GHz range. Such high frequency systems are mentioned in [15]. Figure 6 is for a building of modest size where the delay spread is $100\ ns$ and Fig. 7 is for a larger building with a delay spread of 250ns. The parameter L for these Figures is given in Table I.

We note from Figs. 6 and 7 that selection diversity plus coding does not lose much in performance as the delay spread increases. Note, however, that MRC actually improves in performance as delay spread increases. This is due to increased spread spectrum diversity; that is, increased L in Table I. For instance, for a 120 active users. Thus, the noncoherent integrator would support 60 users which is within system requirements. For more details see [6-9]. Note that to attain this result we have a diversity order of 10; that is, $L = 5$ (see Table I) and two antennas. From Fig. 6 we see that when $T_m = 100\ ns$, that is, the small building, we get 30 users when we apply the 50 percent reduction due to differential demodulation (see the receiver structure in Fig. 5).

One notes from the discussion just presented that up to a certain extent DSSS gets better, or stays about the same, in performance as the application gets more difficult; that is, as the delay spread increases. Other techniques, such as TDMA and FDMA, must reduce the system data rate as delay spread increases in order to avoid intersymbol interference. This leads to a direct loss in user number. Of course, in reducing system data rate, the objective is to avoid intersymbol interference. Equalization could be suggested for this application but such techniques are costly relative to the simple noncoherent integrator in Fig. 5. In addition, many spectral nulls could exist in the wideband cases and thus, any equalization procedure would have to be based on nonlinear techniques. Recall from Fig. 4 it is precisely the multipath which leads to SS diversity when the in-phase paths add in power constructively and thus enchanced performance for our DSSS system.

We close this section by pointing out that the simple receiver of Fig. 5 has been analyzed [9] for the precise statistical model in [16] for indoor digital radio as well as for the Turin's model [11]. Results were found to be about the same as for various versions of the Turin's model [11]. Thus, spread spectrum is also robust to changes in propagation parameters and only delay spread matters.

Multipath Outage

Average error probability is a meaningful indicator of performance over a Gaussian channel. For multipath fading channels, a more appropriate measure is fading outage. Let BER_0 be some nominal bit error rate for an indoor, digital radio system. Let β represent the normalized path gain for a particular path in a multipath environment. The BER as a function of β is denoted as BER (β). The multipath outage is the probability distribution of $BER(\beta)$, namely;

$$M_0 = F(BER_0) = P\{BER(\beta) \geq BER_0\}.$$

If the fading is time varying, the multipath outage is the percentage of time the BER requirement, BER_0, is not met. For static fading, it is the fraction of the useful area over, say a building, that the bBER criterion is not satisfied. The latter case applies in indoor digital radio as terminals move slowly and operating carrier frequencies are in the low gigahertz range.

As we illustrate in Fig. 8, $BER(\beta) \geq BER_0$ as long as $\beta \leq \beta_0 = BER^{-1}\{BER_0\}$; that is, the value of β that produces BER_0. Then, if M_0 is the multipath outage,

$$M_0 = P\{BER(\beta) \geq BER_0\}$$
$$M_0 = P(\beta \leq \beta_0) \qquad \beta_0 = BER^{-1}(BER_0)$$

which is easily computed given the probability distribution function for β, the path gain.

In [7], we considered the case when we used an exact calculation of the error probability and also a calculation based on the Gaussian assumption for the interference and we examined the differences. The case for maximal ratio combining, the coherent weighted integration over all path gains, follows from equation (10a) of [7]. To keep the analysis simple we use a Gaussian assumption for the interference and, neglecting additive white Gaussian noise,

$$\begin{aligned} BER(\beta) &= Q(\sqrt{2\gamma_0\beta^2} \ \ and \\ Q(x) &= \frac{1}{\sqrt{2\pi}}\int_x^{\infty} e^{\frac{-z^2}{2}}dz \end{aligned} \tag{1}$$

where for a SS sequence length of N, K active users, and L paths per user,

$$\gamma_0 = \frac{3N}{2(KL)} \tag{2}$$

Also,

$$\beta^2 = \frac{\sum_{i=1}^{L} \beta_i^2}{2p_0} \tag{3}$$

and

$$2p_0 = E(\beta_i^2) \tag{4}$$

Here, use has been made of the material in Section IV of [7] on invoking a Gaussian assumption for the multi-user interference.

Thus, as it is easier to work with β^2,

$$M_0 = P(\beta^2 \leq \beta_0^2) \tag{5}$$

where

$$\beta_0^2 = \frac{[Q^{-1}(BER_0)]^2}{2\gamma_0} = a \tag{6}$$

For β_i Rayleigh distributed with power, $E(\beta_i^2) = 2p_0$, as in (4), it follows from reference [17], equation (5.2-15), that the multipath outage in (5) is given by

$$M_0 = 1 - e^{-a} \sum_{k=1}^{M} \frac{a^{k-1}}{(k-1)!} \tag{7}$$

where the parameter a is given in (6).

Computations of the multipath outage in (7) are given in Tables II and III. Table II is for a single antenna system and Table III is for a two-antenna system. In both tables the multipath delay spread is 250 nsec and thus, L is given in Table I, part C, for *no coding*. For a single antenna $M = L$ and for two antennas, $M = 2L$. For instance, in Table II the probability that the BER exceeds 10^{-3} is 1.47×10^{-3} for a 512 length code and 26 active users. Thus for non-packet speech and a changing environment, the chances of bad speech bits is 0.147 percent. For data with a BER_0 requirement of 10^{-5}, the error rate requirement is not satisfied 2.04 percent of the time. Moving to say a packet speech application, say with packets speech interpolation. Moving to $K = 52$ active users in Table III and a code length of 255 chips, one sees that roughly 7 percent of the terminal sites in a building area are not useful. For a $N = 512$ length code, a non-useful site almost never occurs. More precise results for selection diversity can be found in [7].

V. Power Control Algorithm

As discussed earlier, and as illustrated in Figure 1, a star network architecture is assumed and the a near/far problem exists; namely, an unfaded signal of a user close to the PBX will interfere with all the users. An algorithm to overcome this is as follows [9]. The base station continuously transmits a narrowband tone or a wideband common code to all receivers. The user's receiver measures the received average power. Since the channel is reciprocal, the transmitter power for a particular user is adjusted, on the average, according to the average attenuation experienced in the received tone. This results in all signals arriving at the base station at approximately equal power levels.

On the downstream mode average power is easily exercised by the base station since all transmitters are co-located.

VI. Experiment

Two links of the complete DSSS system described herein, have been constructed and are described in reference [10]. In this implementation, PN sequences of length 127 and chip rate of 10 MHz were employed. Prototype SAW matched filters were used in the implementation. The input binary data rate was 78.7 kHz. The basic time-resolving power of these sequences is 100 nsec and thus, one-to-two resolved paths can be expected in 100 ns delay spread environments. Two resolved paths are shown in Fig. 4. Note the 20 dB fade notch that exists in the frequency domain description of the indoor, multipath medium under discussion. Linear equalization would be difficult in such a situation. However, the DSSS receiver resolves two paths and integrates their energy (see top trace in Fig. 4) to yield excellent detection performance. Figure 9 corresponds to an error free transmission. As shown in this figure, the system works well in an environment that has a combination of flat and dispersive fades.

A reference receiver/transmitter pair were constructed to operate in the 1 GHz range. In addition, an interfering transmitter was constructed and used to conduct interference tests. Results can be found in [10] and are close to theoretical results. Finally, Fig. 10 illustrates the *frequency capture* phenonmenon [10]. Note that as the reference receiver is increasingly frequency detuned, the SAW matched filter output steadily drops to its correlation side-lobe voltage level. Recall earlier in this article, this was claimed as an advantage for the system, allowing frequency reuse in neighboring LAN's or in neighboring cells of a cellular system.

VII. Conclusion

Our main conclusion is that direct sequenc spread spectrum modulation is a promising modulation technique for inddor digital radio local area networks that use a star network topology. Slow multipath fading is the main performance impairment in such systems and here this modulation technique offers inherent diversity which can ease the system implementation. The main receiver element is a passive correlator which is based on SAW technology. The interference rejection of a SAW-correlator based, differentially coherent integrator, has been examined both theoretically and experimentally. Expected user population levels are promising for present and future application.

References

[1] R. Skaug, J.F. Hjelmstad, "Spread Spectrum in Communication," Peter Peregrinus Ltd, London, 1985.

[2] D.L. Schilling, et al, "Spread Spectrum Goes Commer-

cial," IEEE Spectrum, pp. 40-45, August 1990.

[3] Further Notice of Inquiry and Notice of Proposed Rulemaking, "Authorization of Spread Spectrum and Other Wideband Emissions Not Presently Provided for in the FCC Rules and Regulations," May 21, 1984.

[4] D. Newman, Jr., "FCC Authorizes Spread Spectrum," *IEEE Communications Magazine*, pp. 46-47, July 1986.

[5] K. Pahlavan, "Wireless Communications for Office Information Networks," *IEEE Communications Magazine*, vol. 23, pp. 19-28, June 1985.

[6] M. Kavehrad, "Performance of Non-diversity Receivers for Spread Spectrum in Indoor Wireless Communication," *AT&T Tech. Jour.*, vol. 64, No 6, July-Aug. 1985.

[7] M. Kavehrad and P.J. McLane, "Performance of Low-Complexity Channel Coding and Diversity for Spread Spectrum in Indoor, Wireless Communication," *AT&T Tech. Jour.*, vol. 64, pp. 1927-1965, Oct. 1985.

[8] M. Kavehrad and P.J. Mclane, "Performance of Direct Sequence Spread Spectrum for Indoor Wireless Digital Communication," *Proc. GLOBECOM'85*, New Orleans, LA, Nov. 1985.

[9] M. Kavehrad and B. Ramamurthi, "Direct-Sequence Spread Spectrum with DPSK Modulation and Diversity for Indoor Wireless Communications," *IEEE Trans. on Comm.*, Feb. 1987. Also, *Proc. ICC'86*, Toronto, Canada, June 1986.

[10] M. Kavehrad and G. E. Bodeep, "An Experiment with Direct-Sequence Spread Spectrum and Differential Phase Shift Keying Modulation for Indoor, Wireless Communications," *Proc. ICC'87*, Seattle, WA, June 1987 and *Jour. on Selected Areas in Comm.*, June 1987.

[11] G.L. Turin, "Introduction to Spread-Spectrum Anti-Multipath Techniques and their Application to Urban Digital Radio," *Proc. IEEE*, vol. 68, pp. 328-353, Mar 1980.

[12] J.G. Proakis, *Digital Communications*, New York: McGraw-Hill, 1983.

[13] W.R. Shreve, "Signal Processing Using Surface Acoustic Waves," *IEEE Communications Magazine*, vol. 23, pp. 6-12, Apr. 1985.

[14] M. Kavehrad and P.J. McLane,"Spread Spectrum Wireless PBX," U.S. Patent 4,672,658, June 9, 1987.

[15] R.S. Swain, "Cordless Telecommunications in the UK," *BR. Telecom Tech. Journal*, vol. 3, pp. 32-38, Apr. 1985.

[16] A.A. M. Saleh and R.A. Valenzuela, " A Statistical Model for Indoor Multipath Propagation," *Proc. ICC'86*, Toronto, Canada, June 1986 and *IEEE Jour. on Selected Areas in Communications*, vol. JSAC-5, no. 2, Feb. 1987.

[17] W.C. Jakes, Jr., *Microwave Mobile Communications*, John Wiley and Sons, New York, 1984.

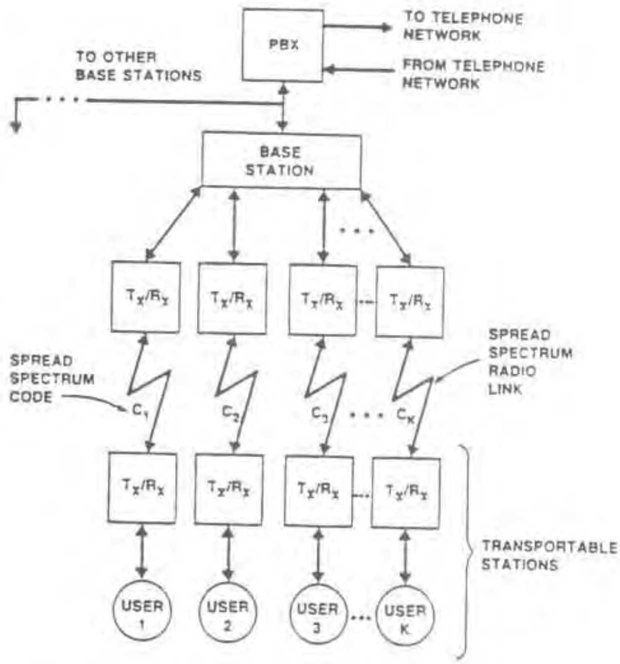

Figure 1 - A star-connected, indoor, wireless, local area network. Each user has a unique spread-spectrum code.

Table I Transmission Parameters for Different Sequence Lengths

N	No Coding	(7, 4) Code	(15, 7) Code
(a) Bandwidth in MHz of various spread-spectrum sequence lengths for a source rate of 32 kb/s			
127	4.06	7.11	8.70
255	8.16	14.20	17.50
512	16.40	28.67	35.11
(b) Number of discrete multipath components when $T_m = 100$ ns			
127	1	1	1
255	1	2	2
512	2	3	4
(c) Number of discrete multipath components when $T_m = 250$ ns			
127	2	2	3
255	3	4	5
512	5	8	9

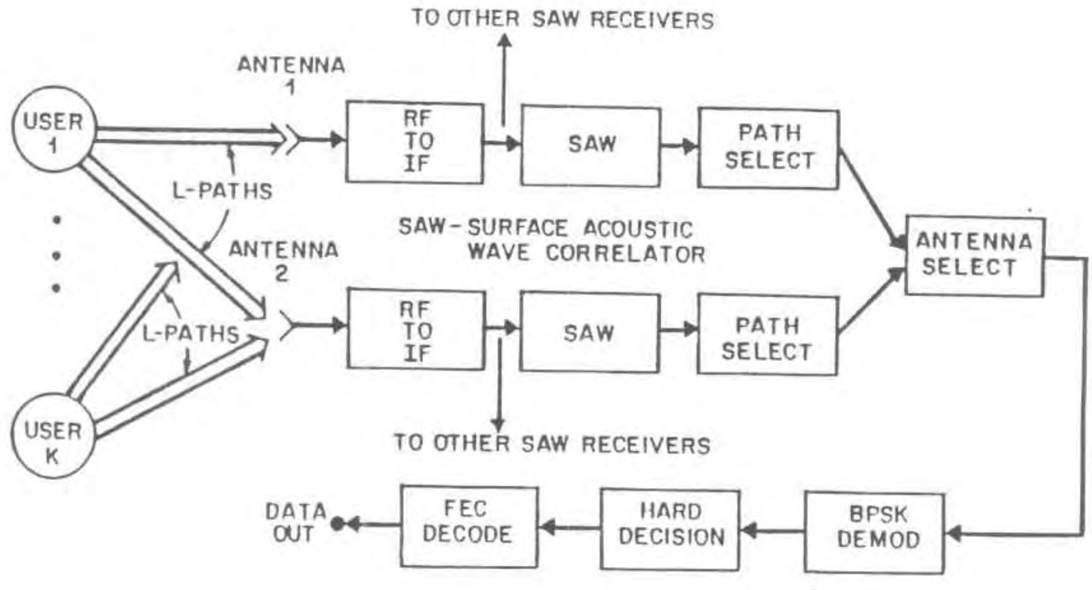

Figure 2 - Per-user receiver for spread-spectrum, direct-sequence receiver using selection diversity.

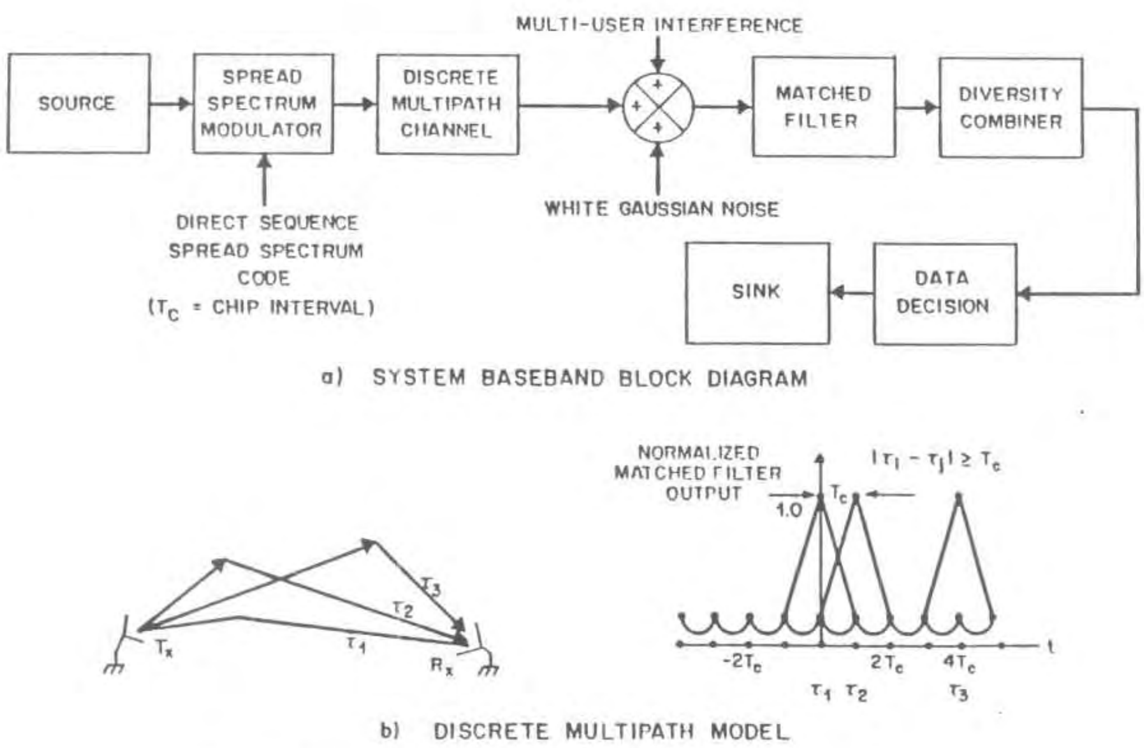

Figure 3 - Multiuser spread-spectrum system for (a) a baseband system and (b) a discrete multipath model.

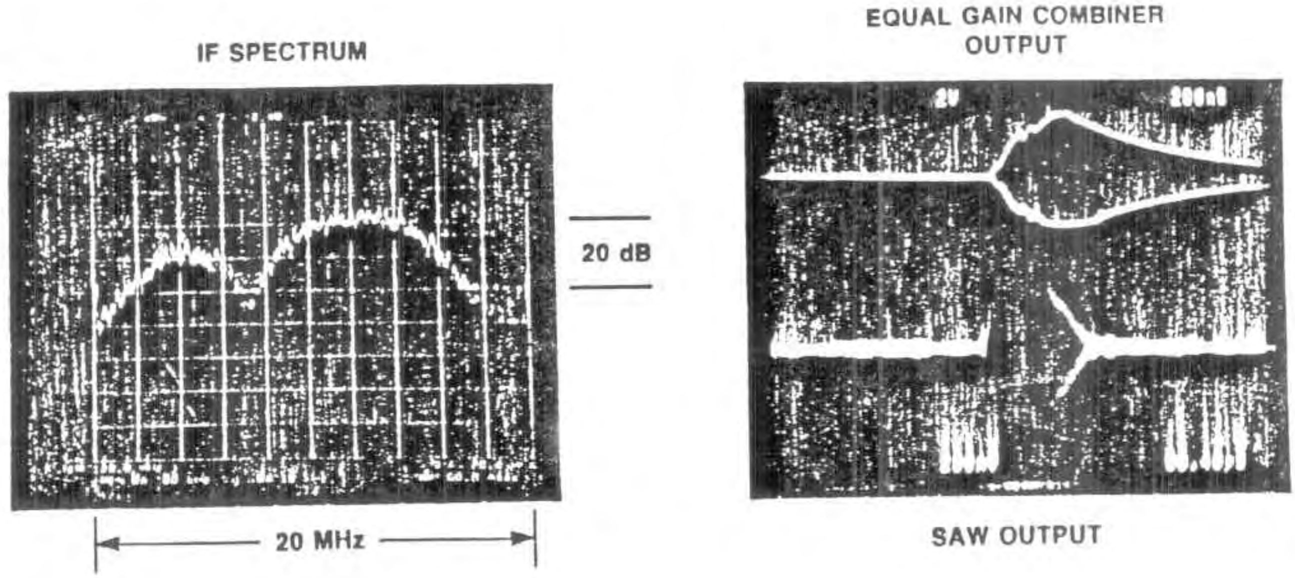

Figure 4 - Correlation peaks due to multipath fading and a 20 dB notch on the IF spectrum.

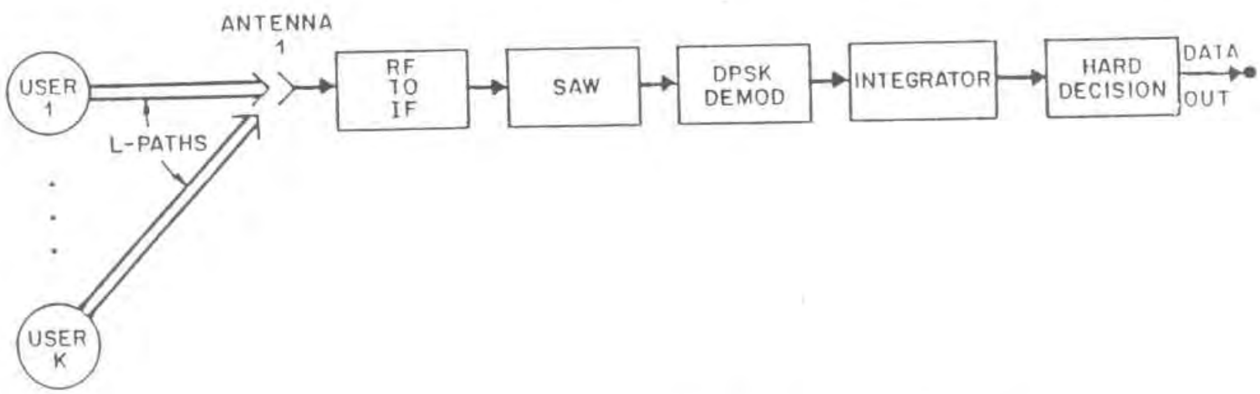

Figure 5 - Per-user receiver for spread-spectrum, direct-sequence receiver using pre-detection combining

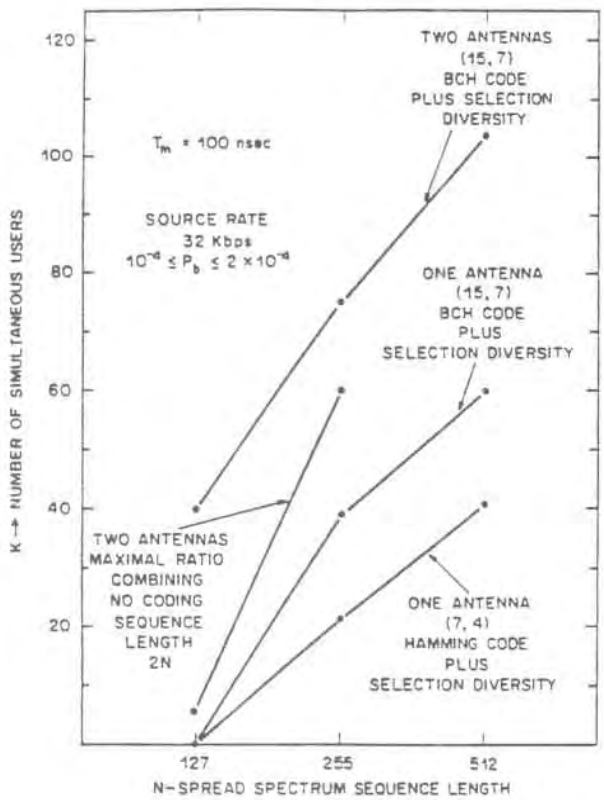

Figure 6 - Number of simultaneous users versus spread-spectrum sequence length when T_m = 100 ns

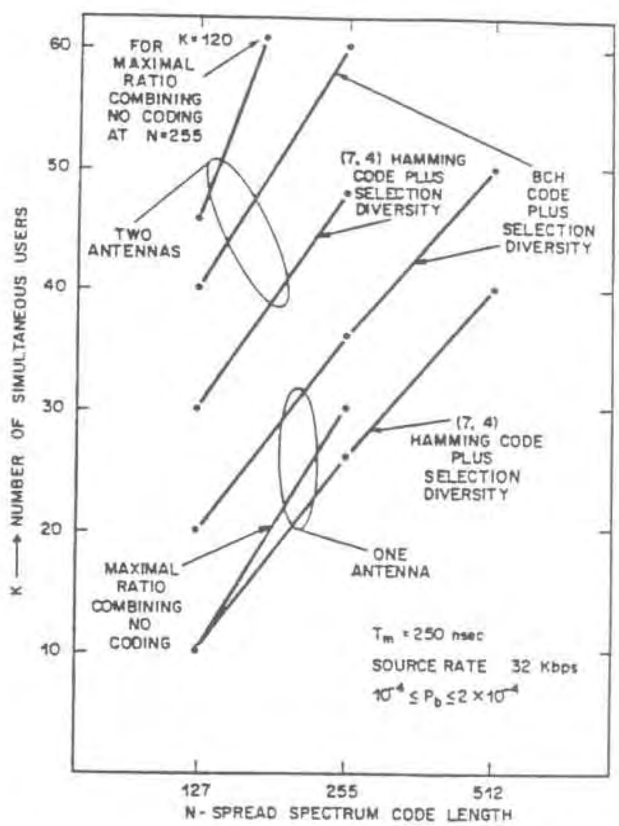

Figure 7 - Number of simultaneous users versus spread-spectrum sequence length when T_m = 250 ns.

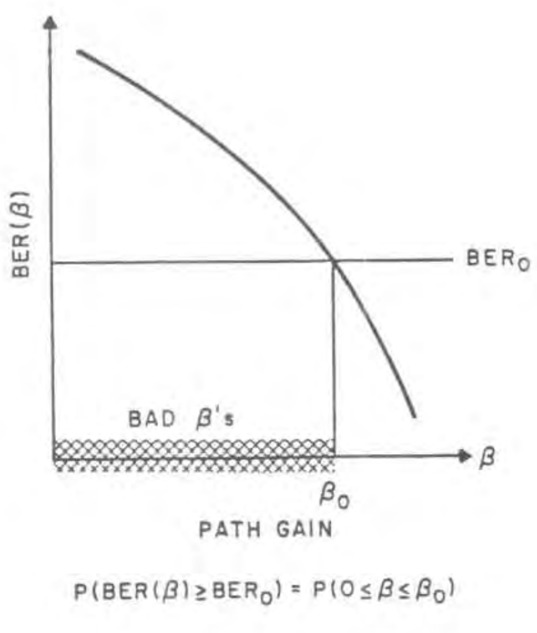

Figure 8 - Multipath outage analysis with respect to path gain, β.

Table II Multipath Outage for a Maximal Ratio Combining Receiver: Single Antenna Case

		$K = 13$		$K = 26$	
BER_0	x_0	$N = 255$	$N = 512$	$N = 255$	$N = 512$
10^{-1}	1.28	9.12×10^{-5}	1.26×10^{-8}	6.86×10^{-4}	3.81×10^{-7}
10^{-2}	2.326	2.85×10^{-3}	4.33×10^{-6}	1.36×10^{-2}	1.15×10^{-4}
10^{-3}	3.09	1.34×10^{-2}	6.42×10^{-5}	7.56×10^{-2}	1.47×10^{-3}
10^{-4}	3.717	3.47×10^{-2}	3.51×10^{-4}	1.68×10^{-1}	6.98×10^{-3}
10^{-5}	4.263	6.72×10^{-2}	1.19×10^{-3}	2.84×10^{-1}	2.04×10^{-2}

Delay Spread = 250 nsec
Bit Rate = 32 *kbps*
Single Antenna System $BER_0 = Q(x_0)$

Table III Multipath Outage for a Maximal Ratio Combining Receiver: Two Antennas Case

		$K = 26$		$K = 52$	
BER_0	x_0	$N = 255$	$N = 512$	$N = 255$	$N = 512$
10^{-1}	1.280	2.62×10^{-7}	6.11×10^{-16}	1.45×10^{-6}	5.77×10^{-12}
10^{-2}	2.326	2.45×10^{-4}	7.37×10^{-11}	9.82×10^{-4}	5.00×10^{-8}
10^{-3}	3.090	5.18×10^{-3}	1.57×10^{-8}	1.47×10^{-2}	7.79×10^{-6}
10^{-4}	3.717	3.30×10^{-2}	3.51×10^{-6}	6.67×10^{-2}	1.65×10^{-4}
10^{-5}	4.263	1.18×10^{-1}	5.09×10^{-4}	1.70×10^{-1}	1.33×10^{-1}

Delay Spread = 250 nsec
Bit Rate = 32 *kbps*
Two Antenna System $BER_0 = Q(x_0)$

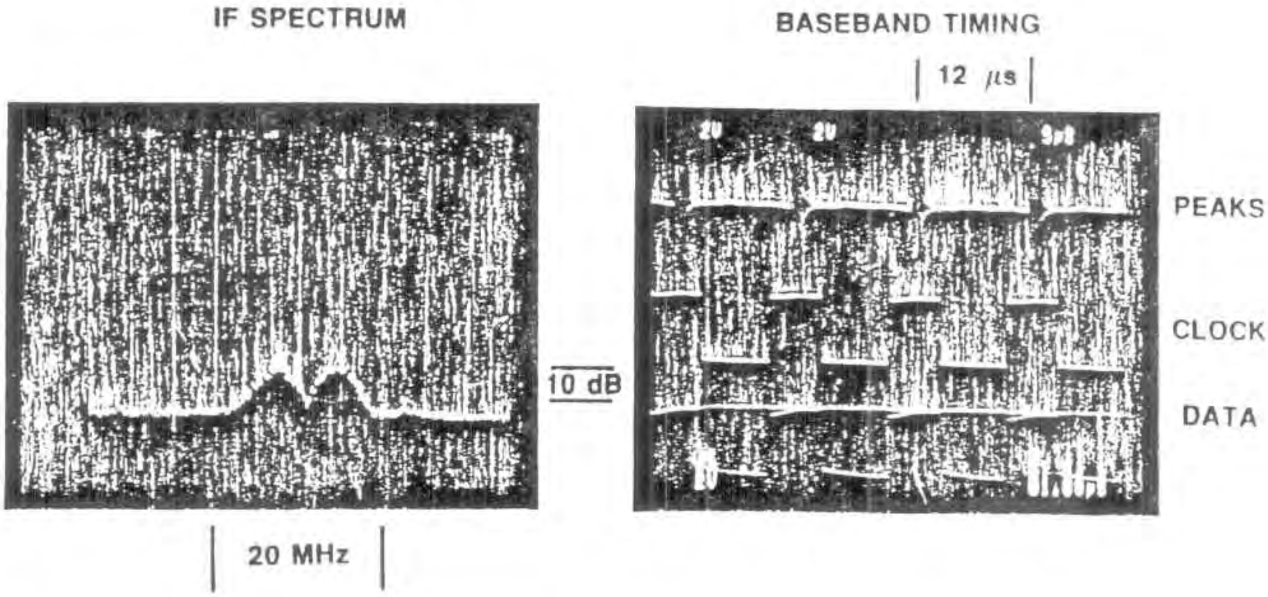

Figure 9 - Correlation peaks due to multipath fading and a 10 dB fade notch on the IF spectrum.

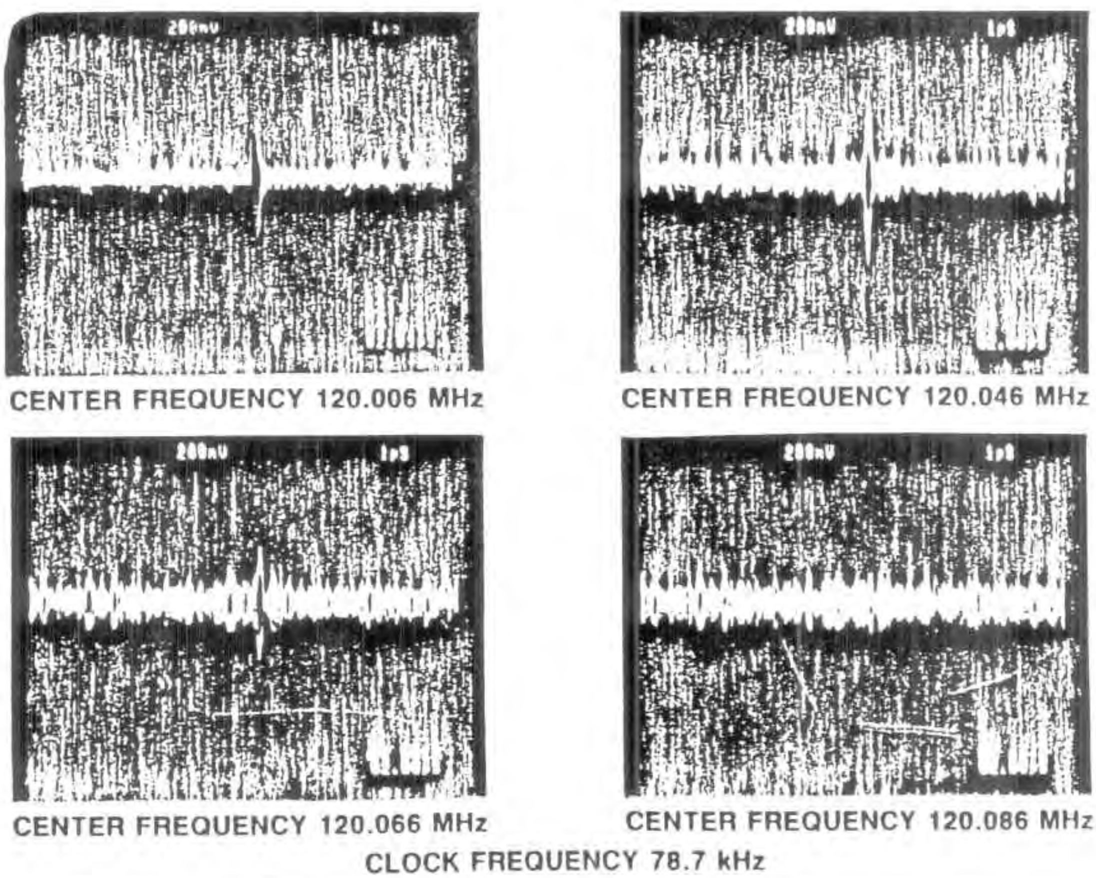

Figure 10 - Effect of frequency shift on correlation peak.

Spectral Efficiency Using CDMA for Personal Communications Networks*

Donald L. Schilling
Dept. of EE
CCNY
New York, NY 10031

Laurence B. Milstein
Dept. of ECE
U. of CA. San Diego
La Jolla, CA 92093

Raymond L. Pickholtz
Dept. of EECS
George Washington U.
Washington, DC 20052

Frank Miller
Millicom, Inc.
New York, NY 10022

Abstract - Spread spectrum techniques have been used for about three decades as a means for communications in a hostile environment. In particular, direct sequence and frequency hopping spread spectrum systems afford the opportunity for some measure of protection against intentional jamming. When the hostile jamming environment is removed and we examine spread spectrum primarily in terms of the CDMA and mutual interference effects, the issues for design and evaluation are shifted drastically. Recently, spread spectrum systems have been given a second look from the perspective of applications which require exactly these features. Entirely new opportunities such as personal communication networks (PCN) and digital cellular radios have created the need for research on how spread spectrum systems can be "re-optimized" for most efficient use of spectrum and other features in these non-hostile environments. In this paper, we discuss some of the issues relevant to CDMA PCNs, and describe an experiment which is designed to test the feasibility of overlaying a spread spectrum network on top of existing narrowband microwave users.

1.0 Introduction

Spread spectrum techniques have been used for about three decades as a means for communications in a hostile environment. In particular, direct sequence and frequency hopping spread spectrum systems afford the opportunity for some measure of protection against intentional jamming. In military systems, the unique addressability attribute of spread spectrum, which allows such systems to operate as a code division multiple access (CDMA) system, was given a secondary role. A rare exception is tactical packet radio; but even here, anti-jamming capability was a major selling point.

* Portions of this research were supported by SCS Mobilecom, Inc., and by the NSF I/UCRC for Ultra-High Speed Integrated Circuits and Systems.

When the hostile jamming environment is remove and we examine spread spectrum primarily in terms of the CDMA and mutual interference effects, the issues for design and evaluation are shifted drastically. Recently, spread spectrum systems have been given a second look from the perspective of applications which require exactly these features. Entirely new opportunities such as personal communication networks (PCN) and digital cellular radios have created the need for research on how spread spectrum systems can be "re-optimized" for most efficient use of spectrum and other features in these non-hostile environments.

For example, it may be possible to achieve a greater capacity per unit bandwidth with CDMA than with either frequency division multiple access (FDMA) or time division multiple access (TDMA) when the sources are homogeneous and when one can exploit the statistical source characteristic better with CDMA. In addition, since CDMA is a distributed form of random access with inherent interference suppression, many of the frequency and time assignment rules used in FDMA and TDMA, as well as their management, may be avoided. CDMA codes may be designed which inherently reject multipath, which is a major concern in terrestrial mobile radio communications. CDMA signals spread their power over large bandwidth, so that the effect of such a transmission on a narrowband receiver is often just an imperceptible rise in its noise floor. Hence it may be possible to overlay a spread spectrum CDMA system on an existing narrowband user without adversely affecting either. Moreover, because of the broadband noise-like character of CDMA signals, it is possible to use newly developed signal processing techniques to perform narrowband interference excision. This will clearly reduce the interference for the spread spectrum users, but it will also help the narrowband user, since CDMA is interference-limited and with reduced interference resulting from such excision, it is possible to operate each CDMA transmission at a reduced power level.

Finally, since spread spectrum uses noise-like codes from a large signal space, a certain amount of privacy is inherent.

In this paper, we will address only a few of these issues and describe a proposed new personal communication network and an FCC approved experiment to demonstrate the feasibility of a direct sequence spread spectrum CDMA overlay in the frequency band 1850-1990 MHz. The main considerations in this instance are the capacity improvements given the cell geometry, CDMA mutual interference, and how such interference is effected by presumed propagation laws.

2.0 Design Considerations

The primary focus for any proposed multiple access method for communications in the radio spectrum is how many voice channels (or bits per second for data) can be accommodated per unit bandwidth. In contrast with FDMA or TDMA, which divide either frequency or time into disjoint, non-overlapping and non-interfering regions, CDMA allows all users to simultaneously use full time and bandwidth. The limitation on CDMA then, is due to the mutual interference, rather than on the number of orthogonal slots available as in FDMA or TDMA.

To illustrate the capacity calculation for CDMA, we first calculate the actual energy per bit to noise density, $(E_b/N_o)_{act}$, which determines probability of error performance measure. If P is the power in a CDMA signal, S is the one-sided power spectral density of the CDMA signal (assumed, for simplicity, constant over the bandwidth of interest), B is the spread bandwidth and R is the symbol rate, then we have

$$\left(\frac{E_b}{N_o}\right)_{act} = \frac{P}{N_oR} = \frac{S}{N_o}\frac{B}{R} > \left(\frac{E_b}{N_o}\right)_{rqd} \qquad (2.1)$$

That is, we require that the power spectral density of each CDMA signal to be large enough so that the actual $(E_b/N_o)_{act}$ is larger than the minimal $(E_b/N_o)_{rqd}$ required to achieve a specified performance. This leads to

$$S \geq N_o \left(\frac{E_b}{N_o}\right)_{rqd} \frac{R}{B} \qquad (2.2)$$

The factor B/R is the so-called processing gain. It is evident that there is a range of values of B/R for which the power spectral density is less than the thermal noise spectral density, N_o. This is the basis of the use of spread spectrum for low probability of intercept (LPI) communications, but it also indicates that spread spectrum signals may be imperceptible to normal users.

The actual $(E_b/N_o)_{act}$ is calculated using the effect of both the thermal noise density N_o and the combined effect of all the other [M-1] CDMA users, giving the $(E_b/N_o)_{act}$ at the k^{th} user to be

$$\left(\frac{E_b}{N_o}\right)_{act,k} = \frac{P_k/R}{N_o + \frac{\lambda}{B}\sum_{\substack{i=1\\ i\neq k}}^{M-1} P_i} \qquad (2.3)$$

Note that sum represents the total power of all the other users as seen by the k^{th} receiver, and λ is a quantity which depends on user activity (e.g., data burst fraction, talk spurts, etc.).

In order to provide equal reception quality to each user, we must equalize the power, as seen by each receiver. This is one of the most difficult tasks in a ground mobile CDMA system, since it requires power control over a very large dynamic range. Without this power control, close-in transmitters overwhelm those remotely located, giving rise to the so-called near-far problem. With perfect power control, (2.3) becomes:

$$\left(\frac{E_b}{N_o}\right)_{act} = \frac{P/R}{N_o + \lambda(M-1)(P/B)} \qquad (2.4)$$

From (2.4) and (2.1), we get, for $M \gg 1$ and $MS \gg N_o$,

$$M \leq \frac{B/R}{\lambda(E_b/N_o)_{rqd}} \qquad (2.5)$$

For voice communications, the activity would conservatively be $\lambda = 50\%$ and $(E_b/N_o)_{rqd} = 3$ dB $= 2$, to achieve a bit error rate of 10^{-3} after decoding. Then, for a code excited linear prediction (CELP) voice encoder of rate 8 kbps., used in conjunction with a rate 1/2 forward error correction code, a 50 MHz band using CDMA could accommodate about $M = 50/16 \times 10^3 = 3125$ users. This picture, however, is somewhat optimistic, due to the effects of co-system interference from the adjacent cells, which might cut the number by one half to one third, depending on the propagation conditions and the location of the user.

It is easy to compare these figures with an FDMA system which can use only $1/7^{th}$ of the total bandwidth in each cell in order to accomplish frequency management and reuse geographically. Thus, for a standard FDMA system using 30 kHz/channel, we obtain

$$M \leq 50 \frac{10^6}{7x30x10^3} = 238$$

It is important to note how sensitive the estimate for the number of users are to the parameters such as activity and external interference. This is because CDMA is interference limited. This is not the case in FDMA or TDMA, where channels are laid out to avoid mutual interference. Nevertheless, CDMA has the potential to provide not only greater total capacity at acceptable levels, but many additional features as described in Section 1.

In the future, it may be possible to include an adaptive array antenna to do beamforming on desired signals while nulling on undesired signals, thereby providing a further opportunity to increase capacity and improve performance.

3.0 Spread Spectrum Overlay

One of the most interesting aspects of the use of DS CDMA for cellular radio transmission is the possibility of overlaying the DS radio network on top of existing users occupying the frequency band of interest. That is, it is not necessary to supply to the spreads spectrum users a frequency band which is completely devoid of other users. Rather, if the frequency band is partially occupied by various narrowband users, it is often possible to superimpose the DS signals on the same band in such a manner that both sets of users can co-exist.

For example, consider the interference caused by the spread spectrum network to the existing narrowband users. An analysis of this situation is presented in [1], and typical results are reproduced in Fig. 1. The curve shown in Fig. 1 corresponds to the average probability of error of an otherwise ideal BPSK receiver when operating in the presence of an unwanted DS signal. The abscissa is labeled $\frac{T_1}{T_c}\frac{P_1}{P_2}$, where T_1 and P_1 are the duration of a bit and the average power, respectively, of the BPSK waveform, and T_c and P_2 are the chip duration and average power, respectively, of the spread spectrum signal. The results correspond to $\frac{E_1}{N_o} = 10.5$ dB, where E_1 is the energy-per-bit of the BPSK signal, and N_o is the one-sided power spectral density of the thermal noise. It can be seen that even when the level of the BPSK signal is below that of the DS waveform, the narrowband receiver can still perform well if the ratio of the bandwidth of the spread spectrum signal to that of the BPSK waveform is sufficiently large.

Similar results can be generated regarding the interference seen by the DS signal. This, of course, is virtually self-evident, due to the anti-jam property of spread spectrum waveforms.

Finally, note that the discussion up to this point has been totally general, i.e., it applies to any DS-to-narrowband overlay. However, there are specific characteristics of the PCN which further enhance the prospects for a successful overlay. The key system aspect in this regard is the fact that the antennas for the narrowband users are typically located on towers which are hundreds of meters above the ground, whereas the PCN antennas are typically on the order of 6m above ground. Hence each set of users will only see the sidelobes of the other set of users' antenna patterns.

4.0 A Proposed PCN

In the U.S., Millicom, Inc. has recently been granted a license by the FCC to operate as a co-primary user in the frequency band 1850-1990 MHz. With this license, Millicom and SCS Mobilecom will conduct field tests of a PCN system employing direct sequence spread spectrum CDMA. The novel application seen here is that the band chosen for experimentation is one which is used today for microwave transmission. The field tests are intended to verify that spread spectrum can share a band with existing users and thereby increase the utilization efficiency of a frequency band. These tests will also provide important quantitative information, such as how many CDMA users can operate in the vicinity of a microwave receiver without degrading the microwave user's performance, and how many CDMA users can operate in the vicinity of a microwave transmitter before the CDMA user's performance is degraded.

The PCN system envisaged by Millicom and SCS is shown in Fig. 2. Here we see that users will be connected to low capacity cells, called "microcells", that are intended to operate with approximately 50 simultaneous users each. Since the cells are spaced closely together, the power transmitted by each user to a cell can be made small, typically 1mW, thereby minimizing interference to any existing microwave user.

The proposed experiments fall into two categories: measurement of the interference produced by the spread spectrum PCN on the existing microwave users, and measurement of the interference produced by the existing microwave users on both the mobile user and the cell. These experiments will be performed in Houston and Orlando during 1990 and 1991.

Consider again Fig. 2. This figure shows a typical, fixed location, existing microwave transmitter-receiver site. The mobile users 1 and 2 each transmit to the cell using the frequency band 1860-1910 MHz and receive from the cell using the band 1930-1980 MHz. Mobile user 3-50 is a transmit-only user which simulates 48 users transmitting from the same site. The power level of mobile users 1 and 2 will be adjustable from 100μW to 100mW, the power level of mobile users 3-50 will be adjustable from 4.8mW to 4.8W, and the power level of the cell will be adjustable from 5mW to 5W. Each adjustment can be made independently of the others.

4.1 Measurement 1: Measurement of the Interference Produced by PCN on Existing Microwave Receiver

The four vans, which include the mobile users as well as the cell, shown in Fig. 2, will be moved relative to a microwave receiver, and the bit error rate (BER) measured at each position. The measured BERs will be compared to the interference-free BER obtained when the mobile system is off. Different transmit powers from the cell and from the mobile users will be employed in order to determine the robustness of the system.

Measurements will be taken during different times of the day and night. In addition, two or more receiver sites will be tested.

4.2 Measurement 2: Measurement of the Interference Produced by the Existing Microwave Transmitters on the PCN

The position of the four vans shown in Fig. 2 will be varied relative to the existing microwave transmitters to determine the sensitivity of the PCN to such interference. Both qualitative voice measurements and quantitative bit-error-rate measurements will be made.

The robustness of the system to fading will also be determined. This measurement of the effect of the propagation characteristics of the channel on the PCN will be made by positioning the cell and mobile users in different parts of Houston and Orlando. BER measurements will be taken, and a comparison to r^2, $r^{3.6}$ and r^4 curves will be made in an attempt to better characterize this PCN channel.

5.0 Conclusion and Future Directions

Personal communication networks using CDMA have numerous advantages as compared to FDMA and TDMA:

- They can be used in a frequency band that has existing users, and therefore this means of communication represents an effective, efficient mode of frequency band utilization.
- CDMA is more robust in the presence of multipath. For example, if the direct path is 600 feet and the multipath is 800 feet, the two returns are separated by 150ns. Using the chip rate of 25Mchips/s means that the two returns are uncorrelated.
- CDMA has the potential of allowing a larger number of users, that is, of being a more efficient system. This improvement can also be translated into lower power and hence longer life for batteries.

In this decade, we are likely to see the CDMA PCN widely used for voice communications, facsimile transmission and data transmission. Its versatility could well result in this system attaining a major share of the world's communication market.

References

[1] R.L. Pickholtz, L.B. Milstein and D.L. Schilling, "Spread Spectrum for Mobile Communications", Submitted IEEE Trans. on Vehicular Technology.

[2] T.S. Rappaport and L.B. Milstein, "Effect of Path Loss and Fringe User Distribution on CDMA Cellular Reuse Efficiency", Globecom'90.

[3] M.B. Pursley, "Performance Evaluation for Phase-Coded Spread Spectrum Multiple-Access Communication, Part I: System Analysis", IEEE Trans. Comm., 8/77.

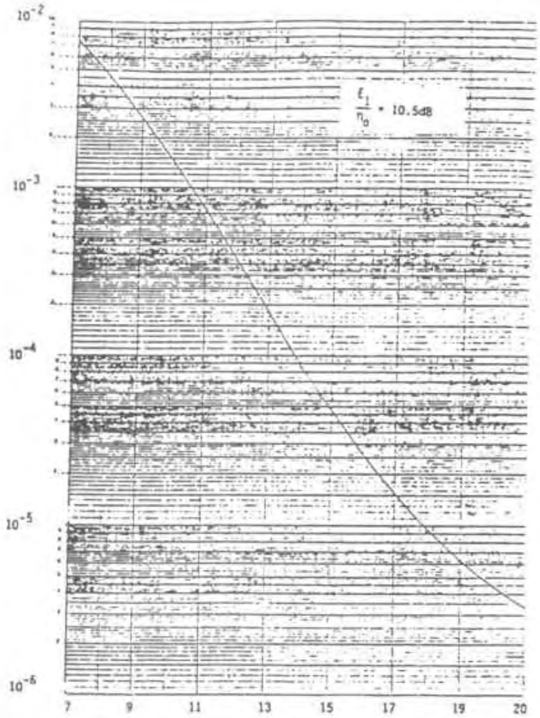

FIGURE 1

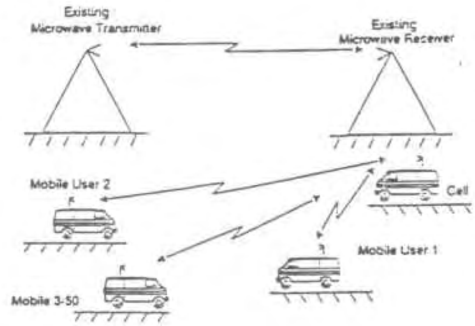

FIGURE 2

AN ISM BAND SPREAD SPECTRUM LOCAL AREA NETWORK: WaveLAN

Bruce Tuch
NCR Corporation
Utrecht the Netherlands

Invited Paper

Abstract- Until recently High Speed Data Communications Cordless Local Area Networks (CLANS) have not been getting much attention both in marketing and research. This paper discusses the design philosophy used during the development of WaveLAN. The technical trade offs, a sample of channel measurements and standard LAN system Benchmark tests are presented.

I. INTRODUCTION

CLAN development has been hampered by the relatively large, when compared with voice, spectral requirements and lack of fundamental research to define and overcome perceived channel impairments using consumer oriented technology. Without a possible spectral allocation the risk for no return on investment for private research and development is quite high. The allocation of the ISM band using Spread Spectrum technology, by the Federal Communication Commission (FCC) in 1985, has led the way for practical research and development activities with an end product as goal.

In chapter II the technical requirements which influence Spectrum, LAN Protocol and security are discussed. In chapter III the Processing Gain/Data Rate trade off is discussed and some channel models and measurements are shown. Chapter IV covers the radio architecture, technology and implementation issues. A SNR Outage prediction used to estimate link reliability, due to external noise, is given in chapter V. In chapter VI the Simulation and Measurements of the radio in a multipath channel is covered. Standard Benchmark tests results, which measure LAN performance, are given in Chapter VII.

II. REQUIREMENTS of a CLAN

Wireless based data communication systems have been low speed, bandwidth allocation driven products. Since this is a LAN it must "feel" like one, cordless or not. An important axiom in WaveLAN product development has been:

Except for the benefits of cordless operation, the end user should observe the least possible difference with standard installed wired based LAN products.

A. The Spectrum

To facilitate high speed data communications, in the Mega bits/s range, the ISM Spread Spectrum band is used. It is noted that Spread Spectrum Modulation is a FCC requirement, stimulating research for commercial applications in these bands. Protocol based Spread-Spectrum systems using Code Division Multiple Access (CDMA) techniques have been investigated for use with PBX connection oriented applications. Combination of voice statistics together with CDMA has been proposed which predicts spectrally efficient system performance and is under field trial [26]. Data communications is fundamentally different than voice in its statistical properties. There is no user defined pause time which can be used to maximize the system capacity. Also the basic structure of connection oriented fixed bandwidth/user system is different than a shared bandwidth data packet communication network. The throughput available per user is a function of the total system load. CDMA systems with dynamic rates as a function of total CLAN load can be envisioned, but the complexity evolved using switched or programmable correlators, compared with more conventional structured time domain multiplex approaches, does not seem promising. Since the cost consequence for a CDMA implementation is not negligible and the lack of "real time" voice statistics in LAN communication, CDMA as a protocol technique has not been chosen. The Spread-Spectrum Modulation method and medium access protocol are two separate entities.

B. The Protocol Choice

In keeping in stride with our development axiom, an already accepted IEEE 802 standard should be used if possible. This is quite important from an end-user marketing perspective when introducing new technology. An advantage in having a standard interface "at the lowest level possible" is in various software development activities; applications already available for existing LAN equipment can easily be adapted, quickening the development cycle. System bandwidth sharing, due to adjacent CLAN usage with electromagnetic overlap, must be taken into account in any radio design. This can be implemented [15] with the usual spectrum "break up" into multiple channels. Due to the nature of three dimensional indoor propagation the amount of frequencies needed is strongly dependant on various topological considerations. It is not clear at this point what reuse frequency set is needed and most likely, due to the variation of user topologies and requirements, never will be. Therefore the protocol must not "break down" due to co-frequency adjacent CLAN interference but take on bandwidth sharing responsibility. A standard bus based protocol is 802.3 Carrier Sense Multiple Access/Collision Detect (CSMA/CD), which has the largest installed base in the LAN market. Due to the large dynamic range of the radio medium, bandwidth efficient collision detection is technically difficult. Various mechanisms exist for collision detection implementations but the cost in bandwidth does not seem to outweigh the benefits of overall throughput in normal loading conditions. Therefore Carrier Sense Multiple Access/Collision Avoidance (CSMA/CA) is closest to an IEEE Standard, which, due to its random access nature, is robust with respect to protocol level bandwidth sharing and radio channel characteristics. Standard activity within the IEEE 802 committee for a new Wireless Media Physical Layer Protocol, 802.11, is now under way.

C. Security

Transmission of data via radio signals gives the perception of lack of privacy of communication due to the "open media". The design of any CLAN must address this issue. WaveLAN has three levels of security:

a. Network Identification (NWID).

In each data package a NWID identifying separate CLAN systems. Only data with the proper NWID is accepted for upper level software transport. Besides giving a first level of security, this optimizes the bandwidth sharing facility of the CSMA protocol.

b. Spread Spectrum Modulation.

While not a "military" implementation, it does give a eavesdropping threshold. Another WaveLAN board or equivalent Spread Spectrum Demodulator is needed, not just a amateur radio scanner hooked up to a modem.

c. National Bureau of Standards Data Encryption Standard (NBS-DES).

A DES VLSI option is implemented which gives a very high "standard level" of security.

III. THE PHYSICAL LAYER

A. Processing Gain and Data Rate in the ISM Band.

Within the FCC [21] regulations either Frequency Hopping (FH) or Direct Sequence Spread Spectrum Modulations can be implemented. While Frequency Hopping systems have some interesting diversity and multipath characteristics [29], due to the FCC regulated bandwidth limitation, FH systems are data rate limited to low kB/sec rates.

Note: The modulation bandwidth has been recently increased from 25 kHz to 500 kHz which would allow data rates up to 250 kbit/s.

First out product development is in the 902 - 928 MHz ISM band due to the implementation cost trade offs.

1. How much Bandwidth Spreading?

Since the spread spectrum modulation is not used as an access technique (CDMA) the trade offs involved are data rate, a robust connection in the presence of interference and the irreducible outage due to multipath intersymbol interference. In military Spread Spectrum systems the Processing Gain, which is a measure of system robustness to jamming and eavesdropping by the "enemy" is of vital importance. Various techniques have been developed to allow large Processing Gains (greater than 25 dB) with minimum receiver code acquisition times [3], [8], [37]. It is vital to realize that the characteristics of an "enemy" and the constraints put upon a system which must deal with this attack are quite different for a commercial communication system. In military systems one must assume that the "jammer" will try to constantly hit the system under attack. This is quite different than, for example, a ISM band interference signal which is quite comfortable staying just where it is. The larger the Processing gain of a Spread Spectrum system the higher the cost and spectral inefficiency. In some cases larger Processing Gain can degrade interference immunity with respect to other conventional frequency assignment techniques. Considering the fact that Spread Spectrum is not used as a protocol method nor is it the optimal "robust" modulation technique using a given bandwidth, one could question why use this at all? The first fact is that in the ISM band a minimum processing gain of 10 dB is a requirement. For a fixed transmit power the power density (watts/Hz) decreases in proportion with the Processing Gain. While other techniques of power reduction and spectrum management are possible, this is not the focus of the Part 15 rules and regulations. (Spread Spectrum does not require a standard "spectrum management protocol" and therefore overlay with already existing systems is possible). In terms of maximizing data rate, without Spread Spectrum modulation in the indoor unequalized channel, data rates on the order 300 Kbps can be supported [1],[7]. Due to inherent Spread Spectrum path resolution properties a 2 Mbit/s data rate is achieved within a 11 MHz Spread Spectrum bandwidth. In summary, a Processing Gain is used which takes into account the trade offs in data rate, robust performance, cost and legal considerations.

B. The Channel Model

1. Channel Echo and Multipath

Recently a wealth of information concerning indoor propagation characteristics has become available. Initial studies have shown wide variation in the delay spread parameter, ranging from 30 ns to 250 ns [9]-[11], [28] depending upon the environment, measurement dynamic range and threshold levels. Correlation Bandwidth measurements performed by NCR [34] of a typical office showed large correlation bandwidths (.5 correlation @ 12 MHz) which support the time domain low delay spread measurement data. The discrete indoor channels impulse response [35], [19] is used for system modeling:

$$h(\tau) = \sum_{i=1}^{L} \beta_i \cdot \delta(\tau - \tau_i) \cdot \exp(j\alpha_i) \tag{1}$$

Where:

τ_i the ith path delay.

β_i the ith path gain, with a Rayleigh distributed pdf.

L the number of paths.

α_i the i^{th} path phase, with a uniform pdf within $(0,2\pi]$.

2. Large Scale Power Variation

The channel model of equation (1) gives the microscopic, with respect to distances on the order of wavelengths, properties of the channel. The macroscopic large scale signal variation, on the order of meters between rooms and different areas, is not taken into account. The macroscopic power variation has been successfully modeled [2] as a log-normal distributed random variable, U(r), with pdf:

$$p(u) = (1/\sigma \cdot \sqrt{2\pi}) \cdot \exp(-(u-m(r))^2/2 \cdot \sigma^2) \qquad (3)$$

Where:

m(r) is the (dB) mean power, $n \cdot 10 \cdot \log(r)$ + Constant, as a function of distance.

The parameters most often found in the literature are the attenuation exponent, n, and the standard deviation, σ. Another parameter that has been found useful in the characterization of different environments [16] is a two exponent cross over point. For distances "close to" the antenna, in a Line of Sight path (LOS), the attenuation has been found to be close to free space, $n=-2$, value. At distances in which significant "clutter" occurs an increase in the attenuation exponent is found. Modeling in such a way decreases the Standard Deviation about the best fit regression lines. Characterization of attenuation of indoor environments is still being done by various researchers [20], [30] with great promise of coupling known building topologies with accurate attenuation predictions.

C. Polarization Diversity

A known technique to mitigate Rayleigh fading is the use of spacial diversity. Large Cross Polarization Coupling in the indoor channel has been reported [6]. Therefore the use of Polarization Diversity is an attractive method in limiting antenna size. Measurements have been done to determine the correlation between the receiver signal power between horizontal and vertically polarized receiver antennas.

1. Measurement Set-Up and Procedure

The vertical dipole transmit antenna, located 1 meter above the ground, radiates a Continuous Wave (CW), signal. For reception, vertical and horizontal polarized dipoles (RX System) are fixed (crossing each other) on an arm which is mounted on a rotating post. Each antenna is connected via a DPST RF PIN switch to a Spectrum Analyzer. The PIN Switch, Rotating post and Spectrum Analyzer is under Personal Computer control. The RX System is placed a set distance away from the transmitter which defines a cell location. During one measurement run the post is stepped through 35 positions, each separated from each other by 1/4 wavelength. During each step the received signal power is measured on the vertical and then, via the PIN Switch, horizontal antenna. Also the received power from both antennas is measured twice, with the same delay between measurements that occurs when antennas are switched. Three such measurements are done per cell, with 1 meter distance between the previous RX System position. In this way 135 measurement points are obtained per cell location. The calibrated transmit power, taking into account all cable loss, is 8 dBm.

2. Results

A typical office building has been measured (Cross over 8.5 m, $n= -3.6$, $\sigma= 3.7$ dB). Without a Line of Sight (LOS) path between TX and RX System a large Cross Coupling has been found with a large variation between receiver sights. Also the Correlation Coefficient, between vertical and horizontal polarized antennas received power levels, was found to be $< .13$ in all locations. Correlation of measurements using the same antenna, due to the channel coherence time (people walking in the office and unwanted movement of the TX or RX system) is greater than .85. An example correlation plot, between Horizontial and Vertical switched antennas, is shown in Figure 1. In this measurement the average cell power for Horizontial and Vertical antennas is -46.8 dBm and -49.8 dBm respectively giving 3 dB Cross Polariztion Coupling. This was found to be quite common showing, as was found in [6], that at a significant amount of locations, the received signal power is due to reflections which rotate the transmit polarization. Also the Cumulative Distributions show excellent Rayleigh Fading Characteristics (without LOS) for both horizontal and vertical polarizations, even with negative Cross Correlation Coupling and a vertically polarized receive antenna, as shown in Figure 2.

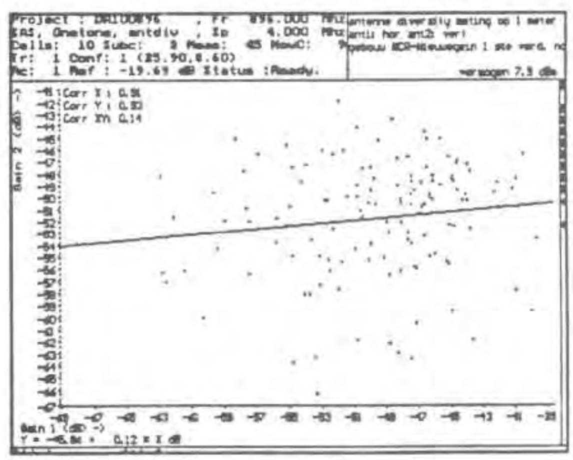

Figure 1. Horizontal vs Vertical Correlation with Cross Correlation Coupling of +3 dB (TX/RX distance of 28 m).

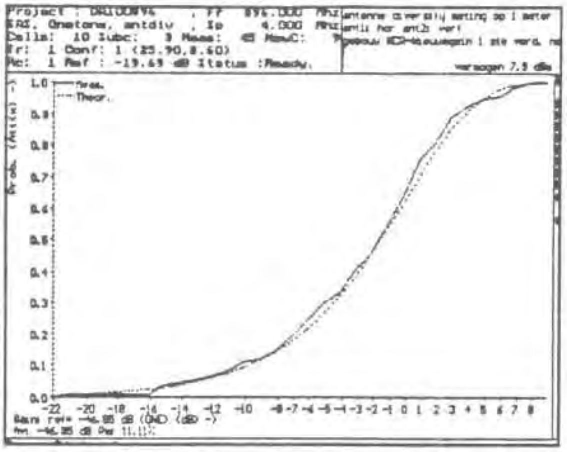

Figure 2. Cumulative Distribution of Vertical Antenna, with respect to cell average power, in a location with -3.7 dB Cross Polarization Coupling (TX/RX distance of 37 meters).

D. Network Topology

Due to the nature of the radio medium, the least number of radio links that achieves total network connectivity will give the best network performance. LAN Operating Systems, Novell being dominant market choice, operate using a central server architecture. Therefore a centralized network topology is implemented by default. While this is a preferred form of operation, it is not required and the implementation of the radio does not prohibit peer to peer configurations.

IV. TECHNOLOGY and THE RADIO ARCHITECTURE

The parameters of the radio modem are listed in Table I and are further clarified in the following discussion.

TABLE I: Radio Parameters

Frequency:	915 MHz
Bandwidth:	11 MHz (peak to null)
Modulation: (Information)	DQPSK
Chip Modulation: (pre filtered)	PSK
Data Rate:	2 Mb/s
Chip Rate: (Chip period, τ_c = 90.9 ns)	11 Mchips/s
Sensitivity: (Including 18 dB Man-Made Noise Factor)	-72 dBm
Output Power	+24 dBm
Antenna Gains (RX/TX)	2 dB

A. Modulation/Demodulation

Using complex notation the transmit signal is represented by [27]:

$$S(t) = RE[U(t) \cdot \exp(j2\pi f_c t)] \qquad (4)$$

Where:

$$U(t) = \sum_{n=-\infty}^{\infty} I_n \cdot g(t-nT)$$

Is the low pass complex envelope of the signal.

T the symbol period of the transmitted information.

g(t) "Spread Spectrum" modulating pulse.

I_n Information Vector, $\exp(j\theta_n)$, with four phase states: $\epsilon\{\pi/4, -\pi/4, 3\pi/4, -3\pi/4\}$.

Equation (4) is composed of two components. One containing the information, described by the complex vector I_n, the other which determines the spread spectrum characteristics of the signal, described by the real Spread Spectrum modulating waveform g(t-nT).

1. DQPSK Information Modulation

In order to simplify the receiver design differential phase modulation has been implemented. In this way no absolute phase reference is needed for demodulation. A known drawback of differential phase modulation is the sensitivity to receiver carrier frequency offset. Cost effective crystals are readily available with accuracies from 50 ppm to 25 ppm. With a 915 MHz carrier this translates into a maximum received frequency offset of 92 kHz. A 1 Mbaud signaling after differential detection gives an unacceptable phase error between symbols of 33 degrees. Therefore a phase compensation technique has been implemented in which this constant offset is adjusted within the preamble of the data frame. The maximum tolerable frequency offset is now a function of the frequency ambiguity function of the post detected spread spectrum signal [3]:

$$A(df) = |\ \mathrm{Sin}(\pi df \cdot T)/\pi df \cdot T\ |^2 \qquad (6)$$

Where:

A(df) gives frequency offset signal's power ratio, with respect to zero frequency offset, at the output detector.

df the offset between carrier frequencies.

T the symbol time (1 μs for 1 Mbaud).

Substitution of f = 92 kHz and T = 1 μs into (6) gives a maximum detected signal power degradation of only .5 dB. This allows cost effective frequency synthesis for applications in all the available ISM bands.

2. Spread Spectrum Modulation

The spectrum determining function in equation (4), $g(t-nT)$, is defined as:

$$g(t) = \sum_{k=1}^{N} X_k \cdot p(t-k\tau_c) \qquad (7)$$

Where:

$g(t)$ the spread spectrum sequence.

$p(t)$ the "chip" pulse:

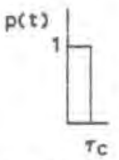

A unit pulse is given here as an example. Actually pre-filtered pulses are used improving the spectral characteristics of the transmit signal.

τ_c the chip duration such that $N = T/\tau_c$ is an integer.

X_k the kth chip's coefficient $\epsilon\{1,-1\}$

The correlation properties of the signal are determined by the real coefficient vector X_k. The Barker sequence is known to have excellent, bounded by one, odd periodic autocorrelation properties, important for robust multipath reception. An extended list of complex Barker Sequences [38] (unit magnitude and phase angles which are multiples of 6 degrees) has been published. Taking into account the trade-offs (Chap. III Sec.A) the 11 chip Barker sequence is used:

$$\overline{X} = [1\ -1\ 1\ 1\ -1\ 1\ 1\ 1\ -1\ -1\ -1]$$

It is noted, looking at (7) and (4), that a real barker sequence causes the signal to pass through the origin of the complex plane. The carrier is Phase Shift Keyed, PSK, with the Barker chip code. As will be shown the sideband regeneration, after chip pulse filtering, noise floor and power stage efficiency requirements are easily met using this signal structure.

3. The Output Spectrum

Given the scarcity of spectral resources, the efficient use of the spectrum is quite important. The theoretically most spectrally efficient modulation pulse shape is the $\mathrm{Sin}(x)/x$, which gives a "brick wall" rectangular frequency transfer function. One common physically realizable pulse which approximates this is the Raised Cosine. An implementation obstacle with this class of pulse shaping is that the transmit signal has a non constant envelope and the need for linear power amplification. Various forms spectrally efficient constant envelope modulation containing memory, Tame Frequency Modulation as an example, have developed [33]. One requirement is flexibility in the data symbol sequence which is transmitted. Due to the Spread-Spectrum modulation structure, the transmitted Barker chip sequence is fixed, limiting the modulation types that can be used. The output spectrum from a random data stream using equations (4),(7) (unit chip pulse) has been calculated [32]:

$$\Phi_{uu}(f) = T \cdot \mathrm{Sinc}^2(\pi f \tau_c) \cdot [11 - 2 \cdot \sum_{k=1}^{5} \mathrm{Cos}(4\pi f \cdot k\tau_c)] \qquad (8)$$

Due to the $[\mathrm{Sin}(x)/x]^2$ envelope of equation (8) the first sidelobes are only 12 dB down with a $(1/f)^2$ spectral roll-off. The main lobe is quite compact, with the first zero at 5.5 MHz. A 3 pole filter with a 7 MHz bandwidth has been implemented, substantially reducing the spectral power outside the main lobe. Since the filtered waveform is not of the constant envelope class, the linearity of the I and Q modulator and power driver stages was a design consideration. Since the out of band spectral requirements are not severe, a class B amplifier end stage operated with 1 dB "backoff" from its compression point gives an efficiency of 60% while keeping the first side-lobe 23 dB down and the noise floor > 45 dB as shown in the actual output spectrum in Figure 5. With a more stringent adjacent channel (another physically separated CLAN) interference requirement, using bias or feedback compensation techniques [31], [36], gives reasonable amplifier efficiencies using linear modulation with low adjacent channel suppression.

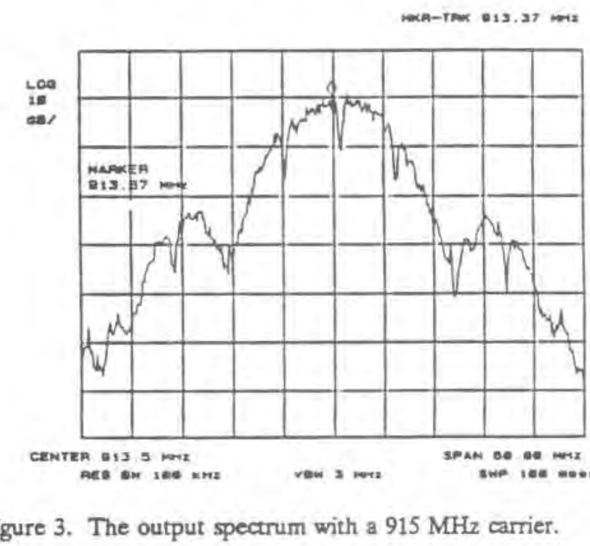

Figure 3. The output spectrum with a 915 MHz carrier.

4. Spread Spectrum Demodulation

Implementation of a Spread Spectrum Modulator is relatively inexpensive. It is the demodulation process which must bear the cost burden. One of the most important characteristics of PSK chip modulation, equation (7), is that it is a linear modulation process and the principle of superimposition applies. This will prove to be quite important when dealing with multipath reception. Therefore the demodulation structures used must maintain the systems linearity (at least up to a specified input signal level power). Demodulation schemes with hard-decision chip decision decoding while simpler to implement, are not used. The despreading process is performed by using a filter, $h(t) = g(t-T)$, matched [19] to $g(t)$ of equation (7).

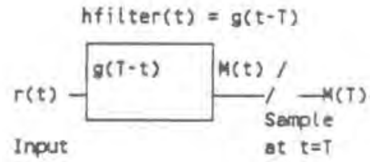

Figure 4. Matched Filter Correlation.

Substitution of the transmit signal (4) into the channels impulse response (1) gives:

$$r(t) = \sum_{n=-\infty}^{\infty} \sum_{i=1}^{L} I_n \cdot \beta_i \cdot \exp(j\alpha_i) \cdot g(t-nT-\tau_i) \qquad (10)$$

Following [18], the received signal (10) for n=0 and n=-1 (present and previous symbol are taken into account) are presented to the matched filter and assuming, without loss of generality, the first path is chosen for detection by the receiver using maximum selection, $\beta_1 > \beta_i$, and this path has zero channel delay, $\tau_1 = 0$, gives:

$$M(T) = I_0 \cdot [T \cdot \beta_1 \cdot \exp(j\alpha 1) + B1 \cdot \tau_c] + I_{-1} \cdot B1 \cdot \tau_c + I_{-1} \cdot [T \cdot \beta_k \cdot \exp(j\alpha k) + B2 \cdot \tau_c] \qquad (11)$$

Where:

$$k \mid [\tau_k = (T + \tau_1) = T]$$

$$B1 = \sum_{\substack{i \mid \tau_i < T \\ i \neq 1}} \beta_i \cdot \exp(j\alpha_i)$$

$$B2 = \sum_{i \mid \tau_i > T} \beta_i \cdot \exp(j\alpha_i)$$

M(T) is the the match filter output at the sample moment T.

In the derivation of (10):

a. The Barker sequence is used having unity bounded odd/even periodic and aperiodic correlation function.
b. The use of superimposition was used due to linear structure of the modulation.

It was important in the system design structure to maintain linearity. Equation (11) shows the robust structure Spread Spectrum modulation has with respect to multipath delay. Two terms, $T \cdot \beta_1$, $T \cdot \beta_k$ are multiplied by a factor T the others by τ_c. The ratio, T/τ_c, being the "Processing Gain" of the system. Since $\tau_k - \tau_1 = T$, only the significantly attenuated path, β_k, at one symbol delay contributes to intersymbol interference (ISI). Without the path delay resolution of spread spectrum, path delays significantly less than the symbol period contribute to ISI [4].

5. DQPSK Information Demodulation

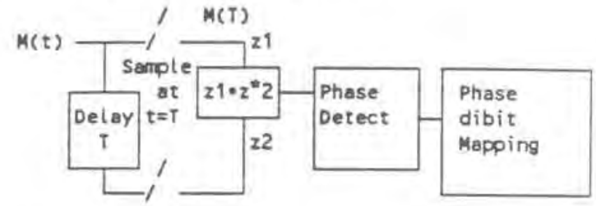

Figure 5. DQPSK Information Demodulator

Performing the complex conjugate multiplication shown in Figure 5 to the matched filter output from (11) gives:

$$M(T) \cdot M^*(0) = (\beta_1 \cdot T)^2 \cdot \exp[j(\theta_0 - \theta_{-1})] + ISI \qquad (12)$$

Taking the phase of the (12) gives the decision variable for Gray dibit decoding.
Equation (12), together with the path selection criteria, describes WaveLAN Spread Spectrum demodulation in a multipath channel.

6. Antenna Diversity

While the path resolution of Spread Spectrum gives "path diversity", with select largest implemented, a significant amount indoor channels (offices with cubicle dividers) have small delay spreads, < 50 ns. Therefore switched antenna diversity has been implemented using two cross polarized antennas, etched onto a printed circuit board, at the receiver. The selection criteria is based on a post processed signal quality level. Signal quality is a measure of an averaged correlation peak to side lobe ratio. This ratio decreases as a function of thermal noise, severe multipath and interference. This gives an excellent method to "probe" the channel's integrity.

V. DISTANCE vs OUTAGE MODEL

Spread-Spectrum modulation is robust with respect to intersymbol interference. Link Outage within indoor office environments will be due to insufficient Signal to Noise ratio as opposed to the irreducible multipath delay.
The question that is addressed here is: "What can the distance be, in an environment, characterized by its large scale parameters n, σ and cross over point, between the Terminal and the LAN Server?" From Table I an input power level of -72 dBm is needed in order to achieve 10E-8 BER. For received signals below this value the link is not reliable and a "link outage" has occurred.

Note: The Bit Error Ratio (BER) parameter does not strongly influence the outage of the link, due to the exponential relationship between BER and input power level. Accurate predictions using an on/off channel model [29] is reported.

The Outage can then be expressed as:

$$P[Pin < -72 \text{ dBm}]$$

Where:

P[•] the probability of the event [•]
Pin the received input power of the signal

From the Power Budget of Table I the transmit power is 24 dBm. Therefore a total radio link gain, LG, of -96 dB is permissible before outage occurs giving the outage criteria:

$$\text{Outage}(r) = P[\text{LG dB} < -96 \text{ dB}] \tag{14}$$

Numerical techniques are used to solve for outage using the large and small scale channel statistics.

A. Outage Calculations

The Large Scale parameters derived from measurement of a typical office (not including the corridor):
$n = 3.6$
$\sigma = 3.7$ dB
Cross over point ($n = -2$ to $n = -3.6$) = 8.5 m

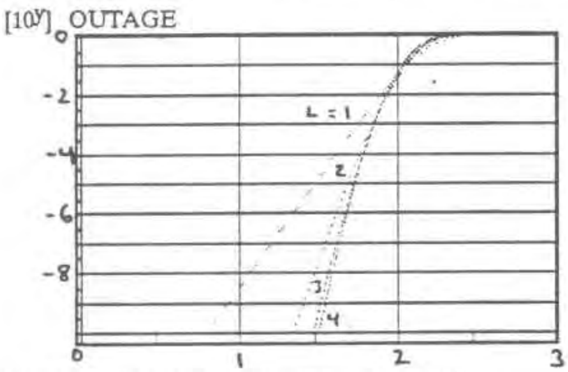

Figure 6. Outage vs Distance in meters [10^x] (L is a parameter).

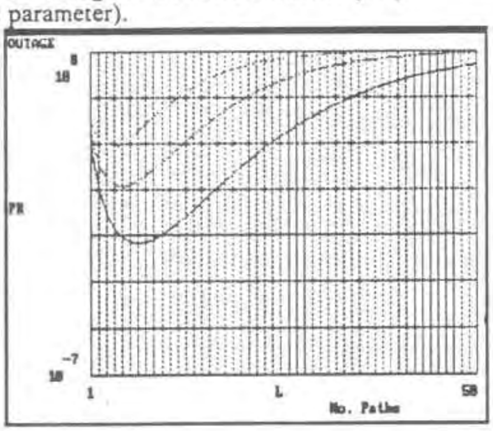

Figure 7. Outage vs L

From Figure 6, which characterizes a typical office, an Outage of .1% (1%) is expected at a Server to Station distance of 50 meters (75 m). In such an environment a one path, L=1, is assumed due to the low delay spread environment [11]. At small Outages, <.1%, a significant improvement is seen with two paths, as in [19], [23], all paths have equal power. With greater Outages, increasing the number of paths does not give improvement, as further shown in Figure 7. There is an optimal number of paths as a function of the minimum outage, the larger outage the smaller the optimal number of paths; for an Outage minimum of 1%, L = 3 is optimum. The reason for an optimal number of paths is due to the selection diversity implementation. While more paths help mitigate the Rayleigh fading, the average power of each path is less.

VI. SIMULATION and MEASUREMENTS

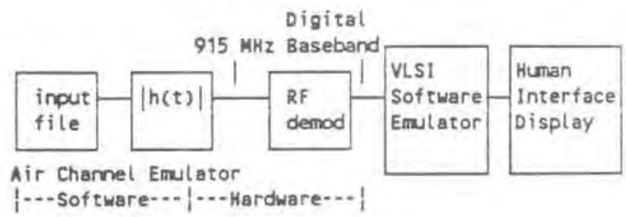

Figure 8. Block Diagram of Receivers simulation Set Up.

The WaveLAN modulation structure and some of the practical reasoning behind the various implementation decisions has been discussed. Software simulation for the modem algorithm development and system testing was extensively used. Since the software simulation structure mapped the VLSI processing exactly, VLSI verification and error detection was accomplished. Replacement of the actual VLSI in the software emulation block of Figure 8, does not alter system performance.

A. Channel Perturbations and Decision Region Diagrams

In order to test the spread spectrum's data recovery algorithms, test impulse responses are generated from a given power delay profile $<|h(\tau)|>$ as done in [5]. The sampled value of the delay profile gives the average power of the Rayleigh distributed path's gain. The phase is assumed to have a uniform distribution $(0,2\pi)$.

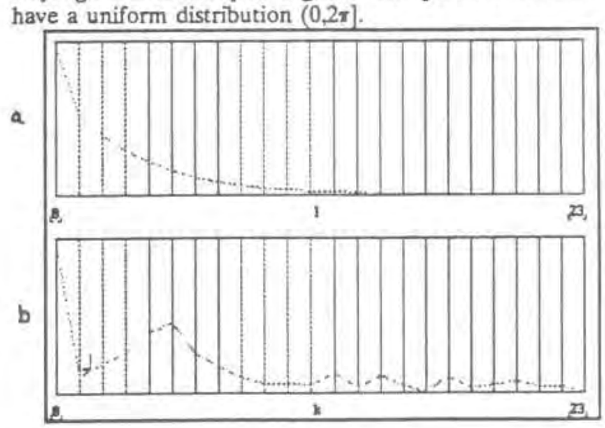

45 ns/div

Figure 9. (a) Exponential Power Delay Profile, (b) one particular impulse response.

Figure 9(a) shows the exponential profile with rms delay spread $\tau rms = 150$ ns. Using this power delay profile and the impulse response model of equation (1), impulse responses are generated with a sample shown in Figure 9(b).

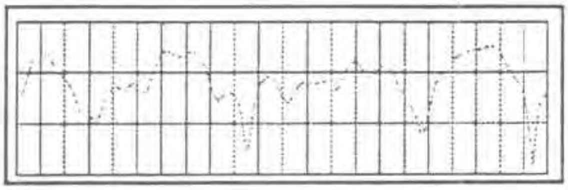

x= 1 MHz/div
y= 10 dB/div

Figure 10. Frequency Transfer Function

Figure 10 shows the frequency domain spectrum of the channels transfer function, $|H(jw)|$. Note that significant "frequency selective" fading is present within the pass band of the modulated signal of Figure 3. A random data sequence is demodulated, using the receiver structure of Figure 5. In Figure 11 the output of the demodulation process is shown.

Figure 11. Post Correlation Signals

Figure 11 (a),(b) shows the I and Q outputs of the digitally correlated data. In Figure 11(c), the correlated data modulus, a second resolvable path is clearly seen. The first path is chosen for data extraction, due to our switched path implementation. Figure 11 (d) shows the sample and hold of the correlation peak, variation here is due to bit quantization and clock tracking algorithms.

Figure 12. DQPSK Vector Data Display

The differentially demodulated information vector, Figure 12, with 5,000 random symbols processed, shows clearly defined decision regions and minimal ISI perturbation.

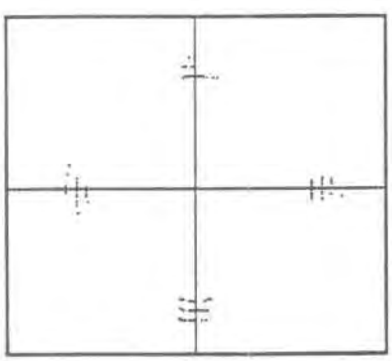

VII. LAN PERFORMANCE

Standard Lan Benchmark testing was performed to compare with standard wired LAN products [14], [17]. Since this is a total system based test, the total system configuration is important. Especially with higher medium data rates a part of the throughput is determined by the Server Speed itself.

A. Test Set-Up

Network
System: Novell SFT Netware version 2.15.

Configuration: Server PC with Intel 80386 processor/16 MHz. Six stations with Intel 80286 processor/8 MHz.

Benchmarks: Novell Perform 3 test and PC Magazine LABS Network Speed Under Load Test rev. 2.

	WaveLAN	Arcnet	Token Ring	Ethernet	StarLAN
Medium Data Rate	2 Mbps	2.5 Mbps	4 Mbps	10 Mbps	1 Mbps
System Throughput (Perform 3)	1 Mbps	1.1 Mbps	2.5 Mbps	3.6 Mbps	.8 Mbps
File Transfer Time (PC Magazine)	580 s	400 s	320 s	300 s	700 s

The effect of multiple electromagnetically overlapping LANS on the throughput and bandwidth sharing has been measured.

#CLANs	#WS	S	S•#CLANs
1	1	.6 Mbps	.6 Mbps
1	3	.8 Mpbs	.8 Mbps
1	6	1 Mpbs	1 Mpbs
2	3	.44 Mpbs	.9 Mpbs
3	3	.3 Mpbs	.9 Mpbs

Where:

S gives the individual LAN system throughput (Novel Perform 3 test).

#CLANs the total number of overlapping LANs.

#WS the number of workstations/LAN.

S•#CLANs gives the total system throughput of all the overlapping CLANs.

As expected the available bandwidth is shared between different overlapping LAN users of the medium.

VIII. CONCLUSION

Various design and implementation issues of the first High Speed CLAN on the market has been discussed. Without channel equalization high data rates are achievable using the existing FCC Spread Spectrum ISM band regulations. WaveLAN, using 11 MHz of bandwidth achieves 2 Mbit/s raw data rate for indoor operation. In the 2.45 GHz and 5.7 GHz

ISM bands there is respectively 83.5 MHz and 125 MHz of bandwidth available now. A great opportunity exists to further increase system capacity, helping solve the end-user's LAN connectivity problems of today.

REFERENCES

[1] A. S. Acampora and J.H. Winters, "System Applications for Wireless Indoor Communications", IEEE Communications Magazine Vol. 25, No. 8, August 1987.

[2] S.E. Alexander, "Characterizing Buildings for Propagation at 900 MHz", Electron Lett. Vol. 19 No. 20 Sep. 1983.

[3] Charles R. Cahn, "Spread Spectrum Applications and State of the Art Equipments", NATO, AGARD Lecture Series No. 58, July, 1973.

[4] Justin C-I Chuang, "The Effects of Delay Spread on 2-PSK, 4-PSK and 16-QAM In a Portable Radio Environment", Globecom 1987.

[5] Justin C-I Chuang, "The Effects of Time Delay Spread on Portable Radio Communications Channels with Digital Modulation", IEEE Journ. on Selected Areas in Communications, SAC-5, June 1987.

[6] Donald C. Cox, Roy R. Murray, Hamilton W. Arnold, A. William Norris, and Marvin F. Wazowicz, "Cross-Polariztion Coupling Measured for 800 MHz Radio Transmissions In and Around Houses and Large Buildings", IEEE Trans. on Ant. and Prop. Vol. Ap-34 No. 1, Jan. 1986.

[7] Donald C. Cox, "Universal Digital Portable Radio Communications", Proc. of The IEEE, Vol. 75. No. 4, April, 1987.

[8] Klaus Dostert, "Ein Neues Spread-Spectrum Empfängerkonzept Auf Der Basis Angeapfter Verogerungsleitungen Für Akustische Oberflächenwellen", Universität Kaiserslautern, Dissertation 1980.

[9] D.M.J. Devasirvatham, "A Comparison of Time Delay Spread Measurments within Two Dissimilar Office Buildings", ICC'86, June 23-25, 1986.

[10] D. M. J. Devasirvatham, "Time Delay Spread Spectrum Measurments of Wideband Radio Signals Within a Building", Electronic Letters, Vol. 20, Nov. 1984.

[11] D.M.J. Devasirvatham, R.R. Murrayand C. Banerjee, "Time Delay Spread Measurements at 850 MHz and 1.7 GHz Inside a Metropolitan Office Building", Electron Lett. Vol. 25 No. 3, Feb. 1989.

[12] Datapro Reports on PC & LAN Communications: LAN Hardware evaluation 800-101 Token Ring Network Adapters, NSTL reports;, June 1990.

[13] Grand Prix, comparision between various Arcnet, Ehternet and Token Ring boards, LAN Magazine, January 1990.

[14] W. Diepstraten and H.J.M. Stevens, "WaveLAN System Test Report", NCR Corporation TR No. 407-0023871 rev A.

[15] William C. Jakes, Jr., "Microwave Mobile Communications", John Wiley & Sons, 1974.

[16] Donald Johnson, "Indoor Coverage Area Modeling", NCR Research and Development, 1988.

[17] A. Kamerman, "Perfomance of WaveLAN and other LANs", NCR Systems Engineering Design Document.

[18] M. Kavehrad, "Direct-Sequence Spread Spectrum with DPSK Modulation and Diversity for Indoor, Wirless Communciations", IEEE Trans. Commun.,vol. Com-35, Feb. 1987.

[19] M. Kavehrad and G. E. Bodeep, "Design and Experimental Results for a Direct Sequence Spread-Spectrum Radio Using Differential Phase-Shift Keying Modulation for Indoor, Wireless Communications", IEEE Journal on Sel. Areas in Communications, Vol. SAC-5, No.5, June 1987.

[20] Jean-Francois Lafortune and Michel Lecours, "Measurements and Modeling of Propagation Losses in a building at 900 MHz", IEEE Tran. Vehicular Tech, Vol. 39, No. 2, May 1990.

[21] Michael J. Marcus, "Regulatory Policy Considerations for Radio Local Area Networks", IEEE Communications Magazine, Col. 25, No. 7, July 1987.

[22] Novell: LAN Evaluation Report, Novell Advanced Netware, 1986.

[23] K. Pahlavan,"Spread Spectrum For Wireless Local Networks", Proc. IEEE PCCC, Febuary 1987.

[24] K. Pahlavan, "Wireless communications for office information networks", IEEE Commun. Magazine, June 1985.

[25] A. Papoulis, Probability, Random Variables, and Stochastic Processes", McGraw Hill, New York, 1965.

[26] PCN America, Inc., "For Authorization in the Experimental Radio Service of a Spread Spectrum Personal Communications Network, to Serve the Washington, D.C., Metropolitan Area", FCC File No. 1343-E-PC-90, January 1990.

[27] J.G. Proakis, Digital Communications, New York: McGraw-Hill, 1983.

[28] Adel A. M. Saleh and Reinaldo A. Valenauela, "A Statistical Model for Indoor Multipath Propatation", IEEE Journal SAC Vol. SAC-5 No. 2, Feb. 1987.

[29] Adel A. M. Saleh and Leonard J. Cimini, JR., "Indoor Radio Communciations Using Time-Division Multiple Access with Cyclical Slow Frequency Hopping and Coding", IEEE Journal on Selected Areas in Communications, Vl. 7, No. 1, January 1989.

[30] Scott Y. Seidel and Theodore S. Rappaport, "900 MHz Path Loss Measurements and Prediction Techniques for In-Building Communication System Design", Vehicular Technology Conference, St. Louis, MO, May 1991 (Future presentation).

[31] Sirikiat Ariyavisitakul and Ting-Ping Liu, "Characterizing the Effects of Nonlinear Amplifiers on Linear Modulation for Digital Portable Radio Communciations", IEEE Trans. on Vehicular Technology, Vol. 39, No. 4, November 1990.

[32] Carl-Erik Sundberg and Nils Rydbeck, "Recent Results on Spectrally Effecient Constant Envelope Digital Moduahion Methods", CH1435-7/79/0000-0227 IEEE 1979.

[33] Kiwi Smit "Spectrum of 11 chip Barker Sequence", NCR Systems Engineering Design Report.

[34] Bruce Tuch, "Radio Propagation Measurement Report", NCR Systems Engineering, 1987.

[35] George L. Turin, "Introduction to Spread-Spectrum Antimultipath Techniques and Their Application to Urban Digital Radio", Proc. of the IEEE, Vol. 68, No. 3, March 1980.

[36] Yoshihiko Akaiwa and Yoshinori Nagata, "Highlty Efficient Digital Mobile Communications with a Linear Modulation Method", IEEE Journal on Selected Areas in Communiations, Vol. SAC 5, No. 5, June 1987.

[37] Shen Yunchun and C.P. Tou, "A Scheme for Further Strengthening Interference Protections of Spread Spectrum Communication Systems", IEEE EMC Symposium 1990, Washington.

[38] Ning Zhang and S.W. Golomb, "Sixty-Phase Generalized Barker Sequences", IEEE Trans. on Information Theory, Vol. 35, No. 4, July, 1989.

Bruce Tuch received the BEEE degree (Honors) from the State University of New York at Stony Brook, in 1979 and M.S. Degree from The Technical University Eindhoven, Holland, in 1983. From 1982 to 1985, he worked on High Frequency Integrated Circuit Design for commercial Tuner development at Philips Corporation, Component Laboratories (ELCOMA). He joined NCR in 1985 and is Project Leader within the Wireless Indoor Network Division at NCR Systems Engineering, Utrecht the Netherlands. His research interest are in indoor digital transmission systems and analog integration. Bruce is a member of Tau Beta Pi.

PERFORMANCE OF SPREAD SPECTRUM AND DECISION FEEDBACK EQUALIZERS OVER WIDEBAND MEASUREMENTS OF THE INDOOR RADIO CHANNEL

K. Pahlavan
Worcester Polytechnic Institute
Worcester, MA

M. Chase
Kodak EPS
Billerica, MA

S. J. Howard
Raytheon Company
Marlboro, MA

Abstract

The measured multipath profiles from five different indoor areas are used for the performance analysis of a spread spectrum system and a modem with a Decision Feedback Equalizer (DFE). The results are compared with the analytical performance predictions for both cases. For the DFE modem, the analytical results are shown to agree closely with the performance determined over the real channels. The DFE modem showed acceptable performance at data rates on the order of ten megabits per second. The performance of the spread spectrum multiple access orthogonal codes over the real channel measurements is then compared with an analytical bound. The results reveal that the standard techniques used for performance predictions provide optimistic results.

Introduction

The severe multipath fading, which is characteristic of the indoor radio channels, limits the performance of various modems over the indoor radio channel. Usually there are analytical solutions in the literature which are used for performance predictions of these systems. It is desirable to predict the real performance of these systems over the measured channel responses and compare it with the analytical predictions.

The results of wideband channel measurements in five indoor areas are used for performance predictions of the decision feedback equalizer modem and a spread spectrum system. The analytical results for DFE modems are those originally developed for the troposcatter [1] and microwave line-of-sight channels [2]. The spread spectrum system uses orthogonal codes in a CDMA environment with a coherent RAKE receiver. The performance predictions are based on the asymptotic approximations used for performance evaluation of maximum ratio combiner receivers [3].

The first section provides details of the measurement data base used for performance prediction on the actual channels. In the second section, the performance predictions for the DFE and the spread spectrum systems are evaluated over the measured channels and the results are compared with the results of analytical approximations. The last section provides the summary and conclusions.

1. The Data Base

For the modeling of the fading multipath indoor radio channels, the complex low-pass impulse response of the channel is represented by $h(x,\tau)$, where τ is the delay and x is a variable representing the location of the transmitter and the receiver. The complex low-pass impulse response of the channel is mathematically represented by:

$$h(x,\tau) = \sum_k \beta_k(x)\, e^{j\theta_k(x)}\, \delta(\tau - \tau_k(x)) \qquad (1)$$

where a transmitted impulse is received as the sum of several impulses with amplitude β_k, phase θ_k and arrival delay τ_k. This model is defined by the set of parameters $\{(\beta_k, \tau_k, \theta_k)\}$.

The experimental measurements used in this paper are performed at 910MHz [4,5]. A 5 nsec RF pulse is transmitted every 500 nsec. The envelope of the received signal is averaged over 64 observations. The averaging takes 15-20 msec and the result is stored as a channel profile. From each of these profiles, a set of (β_k, τ_k) representing delay and amplitude of the arriving paths is determined. The θ_k associated with each path is assumed to have a uniform distribution [5].

The multipath profiles used for performance predictions were measured in 288 locations in five factories [4]. Area A (Infinet Inc., N. Andover, MA) is a typical electronics shop floor having circuit board design equipment, soldering and chip mounting stations. Area B (also in Infinet Inc.) includes test equipment and storage areas for common electronic equipment partitioned by metallic screens. Area C (Norton Company, Worcester, MA) has grinding machines, huge ovens, transformers and other heavy machinery. Area D (General Motors, Framingham, MA) is a car assembly line "jungle" comprising all kinds of welding and body shop equipment. Area E (also in General Motors) is a vast open area used for final inspection of the new cars coming out of the assembly line.

2. Performance Predictions

From the measured multipath profiles explained in section 1, a set impulse responses are formed by associating independent uniform random phases with each arriving path. The resulting impulse responses are used for the performance analysis based on the actual measured data. The performance of a DFE modem and a spread spectrum system are evaluated over these responses and the results are compared with a theoretical bounds.

The DFE Modem

Using the method described in [2], the overall impulse response after equalization and the bit error rate of the BPSK/DFE modems are calculated for each channel impulse response. The BERs determined from the complex channel impulse responses are used for calculation of average probability of error in each area. The DFE uses three T/2-spaced forward taps and three T-spaced feedback taps. As shown in [6,7], three forward and three feedback taps provide a suitable compromise between the complexity of the hardware and the performance gain from the implicit diversity in the indoor radio channels.

The theoretical results presented for the BPSK/DFE modem are based on the analysis provided in [1]. This work assumes an infinite number of feedback taps which results in complete removal of the ISI due to the past decisions. In this work, the Laplace transform of the probability density function of the signal to noise ratio after equalization is given by:

$$Y(s) = \prod_{k=0}^{K}\left(1+\frac{E_b}{N_0}\lambda_k s\right)^{-D}, \qquad (2)$$

$$= \sum_{i=1}^{D}\sum_{k=0}^{K} A_{ik}\left(1+\frac{E_b}{N_0}\lambda_k s\right)^{-i},$$

where K+1 is the number of forward filter taps, D is the external diversity, A_{ik}'s are the coefficients of the polynomial after partial fraction expansion of the first part of the equation and the λ_k's are the eigenvalues of the matrix $G^{-1}C(t_0)$. The elements of the matrix $C(t_0)$ are given by

$$C_{kl}(t_0) = \int_{u=-\infty}^{\infty} g(t_0-k\tau_s-u)g(t_0-l\tau_s-u)Q(u)\,du$$

where τ_s is the equalizer tap spacing, g is the overall impulse response of the pulse shaping filters (raised cosine, 50% roll-off), and $Q(u)$ is the delay power spectrum of the channel. The elements of matrix G are given by

$$G_{kl} = g(k\tau_s - l\tau_s) + \frac{E_b}{N_0}S^2\sum_{i=1}^{I} C_{kl}(t_0 - iT)$$

where E_b is the average energy per bit, N_0 is the power spectral density of the additive noise, S^2 is the variance of the ISI, I is the number of future symbols with significant ISI , t_0 is the sampling instant, and T is the symbol period.

The delay power spectrum used for these calculations is obtained by averaging the received power at different delays over all measured locations. The shape of the equivalent delay power spectrum is exponential with the decay rate of 15 nsec.

Defining $b_j = E_b\lambda_j/N_0$, and taking the inverse-Laplace transform from (2), the probability density function of γ is :

$$f_\Gamma(\gamma) = \sum_{i=1}^{D}\sum_{k=0}^{K}\frac{A_{ik}\,\gamma^{k-1}}{(b_j)^k(k-1)!}\exp\left(\frac{-\gamma}{b_j}\right).$$

The average probability of error for the modem is given by:

$$\overline{P_e} = \frac{1}{2}\int_0^\infty erfc(\sqrt{\gamma})f_\Gamma(\gamma)d\gamma \qquad (4)$$

$$= \sum_{i=1}^{D}\sum_{k=0}^{K} A_{ik}\left(\frac{1-u_j}{2}\right)^k\sum_{i=0}^{k-1}\binom{k-1+i}{i}\left(\frac{1+u_j}{2}\right)^k$$

where

$$u_j = \left(\frac{b_j}{1+b_j}\right)^{\frac{1}{2}}.$$

Fig. 1 represents the average probability of error versus the data rate at SNR=40dB for the bound using the equivalent delay power spectrum, results from computer generated channel profiles and the results for the measured channel profiles in five different areas. The computer simulated profiles are generated from the model suggested in [8] with the same performance prediction method used for the actual measurements.

For the low data rates in the area E, which is a vast open area, the performance is better than the predicted values for the lower bound. As the data rate increases, the symbol duration decreases and the ISI caused by the multipath increases. The performance of the BPSK modem is degraded with the additional ISI. However, the BPSK/DFE modem takes advantage of the additional ISI and uses that as a source of inband or implicit diversity to improve its performance [1,6].

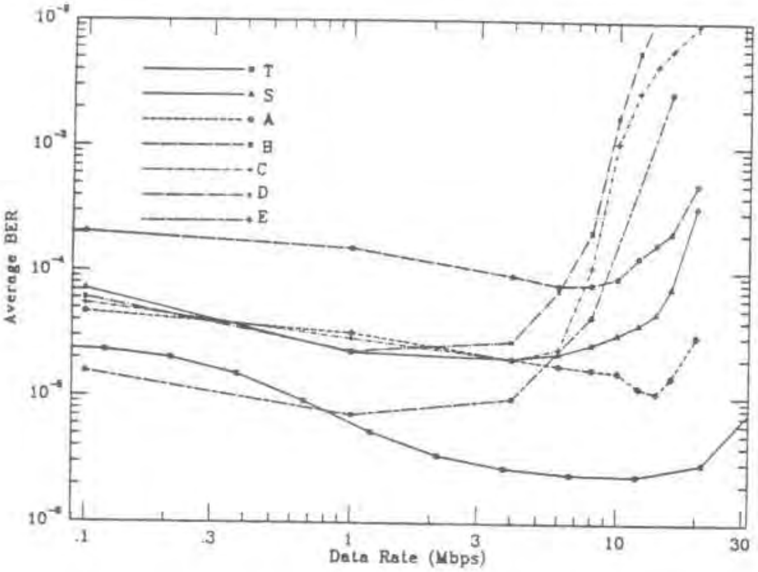

Fig. 1. Average probability of error versus data rate for a BPSK/DFE modem in each of the 5 areas, the computer simulated channel model (S), and the theoretical results (T). The SNR is 40 dB.

3. The Spread Spectrum System

The system [9,10] consists of K users, each assigned a set of sequences $V^{(k)}$ consisting of M-ary orthogonal sequences, each of length N;

$$V^{(k)} = \{V_1^{(k)}, V_2^{(k)}, \cdots V_M^{(k)}\}$$

where

$$V_\lambda^{(k)} = \{V_{\lambda,0}^{(k)}, V_{\lambda,1}^{(k)}, \cdots V_{\lambda,N-1}^{(k)}\}$$

and $V_{\lambda,n}^{(k)} = exp(j\theta_{\lambda,n}^{(k)})$ is a complex r^{th} root of unity (r-phase modulation). M-ary equally likely data symbols are transmitted at a rate of one every T seconds.

The chip duration T_c is $1/W$, W being the available bandwidth. The chip waveform is defined for $0 \le t < T$, is zero outside the range, and is normalized so that the energy per chip is equal to T_c. The received signal with noise and $W >> (\Delta f)_c$ (the coherence bandwidth) is

$$r(t) = \sum_{k=1}^{K} \sum_{i=0}^{L_1-1} a_i^{(k)} X_k(V_\lambda^{(k)}, t - \frac{i}{W}) + n(t)$$

where $a_i^{(k)}$ are samples of the channel impulse response for the k^{th} user and the i^{th} path.

A coherent RAKE receiver is used to determine an upper bound on performance. The decision variable Z_λ for the first user and the symbol λ with the receiver phase locked to the first user is

$$Z_\lambda = \mathrm{Re}\{\sum_{k=1}^{K} \sum_{l=0}^{L_1-1} a_l^* \int_0^T r(t) X_1^*(V_1^{(1)}, t - \frac{l}{W}) dt\}$$

The statistics of the difference of decision variables are assumed to follow a Gaussian distribution. Therefore, the probability of error can be expressed as

$$Pr(\epsilon) \simeq \frac{M-1}{2}\, erfc(\sqrt{\frac{\gamma}{2}})$$

The energy per bit is

$$E_b = \frac{A^2}{2} \frac{NT_c}{\log_2 M}$$

and

$$\gamma = \frac{[NT_c \sum_{l=0}^{L_1-1} |a_l|^2]^2}{\Omega}$$

where

$$\Omega = \sum_{l=1}^{L_1-1} \sum_{i=0}^{L_1-1} [\mathrm{Re}(a_l^* a_i^{(1)})]^2 Y_a(\frac{l-i}{W})$$

$$+ \sum_{k=2}^{K} \sum_{l=0}^{L_1-1} \sum_{i=0}^{L_1-1} [\mathrm{Re}(a_l^* a_i^{(k)})]^2 Y_b(\frac{l-i}{W})$$

$$+ \frac{N_o}{E_b} \frac{(NT_c)^2}{2\log_2 M} \sum_{l=0}^{L_1-1} |a_l^*|^2$$

$Y_a()$ and $Y_b()$ are related to the variances of the auto- and cross-correlation functions of the transmitted sequences. The first term represents the self-interference, the second term interference from other users and the last term is noise.

The results of the simulations are compared with the asymptotic approximation for maximal-ratio coherent detection [3]

$$Pr(\epsilon) \simeq \frac{1}{2} \frac{(DL - \frac{1}{2})!}{\sqrt{\pi}(DL)!} \frac{2^{DL}}{\Gamma^{DL}}$$

where D is the order of external diversities, Γ is the signal-to-noise ratio and L is the internal diversity. Usually [11,12] the order of internal deversity is determined by dividing the maximum delay spread with the chip duration. If this technique is used, the order of diversity for a system with bandwidth of 25MHz and a maximum delay spread of 100-200 nsec is between three and six.

Fig. 2 and 3 show the results of 2 and 5 active transmitters, respectively, over the measured indoor channels without power control for one order of external diversity. The asymptotic approximations are also shown for one and two orders of internal diversity and one and two orders of external diversities. Fig. 4 shows the performance over the measured indoor channels with power control and for 2, 5, 10 and 15 active transmitters.

Summary and Conclusions

Performance of DFE/BPSK modem and an M-ary orthogonal codes spread spectrum systems over measured channel impulse responses in five indoor areas were presented. It was shown that the data rates in the order of 10Mbps is feasible for the DFE/BPSK modems in the measured channels. The results of performance predictions over the measured channels showed close agreement with the results of analysis originally described in [1]. For the spread spectrum performance the results did not agree closely with those of the analytical predictions. In general, the analytical results were shown to be overly optimistic. In reality the order of diversity predicted by the RMS multipath spread of the channel seemed to provide much larger numbers than those observed from the performance over the real channels.

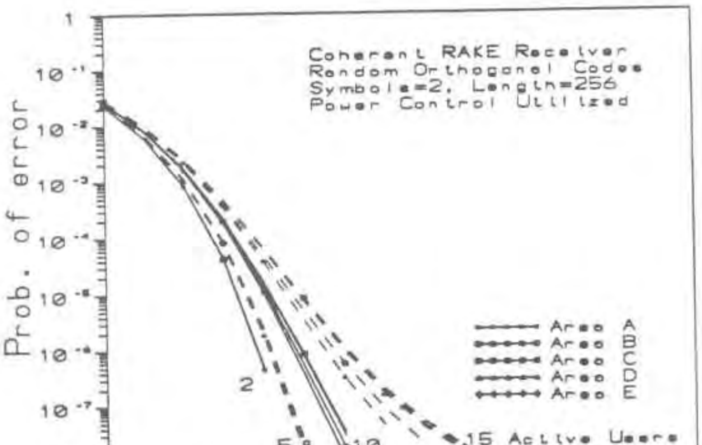

Fig. 4. Average probability of error versus signal to noise ratio for 2, 5 , 10 and 15 users with power control.

REFERENCES

[1] P. Monsen, "Theoretical and measured performance of DFE modem on fading multipath channel," *IEEE Trans. on Commun.*, vol. COM-25, pp. 1144-1153, Oct., 1977.

[2] P. A. Bello and K Pahlavan, "Adaptive equalization for SQPSK and SQPR over frequency selective microwave LOS channels," *IEEE Trans. on Commun.*, vol. COM-32, pp. 609-615, May 1984.(Also presented in ICC 82).

[3] M. Schwartz, W. Bennett and S. Stein, Communication Systems and Techniques. New York: McGraw-Hill, 1966

[4] K. Pahlavan, R. Ganesh, and T. Hotaling, "Multipath propagation measurements on manufacturing floors at 910MHz," *Electronic Letters*, vol. 3, pp. 225-227, Feb. 1989.

[5] R. Ganesh and K. Pahlavan, "Statistical Characterization of Indoor Radio Channels", Proceedings of the IEEE Globecom, Dec. 1989.

[6] T. A. Sexton and K. Pahlavan, "Channel modeling and adaptive equalization of indoor radio channels," *IEEE J. Selected Areas Commun.*, vol. SAC-7, pp. 114-121, Jan. 1989.

[7] S.J. Howard and K. Pahlavan, "Performance of a DFE Modem Evaluated from Measured Indoor Radio Multipath Profiles", *Proceedings of the IEEE ICC*, Atlanta, GA, June 1990.

[8] A. M. Saleh and R. A. Valenzuela, "A statistical model for indoor multipath propagation," *IEEE J. Selected Areas Commun.*, vol. SAC-5, pp. 128-137, Feb. 1987.

[9] P. K. Enge and D. V. Sarwate, "Spread spectrum multiple-access performance of orthogonal codes: linear receivers," *IEEE Trans. Commun.*, vol. COM-35, pp. 1309-1319, Dec. 1987

[10] M. Chase and K. Pahlavan, "Spread-Spectrum Multiplie-Access Performance of Orthogonal Codes Over Measured Indoor Channels," *IEEE Symposium on Spread Spectrum Techniques and Applications*, Sept. 1990, pp. 1-5

[11] K. Pahlavan and M. Chase, "Spread Spectrum Multiple Access Performance of Orthogonal Codes for Indoor Radio Communicaitons", *IEEE Trans. on Comm.*, Vol. 38, No. 5, pp574-577, May 1990.

[12] M. Kavehrad and P. McLane," Performance of Low-Complexity Channel Coding and Diversity for Spread Spectrum in Indoor Wireless Communications," *AT&T Tech. J.* , Vol. 64, No. 8, pp 1927-1965, Oct. 1985.

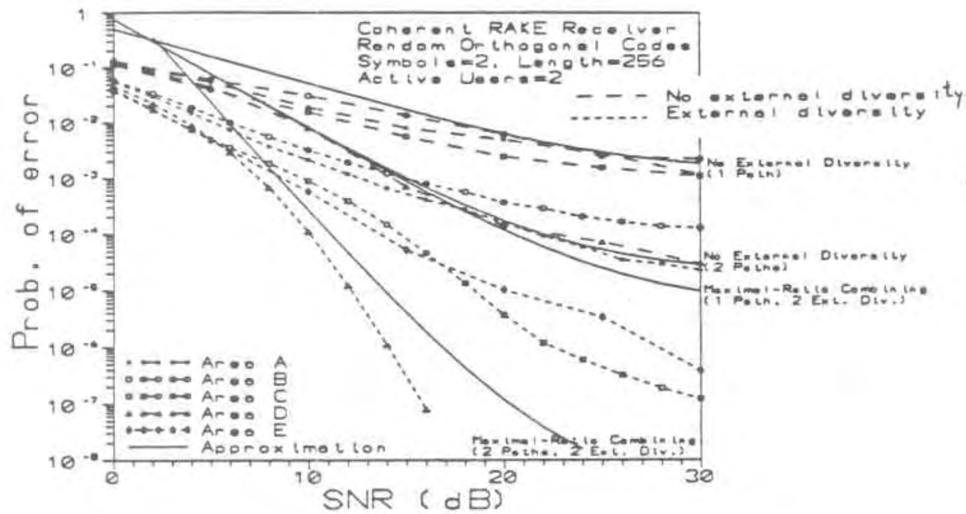

Fig. 2. Average probability of error versus signal to noise ratio for two active transmitters, without power control.

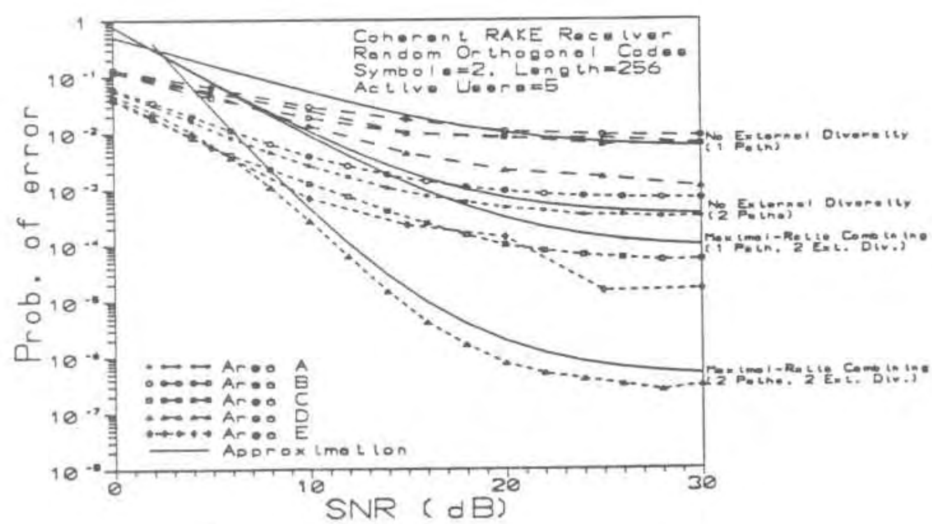

Fig. 3. Average probability of error versus signal to noise ratio for five active transmitters, without power control.

SESSION IV

OTHER EMERGING TECHNOLOGIES

Compound strategies of coding, equalization and space diversity for wideband TDMA indoor wireless channels*

Charles L. Despins, David D. Falconer and Samy A. Mahmoud

Department of Systems and Computer Engineering
Carleton University, Ottawa, Canada, K1S 5B6

Abstract — **Compound strategies of equalization and space diversity in the form of an optimum baseband combiner are attractive for wideband TDMA portable communication radio links in order to combat dispersive fading and cochannel interference. This paper investigates the performance of such a scheme in conjunction with convolutional coding and soft-decision Viterbi decoding via a semi-analytical technique based on the method of moments. This approach avoids a non-fading gaussian noise characterization of interference and provides results for both ideal interleaving and no interleaving. With dual space diversity and three taps per forward filter, it is shown that, at a data rate of 10 Mbits/s, channel coding can be a viable alternative to increasing the space diversity order even in the absence of interleaving.**

I. Introduction

A wideband[2] TDMA access mode is attractive for personal and portable tetherless communications as it provides users with a flexible combination of data rates to accommodate a variety of different applications such as facsimile, still pictures, high quality voice and high resolution video. However, the large irreducible error rates observed [1] when the rms delay spread, typically limited to 50 ns [2] in a medium-size office building, exceeds 5% or 10% of the symbol interval imply that equalization is necessary for signaling rates larger than 1 Mbit/s or 2 Mbits/s. With the aid of macroscopic diversity to alleviate large-scale shadowing effects, an equalizer structure as shown in figure 1 with M L-tap forward filters and a common feedback filter is then an attractive technique to simultaneously combat signal fading, intersymbol interference (ISI) and cochannel interference (CCI) on the radio links between the portables and the base stations. This configuration, first proposed in [3,4] was recently examined for the indoor wireless application with BPSK/QPSK in the presence of ISI [5] and of both ISI and CCI [6,7]. By taking advantage of the channel's implicit diversity effect, it provides an effective microscopic diversity order of $M \times L$ and can be considered as an *optimum baseband combiner* [6,7,8] as it cancels interference by exploiting the latter's *short-term* correlation across the independent diversity paths.

Compact, built-in, dual diversity antennas have been developed [9] for the portables but the extension to the three-antenna case appears difficult considering the small volume of hand-held units. As in [6,7], this paper investigates the viability of using convolutional channel coding with soft-decision Viterbi decoding as an alternative to adding a third explicit diversity branch in order to improve performance. However, the latter is now evaluated via a semi-analytical technique based on a variation of the method of moments [10]. This approach avoids a non-fading gaussian noise characterization of interference [3,4,5,6,7] while providing statistically significant results without resorting to lengthy bit-by-bit simulations [6,7]. In general, such a gaussian assumption is not realistic as CCI is most often dominated by a single interfering source [11]. Coded performance results are obtained for both the optimal case of ideal interleaving, which is infeasible in view of the quasi-static nature of the channel, and no interleaving. The relative performance of the uncoded, two- and three-antenna and coded, two-antenna configurations with coherent BPSK and QPSK are thus compared in terms of both average bit error rate and outage rate with one or two interferers.

II. System description

In figure 1, n $(n=0,..,N)$ indexes the desired $(n=0)$ and N cochannel interfering portables, i $(i=1,...,M)$ indexes the M receiver antennas, $s_{kn} = a_{kn} + jb_{kn}$ represents the k[th] symbol from the n[th] portable, and the $n_i(t) = n_{ci}(t) + jn_{si}(t)$ are uncorrelated, complex,

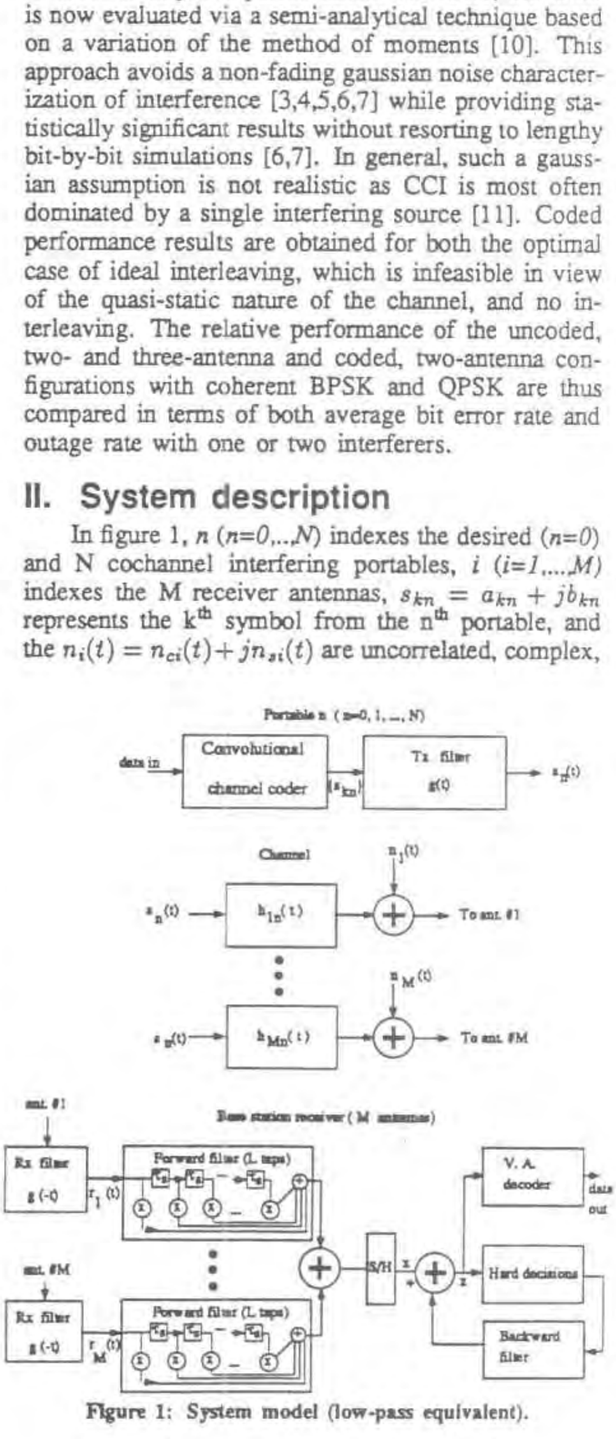

Figure 1: System model (low-pass equivalent).

* This work was supported by the Telecommunications Research Institute of Ontario (*TRIO*) and the Natural Sciences and Engineering Research Council of Canada (*NSERC*).

[2] A "*wideband*" signal's bandwidth is greater than the channel's coherence bandwidth thus causing ISI.

zero-mean white gaussian noise processes with single-sided spectral density N_0. With $\frac{I_n}{S}$ denoting the n^{th} mean interferer-to-carrier ratio, the decision variable z can be expressed as[3] [6,7]

$$z = \mathbf{W}^{*\mathrm{T}}\left(\sum_{k=0}^{K} s_{k0}\mathbf{q}_{k0} + \sum_{n=1}^{N}\sqrt{\frac{I_n}{S}}\sum_{k=-K}^{K} s_{kn}\mathbf{q}_{kn} + \mathbf{V}\right)$$
$$= \mathbf{W}^{*\mathrm{T}}(s_{00}\mathbf{q}_{00} + \mathbf{V_X} + \mathbf{V}) \quad (1)$$

where the sum over the symbol index k has been truncated to $2K$ terms in view of the finite duration of the pulse function f(t) and where it is assumed (as in [3,4]) that the feedback filter cancels the postcursor interference contribution from the desired portable. The $M{\times}L$ element vectors $\mathbf{W}$ and $\mathbf{q}_{kn}$ respectively contain the $\tau_s = \frac{T}{2}$-spaced forward filter tap coefficients and samples of the convolution of the low-pass equivalent impulse response $h_{in}(t)$ with the combined transmitter and receiver filter response $f(t) = \int_{-\infty}^{\infty} g(t+u)\, g(u)\, du$. Since the elements of the AWGN vector $\mathbf{V}$ are independent from those of the interference vector $\mathbf{V_x}$, the elements of the short-term average (interference-plus-noise) covariance matrix $\mathrm{C} = \frac{N_o}{E_S}\mathrm{C}_0 + \mathrm{C_i}$ are obtained from [7,6]

$$\mathrm{C_i} = \sum_{k=1}^{K}\mathbf{q}_{k0}\mathbf{q}_{k0}^{*\mathrm{T}} + \sum_{n=1}^{\mathrm{N}}\frac{I_n}{S}\sum_{k=-\mathrm{K}}^{\mathrm{K}}\mathbf{q}_{kn}\mathbf{q}_{kn}^{*\mathrm{T}} \quad (2)$$

and from [7,6]

$$\mathrm{C}_0(((\mathrm{i}-1)*\mathrm{L})+\mathrm{k},((\mathrm{j}-1)*\mathrm{L})+\mathrm{l}) = \mathrm{f}((\mathrm{k}-\mathrm{l})*\tau_s)\,\delta_{ij}$$
$$for \quad i,j = 1,...,M; \qquad k,l = 1,...,L. \quad (3)$$

III. Performance evaluation

For a particular static channel realization, the probability of bit error can be written in terms of the decision variate z in figure 1 as

$$P_b = Pr(Re(z) < 0 \mid a_{00} = +1) \quad (4)$$

An efficient algorithm has been proposed [10] to compute such a probability of error in the context of a binary symmetric channel with pulse-amplitude modulation. It involves the numerical quadrature of a Laplace inversion integral which is approximated via the trapezoidal rule as [10]

$$P_b = \Delta y\left[\frac{1}{2}G(s_0) + \sum_{u=1}^{U} G(s_0 + ju\Delta y)\right] \quad (5)$$

where the function $g(s)$ in $G(s) = \frac{1}{\pi}Re\left(s^{-1}g(s)\right)$ denotes the moment-generating function (mgf) of $y = Re(z)$ and where U is large enough such that $G(s_0 + ju\Delta y)$ is negligible for u>U. The numerical quadrature is performed on a straight vertical path through the integrand 's $(s^{-1}g(s))$ single positive saddlepoint s_0 on the $Re(s)$ axis [10] using only a finite number of moments of the decision variate and without explicit knowledge of its probability density function. The saddlepoint s_0 can be found by replacing an initial value[4] of s_0 by [10]

$$s_0 - \left(\left[ln(s^{-1}g(s))\right]'\big|_{s=s_0}\right)\left(\left[ln(s^{-1}g(s))\right]''\big|_{s=s_0}\right)^{-1} \quad (6)$$

and repeating this until the change in s_0 is negligible.

By generating a large number (i.e. 10000) of independent channel sets, statistically significant outage and average error rates can thus be obtained. For each set of transmitter to receiver antenna channel realizations $h_{ni}(t)$, $i = 1,...M;\ n = 0,...N$, the procedure to find P_b thus involves the following steps:

1. Find all the $\mathbf{q}_{kn}$ $\mathrm{k} = -\mathrm{K},...\mathrm{K};\ \mathrm{n} = 0,...\mathrm{N}$ vectors from the impulse responses $h_{ni}(t)$.
2. Find the interference-plus-noise covariance matrix C from equations 2 and 3.
3. Find the optimum tap weight vector $\mathbf{W}_{opt} = \mathrm{C}^{-1}\mathbf{q}_{00}$ [4] and all the $\mathbf{W}^{*\mathrm{T}}\mathbf{q}_{kn}$ $\mathrm{k} = -\mathrm{K},...\mathrm{K};\ \mathrm{n} = 0,...\mathrm{N}$.
4. Compute the saddlepoint search starting point and find the saddlepoint from equation 6.
5. Use the trapezoidal rule to find P_b as per equation 5.

Expressions describing the moment-generating function of the decision variate y are now given for the uncoded case as well as for the coded cases with both ideal interleaving and no interleaving.

III.A Uncoded BER

By expanding equation 1 and by defining $A_{kn} = \sqrt{\frac{I_n}{S}}\, Re(\mathbf{W}^{*\mathrm{T}}\mathbf{q}_{kn})$ and $B_{kn} = \sqrt{\frac{I_n}{S}}\, Im(\mathbf{W}^{*\mathrm{T}}\mathbf{q}_{kn})$, the decision variable becomes

$$y = a_{00}\,A_{00} + \sum_{k=1}^{K} a_{k0}\,A_{k0} - \sum_{k=0}^{K} b_{k0}B_{k0}$$
$$+ \sum_{n=1}^{N}\sum_{k=-K}^{K}\left[a_{kn}\,A_{kn} - b_{kn}B_{kn}\right] + Re(\mathbf{W}^{*\mathrm{T}}\mathbf{V})$$
$$= a_{00}A_{00} + \eta + \xi \quad (7)$$

where η is the sum of ISI, cross-rail interference[5] and CCI and where ξ is the AWGN. Setting $a_{00} = 1$ in order to compute P_b from equation 5, and because the interference and the noise are statistically independent, the mgf of the decision variable is

$$g(s) = \varepsilon\left[\mathrm{e}^{-sy}\right] = g_\eta(s)\, g_\xi(s)\, e^{(-A_{00}s)} \quad (8)$$

With all a_{kn} and b_{kn} being independent, the mgf of the interference can be written as [8,12]

$$g_\eta(s) = \quad (9)$$
$$\varepsilon\left[e^{\left(-s\left(\sum_{k=1}^{K}a_{k0}A_{k0} - \sum_{k=0}^{K}b_{k0}B_{k0} + \sum_{n=1}^{N}\sum_{k=-K}^{K}(a_{kn}A_{kn} - b_{kn}B_{kn})\right)\right)}\right]$$
$$= \prod_{k=1}^{K}cosh(A_{k0}s)\prod_{k=0}^{K}cosh(B_{k0}s)\prod_{n=1}^{N}\prod_{k=-K}^{K}cosh(A_{kn}s)\,cosh(B_{kn}s)$$

whereas the mgf of the AWGN component is [8,12]

$$g_\xi(s) = exp\left(\frac{N_0 s^2}{4}sum\left(|\mathbf{W}|^2\right)\right) \quad (10)$$

[3] For the case of n=0 (desired signal), $\sqrt{\frac{I_n}{S}} = 1$.

[4] The saddlepoint search starting point can be determined by replacing all interference terms by gaussian noise of equal variance [10].

[5] For BPSK, all $b_{kn} = 0$ which eliminates the cross-rail interference.

III.B Coded BER

Recall that the bit error rate upper bound for soft-decision Viterbi decoding of a rate 1/n convolutional code can be expressed as $P_b = \sum_{d=d_{free}}^{\infty} \beta_d P_2(d)$ where β_d is obtained from the first derivative of the code's transfer function and $P_2(d)$ is the pairwise error probability for sequences that differ in d bits. For QPSK[6], the pairwise error probability can thus be expressed as

$$P_2(d) = \tag{11}$$
$$\begin{cases} Pr\left(\sum_{i=0}^{d_e-1} (Re(z_i) + Im(z_i)) \leq 0 | s_{i0} = 1+j\right) & d\ even \\ Pr\left(\sum_{i=0}^{d_0-1} (Re(z_i) + Im(z_i) + Re(z_{d_o})) \leq 0 \left| \begin{matrix} s_{i0} = 1+j \\ a_{d_o0} = 1 \end{matrix} \right.\right) & d\ odd \end{cases}$$

where $d_e = \frac{d}{2}$ and $d_o = \frac{d-1}{2}$. The moment generating functions required to determine these pairwise error probabilities are now described for both the ideally-interleaved and non-interleaved cases.

Ideal interleaving (random errors)

Assuming that successive symbols fade independently which is equivalent to interleaving of infinite depth, the successive bits[7] z_i appearing at the Viterbi decoder input have all been subjected to independent fading. The determination of the 10000 static channel P_b's can thus be done similarly to the uncoded case. However, instead of generating one set of $h_{ni}(t)$ $i = 1:M;\ n = 0:N$, one generates $d_{free} + D$ such sets where D is such that $P_2(d_{free} + D) \ll P_2(d_{free})$, i.e. $P_b = \sum_{d=d_{free}}^{d_{free}+D} \beta_d P_2(d)$. Each $P_2(d)$ is evaluated using the mgf of $y = \sum_{i=0}^{d-1} Re(z_i)$ i.e. [8,12]

$$g(s) = \prod_{i=0}^{d-1} e^{-A_{00i}s}\, g_{ni}(s)\, e^{\frac{N_0 s^2}{4R_c} sum(|W_i|^2)} \tag{12}$$

where each of the $g_{ni}(s)$ are obtained from equation 9.

No interleaving (burst-error case)

Only one set of $h_{ni}(t)$, $i = 1:M;\ n = 0:N$ need now be generated to compute each of the 10000 P_b's. However the determination of the mgf required for each $P_2(d)$ is more complex as successive symbols do not fade independently and interfere with each other because of symbol dispersion. The analysis is made tractable by assuming that, for a given $P_2(d)$, the d bits that differ between two paths are successive bits[8]. The mgf of the decision variate can be expressed as $g(s) = g_\lambda(s) g_\eta(s) e^{\frac{4N_0 s^2}{4R_c} sum(|W|^2)}$ where the last term is the AWGN mgf [8,12]. With $X_{kn} \triangleq A_{kn} + B_{kn}$ and $Y_{kn} \triangleq A_{kn} - B_{kn}$, expanding the sums of z_i terms in equation 11 then yields the CCI mgf for d even as [8,12]

$$g_\eta(s) = \prod_{n=1}^{N} \prod_{k=-K}^{(d_e-K-1)} cosh\left(\sum_{l=-K}^{k} X_{ln}s\right) cosh\left(\sum_{l=-K}^{k} Y_{ln}s\right)$$
$$\prod_{k=d_e-K}^{K} cosh\left(\sum_{l=k-(d_e-1)}^{k} X_{ln}s\right) cosh\left(\sum_{l=k-(d_e-1)}^{k} Y_{ln}s\right) \tag{13}$$
$$\prod_{k=K+1}^{(d_e+K-1)} cosh\left(\sum_{l=k-(d_e-1)}^{K} X_{ln}s\right) cosh\left(\sum_{l=k-(d_e-1)}^{K} Y_{ln}s\right)$$

For d odd [8,12],

$$g_\eta(s) = \tag{14}$$
$$\prod_{n=1}^{N} \prod_{k=-K}^{(d_o-K)} cosh\left(\sum_{l=-K}^{k} X_{ln}s\right) \prod_{k=-K}^{(d_o-K-1)} cosh\left(\sum_{l=-K}^{k} Y_{ln}s\right)$$
$$\prod_{k=d_o-K+1}^{K} cosh\left(\sum_{l=k-d_o}^{k} X_{ln}s\right) \prod_{k=d_o-K}^{K} cosh\left(\sum_{l=k-(d_o-1)}^{k} Y_{ln}s\right)$$
$$\prod_{k=K+1}^{(d_o+K)} cosh\left(\sum_{l=k-d_o}^{K} X_{ln}s\right) \prod_{k=K+1}^{(d_o+K-1)} cosh\left(\sum_{l=k-(d_o-1)}^{K} Y_{ln}s\right)$$

With the first d bits set to 1, the same process with the $n=0$ terms yields the signal mgf, for d odd, as [8,12]

$$g_\lambda(s) = \tag{15}$$
$$\begin{cases} \prod_{k=(d_o+1)}^{(d_o+K)} cosh\left(\sum_{l=k_o-1}^{K} X_{l0}s\right) \prod_{k=d_o}^{(d_o+K-1)} cosh\left(\sum_{l=k_o}^{K} Y_{l0}s\right) \\ \prod_{k=0}^{K} e^{-\sum_{l=0}^{k} 2A_{l0}s} \prod_{k=K+1}^{(d_o-1)} e^{-\sum_{l=0}^{K} 2A_{l0}s - \sum_{l=0}^{d_0} X_{l0}s} & ;for\ d_o > K \\ \prod_{k=0}^{(d_o-1)} e^{-\sum_{l=0}^{k} 2A_{l0}s}\, e^{-\sum_{l=0}^{d_o} X_{l0}s}\, cosh\left(\sum_{l=1}^{d_o} Y_{l0}s\right) \\ \prod_{k=d_o+1}^{2d_o} cosh\left(\sum_{l=k_o-1}^{d_o} X_{l0}s\right) \prod_{k=d_o+1}^{(2d_o-1)} cosh\left(\sum_{l=k_o}^{d_o} Y_{l0}s\right) \\ ;\quad for\ d_o = K \\ \prod_{k=d_o+1}^{K} cosh\left(\sum_{l=k_o-1}^{k} X_{l0}s\right) \prod_{k=K+1}^{(d_o+K)} cosh\left(\sum_{l=k_o-1}^{K} X_{l0}s\right) \\ \prod_{k=d_o}^{K} cosh\left(\sum_{l=k_o}^{k} Y_{l0}s\right) \prod_{k=K+1}^{(d_o+K-1)} cosh\left(\sum_{l=k_o}^{K} Y_{l0}s\right) \\ \prod_{k=0}^{(d_o-1)} e^{-\sum_{l=0}^{k} 2A_{l0}s}\, e^{-\sum_{l=0}^{d_o} X_{l0}s} & ;\quad for\ d_o < K \end{cases}$$

where $k_0 = k - (d_0 - 1)$. For d even [8,12], we have

$$g_\lambda(s) = \begin{cases} \prod_{k=d_e}^{(d_e+K-1)} cosh\left(\sum_{l=k_e}^{K} X_{l0}s\right) cosh\left(\sum_{l=k_e}^{K} Y_{l0}s\right) \\ \prod_{k=0}^{K} e^{-\sum_{l=0}^{k} 2A_{l0}s} \prod_{k=K+1}^{(d_e-1)} e^{-\sum_{l=0}^{K} 2A_{l0}s} & ;for\ d_e > K \\ \prod_{k=d_e}^{K} cosh\left(\sum_{l=k_e}^{k} X_{l0}s\right) cosh\left(\sum_{l=k_e}^{k} Y_{l0}s\right) \\ \prod_{k=K+1}^{(d_e+K-1)} cosh\left(\sum_{l=k_e}^{K} X_{l0}s\right) cosh\left(\sum_{l=k_e}^{K} Y_{l0}s\right) \\ \prod_{k=0}^{(d_e-1)} e^{-\sum_{l=0}^{k} 2A_{l0}s} & ;for\ d_e \leq K \end{cases} \tag{16}$$

where $k_e = k - (d_e - 1)$.

---

[6] The coded BPSK case is not discussed here but is handled similarly [8,12].

[7] Even for QPSK, it is assumed that successive bits are interleaved.

[8] This is realistic given the quasi-static nature of the channel [8,12].

IV. Results

The results on the following page are based on a "*cluster*" channel model developed as a result of measurements [2]. Using the parameters in [2], a mean rms delay spread of 21 ns was found over 10000 sets of independent portable-to-base station antenna impulse response realizations. As complexity is a prime concern for the portable application, the number of forward filter taps L is set to 3 which was found to be nearly optimal[9] [6,8] for a rms delay spread on the order of a quarter of the symbol interval. All parameters are thus normalized to a data rate of 10 Mbits/s yielding a normalized rms delay spread of 0.21T. A fixed sampling phase is employed along with 50% rolloff cosine spectrum pulses and a rate $\frac{1}{2}$, $d_{free} = 5$, *short* constraint length 3 convolutional code in order to minimize complexity. Uncoded BPSK is compared to rate $\frac{1}{2}$ coded QPSK thus maintaining the same rate of information throughput and the same bandwidth.

Although figures 2 and 3 show that the M=2, coded system with ideal interleaving clearly outperforms the M=3 uncoded system, it is seen that, with a single interferer at a SIR of 10 dB, the M=2 non-interleaved coded system still yields positive coding gains with respect to the M=2 uncoded system. For a BER of 10^{-3} and an outage rate of 10^{-2}, the M=2, non-interleaved system recuperates respectively 50% (2.6 dB) and 80% (5.6 dB) of the gain obtained by adding a third space diversity branch. Hence, with only dual space diversity and a short constraint length code, the effective diversity order $M*L$ is sufficiently large to alleviate the effects of the absence of interleaving. Positive coding gains with no interleaving have also been observed [13] with explicit space diversity only but this requires a very large diversity order and a complex code. Results with the same parameters as those of figures 2 and 3 but at a lower data rate of 2.4 Mbits/s (i.e. where the rms delay spread equals 0.05T) show [8,12] that the coding gain in terms of BER=10^{-3} becomes negative (-0.7 dB) while it is much smaller (3.2 dB) in terms of outage rate = 10^{-2}. Hence, as the data rate *increases* thus enabling the receiver to exploit the channel's implicit diversity effect, coding with no interleaving becomes more attractive as an alternative to adding a third explicit space diversity branch. Figure 4 shows however that such a conclusion is valid for a SIR greater than 8.5 dB as the coded system suffers from a "threshold effect" when the interference power becomes too large.

Figures 5 and 6 show that the dual space diversity configuration cannot cancel two cochannel interferers with a total SIR of 10 dB thus resulting in large irreducible average bit error rates and outage rates unless a third explicit space diversity branch is added. The M=2, coded, non-interleaved system's irreducible BER is found to be larger than the M=2, uncoded system's irreducible BER. The reverse is however true in terms of outage rate. This results in a coding gain which is nil in terms of a BER of 10^{-3} but as high as 13 dB in terms of an outage rate of 10^{-2}. However, a more stringent performance criterion (e.g. an outage rate of 10^{-3}) would make the use of a third space diversity branch essential. Figure 7 then shows that the M=2, coded system's irreducible average bit error rate only becomes smaller than the M=2, uncoded system's average bit error rate when the SIR becomes larger than 15 dB. At that point, the coded system's irreducible outage rate is sufficiently low [8] to satisfy even a strict performance criterion of 10^{-3} outage rate.

[9] This assumes BPSK and an arbitrary fixed equalizer sampling phase [6,8].

V. Conclusion

At a data rate of 10 Mbits/s, the use of a simple, short constraint length convolutional code has been shown to be viable alternative to increasing the explicit space diversity order of a dual space diversity optimum baseband combiner with 3 taps per forward filter. With the large effective diversity order obtained as result of exploiting the channel's implicit diversity effect, such a conclusion holds even in the absence of interleaving. This is particularly true when a single cochannel interferer is dominant which is most often the case in a high-capacity, small-cell, frequency reuse radio system [11]. As opposed to average bit error rate, coding is also more attractive in terms of outage rate which is the criterion of interest for portable communications.

References

[1] J. Chuang, "The effect of time delay spread on portable radio communication channels with digital modulation," *IEEE Journal on Selected Areas in Communications*, vol. SAC-5, no. 6, pp. 879–889, June 1987.

[2] A. Saleh and R. Valenzuela, "A statistical model for indoor multipath propagation," *IEEE Journal on Selected Areas in Communications*, vol. SAC-5, no. 2, pp. 128–137, February 1987.

[3] P. Monsen, "MMSE equalization of interference on fading diversity channels," *IEEE Transactions on Communications*, vol. COM-34, no. 1, pp. 5–12, January 1984.

[4] P. Monsen, "Theoretical and measured performance of a DFE modem on a fading multipath channel," *IEEE Transactions on Communications*, vol. COM-25, no. 10, pp. 1144–1153, October 1977.

[5] T. Sexton and K. Pahlavan, "Channel modeling and adaptive equalization of indoor radio channels," *IEEE Journal on Selected Areas in Communications*, vol. SAC-7, no. 1, pp. 114–120, January 1989.

[6] C. Despins, D. Falconer, and S. Mahmoud, "Coding and optimum baseband combining for wideband TDMA indoor wireless channels," *Canadian Journal of Electrical and Computer Engineering*, vol. 16, no. 3-4, April 1991.

[7] C. Despins, D. Falconer, and S. Mahmoud, "Coding and optimum baseband combining for wideband TDMA indoor wireless channels," in *Proceedings of the 1990 IEEE Global Telecommunications Conference*, (San Diego, Ca.), pp. 1832–1837, December 1990.

[8] C. Despins, "Coding and optimum baseband combining for wideband TDMA indoor wireless channels," *Ph.D. thesis, Dept. of Systems and Computer Engineering, Carleton University (Ottawa, Canada)*, 1991.

[9] K. Tsunekawa, "Diversity antennas for portable telephones," in *Proceedings of the IEEE 1989 Vehicular Technology Conference*, (San Francisco, Ca.), pp. 50–56, May 1989.

[10] C. Helstrom, "Calculating error probabilities for intersymbol and cochannel interference," *IEEE Transactions on Communications*, vol. COM-34, no. 5, pp. 430–435, May 1986.

[11] R. Bernhardt *Private communication*, March 1989.

[12] C. Despins, D. Falconer, and S. Mahmoud, "Compound strategies of coding, equalization, and space diversity for wideband TDMA indoor wireless channels," *to be submitted to IEEE Transactions on Communications.*

[13] Y. Miyagaki, N. Morinaga, and T. Namekawa, "Effect of compound strategies of error correcting coding, bit interleaving and diversity combining in mobile radio data transmission," *Transactions of the Institute of Electronics and Communications Engineers of Japan*, vol. J67-B, no. 6, pp. 599–606, June 1984.

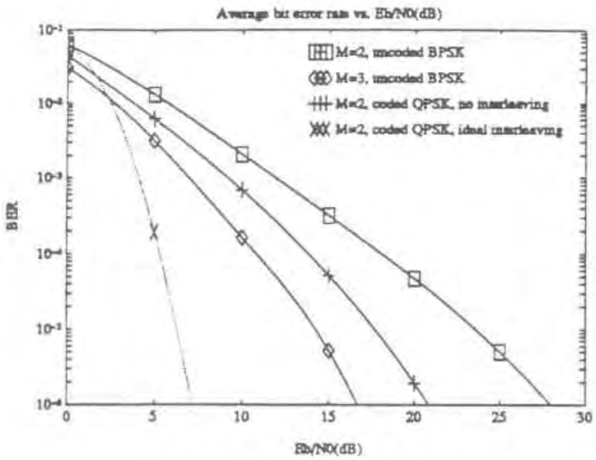

Figure 2: Average BER vs. $\frac{E_b}{N_0}$. N=1 interferer, $SIR = 10\ dB$.

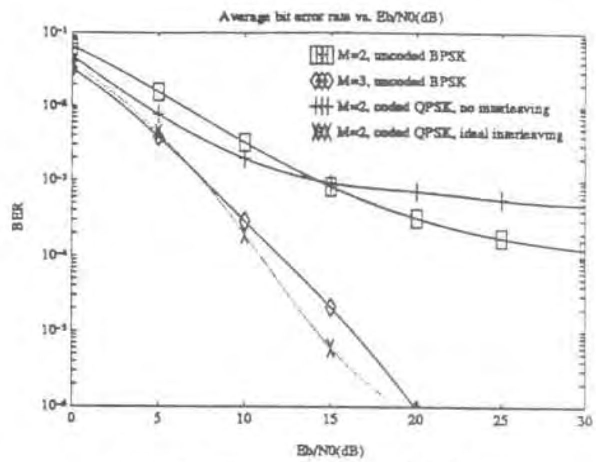

Figure 5: Average BER vs. $\frac{E_b}{N_0}$. N=2 equal-power interferers, $SIR_{tot} = 10\ dB$.

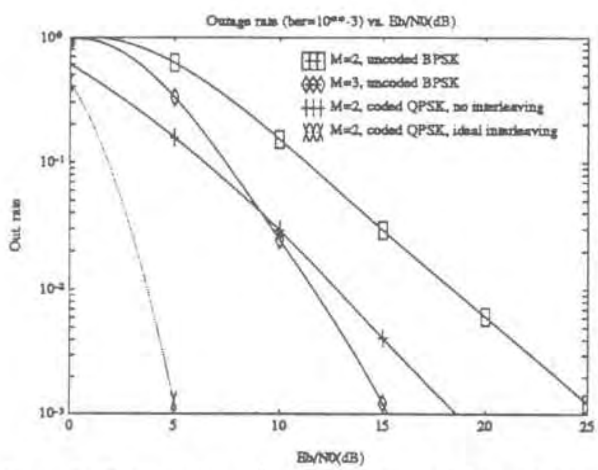

Figure 3: Outage rate vs. $\frac{E_b}{N_0}$. N=1 interferer, $SIR = 10\ dB$.

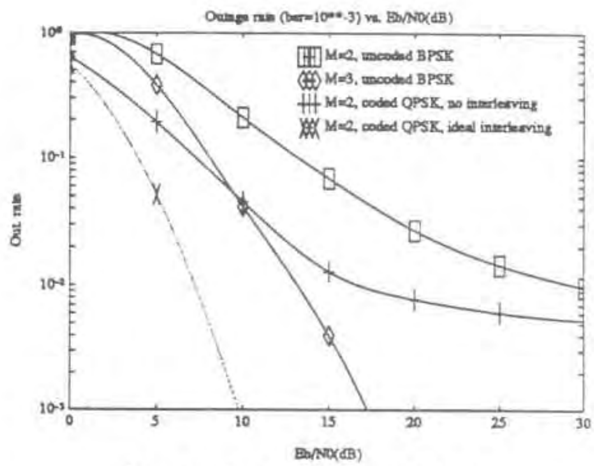

Figure 6: Outage rate vs. $\frac{E_b}{N_0}$. N=2 equal-power interferers, $SIR_{tot} = 10\ dB$.

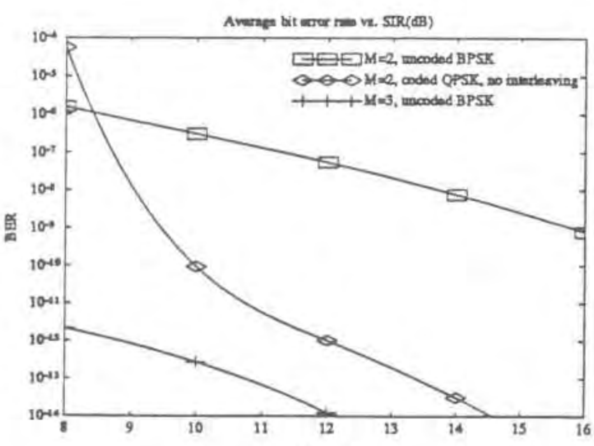

Figure 4: Average BER vs. SIR for N=1 interferer. $\frac{E_b}{N_0} = 30\ dB$.

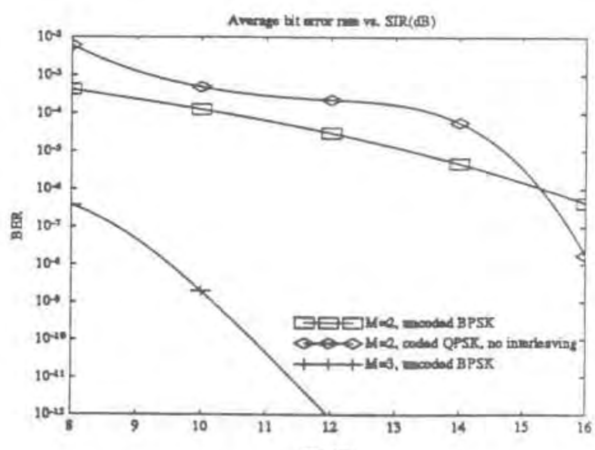

Figure 7: Average BER vs. SIR_{tot} for N=2 equal-power interferers. $\frac{E_b}{N_0} = 30\ dB$.

EQUALIZATION, DIVERSITY AND CODING FOR WIDEBAND TDMA INDOOR WIRELESS CHANNELS

C. L. Despins, D.D. Falconer and S.A. Mahmoud

Dept. of Systems and Computer Engineering
Carleton University
Ottawa Ontario Canada K1S 5B6

IEEE Workshop on Wireless Local Area Networks
Worcester Polytechnic Institute
May 9-10 1991

TYPICAL CHARACTERISTICS OF A 800 mhz INDOOR WIRELESS CHANNEL

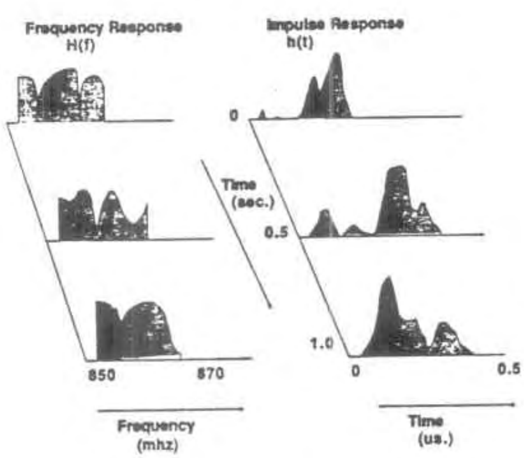

A DISPERSIVE CHANNEL

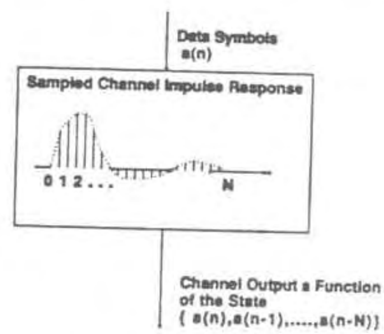

Remedies

- Decision feedback equalizer (DFE)
- Sequence estimation

CO-CHANNEL INTERFERENCE IN CELLULAR RADIO

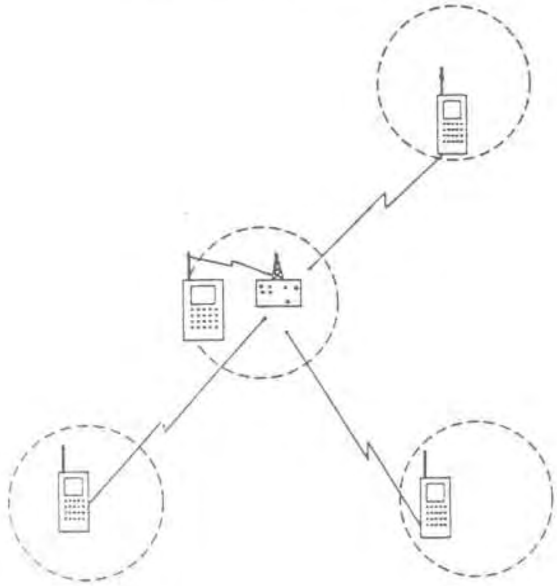

INTERFERENCE

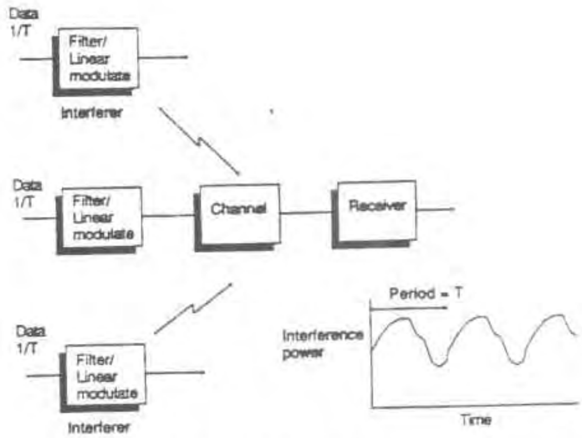

SOME APPLICATIONS OF INTEREST:

- Crosstalk in digital transmission on multipair cables.
- Radio: co- and adjacent-channel interference.
- Dual-polarized radio system crosstalk.
- Residual echo in full-duplex 2-wire transmission.
- Magnetic recording.

ROLE OF ADAPTIVE EQUALIZATION IN TDMA CELLULAR RADIO

- Compensation of frequency selectivity (for delay spread > 10% to 20% of symbol interval).
- Realization of implicit diversity to combat multipath.
- Suppression of interference (temporal nulling).
- Equalizer's tracking ability becomes an issue in channels with doppler/symbol rate > 0.001.

ROLE OF DIVERSITY IN TDMA CELLULAR RADIO

- Compensation of fading and shadowing.
- Suppression of interference (spacial nulling).
- Degree of space diversity may be limited by hardware considerations.

ROLE OF CODING IN TDMA CELLULAR RADIO

- An alternative to diversity to combat fading, multipath and interference.
- A means of reducing bit error rate and outage probability.

EQUALIZATION, DIVERSITY AND CODING FOR WIDEBAND TDMA INDOOR WIRELESS CHANNELS

- To determine performance of wideband TDMA indoor radio links employing baseband combining with coherent BPSK or QPSK modulation, in the presence of fading, frequency selectivity, and co-channel interference.

- To determine whether convolutional coding is a viable alternative to increasing the order of space diversity.

System Model

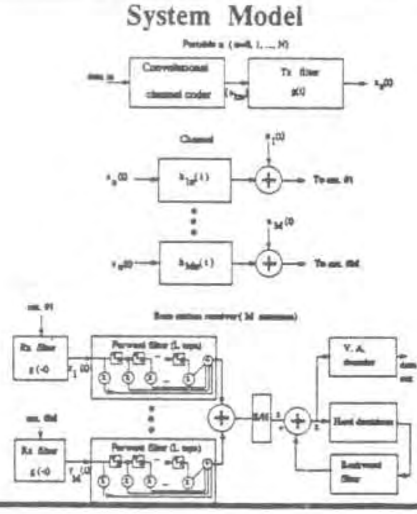

System parameters

- 10000 sets of portable-to-base station antenna impulse response realizations.
- "*Cluster*" channel model.
- Average rms delay spread = 0.21T.
- 3 $\frac{T}{2}$−spaced forward filter taps.
- Fixed receiver sampling phase.
- Random interferer timing phase.
- 50% rolloff cosine spectrum pulses.
- Rate $\frac{1}{2}$, d_{free}=5, constraint length 3 convolutional code.

BER VERSUS SIGNAL-TO-INTERFERENCE PLUS NOISE RATIO

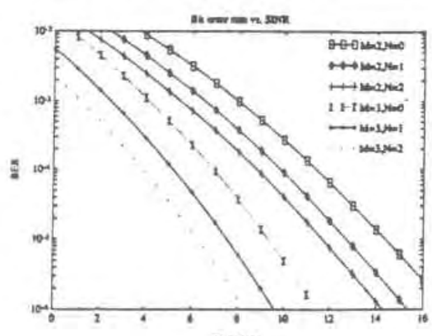

- BPSK, interferer-to-noise ratio $E_{S_n}/N0=1$ for n=1,2.
- t_0=0.0T, t_1=0.125T, t_2=0.25T.
- σ_d=0.25T, exponential delay profile.
- Rectangular pulse shape, L=3, L1=2, L2=0.

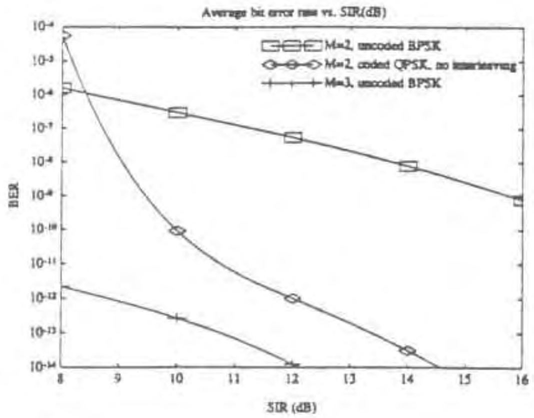

• N = 1 interferer, E_b/N_0 = 30 dB.

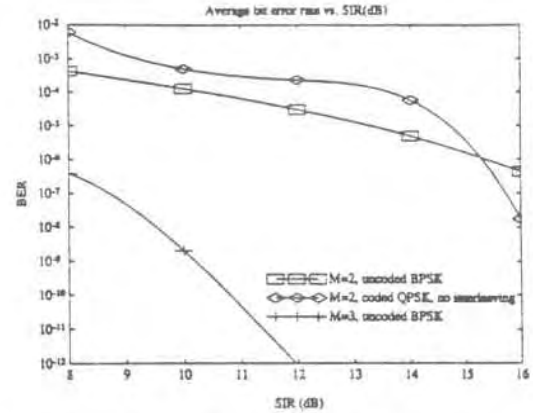

• N = 2 equal-power interferers, E_b/N_0 = 30 dB.

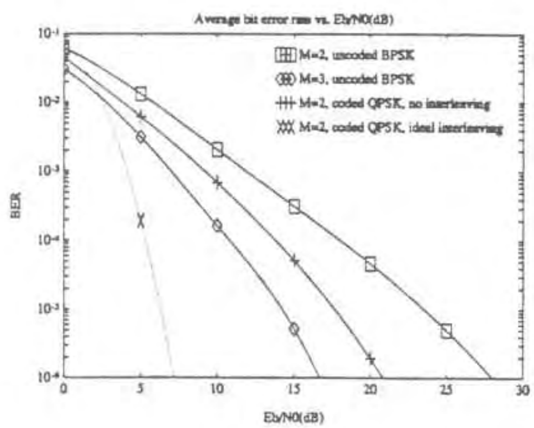

• N = 1 interferer, SIR = 10 dB.

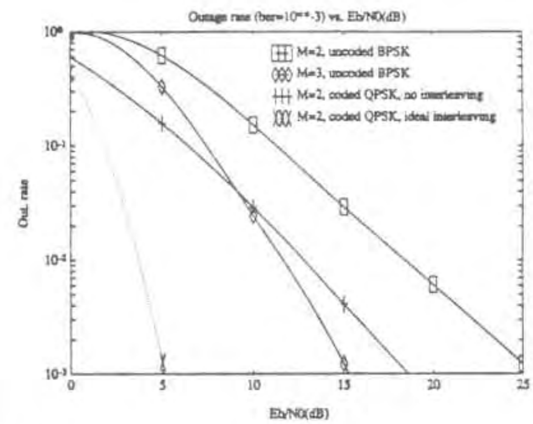

• N = 1 interferer, SIR = 10 dB.

SUMMARY

- A combination of adaptive equalization and diversity combining is effective in exploiting multipath to combat intersymbol and cochannel interference.
- With adequate interleaving, in the presence of one or two dominant interferers, coding is an effective way to reduce the required degree of diversity.
- Coding is still effective, but less so, with no interleaving, or non-ideal interleaving.

MOTOROLA
ALTAIR

The Brightest Star in Wireless Network Communications

MOTOROLA INC.

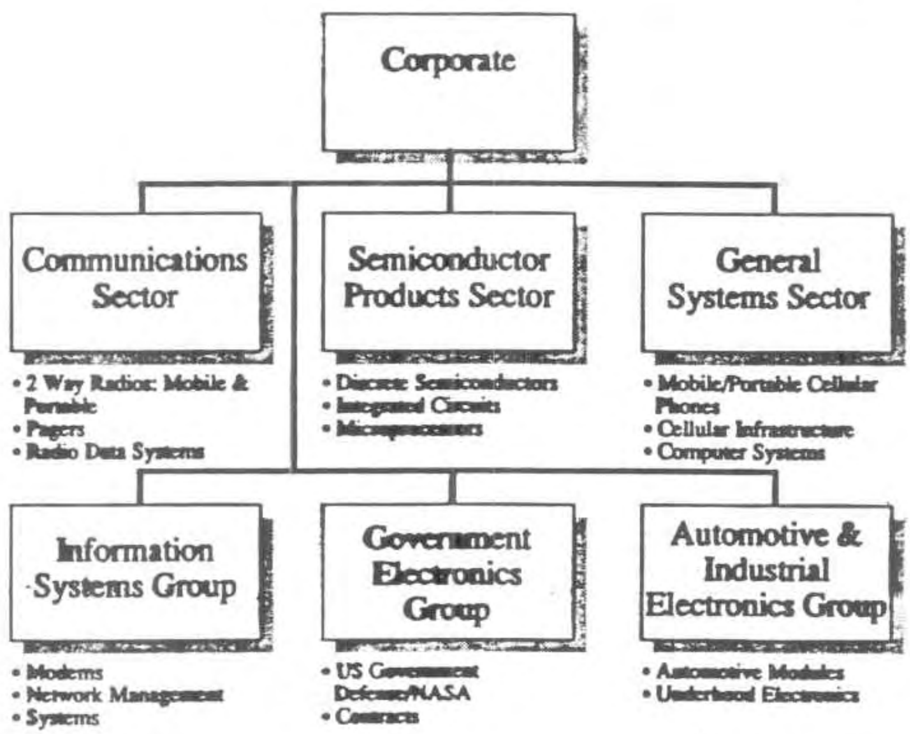

MOTOROLA
ALTAIR

Key Customer Requirements

- Transparency
- Compatibility
- Performance

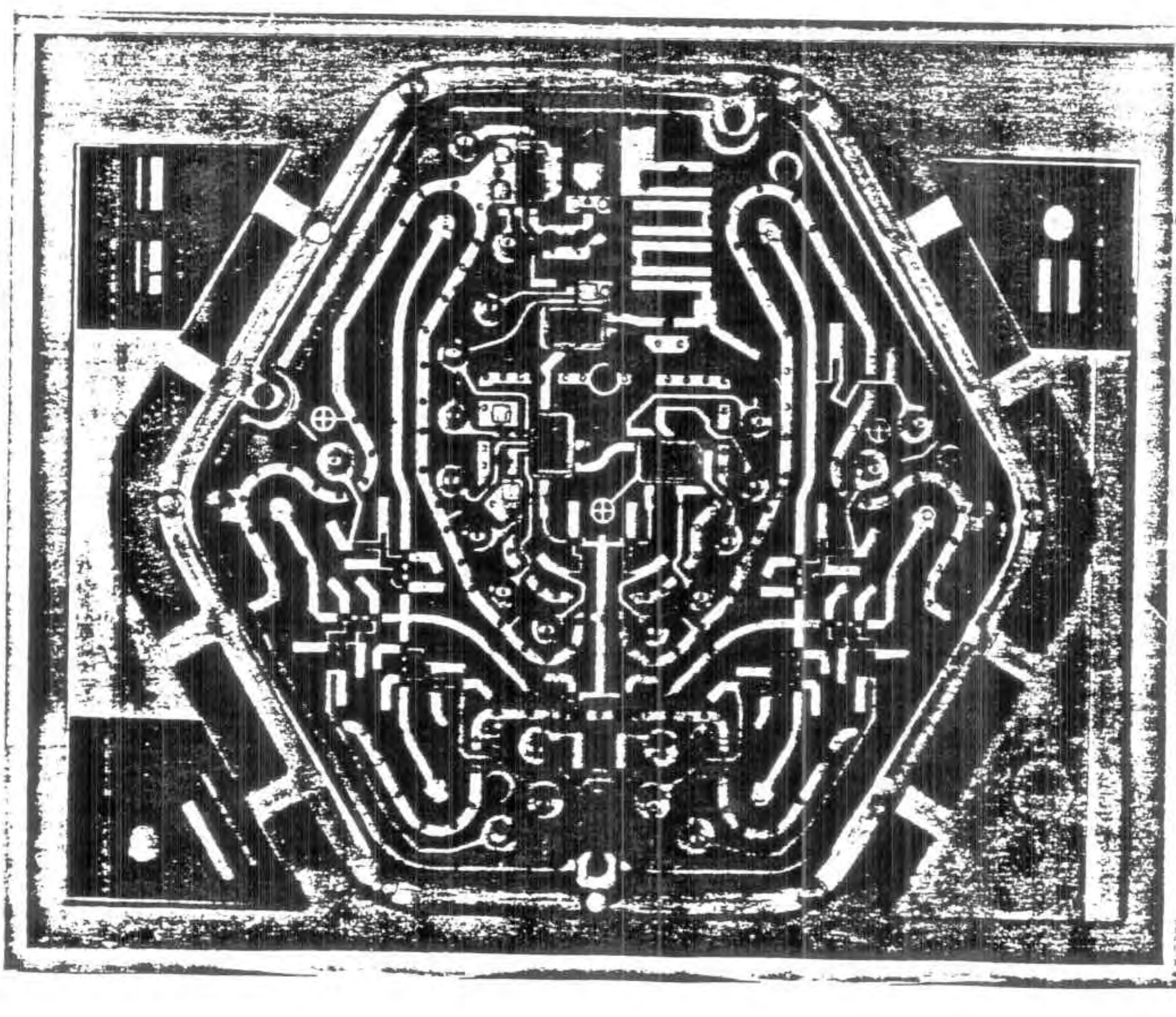

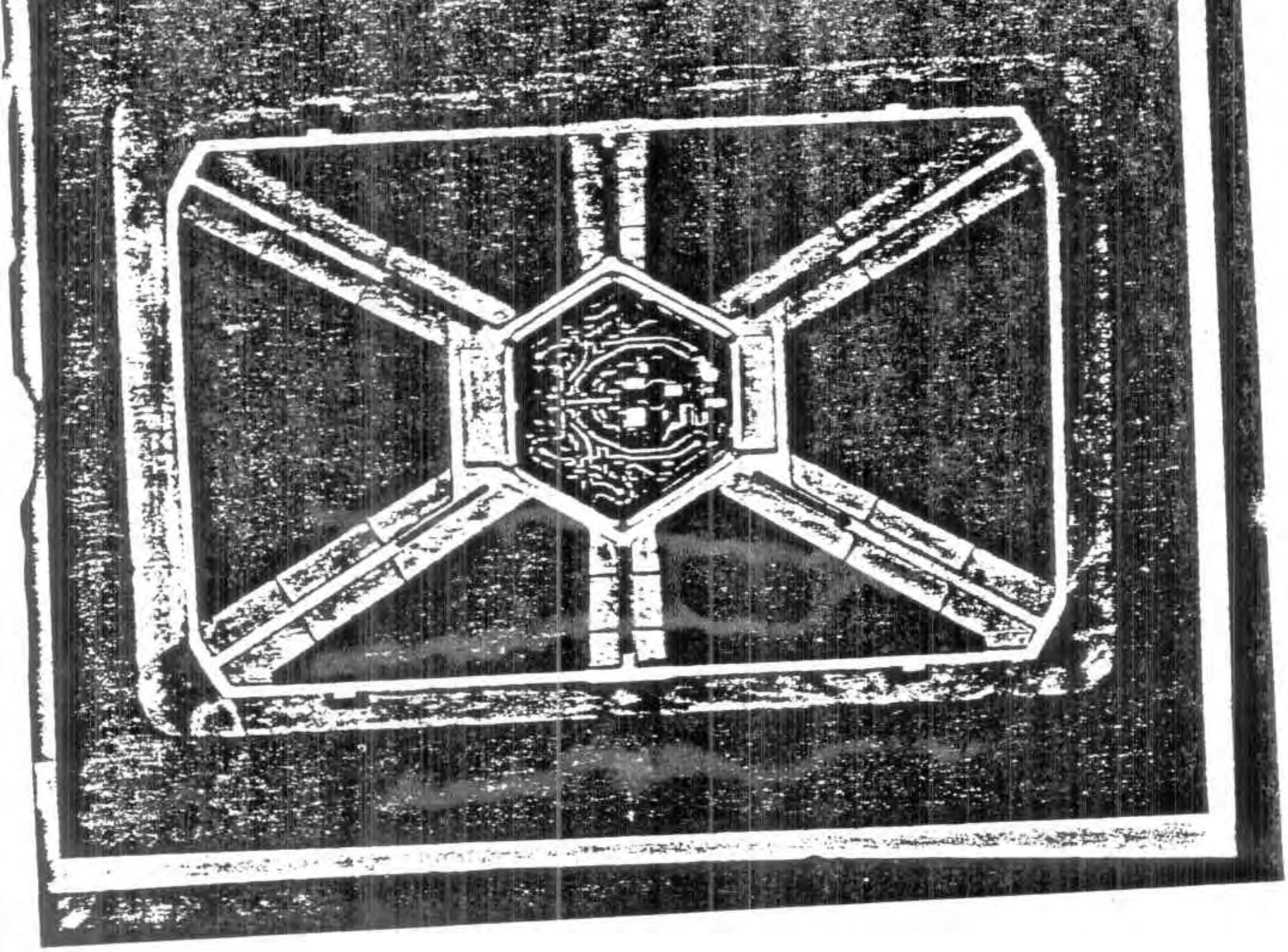

WIN ARCHITECTURE CHOICES FOR HIGH SPEED DATA TO THE DESKTOP

- MEDIA REPLACEMENT
  - PRO: TRANSPARENT TO DRIVERS / NOS / APPLICATIONS
  - CON: EXTRA BOX
- LAN REPLACEMENT
  - PRO: INTEGRATED SOLUTION
  - CON: SOLUTIONS ARE COMPUTER DEPENDENT

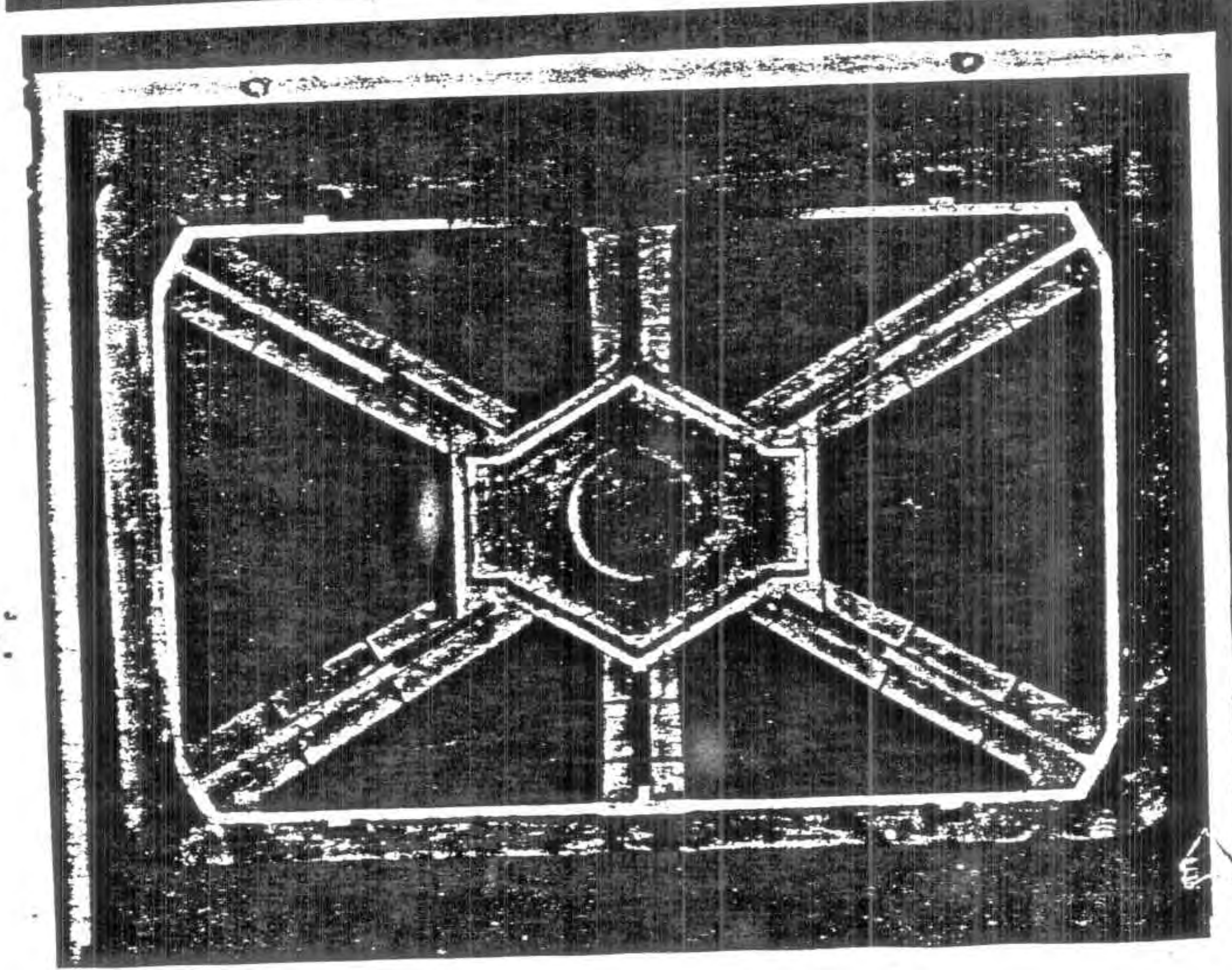

MEDIA REPLACEMENT ARCHITECTURE

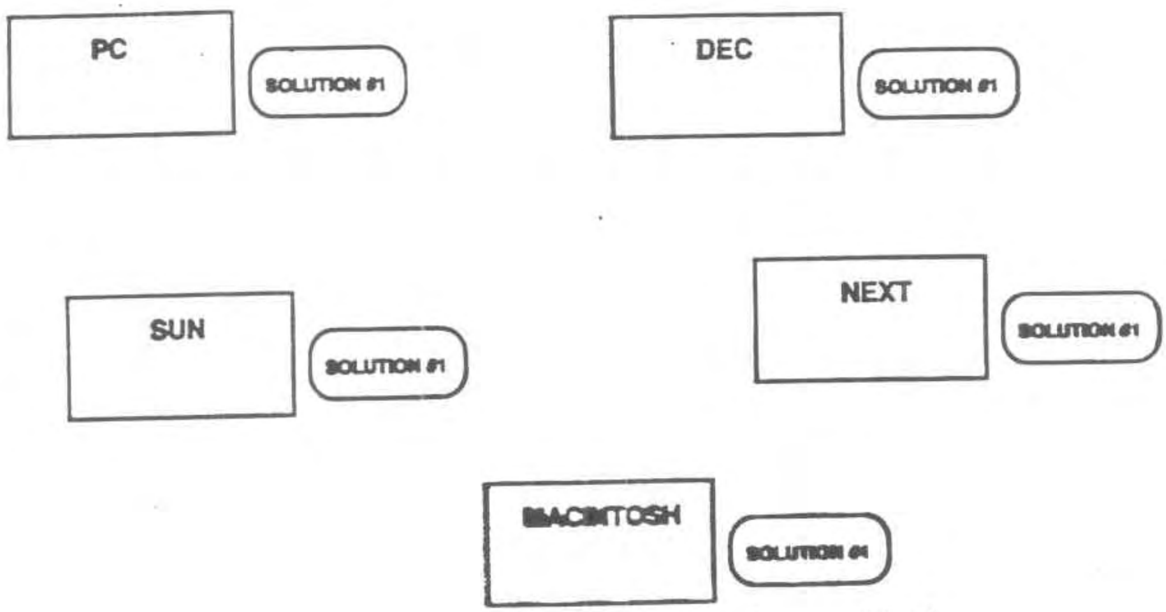

LAN REPLACEMENT ARCHITECTURE

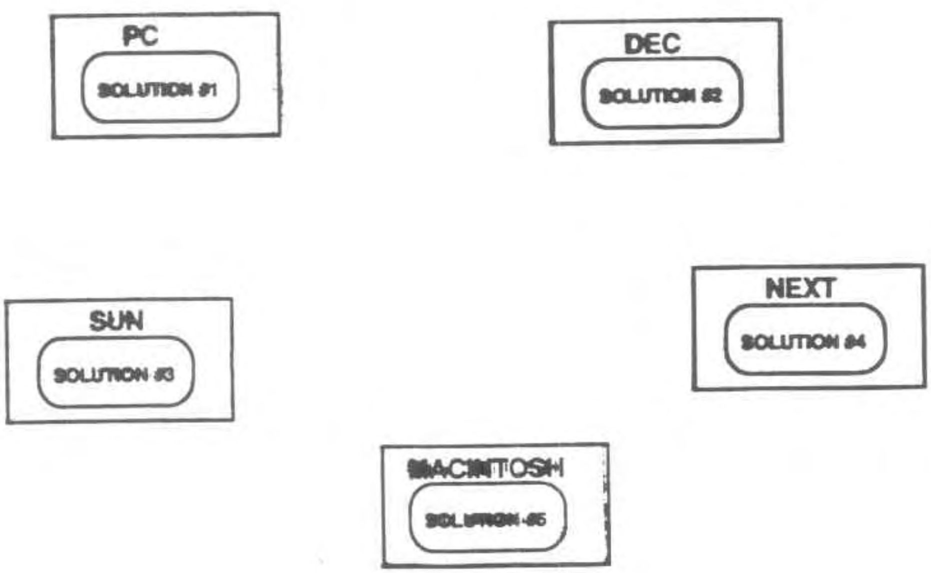

Design Objectives

- End User Installable
- Replace "Horizontal" Ethernet Wiring
- Perform Greater than or Equal to Wire
  - Security
  - Ethernet Compatible Speeds (10 Mbps)
  - User Transparent

MOTOROLA
ALTAIR

Product Overview
Altair System Components

User Module (UM)

Connected to Ethernet Devices
- Personal Computers
- Printers
- Other Ethernet Devices

Control Module (CM)

Connected to Ethernet Servers and Wired Networks

MOTOROLA
ALTAIR

Typical Altair Microcell

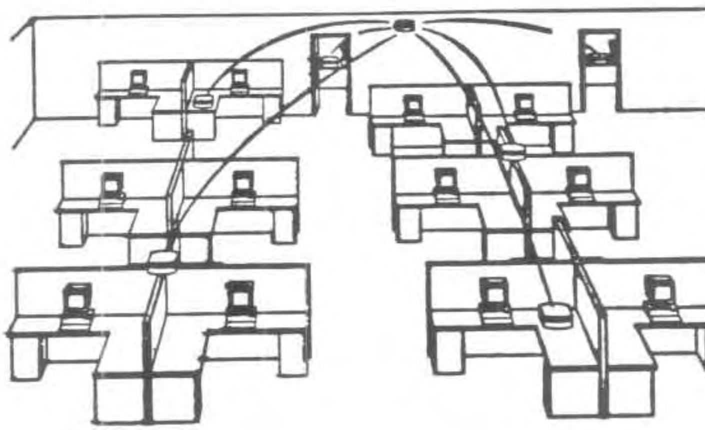

MOTOROLA
ALTAIR

The Altair Microcell

- One Control Module
  - The "Traffic Cop"
  - Supports Up to 32 Ethernet Devices
  - Coverage Area Typically 5,000 sq. ft.
- User Modules
  - Each UM Can Connect 1-6 Ethernet Devices
  - Different UM: Connected Ethernet Device Ratios for Reaching Maximum 32 Ethernet Devices per Microcell

MOTOROLA
ALTAIR

Ease of Installation

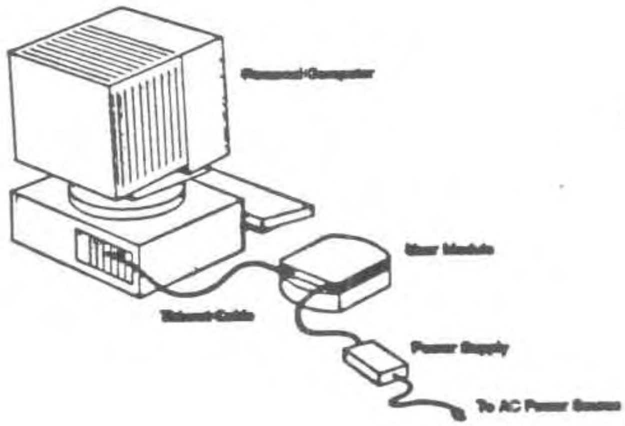

Motorola Confidential Proprietary

MOTOROLA INC.
Radio Telephone Systems Group

Arlington Ridge 3209 Building

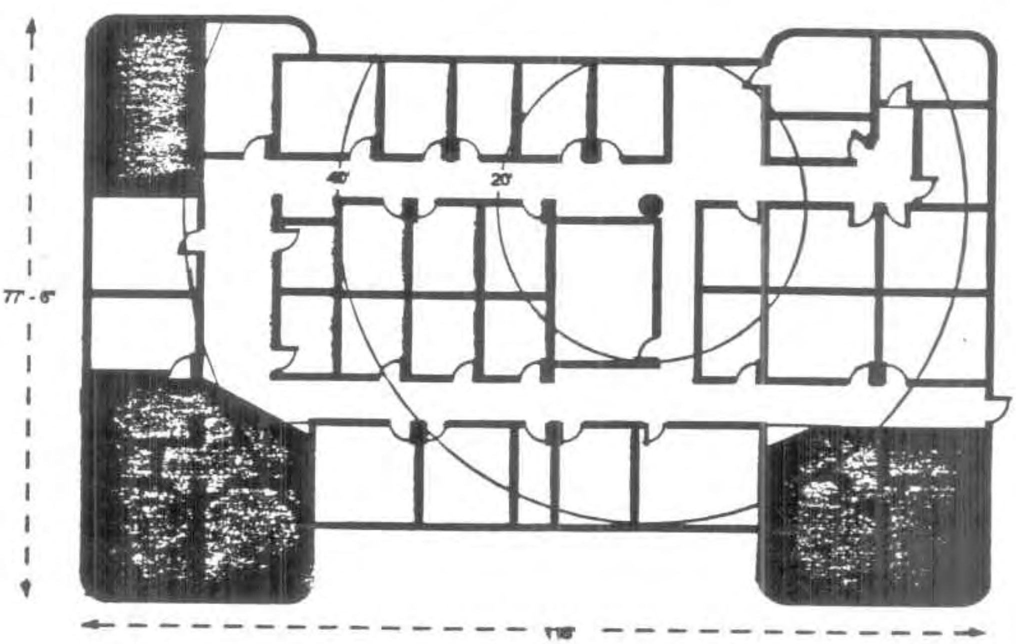

1990 Strategic Operations - RMTR
7 September 1990

Motorola Confidential Proprietary

M. L S. 1st Floor

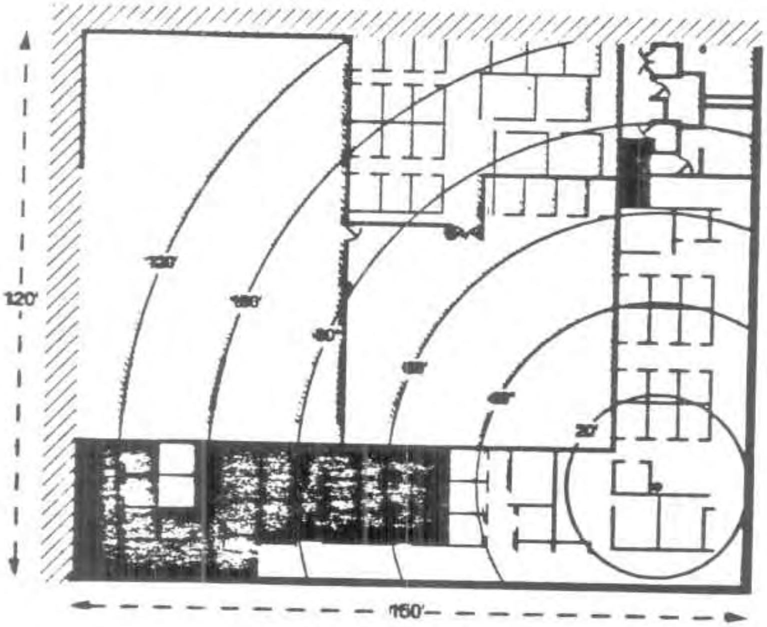

MOTOROLA
ALTAIR

Altair Deployment Flexibility

Extends the Reach of Existing LANS for New Users

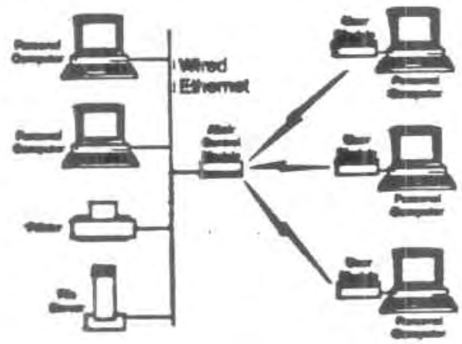

Wireless for New LANS

MOTOROLA
ALTAIR

Altair Is *Complementary* to Structured Distribution Systems

- Extends the Capabilities of an SDS System
- Facilitates the Inherent Advantages of an SDS
- Offers Enhanced Flexibility to Non-Serviced SDS Portions of a Building

MOTOROLA
ALTAIR

Altair Transparency

- Altair Is a Media-Replacement
- Compatible with Any Standard Ethernet 802.3 Network
  - Personal Computers
  - Terminals
  - Ethernet Cards
  - Other Ethernet Devices
  - Printers
- Altair Requires No Hardware or Software Modifications to Existing Ethernet Equipment

MOTOROLA
ALTAIR

Altair System Operations

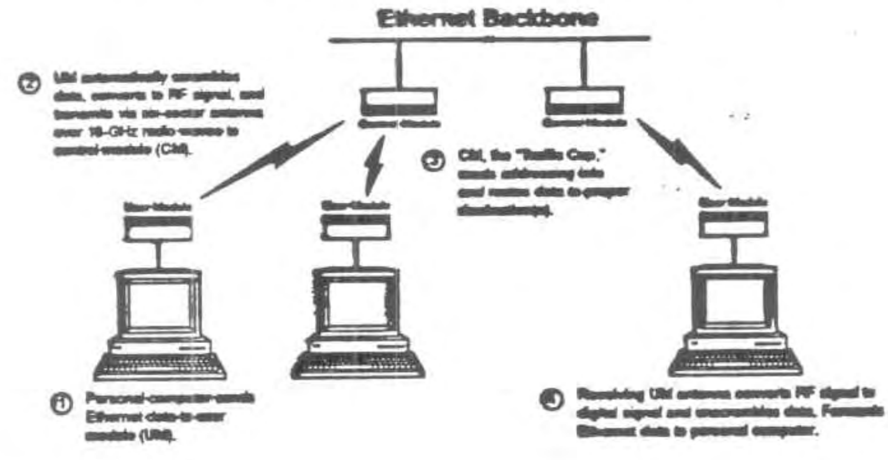

A System That Expands

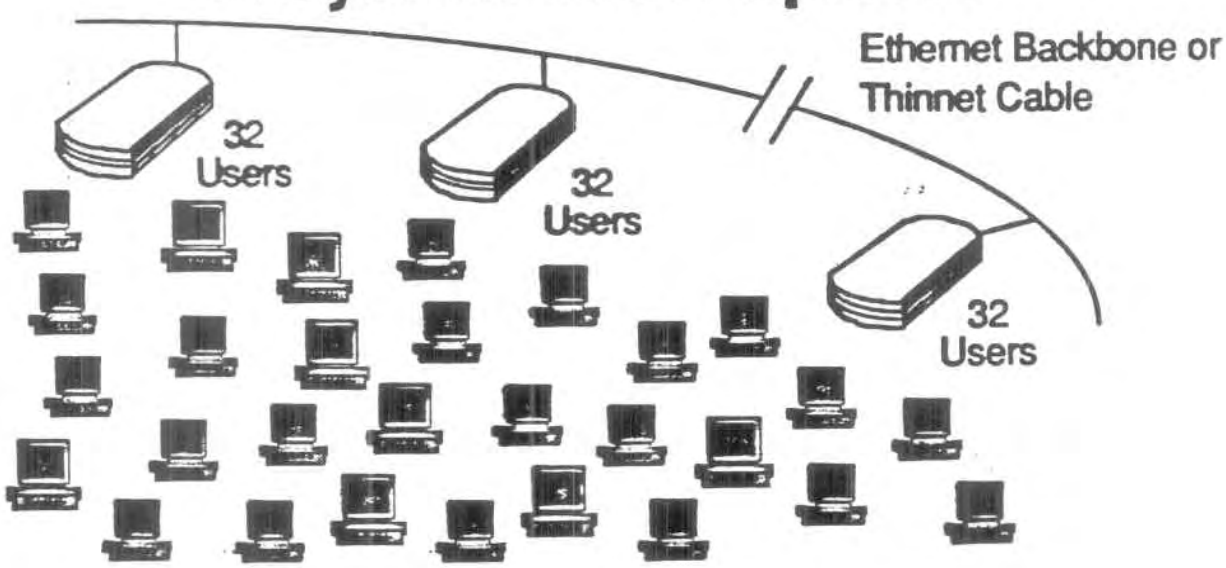

MOTOROLA
ALTAIR

Product Overview
Altair Data Security Attributes

- Design Goal
  - "Easiest" Place to Invade a Building's Network Is via the Traditional Wire; Not via Altair Network

Security

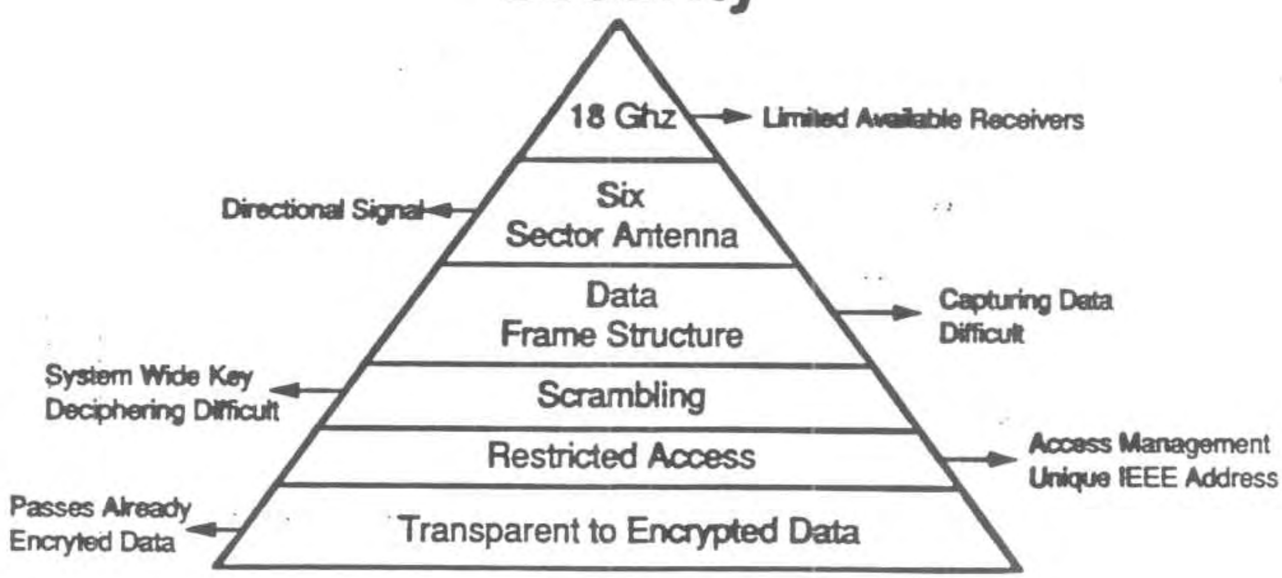

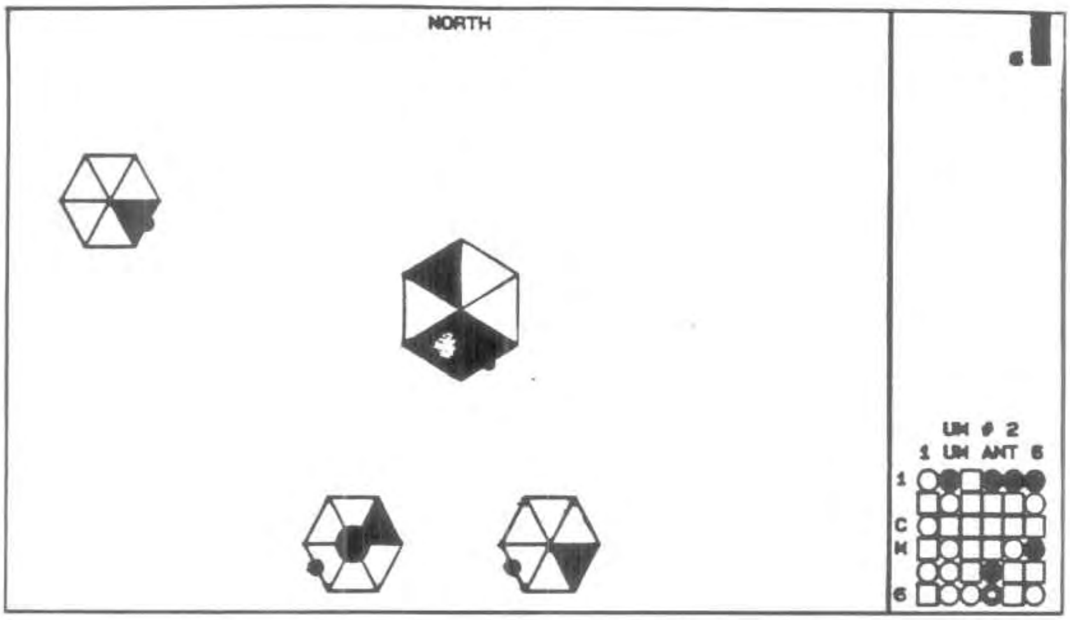

MOTOROLA
ALTAIR

Licensing and Frequency Utilization

Keys to High Speed, High Capacity, and Interference-Clear Communications

- An Altair Microcell Transmits and Receives, Requiring Only One of Two Available Frequencies
  - Second Neighboring Microcell Can Be Added Using Second Frequency
- Still More Altair Microcells Can Be Added with "Frequency Reuse"
  - Using Same Exact Frequencies Over and Over in a Building

MOTOROLA
ALTAIR

Licensing and Frequency Utilization

Keys to High Speed, High Capacity, and Interference-Clear Communications

- FCC Modified Digital Termination Service (DTS) Band Rules to Permit Low Power Radio in Buildings
  - 5 Licenses per Given 35 Mile Diameter
  - Each License Has Two Frequencies: DTS Requires One for Transmit and One for Receive

MOTOROLA
ALTAIR

Horizontal Frequency Reuse

Multiple Altair Microcells

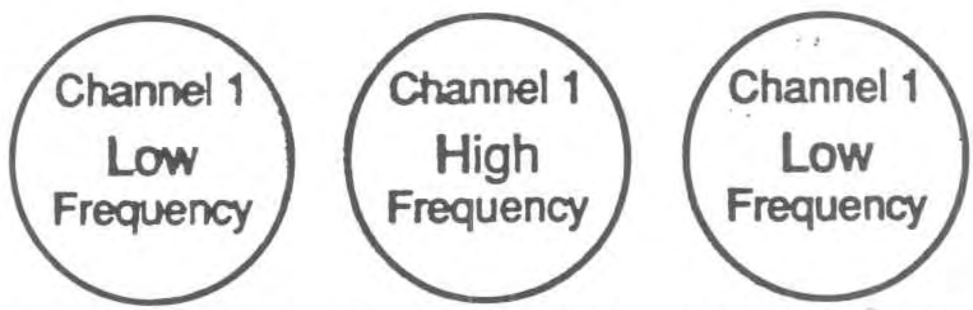

Altair Microcell #1 Altair Microcell #2 Altair Microcell #3

MOTOROLA
ALTAIR

Vertical Frequency Reuse
Multiple Altair Microcells

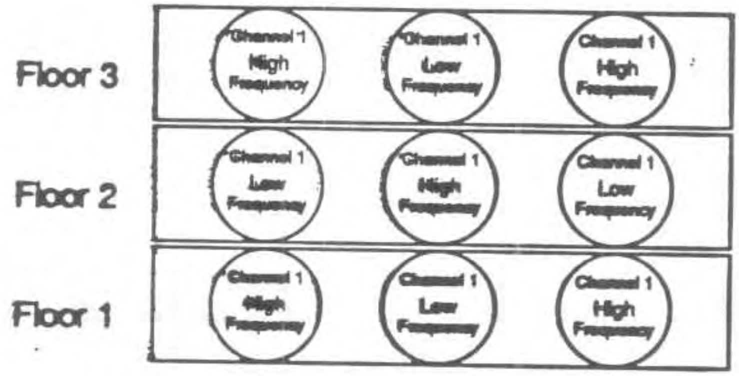

MOTOROLA
ALTAIR

Frequency Management Center

1-800-233-0877 - 7 Days/Week, 24 Hours/Day Support

- Manages Compliance with FCC Regulations
- Coordinates Frequency Use
- Maintains Central Database of All Altair Installations
- Provides Technical Assistance

Considerations for the Design of High Speed Wireless Optical Networks

K. S. Natarajan
K. C. Chen
P. D. Hortensius

IBM Research
T. J. Watson Research Center
Yorktown Heights, NY 10598

Abstract

We describe a conceptual design framework for wireless local area network communication between mobile computer users. The fundamental network architecture discussed is similar to the pioneering investigations of indoor infrared data networks by Gfeller at the IBM Zurich Research Laboratory [1]. Here we assume a base station which is typically attached to the ceiling and is connected to an established wired local area network. Each mobile computer has a transceiver to communicate with a base station via an optical wireless link. Therefore, there exist two main issues to study - the physical link and appropriate network protocols. We assume that if a user is located in an area that is within the range of more than one base station, the user is served by only one base station. Within each cell, users transmit/receive to/from the base station on a shared channel. We assume no code division multiple access, hence if a base station receives messages simultaneously from several sources, then all the messages collide and are lost. We review the conditions under which such collisions occur and suggest some partitioning mechanisms to avoid collisions.

Introduction

Portable computing using "luggables", "laptops", "notebooks", or "palmtops" is becoming more and more pervasive and more computationally powerful. However, currently, when one uses a portable computer, the vital communication link to a computer network still relies on tethered connection to common local area networks such as Ethernet and Token Ring. Flexibility and portability which are critical in portable computing are restricted in such an environment. Reliable and efficient wireless networking to support portable computing is a requirement for portable computing and other mobile information technologies. Multiple access wireless communication is typically accomplished by radio frequency (RF) communication techniques. An alternative for indoor environments which can potentially provide much higher data bandwidth and is currently immune from the regulatory problems of RF allocation is free space optical (most likely, infrared) transmission.

The Physical Link

Several earlier investigations have been conducted [1-3] into the characteristics of the free space optical data links. For the indoor wireless optical links under consideration the physical link between the base station and mobile transceiver has the following characteristics:

- Wide Beam Transmission: To avoid an aiming procedure the optical source at both the mobile and base station emit their power into a wide solid angle.
- Propagation: Optical transmission typically uses line-of-sight propagation. However, as demonstrated by Gfeller [1], signals can be successfully transmitted using a diffuse propagation path.
- Multi-Path Effects: In addition to a primary propagation path (either line-of-sight or diffused), other secondary propagation paths may create *interference* power which smears the pulse waveform and results in intersymbol interference.
- Power Considerations: We intend to minimize the power consumption at both transmitter and receiver in order to maximize the battery life of portable transceivers.
- System Complexity: The network must be applicable to portable systems hence its complexity must be contained to that which can be implemented just a few VLSI chips

According to studies recently conducted at the IBM Thomas J. Watson Research Center [4, 5], we have determined several important observations of such a physical link:

- Not suprisingly the link performance depends heavily on received power. The free space optical channel is clearly a power limited channel.
- While the optical bandwidth is very high when low-cost device technology is used the channel must be treated as a bandwidth limited channel.
- Multi-path effects create power leakage to subsequent bit periods which can degrade

the bit error rate performance. This is especially a problem in high data rate systems ($\geq$ 10Mbps).

- Short pulses can resist and even take advantage of multi-path effects, hence improving bit error rate performance.
- Blocking of direct-path propagation reduces the received power and enhances the multi-path effects.

For high speed wireless optical communication a major consideration in the design of the physical transmission system is the channel capacity of the indoor environment. Past experience in examining free space optical systems indicates that the noise in the channel and receiver approaches additive white Gaussian noise (AWGN) quite closely. Hence we need only calculate the band-limited AWGN channel capacity via a well known result from information theory [6]. The only modification is that we model the multi-path effect as a channel filter. With a 10 Mbps system, we only utilize around 10% of the theoretic channel capacity at a SNR of 25dB. However, our experience is that it is difficult to design cost efficient systems above several Mbps. To further increase the transmission rate for future high bandwidth applications several possible directions may be appropriate.

- Modulation, Coding, and Multiple Access Protocols: This is the *traditional* approach. However, there is a need for a great deal of innovation in the areas of coherent modulation and detection, (coded) incoherent modulation and decoding algorithms, signal processing (channel estimation and timing recovery), and efficient multiple access protocol(s).
- Optical Code Division Multiple Access (CDMA): This approach may provide tremendous advantages in wireless optical networking because of its theoretically efficient channel utilization. However, it suffers from practical implementation issues. To support a large number of (simultaneous) users, a large processing gain (spreading ratio) is required. The final chip rate will be extremely high. New technologies such as integrated optics and optical signal processing may be necessary.
- Subcarrier Multiplexing: A technology from satellite communication and cable television which is popular in optical fiber communication research. In such a system many network access and control issues would be addressed in the physical layer transmission.

The Wireless Optical Network

We now consider some of the networking issues in creating multicell wireless extensions to existing local-area networks. In a typical LAN environment, a user who wishes to communicate with remote facilities or use shared resources (eg. file servers, print servers, etc...) gains access to a network via a fixed connection point. The location of users is mostly *static* i.e., users do not frequently change the connection point through which they access the network. However, in a mobile wireless environment mobile transceivers are expected to change their physical location frequently. In such a *mobile* environment, users cannot be restricted to only gain access to the network via a predetermined connection point. Two possibilities exist for network support of such users; a) define new networks and protocols to support such movement or b) augment existing networks to support mobile wireless communication links. We believe that a commercially viable system must utilize existing infrastructure as much as possible hence our motivation here is to extend the range of existing wired network systems in such a way that users can have continued and transparent access to the network system irrespective of their access mechanism (wired or wireless, fixed or mobile).

We envision mobiles gaining access to the network via one of a finite number of devices called *Base Stations* that are physically attached to the wired backbone network (see Fig. 2). Each base station has both processing and storage capability to perform store-and-forward communication functions. Each base station essentially serves as a bridge between the wired backbone network on one side and a collection of wireless mobiles on the other side. Consider the network shown in Fig. 2. It consists of three base stations H_1, H_2 and H_3 attached to a wired network. All communication traffic originating from (or destined for) mobile A is handled via H_1. Similarly, all traffic from/to mobiles B and C is handled via H_2. The communication needs of mobiles D, E and F are handled by H_3.

A cell corresponding to a base station H consists of the geographic area within which a mobile can communicate with base station H. The owner of mobile A, denoted as $Owner(A)$, is the base station that is responsible for handling the communication needs of mobile A. The Domain Table of a Base Station H, denoted as $Domain(H)$, includes all mobiles that have H as their owner. In order to perform the store-and-forward function each base station maintains a Routing Table containing pairs of the form $<$ *Node id, Base Station id* $>$ where a pair $<NID$, $SID>$ means traffic for mobile NID should be sent to Base Station SID (see Fig. 3). Suitably defined protocols can enable each base station to create and dynamically maintain its Domain and Routing Tables.

The example in Fig. 2 showed three non-overlapping cells. In general, cells can overlap, i.e., a mobile may be able to physically communicate with more than one base station. An example of such a network is shown in Fig. 4. In this figure, mobile A can communicate with H_1 while mobile B can communicate with two base stations H_1 and H_2. A mobile located in a physical area with a *degree of overlap* of k is within communication range of k base stations.

We assume that if a mobile is located in an area with a degree of overlap of k, its communication needs are handled by exactly one base station, namely the one that owns it. In Fig. 4, H_1, H_2 and H_3 are three base stations. Let $\{A, B, C, D, E, F, G\}$ be a set of seven mobiles. mobiles A, B and C are within the cell corresponding to base station H_1. mobiles B, C, D

and E are within the cell corresponding to H_2, mobiles E, F and G are within the cell corresponding to H_3. An assignment of mobiles to the base stations is shown in Fig. 4. mobiles A, D, F and G have unique choices for their owner while mobiles B, C and E have two choices each for their owner.

When a mobile is in an overlapping area, it's transmissions can be heard by more than one base station (i.e., the mobile's owner and other potential owners) in whose cells the mobile is located. For example, in Fig. 4, uplink transmissions from B will interfere with transmissions by A, C, D and E. However B does not interfere with F because B and F can never transmit to the same base station. For the same reason, B and G do not interfere with one another. The interference is not limited to uplink transmissions alone. In fact, a mobile, such as B, who is within an overlapping cell area can receive broadcast signals from multiple base stations (B can hear from H_1 and H_2). If such a mobile receives broadcast messages from more than one base station at the same time, then the messages will collide and B will not receive any of them correctly. Thus the transmission and reception of messages in a cell of a multicell network that uses identical communication wavelengths in different cells requires control of interference that may occur due to:

- Uplink transmission from mobiles who lie in overlapping areas (even though a mobile is owned by exactly one base station, it's transmissions are heard by all base stations that can potentially own him).
- Downlink transmissions from base stations if their overlapping cell areas contain one or more mobiles.

Network control algorithms for avoiding inter-cell interference in wireless channel usage are required.

Mobiles within a cell gain access to the network by sharing the wireless channel in a multiaccess-broadcast mode. A key consideration in the design of the media access protocol in a mobile network is that the set of mobiles within a cell can change with time. This has the following implications for the base station responsible for the cell. The base station can not assume that:

- the number of mobiles desiring access to the channel is fixed, and
- the identity of mobiles accessing the channel is fixed over any extended period of time.

Media access protocol design

Mobiles within a cell gain access to the network by sharing the wireless channel in a multiaccess-broadcast mode. Important factors to consider in designing multiaccess channel protocols for mobile networks include:

- The applications that are to be supported by the wireless network. Diverse traffic needs can require different bandwidth and performance requirements be provided by the system. For example, data traffic can require low average delay while voice traffic typically requires guaranteed bandwidth and real-time delivery. The multiaccess protocol must be capable of satisfying the diverse requirements simultaneously.
- Following parameters -
- Channel speed (100kbps - 10 Mbps currently, potentially much higher in the future).
- Propagation delay - primarily a function of the size of the cells of the network. In an infrared environment, cell sizes are small (tens of feet) and the propagation delay is negligible.

Mobility Issues

The network is assumed to provide multiple, overlapping cell coverage for the geographic area of interest. We need control algorithms for automatic and transparent management of domain and owner relationships as well as the dynamic maintenance of routing tables at the base stations.

As the mobile moves from one physical location to another, the base station responsible for handling the communication needs of the mobile must change. The functionality of mobile communication means that mobiles can communicate with one another using symbolic names and without any specific reference to their physical location. The issues to be addressed include design of protocols for accomplishing the following functions.

- Establishment of unique ownership for each mobile that becomes active (turned ON for the first time) in the system
- Detection of movement of mobiles as they cross from one cell to another
- Handling the change of ownership of mobiles as they move from one cell to another
- Mechanisms for assigning a unique owner to a mobile that lies in an overlaping cell area (i.e., the mobile can be potentially served by more than one base station)
- Readjustment of routing related information at base stations that are affected by the movement of a mobile

A subtle but important design consideration, is that the mobiles are likely to be run with batteries whose life must be prolonged as long as possible (efficient use of battery power). It is undesirable to design protocols that place excessive demand on the mobile battery power. For example, a network protocol which relied on constant pinging from the mobile would waste precious battery power. The power consumption also varies widely between transmission and reception (a factor of 10) hence one should take advantage of the asymmetry in the transmit/receive power. Finally, the base station generally is powered from the building ac power supply hence it is more important to minimize uplink transmissions compared to downlink broadcasts.

Network control of interference

The basic idea of network control is to avoid intercell interference by permitting *simultaneous wireless communication to occur only in non-overlapping cells*, i.e., wireless operations occur within a cell if and only if no wireless operations are occurring at the same time in any of the neighboring cells. An important objective is to attempt to maximally reuse bandwidth in spatially disjoint cells of the wireless network. Possible approaches include centralized as well as distributed control algorithms

Variants of random access schemes (such as Carrier Sense Multiple Access protocol) as well as contention-free schemes (such as roll-call polling) show promise for satisfying many of the mobility and media access protocol requirements. The challenge is to provide systems which are able to utilize existing network cabling and network devices by simply extending the network protocols.

Conclusions

We have discussed both physical link and network protocol design considerations for wireless infrared networking. It is clear that free space optical networks face many limitations especially at high signalling rates. Above 10Mbps new and novel work will be required to establish reliable links. At the same time the network management and control issues are also formidable if full LAN service is to made transparently available to the mobile user.

[1] F. Gfeller and U. Bapst, "Wireless In-House Data Communication via Diffuse Infrared Radiation," *Proc. IEEE*, vol. 67, no. 11, pp. 1471-1486, Nov. 1979.

[2] T.S. Chu and M.J. Gans, "High Speed Infrared Local Wireless Communication," *IEEE Communication Magazine*, vol. 25, no. 8, pp. 1-10, Aug. 1987.

[3] C.S. Yen and R.D. Crawford, "The Use of Directed Optical Beams in Wireless Computer Communication," *Proc. Globecom'85*, pp. 1181-1184, 1985.

[4] K.C. Chen, "On-Off Keying Optical Transmission and Channel Capacity for Indoor High Rate Wireless Data Networks," *submitted for publications*, 1991.

[5] P.D. Hortensius, "Infrared Communication Research and Development," *IBM Internal Research Report*, 1991.

[6] R. Blahut, *Principles and Practice of Information Theory*, Reading, MA: Addison Wesley, 1987.

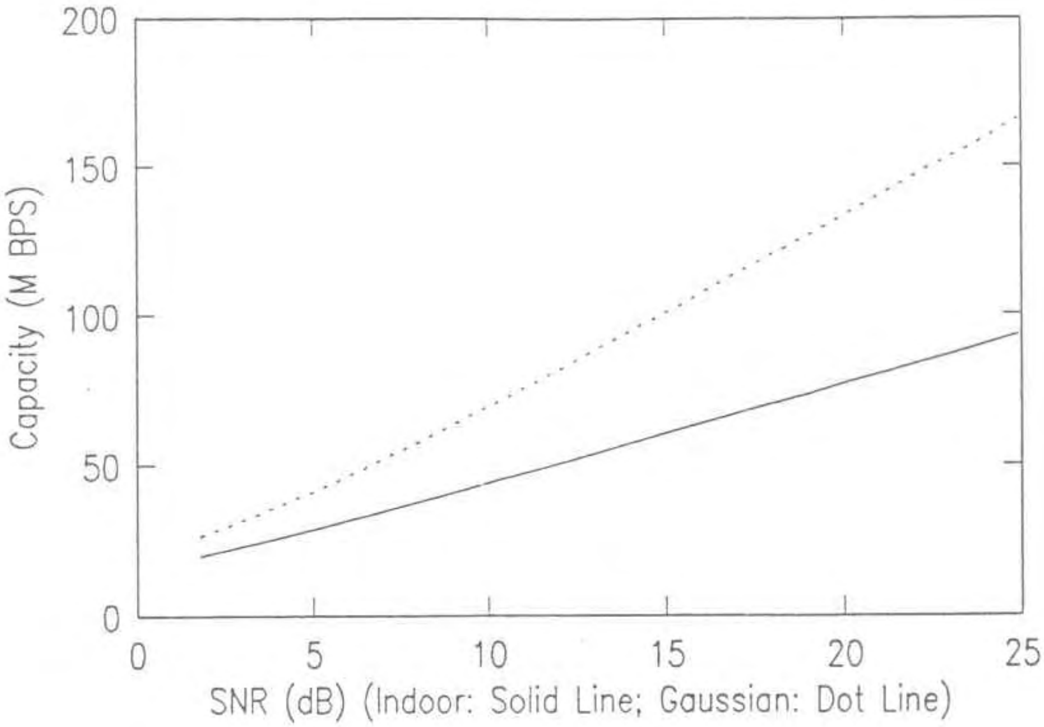

Figure 1 Capacity of Indoor Channel

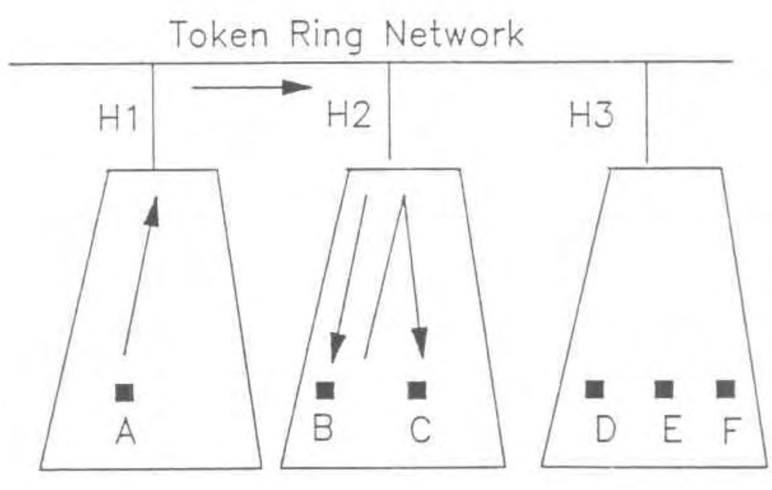

Figure 2 Three Non-Overlapping Cells

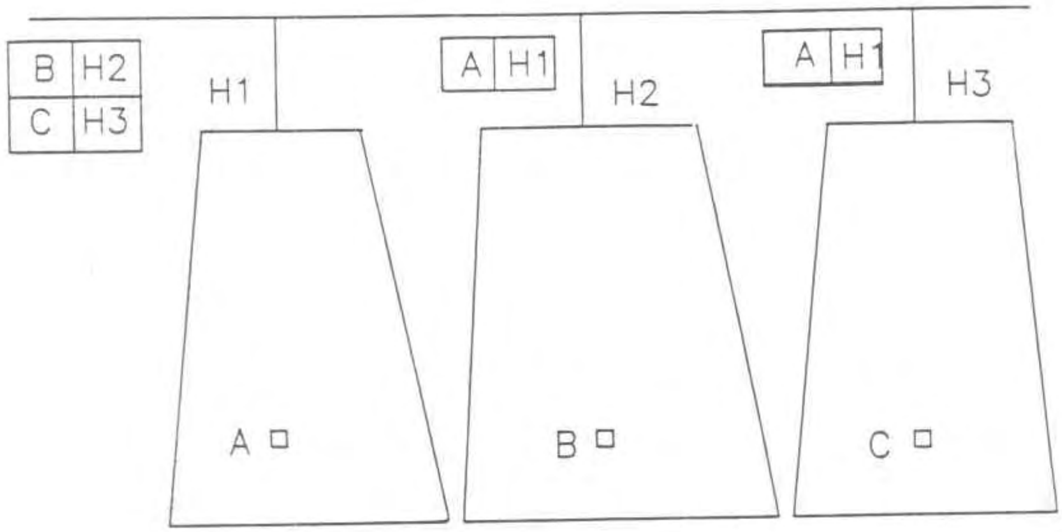

Figure 3 Routing Tables at Header (Base) Stations

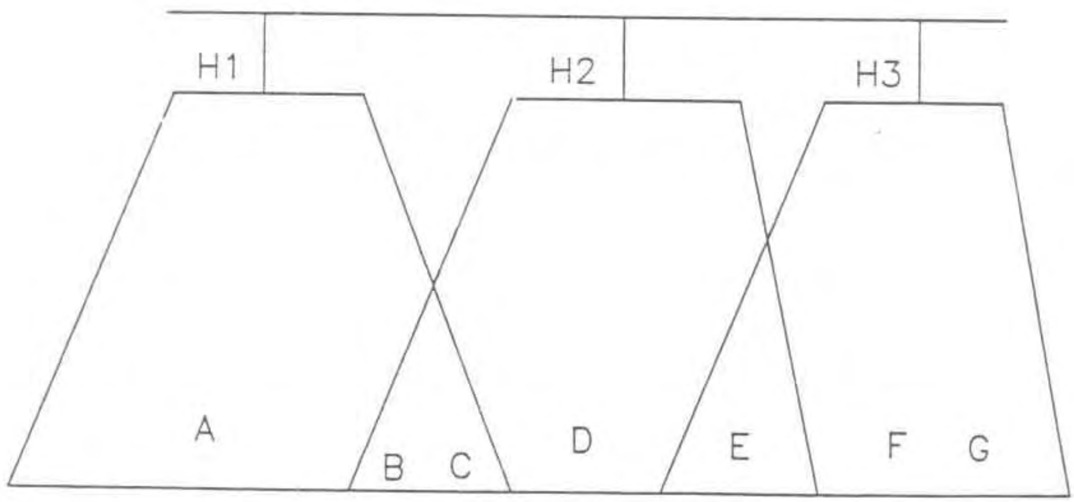

OWNER(A) = H1
OWNER(B) = H1
OWNER(C) = H2
OWNER(D) = H2
OWNER(E) = H2
OWNER(F) = H3
OWNER(G) = H3

Figure 4 Three Overlapping Cells